ACTIVITY-DEPENDENT REGULATION OF ETHER À GO-GO K^+ CHANNELS

by

Daniel David Marble

A dissertation submitted in partial fulfillment
of the requirements for the degree of
Doctor of Philosophy
(Molecular, Cellular and Developmental Biology)
in The University of Michigan
2008

Doctoral Committee:

Associate Research Fellow Gisela F. Wilson, Univeristy of Wisconsin, Co-Chair
Associate Professor Kenneth M. Cadigan, Co-Chair
Professor Richard I. Hume
Professor Lori L. Isom
Professor Michael D. Uhler
Assistant Professor Anatoli N. Lopatin

To the three most exceptional women in the world,
my daughter Alexandria Jean,
my wife Katina Jean,
and my late mother Carla Jeanne.

ACKNOWLEDGEMENTS

The number of people who I can thank for contributing to my love of science and helping me throughout my graduate career is too high to count. But I'll try. First, I have to recognize Gisela Wilson and her immeasurable wisdom and undeserved patience in assisting me through this process of becoming a scientist. Other members of the Wilson lab that have gone out of their way in numerous instances to facilitate my work include Andrew Hegle, Dylan Clyne, Elizabeth Stevenson, Eric Snyder II, Sarah Telfer, Katherine MacNair and Divya Sharma. I especially thank Andy for making the lab an enjoyable workplace as well as for being a swell scientitian.

I must also thank all the members of my thesis committee that have selflessly contributed their time and insight to this work, including Richard Hume who has gone out of his way for me over the years. Additionally, I am grateful to all the individuals associated with MCDB, including the Cadigan, Hume, Kuwada, Duan, and Bodmer labs, and the departmental staff including Mary Carr and Diane Durfy. I especially would like to acknowledge David Parker, Margaret Liu, Yan Liu, Susan Klinedinst, R. J. Wessells, Peter Schleuter, Sean Low, Shlomo Dellal, and Jamila Power. Members of the Isom lab, Henriette Remmer, and Sushama Pavgi are others in the University of Michagan community that also deserve thanks.

Most importantly I need to thank my wife Katina, who has been exceedingly supportive of me, ever since we have known each other. It is unlikely I would be the person I am, have it not been for her.

PREFACE

Some data presented in this thesis have been previously published or are in preparation for publication at the time of this writing. Chapter II (Marble et al., 2005) was published in the Journal of Neuroscience (J Neurosci 25(20) 4898-4907) and the Appendix (Hegle et al., 2006) in the Proceedings of the National Academy of Sciences of the United States of America (PNAS 103(8) 2886-2891). Chapters III and IV have been submitted for publication.

All of these chapters were written collaboratively with my thesis advisor, Gisela F. Wilson. In Chapter II much of the *in vitro* and heterologous expression data were collected by Eric Snyder and Andrew Hegle, respectively. Dylan Clyne contributed the majority of the oocyte and *in vitro* data presented in Chapter III and Andrew Hegle again performed all of the heterologous expression experiments found in Chapter IV. I am immensely appreciative of Gisela and all the others, including the Leslie Griffith lab, who contributed immensely to this work, both experimentally and in writing.

TABLE OF CONTENTS

LIST OF TABLES

LIST OF FIGURES

APPENDIX: A VOLTAGE-DRIVEN SWITCH FOR ION-INDEPENDENT SIGNALING BY ETHER À GO-GO K^+ CHANNELS

ABSTRACT

The *Drosophila ether á go-go* (*eag*) gene encodes a partially inactivating, voltage-gated K^+ channel expressed at neuromuscular and CNS synapses. Recordings from the larval neuromuscular junctions (NMJs) of *eag* mutants, compared to wild type, reveal a high level of spontaneous activity in the motor nerve and broader evoked excitatory junctional potentials. Also, EAG is one of the few K^+ channels that demonstrate a role in learning and memory as assayed by habituation and courtship conditioning protocols.

The goals of my thesis are to better understand the mechanisms by which neuronal activity affects EAG function and how EAG channels contribute to neuronal function. Since neuronal activity changes Ca^{2+} concentrations within the cell, I focused on how Ca^{2+}-dependent mechanisms could regulate EAG channels. Proteins that modulate EAG current include calmodulin (CaM), the calcium (Ca^{2+})/calmodulin (CaM)-dependent protein kinase II (CaMKII) and the Camguk/CASK (CMG) adaptor protein. Phosphorylation of EAG by CaMKII and association with CMG produce relatively long-term effects by regulating EAG surface expression, whereas CaM binding acutely down-regulates EAG current. In addition, EAG channels regulate CaMKII activity by a mechanism not dependent on ion conduction, but rather, depends on conformational changes associated with the position of the voltage sensor.

The temporal difference in the regulation of EAG by increased intracellular Ca^{2+} suggests a model in which CaM binding affects short-term plasticity, whereas CaMKII and CMG regulation of EAG affect more long-term, homeostatic adjustments to increased neuronal activity. *In vivo*, signaling deficient channels fail to rescue high levels of spontaneous activity characteristic of *eag* mutants, suggesting that voltage-dependent, conductance-independent EAG signaling plays a role in the homeostatic regulation of neuronal activity. These results identify, until now, an unknown function for voltage sensing of EAG and suggest this mechanism may serve as a direct link between neuronal activity and the state of intracellular messengers. Transgenic expression of EAG channels that cannot bind CaM or be phosphorylated by CaMKII show Ca^{2+}/CaM and CaMKII independently modulate EAG currents. Inhibition of EAG by CaM binding is necessary for facilitation at the larval NMJ, and phosphorylation of EAG at its CaMKII site is essential for proper synaptic function.

CHAPTER I

INTRODUCTION

A. THESIS OVERVIEW

The *Drosophila ether á go-go* (*eag*) gene encodes a partially inactivating, voltage-gated K^+ channel expressed at neuromuscular and CNS synapses. Recordings from the larval neuromuscular junctions (NMJs) of *eag* mutants reveal a high level of spontaneous activity in the motor nerve and evoked excitatory junctional potentials (EJPs) that are larger than those of wild type larvae. Of the dozens of K^+ channels now identified, EAG is one of the few that demonstrate a role in learning and memory as assayed by courtship conditioning protocols. Because the basic characteristics of many K^+ channel currents are very similar, my working hypothesis has been that regulation of EAG is a key determinant of the unique role of EAG in physiology and learning.

The goals of my thesis are to better understand the mechanisms by which neuronal activity affects EAG function and how EAG channels contribute to neuronal function. Because neuronal activity changes calcium (Ca^{2+}) concentrations within the cell, I focused on how Ca^{2+}-dependent mechanisms that could affect EAG channels. Several proteins regulate EAG current when the channel is studied in heterologous

expression systems. These include Ca^{2+}/calmodulin (CaM)-dependent protein kinase II (CaMKII) and the Camguk/CASK (CMG) adaptor protein and calmodulin (CaM). Phosphorylation of the channel by CaMKII and association with CMG produce relatively long-term effects by regulating EAG surface expression (Chapter II), whereas CaM binding acutely down-regulates EAG current (Chapter III). In addition, EAG channels, in turn, regulate CaMKII activity by a conductance-independent mechanism that involves a direct interaction with the kinase (Chapter IV).

The temporal difference in the regulation of EAG by increased intracellular Ca^{2+} suggests a model in which CaM binding affects short-term plasticity, whereas CaMKII and CMG regulation affect more long-term, homeostatic adjustments to increased neuronal activity. To test these predictions, I transgenically expressed *eag* constructs containing site-specific mutations that disrupt regulation. Four constructs, including the CaM binding mutant (*eag*-FFSS), the CaMKII binding mutant (*eag*-LAKK), the CaMKII phosphorylation site mutant (*eag*-T787A), and the non-conducting mutant (*eag*-F456A), were examined for their ability to rescue the NMJ phenotype observed in eag^{sc29} larvae relative to the rescue observed using wild type *eag*. My results suggest that acute inhibition of EAG current by CaM binding makes a major contribution to short-term plasticity at this synapse: the interaction of CaM with EAG is necessary for facilitation, whereas other features of the *eag* phenotype are rescued as effectively by the CaM-binding mutant as by the wild type channel. In addition, *eag*-LAKK (signaling-deficient) and *eag*-F456A (conductance-deficient) transgenics revealed phenotypically distinct effects, failing to rescue either spontaneous activity or EJC amplitudes, respectively. Finally, *eag*-T787A transgenics were indistinguishable from eag^{sc29} larvae, consistent

with the role of phosphorylation in regulating the surface expression of EAG. The implied change in surface expression appears to affect both the conductance and signaling functions of EAG, even at basal activity levels, suggesting that EAG may be an important target for both short-term and homeostatic mechanisms of plasticity.

B. CLASSIFICATION AND STRUCTURE OF K^+ CHANNLES

All fully sequenced genomes, including: eubacteria, archaebacteria, and eukaryia, include at least one K^+ channel (Littleton and Ganetsky, 2000). No other ion channel demonstrates such ubiquity. The more than 90 different K^+ channels encoded by the human genome are greater than the number of sodium, calcium and chloride channels combined (see Gutman et al., 2005 for review). Although all K^+ channels are functionally related by their shared ability to selectively conduct K^+ ions, the number and diversity of K^+ channel structures underscores the large variability within this group and suggests a corresponding functional diversity that is unique in comparison to other ion channels.

There are several ways of classifying K^+ channels based upon their structural characteristics. All known K^+ channels consist of a 4-fold symmetrical ion pore (Gutman et al., 2005), but K^+ channel classes differ in the mechanism by which this 4-fold symmetry is accomplished. Functional channels are either tetrameric, containing four pseudo-symmetrical subunits, with each subunit contributing one-fourth of the pore structure, or dimers containing two subunits, each making half of the pore.

K^+ channels are further classified according to the number of transmembrane (TM) domains in each channel subunit. There are two broad groups: subunits that

contain either two TM domains (the inward-rectifier, K_{ir}, group) or six transmembrane domains as in the voltage gated (K_v) group (reviewed in Miller, 2000), in addition to the pore domain. These two themes, however, come in variations. The K_{ir} group can be further divided into subunits that contain either one (K_{ir}) or two (two pore-domain channels) repeats of the basic 2TM-1pore structure. The largest class of K^+ channels is the K_v group which consists of six TM (voltage-gated, calcium-activated, and sodium-activated channels) or seven TM (calcium-activated/large conductance) K^+ channels.

Another classification scheme for K^+ channels is based on their mechanism of activation. Some K^+ channels, such as those composed of 2TM-1pore subunits, are not gated by an intrinsic voltage sensor, but rather are always in an open conformation (Goldstein et al, 2001; Kubo et al., 2005). Nonetheless, due to the strong voltage-dependent block of the channel pore by intracellular cations at positive membrane potentials (such as the polyamine spermine), these channels preferentially conduct K^+ in the inward direction, and thus, have the appearance of voltage-dependence. It is postulated that outward flow of K^+ through these channels contributes to the resting membrane potential of the cell.

Other channels are regulated by the direct interaction with other ions such as Ca^{2+} and Na^+, namely the Slo and Slack/ Slick family of channels (Bhattacharjee and Kaczmarek, 2006). KATP channels, such as the $K_{ir}6$ group and K_{ir} 1.1 (ROMK), are regulated by intracellular nucleotide binding. Certain K^+ channels have also been shown to have a pH sensitive conductance such as Slo3 and members of the TASK family of two pore-domain channels (Schreiber et al., 1998; Cho et al., 2005).

B1. K_v channels

Probably the most studied group of K^+ channels are the voltage-gated channels, which include EAG. K_v channels make up about half of the known K^+ channels in the human genome (Gutman et al, 2005). The *Drosophila Shaker* (*Sh*) channel is a member of this family, and since it was the first cloned K^+ channel it is often considered an archetype to which other K^+ channels are compared (Papazian et al., 1987; Tempel et al., 1987). *Sh* and all other members of this group are tetrameric channels with each subunit contributing six transmembrane domains and one-fourth of the selectivity filter. K_v channels also have positively charged amino acids within their S4 domains which confer their voltage-sensing capabilities. This family can be further separated into four categories: the Sh/Shab/Shaw/Shal-related families, the KCNQ sub-family, the non-conducting K_v modifying sub-family, and the EAG sub-family (see Table 1.1, Gutman et al., 2005). Many of these pore-forming α-subunits also interact with accessory β-subunits that contribute to channel expression and functionality.

The Sh-related sub-family of K^+ channels makes up almost half of the voltage-gated K^+ channels in the human genome. The roles of Sh-related channels are numerous. They include, however, the presynaptic A-type current involved in regulation of neurotransmitter release (Sheng et al., 1993), the native cardiac transient outward current (Po et al., 1993), and the delayed rectifier K^+ current in rat hippocampal neurons (Murakoshi and Trimmer, 1999). Some Sh-related channels form functional homomeric channels, but the fact that isolated expression of individual α-subunits rarely results in K^+ currents with properties matching those of the corresponding *in vivo* current has made it clear that the pore-forming alpha subunits of K^+ channels often heteromultimerize or

TABLE 1.1

IUPHAR Name	HGNC Name	Other Names
K_v1.1	KCNA1	*Shaker*-related family
K_v1.2	KCNA2	
K_v1.3	KCNA3	
K_v1.4	KCNA4	
K_v1.5	KCNA5	
K_v1.6	KCNA6	
K_v1.7	KCNA7	
K_v1.8	KCNA10	
K_v2.1	KCNB1	*Shab*-related family
K_v2.2	KCNB2	
K_v3.1	KCNC1	*Shaw*-related family
K_v3.2	KCNC2	
K_v3.3	KCNC3	
K_v3.4	KCNC4	
K_v4.1	KCND1	*Shal*-related family
K_v4.2	KCND2	
K_v4.3	KCND3	
K_v5.1	KCNF1	Modifier
K_v6.1	KCNG1	Modifiers
K_v6.2	KCNG2	
K_v6.3	KCNG3	
K_v6.4	KCNG4	
K_v7.1	KCNQ1	*KVLQT*
K_v7.2	KCNQ2	*KQT2*
K_v7.3	KCNQ3	
K_v7.4	KCNQ4	
K_v7.5	KCNQ5	
K_v8.1	KCNV1	Modifiers
K_v8.2	KCNV2	
K_v9.1	KCNS1	Modifiers
K_v9.2	KCNS2	
K_v9.3	KCNS3	
K_v10.1	KCNH1	*eag1*
K_v10.2	KCNH5	*eag2*
K_v11.1	KCNH2	*erg1*
K_v11.2	KCNH6	*erg2*
K_v11.3	KCNH7	*erg3*
K_v12.1	KCNH8	*elk1,elk3*
K_v12.2	KCNH3	*elk2*
K_v12.3	KCNH4	*elk1*

Table 1.1: K_v Channel Sub-families. Gene names are those assigned by the IUPHAR (Catterall et al., 2002) and HGNC (www.gene.ucl.ac.uk). From Gutman et al., 2005.

associate with auxiliary subunits. Sh-like K^+ channels can form heteromultimeric tertiary structures consisting of similar sub-family members. For example, mouse $K_v1.1$ and $K_v1.2$ multimerize with each other in the juxtaparanodal regions of the nodes of Ranvier in the myelinated axons and terminal fields of basket cells in cerebellum (Wang et al., 1993). This combination of channel subunits appears necessary for the rapid membrane repolarizations observed at these locations.

Another major sub-family of the K_v family of K^+ channels is the KCNQ (K_v7) group. Members of this sub-group have several functions, but they are particularly known for being responsible for the M current found in neurons. The M current is a slowly activating and deactivating potassium current that performs a critical role in determining the responsiveness to synaptic inputs as well as the subthreshold excitability of neurons. The M current was first described in peripheral sympathetic neurons, and differential expression of this current produces subtypes of sympathetic neurons with distinct firing patterns; the M current is also expressed in many neurons in the central nervous system (Wang et al., 1998; Selyanko et al., 2002). Importantly the M current is modulated by the neurotransmitter acetylcholine (ACh). When ACh is released muscarinic receptor (mAChR) activation inhibits KCNQ K^+ channels and thus the M current. Activation of phospholipase C by mAChR initiates M current modulation and recovery from inhibition requires ATP and phosphoinositide 4-kinase. Also, breakdown of the second messenger phosphotidylinositol 4,5-bisphosphate is a crucial determinant of M channel modulation (Ikeda and Kammermeier, 2002; Suh and Hille, 2002).

B2. Non-conducting K_v channels and β–subunits

The structural and functional diversity of K^+ channels is further extended by the association of auxiliary subunits with pore-forming α subunits. Both cytoplasmic and integral membrane auxiliary subunits have been identified and are often necessary to fully replicate the properties of the corresponding *in vivo* K^+ current. For example, the channel KCNQ1 is expressed in heart tissue and mutations in that gene have been linked to cardiac arrhythmias (Sanguinetti et al., 1996). When KCNQ1 is expressed heterologously it displays current properties that are unlike that of any known cardiac current. However, when KCNQ1 is co-expressed with minK (which also has been linked to arrhythmias), a current that is almost identical to cardiac I_{Ks} emerges (Barhanin et al., 1996; Sanguinetti et al., 1996). This strongly suggests that K^+ channel and β-subunit interactions are necessary for proper function, and that inhibition of certain protein associations might underlie severe channelopathies.

Functional K^+ channels also can be regulated by an association with non-conducting α-subunits. As described earlier, many K_v channels can heteromultimerize with other similar K^+ channels which results in new properties not found in either homomer. However, there appears to be a large number of K^+ channels (groups K_v5, K_v6, K_v8, and K_v9), all with the 6TM-1 pore structure, that only function when bound to other conducting K^+ channels. For example, $K_v6.3$ decreases the rate of inactivation of Kv2.1 (Sano et al., 2002). Also, $K_v9.1$ or $K_v9.2$ alone have no conductance, but when co-expressed with functional Shab-family K^+ channels, lead to strong inhibition, large changes in kinetics, and shifts in voltage-dependent inactivation (Salinas et al., 1997). Much is not known about the function of many of these obligatory interacting proteins,

but due to the relatively large number of channels (at least ten), and the numerous possible permutations of interactions with other channels, it appears that this group of non-conducting channels may play a significant role in affecting neuronal function. Although members of these K_v sub-families are localized to the plasma membrane of neuronal cells, it is not known if they are voltage-sensitive--unless co-expressed with other conducting K_v channels. Although they do have positively charged residues in their S4 domains, alone they may or may not exhibit gating currents. An intriguing possibility is that these subunits may have other voltage-sensitive, non-conducting functions.

B3. The EAG family

The EAG sub-family of K_v channels consists of the EAG, EAG-related gene (ERG), and Eag-like K^+ channel (ELK) channels. The *eag* gene was originally identified in *Drosophila* mutants that exhibit leg-shaking behavior under ether anesthesia (Kaplan and Trout, 1969), but its identity as a potential ion channel gene was not appreciated until later studies that found an enhancement of neurotransmission defects in *eag/Sh* double mutants when compared to either individual mutation (Ganetzky and Wu, 1983b). The *eag* gene was cloned using chromosomal analysis (Drysdale et al., 1991; Warmke et al., 1991) and soon thereafter, an *eag* homology screen identified a family of highly conserved genes in several invertebrate and mammalian species, which could be separated into the three EAG, ERG and ELK groups. The amino acid sequences encoded by these genes contain the characteristic transmembrane, pore-forming and voltage sensing domains found in *Sh* channels, as well as a cyclic nucleotide-binding domain similar to that of cyclic-nucleotide gated (CNG) channels (Warmke and Ganetzky, 1994).

Interestingly, sequence comparison shows that the EAG family of channels is more closely related to CNG channels than voltage-gated K^+ channels (Guy et al., 1991), and consequently they are now considered part of the same phylogenetic branch of channel evolution (Yu and Catterall, 2004). EAG channels are found in the genomes of all fully sequenced animal species, and similar channels (~25% amino acid identity over the 6TM/pore domains) are found in the genomes of plants, including the inward-rectifying K^+ channels KAT1 and AKT1 (Warmke and Ganetzky, 1994).

B3a. EAG structure

EAG is a typical member of the 6 TM/ 1 pore family of K_v channels. The EAG channel is comprised of four identical subunits, each with six transmembrane domains, a membrane re-entrant pore loop and intracellular N- and C-termini. EAG differs from the majority of other 6 TM/ 1 pore K_v channels by way of its significantly larger intracellular domains. The N- and C-termini of EAG are 225 and 678 amino acids long, respectively (Warmke et al., 1991). Sh channels, for comparison, have 488 fewer intracellular amino acids (Tempel et al., 1987). Although there are other K^+ channels with relatively large intracellular domains, such as dSlo (489 amino acids in cytoplasmic C-terminus), the majority of their intracellular domains are made of single large specialized regions for Ca^{2+}-sensing (Wei et al., 1994). Although the identities of many of the intracellular regions of EAG (based upon homology to other proteins) have been found, the functional roles of the majority have yet to be fully determined.

B3b. N-Terminus and pore

In its N-terminus, EAG contains a stretch of amino acids that form a Per-Arnt-Sim (PAS) dimerization domain (Figure 1.1). This domain is particularly unusual for an ion channel because nearly all eukaryote proteins that contain a PAS domain are cytoplasmic (Crews and Fan, 1999). Examples include the basic helix-loop-helix-PAS transcription factors that reside within the nucleus or shuttle between the nucleus and cytoplasm. One such PAS domain containing transcription factor is *single-minded*, which is a master regulator of ventral midline development in *Drosophila* (Epstein et al., 2000). PAS domains are usually found in proteins that act as internal sensors of light, hypoxia, and redox potential, such as the *Drosophila* circadian protein Period (Per) (Taylor and Zhulin, 1999). In the case of Per, this domain facilitates dimerization with Timeless (Tim), another PAS-containing circadian protein. This association exposes a nuclear localization signal (NLS) in the Per/Tim complex that allows it to directly downregulate transcription of both proteins (Scully and Kay, 2000). Another intriguing role of a PAS domain is in the serine/threonine kinase PASK (Rutter et al., 2000). PASK acts as metabolic sensor in a cell-autonomous manner to maintain cellular energy homeostasis by regulating glucose-stimulated insulin secretion in pancreatic cells, triglyceride storage in liver, metabolic rate in skeletal muscle (Hao et al., 2007).

It is yet to be determined whether the EAG PAS domain is functional, although it is conserved throughout the EAG family of K^+ channels and has been suggested to operate as an oxygen sensor in both EAG and hERG channels (Bauer and Schwarz, 2001). The PAS domain of hERG has been crystallized and is similar in structure to PAS domains found in light sensor photoactive proteins (Morais Cabral et al., 1998). Both

FIGURE 1.1

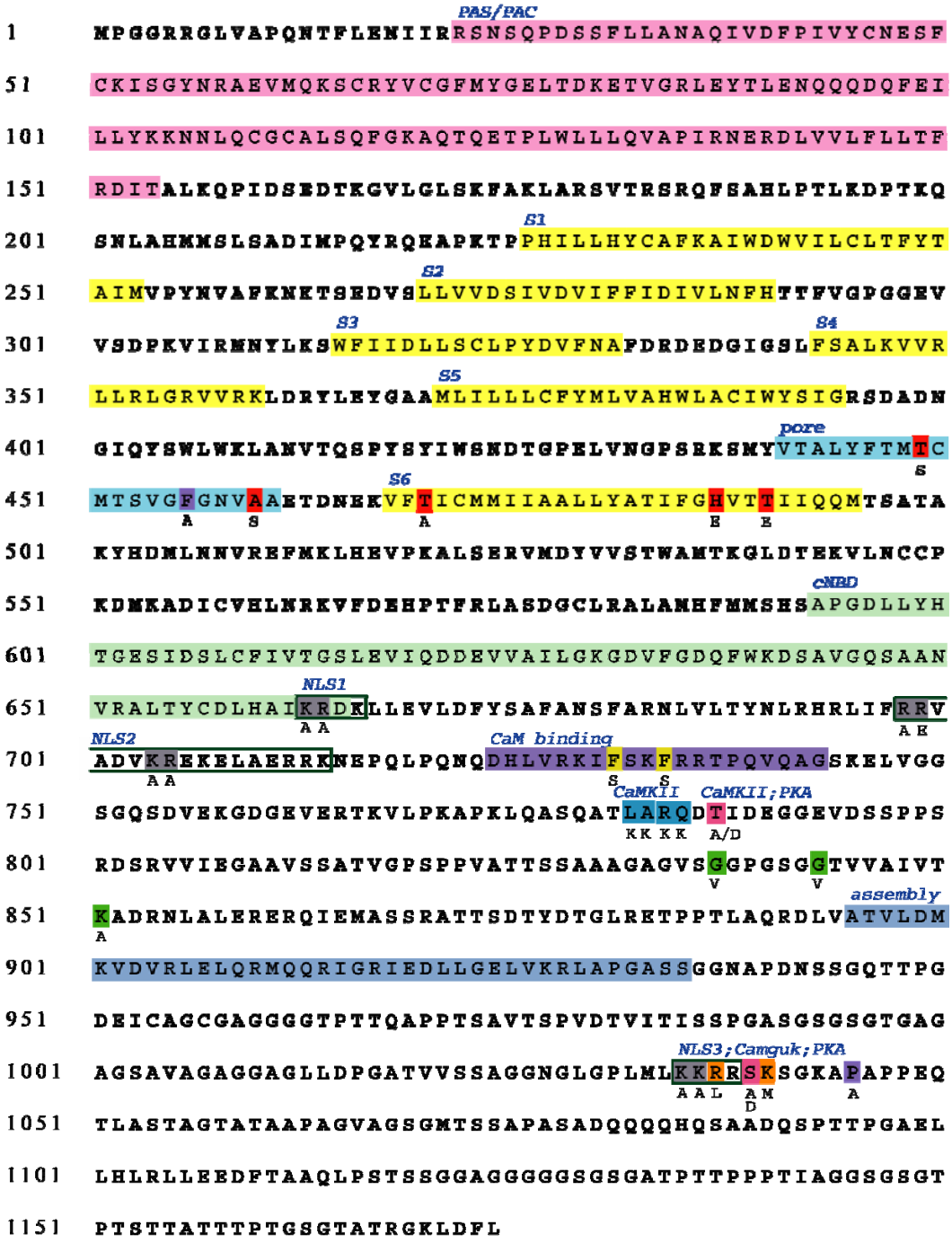

Figure 1.1: *Drosophila* EAG amino acid sequence. Regions of interest are highlighted in color: transmembrane domains are indicated in yellow, known and possible phosphorylation sites are in pink, putative nuclear localization signals are boxed and other domains discussed in text are labeled. Point mutations used throughout this thesis are specified below the respective amino acids.

hERG1 and the alternative transcript hERG1B (which lacks the N-terminal PAS domain) are expressed as a heteromeric channels on the plasma membrane of tumor cells (Crociani et al., 2003). Expression of both hERG isoforms is strongly cell cycle-dependent and blocking of hERG channels dramatically impairs cell growth of tumor cells. These results suggest that modulated expression of different K^+ channels is the molecular basis of a mechanism regulating neoplastic cell proliferation. As tumor progression often involves hypoxia (Guillemin and Krasnow, 1997), the PAS domain of hERG1 may sense environmental oxygen during hypoxic events by altering the heterotetrameric ratio of hERG1B to hERG1, thereby shifting the channel's activation curve to limit K^+ loss (Crociani et al., 2003). Incidentally, gating of hERG channels is modulated by the PAS domain, such that point mutations in the pore facing surface of the PAS domain slows the rate of activation (Morais Cabral et al., 1998; Gomez-Varela et al., 2002). Because the PAS domain is highly conserved throughout the EAG sub-family of channels, similar intramolecular interactions may occur in EAG channels.

The core of the EAG channel consists of four subunits each containing six helical transmembrane domains (S1-S6). A series of positively charged residues in S4 constitute the voltage sensor, and an additional hydrophobic domain between S5 and S6 contains the signature GFG motif that forms the K^+ ion selectivity filter. The S4 domain, which contains five equally spaced positively charged residues, moves in a twisting upward motion in response to depolarizing voltages (Silverman et al., 2003). In EAG, the conformational shifts during voltage sensing also affect the conformation of other transmembrane domains that are hypothesized to contribute to the gating canal through which the S4 domain moves. Using accessibility and perturbation analyses, Silverman et

al. found that activation increases both the charge occupancy and volume of S4 side chains in the gating canal and that mode switching between closed states is due to motion of the S2/S3 side of the gating canal. In addition, EAG gating is strongly regulated by Mg^{2+}. Mg^{2+} ions can bind to the pocket formed by S2, S3, and S4 (Silverman et al., 2004) and the transitional movements of S2 and S3 during depolarization underlie a Mg^{2+}-dependent shift in activation rates.

The essential function of the voltage sensor in ion channels is to respond to changes in electric potential and initiate conformational changes that result in the opening or closing of the pore. In K_v channels this signal is transduced to the pore by means of a linker in the cytoplasmic chain of amino acids between S4 and S5. Biophysical analysis of mutations in this region, as well as its crystallized structure, reveal that the S4-S5 linker both couples voltage sensor movement to pore gating and partially determines the kinetic properties that underlie gating (Sanguinetti and Xu, 1999; Long et al., 2005a; Long et al., 2005b). Experiments that specifically investigated the S4-S5 linker region of EAG show that it functions not only as a mechanical lever, but that specific interactions between the S4-S5 linker and the activation gate stabilize closed channel conformations (Ferrer et al., 2006). Thus, as observed for other K_v channels, interaction of S4-S5 linker with other regions contributes to the kinetic properties of EAG.

One of the most conserved, and therefore important, domains of EAG K^+ channels is the conduction pore (Christie, 1995). This domain consists of the S5 and S6 membrane spanning helices and the selectivity filter which connects the two. Most ion channels are thought to have a very similar pore structure where the selectivity filer dehydrates an ion, distinguishes it for atomic structure and size, coordinates it in a linear

progression across the hydrophobic membrane density, and rehydrates it, all at nearly diffusion-limited rates (MacKinnon, 2004; Long et al., 2005a; Long et al., 2005b; Valiyaveetil et al., 2006). The rest of the pore, consisting of the S5 and S6 helices, forms an inverted teepee structure that contains a water-filled cavity within the membrane near the filter (Doyle et al., 1998). These helices function to regulate conduction properties of the channel, and in the case of gated channels, act as a hinged gate that opens and closes the conduction pathway (Morais Cabral et al., 2001; Jiang et al., 2002).

As a channel transitions between closed and open conducting states, many voltage-sensitive and probabilistic changes occur that can affect the rate of opening and the duration of the open state. One well-studied intermediate state that is mechanistically distinct from either closed or open states is inactivation. Inactivated channels are non-conducting and can transition (referred to as recovery, from inactivation) to the open state or directly to the closed state. For many voltage-gated K^+ channels there are two types of inactivation, N-type and C-type, which differ in the underlying mechanism. N-type inactivation occurs by a "ball-and-chain" mechanism, in which the N-terminus of the protein behaves like a blocker tethered to the cytoplasmic side of the channel and directly occludes the pore (Zagotta et al., 1990; Demo and Yellen, 1991). A similar inactivation mechanism is also found in voltage-gated sodium (Na^+) channels in which a loop between domains III and IV acts as the "ball" (Yu and Catterall, 2003). In contrast, C-type inactivation is thought to occur by a structural collapse of the pore and selectivity filter and happens at a much slower rate than N-type inactivation (Demo and Yellen, 1991; Ogielska and Aldrich, 1999). EAG channels only exhibit C-type inactivation, and

EAG currents only partially inactivate, reaching steady state equilibrium of conduction during longer depolarizations (Robertson et al., 1996).

B3c. C-Terminus

As described earlier, the cytoplasmic C-terminus of EAG is unusually large for K_v channels and contains many putative regulatory regions which have been identified by homology to corresponding regions in other proteins. These putative regions include: a cyclic nucleotide-binding domain (cNBD), a subunit assembly domain, three nuclear localization (NLS) signals, a region with high similarity to the autoinhibitory domain of CaMKII, a CaM binding domain, several Src-Homology 3 (SH3) binding motifs, and numerous consensus sequences for phosphorylation. Additionally, there is a stretch of glycine residues with similarity to the conserved ATP-binding domain of known kinases (Hanks et al., 1988).

Although the cNBD of EAG has not been found to be functional in binding or regulation by cyclic nucleotides (Robertson et al., 1996; Frings et al., 1998), cAMP directly binds to hERG resulting in a hyperpolarizing shift in voltage-dependent activation (Cui et al., 2000). The cNBD of hERG also is important for proper cellular trafficking and protein expression. Removal of the entire cNBD prevents Golgi transit, surface localization and function of hERG channel tetramers (Akhavan et al., 2005). These trafficking defects are also found in other cNBD containing K^+ channels such as the hyperpolarization-activated cyclic-nucleotide-gated (HCN) and ERG3 channels (Akhavan et al., 2005). Therefore, the cNBD domain may be a general device used for proper trafficking, in EAG as well as other channels.

Because the core structure of K_v channels is so highly conserved, the possibility of promiscuous intermolecular multimerizations is quite high. Nonetheless, only certain heteromeric assemblies are favored. This is due to cytosolic assembly domains found in the majority of K_v channels. The assembly of K_v channel α-subunits is primarily mediated by a region within the intracellular amino-terminus known as the tetramerization domain (Li *et al.*, 1992; Shen *et al.*, 1993; Deal *et al.*, 1994; Hopkins *et al.*, 1994; Shen and Pfaffinger, 1995; Xu *et al.*, 1995). In contrast to most other K_v channels, the assembly domain of EAG channels is found in the C-terminus. A sequence of about 40 amino acids in the C-terminus is essential to produce functional tetrameric channels (Ludwig et al., 1997). Particularly, mutations in the first half of this domain greatly affect the homophilic interactions between each subunit's assembly domains. Because the cytosolic portions of EAG are more closely related to cyclic-nucleotide-gated cation (CNG) and plant inwardly rectifying K^+ channels than to other K_v channels (Baumann et al., 1994), and CNG channels also oligomerize via C-terminal domains (Zhou et al., 2004), this may be a common mechanism for these types of channels.

The other regions of the C-terminus, with possible important functions, including the NLS signals, the region with high similarity to the autoinhibitory domain of CaMKII, the calmodulin binding domain, the SH3 binding motifs, and phosphorylation sites will be discussed in more detail later, as they are key to the central topics of my thesis.

C. FUNCTION OF EAG K^+ CHANNELS

C1. Roles of K^+ channels

The fact that there are many more genes encoding K^+ channels than Na^+ and Ca^{2+} channels has led to the suggestion that K^+ channel diversity is a large determinant of the diversity in neuronal firing patterns, action potential shape, and response properties in neurons and muscle fibers. Although exciting new roles of K^+ channels have recently been elucidated (such as conduction-independent cell signaling), there are four main roles of K^+ channels in excitable neuronal cells: setting and maintaining the resting membrane potential, repolarizing the membrane potential during action potentials, hyperpolarizing the membrane after action potentials, and regulating the amount of back-propagation of sub-threshold dendritic potentials. The contribution of a given K^+ channel to these functions depends largely on its current properties, namely, the mechanism of activation (opening), how rapidly the channel activates once the activation criteria have been met, and inactivation and deactivation (closing) which determine how long the channel stays open once activated.

C1a. Resting potential

The flux of K^+ ions across the membrane is the main force setting the membrane potential in both neuronal and non-neuronal cells. The concentration gradient of K^+, which is maintained by the Na^+-K^+ ATPase pump, is the driving force behind this movement of charge. The identity of the channels mediating the background flow of K^+ ions continues to be a matter of some debate. K^+ channels known to control resting membrane potential include the K_{ir} leak channels and the 4 TM/2 pore channels (Gutman et al., 2005). To contribute to the resting potential, a K^+ channel must be open at the resting potential and should not inactivate completely. In neurons, which typically have a

resting potential of -60 to -80 mV, most K_v channels do not appear to meet this basic criterion, because the voltage at which they activate is more positive than the resting potential. However, K_v channels can contribute to the resting potentials of non-neuronal cells which typically exhibit a more depolarized resting potential (~ -30 mV) (Kandel et al., 2000). In addition, some K_v channels could theoretically contribute to K^+ flow at rest, even when they are predominantly closed due to probabilistic transitions between open and closed states. Although the extent of the K_v channel contribution to resting potential remains to be seen, an example is the modified dORK channel which has been used to electrically silence various *Drosophila* CNS neurons *in vivo* by decreasing the input resistance and driving the membrane potential more negative by dozens of mV (Nitabach et al., 2002).

C1b. Action potential repolarization

When extracellular neurotransmitters bind to receptors on neuronal cell membranes this can result in dramatic changes in local ion conductivity causing either excitatory or inhibitory postsynaptic potentials (EPSPs or IPSPs). EPSPs generated at different synapses in the neuron integrate in distance and time to cause a depolarization that, if strong enough, will initiate an action potential by activating Na^+ (and Ca^{2+}) channels. Due to their slower rate of activation, K_v channels open later and begin attenuating the action potential. During this time, the Na^+ current also begins to decrease due to fast inactivation of Na^+ channels (Hille, 2001). K_v channels involved in action potential regulation have much slower inactivation and deactivation rates than Na^+

channels. Both the number of K^+ channels and the speed at which K^+ currents activate play an important role in determining the height and width of action potentials.

Three major classes of K_v currents have been described in mammalian neurons: rapidly inactivating (A-type), slowly inactivating, and non-inactivating currents (Hille, 2001; Hoshi et al., 1990). A-type and delayed rectifier currents play an important role in shaping action potentials during repolarization and in determining the duration of an action potential. Examples of this are the currents carried by $K_v1.2$ and $K_v1.4$ multimeric channels found in numerous parts of the brain (Sheng et al., 1993). These currents expressed in axons and nerve terminals also regulate neurotransmitter release. The non-inactivating outward currents modulate firing frequency upon receptor stimulation by neurotransmitters and/or regulate resting membrane potentials (Molleman et al., 1993).

C1c. After-hyperpolarization and firing frequency

At the end of an action potential Na^+ channels are inactivated, but some K^+ channels remain open, generating a significant outward current which hyperpolarizes the membrane to a potential that is more negative than the resting potential. This phase, referred to as the after-hyperpolarization, increases the magnitude of subsequent depolarizations required for initiating additional action potentials, and also speeds the recovery of Na^+ channels from the inactivated state. Which effect predominates will determine whether action potential firing frequency is increased or decreased, and depends on the characteristics of the K^+ channels involved , as well as the other ion channels present (McCormack and Bal, 1997). K^+ channels that contribute to the after-hyperpolarization are typically either non-inactivating K_v channels, or Ca^{2+}-activated

(K_{Ca}) channels like those found in the suprachiasmatic nucleus that modulate firing frequency and control circadian rhythms (Cloues and Sather, 2003).

C1d. Back-propagation and dendritic integration

The inactivation of Na^+ channels and the hyperpolarization caused by K^+ channels ensure propagation of the action potential away from the soma, down the axon and into nerve terminals where it can induce neurotransmitter release. However, unidirectional propagation of action potentials is not absolute. Action potentials initiated in the axon can subsequently invade the soma and dendrites, providing a retrograde signal informing synapses in the dendritic tree that an output has been generated by the neuron (Hausser et al., 2000). Down-regulation of somal and axonal K^+ channels can affect the extent to which back-propagation occurs. One known role of back-propagation is to trigger dendritic release of neurotransmitter. Action potential back-propagation is extremely effective in two neuronal types where this is known to occur: dopamine neurons of the substantia nigra and mitral cells of the olfactory bulb (Hausser et al., 2000; Chen et al., 1997; Bischofberger and Jonas, 1997). K^+ channels are also present in the dendritic arbors of neurons. Activation of EPSPs and other inward dendritic conductances can be balanced and shaped by outward conductances generated by dendritic K^+ channels. Dendritic channels regulate back-propagation into the dendritic tree and affect the integration of excitatory and inhibitory inputs (Hoffman et al., 1997; Roth and Hausser, 2001).

C2. Roles of EAG

After the *eag* gene was mapped and cloned (Drysdale et al., 1991;Warmke et al., 1991), heterologous expression studies indicated that EAG gives rise to a voltage-gated, outwardly-rectifying, partially inactivating K^+ current (Bruggemann et al., 1993). Although EAG is highly selective for K^+ ions, like many other K^+ channels, EAG is also slightly permeable to other monovalent cations with a preference of $K^+ > Rb^+ > NH_4 > Cs^+ >> Na^+ >> Li^+$. Single channel conductance is quite variable amongst K^+ channels, ranging from several hundred pS for Slowpoke (KCNMA1, the large conductance calcium-activated K^+ channel) to less than 2 pS for hERG. EAG has a relatively small single-channel conductance of 4.9 pS (Bruggemann et al., 1993). Intriguingly, although *eag*, *in vivo*, is predominantly found in neurons in both flies and mammals, an *eag* current has not been identified in central neurons. This is likely due, in part, to the absence of a specific pharmacological blocker of *eag* channels and the inaccessibility of most *Drosophila* neurons for intracellular recording. Thus, our understanding of the *in vivo* function of EAG has been limited to what can be inferred based on the phenotypes displayed by *Drosophila eag* mutants.

C2a. Traditional neuronal functions

A role for *eag* in neuronal function was first suggested by an ether-induced leg shaking phenotype associated with *eag*, as well as *Sh* and *Hk,* mutants (Kaplan and Trout, 1969; Warmke et al., 1991; Drysdale et al., 1991). This initial observation, along with later ones showing physiological and behavioral defects in *eag* mutants, demonstrates that the EAG channel is an important player in neuronal function.

Consistent with a role in controlling neuronal excitability, intracellular recordings from muscle fibers at the neuromuscular junction (NMJ) of *eag* mutant larvae exhibit spontaneous excitatory junctional potentials (EJPs) and larger EJPs in response to motor nerve stimulation (Ganetzky and Wu, 1983; Wu et al., 1983;Griffith et al., 1994). Simultaneous extracellular recordings of the motor nerve show parallel changes in motor neuron action potentials, indicating that the defects observed in muscle are primarily due to alterations in the excitability of the motorneurons, not muscle fibers. The resulting inference is that the current generated by *eag* channels contributes to the maintenance of the neuronal resting potential, action potential repolarization, and firing frequency. These roles are consistent with the properties of heterologously expressed *eag,* although the activation threshold of *eag* may be more depolarized than the resting potential expected for most neurons.

Although *eag* mutants have not been examined for plasticity defects at the larval NMJ, EAG has been shown to participate in mechanisms underlying neuronal plasticity in studies of the giant fiber escape pathway of *Drosophila*. The giant fiber escape pathway is an established model system for analyzing habituation and its modification by memory mutations in an identified neuronal circuit (Krasne and Teshiba,1995; Engel and Wu, 1996). Mutations of *eag* result in enhanced habituation as compared to both *Sh* and wild type flies (Engel and Wu, 1996). Alterations in habituation due to *eag* are as strong as those observed for the memory mutants *rutabaga* (*rut*) and *dunce* (*dnc*), genes that are involved in cAMP metabolism (Davis, 1996). Because habituation represents a change in neuronal responsiveness over time, channels contributing to habituation should confer prolonged modulatory effects. Unlike *Sh*, which has fast opening and closing kinetics,

EAG, has slower kinetics and may contribute more to the physiological mechanisms that underlie habituation and other components of behavioral plasticity.

In addition to the above defects in neuroexcitability and habituation, *eag* appears to be one of the few ion channel genes to exhibit learning defects (Grifffith et al., 1994). These defects were observed using a courtship conditioning paradigm. A courtship index can be constructed by measuring the duration of courtship activity by male flies directed towards female flies (Siegel and Hall, 1979; Griffith et al., 1993). Female flies that have been previously mated are no longer responsive to male courtship activity, and through behavioral and chemical cues indicate this to males. Therefore, wild type males flies learn to decrease their courting behavior. However, *eag* mutants are defective in this operant conditioning paradigm and exhibit an increase in courtship activity. As *eag* phenotypes become more pronounced amongst alleles, however, the ability to measure courtship decreases, due to increasing failure rates of initial conditioning. In other words, *eag* mutants show a significant correlation between severity in potassium conductance and courtship initial failure rates, such that courtship can be measured in weak alleles (i.e. eag^{4PM}, eag^{1} and eag^{1}) with decreasing ability for the null mutation (eag^{sc29}) (Zhong and Wu, 1991; Griffith et al., 1994). These series of observations strongly implicate *eag* in learning and memory. Weak alleles cause defects in memory and strong alleles appear to nearly abolish learning acquisition.

Recent studies have identified behavioral phenotypes associated with eag in other species. The *C. elegans* homolog of *eag*, called *egl*-2, is necessary for proper egg-laying and muscle contraction as well as chemotaxic behavior to volatile odorants (Weinshenker et al., 1999). A gain-of-function mutation in *egl*-2 blocks excitation in neurons and

muscles by causing the channel to open at inappropriately negative voltages. This mutant, as well as EGL-2-GFP conjugated protein expression, suggests EAG is present and functions in vulval muscles, chemosensory neurons, mechanosensory neurons and entertic muscles. Also, as indicated by the chemotaxic phenotype, it is possible that EGL-2 functions in sensory endings and is in fact a component of sensory transduction.

C2b. ERG and ELK channels

Although *eag* was the founding member of the EAG gene family, other members include *erg* and *elk* and each of these genes has unique properties and roles. In *Drosophila,* the gene encoding the ERG channel is called *seizure* (*sei*). Mutations of *sei* are characterized by a temperature-sensitive paralysis combined with hyperactivity in the flight motor pathway (Titus et al., 1997). In the human genome, there are three members of the ERG sub-family: hERG1, hERG2, and hERG3. These proteins are able to form heteromultimers amongst themselves (Wimmers et al., 2001); however, they do not multimerize with either EAG or ELK channels. *In situ* hybridization experiments show that the different *erg* subunits have overlapping expression patterns in several regions of the brain. All three transcripts are expressed in the olfactory bulb, and *erg1* and *erg3* are co-expressed in the reticular thalamic nucleus, cerebral cortex, cerebellum and hippocampus (Saganich et al., 2001). Heteromultimeric ERG channels result in larger current amplitudes upon both depolarization and repolarization (Wimmers et al., 2002). Thus, through heteromeric assembly, hERG channels may contribute significantly to different physiological functions such as modulation of action potential frequency and resting membrane potential.

The best known function of ERG is its contribution to the repolarization of the heart action potential via a current, known as I_{Kr}. Suppressing I_{Kr} function, due to either genetic defects in the *erg* subunit or adverse drug effects, can lead to long-QT (LQT) syndrome that carries increased risk of life-threatening heart arrhythmia and sudden death (Curran et al., 1995; Tseng, 2001). ERG-mediated currents have also been recorded in various types of other cells, such as neuroblastoma cells, smooth muscle fibers and neuroendocrine cells (Schwarz and Bauer, 2004). In these cell types ERG currents serve as threshold currents, which modulate cell excitability. In fact, there are various cell types which do not express classical inward rectifier channels, but instead express ERG channels. In these cells, because of its inward-rectifying properties, the ERG current likely contributes to the resting potential (Schwarz and Bauer, 2004).

Unlike most other K_v channels, ERG channels only exhibit small outward current upon depolarization, yet produces large tail currents when repolarized to negative potentials (Trudeau et al., 1995). This is the result of an inactivation mechanism that is more rapid than activation, which confers inward rectification properties on ERG (Schonherr and Heinemann, 1996; Smith and Yellen, 2002). The resulting inwardly rectifying current has important implications for ERG in cardiac tissue, where it functions alongside HCN pacemaker channels to regulate rhythmic contractions (Trudeau et al., 1995).

There is no known phenotype of *elk* in *Drosophila* or of the three *elk1*, *elk2* and *elk3* genes in mammals. However, because they are highly conserved across species (97% identity between mouse and human *elk1*) and are highly expressed in many tissues, it seems likely that important roles for these channels will be discovered (Ganetzky et al.,

1999). The current properties of heterologously expressed ELK channels differ depending on the isoform expressed. Although all channels are slowly activating, ELK3 currents, which are expressed throughout the human nervous system, are more EAG-like, but do not exhibit the Cole-Moore shift, where prepulse voltage affects outward current, characteristic of EAG currents (Engeland et al., 1998; Zou et al., 2003). ELK2 currents share properties displayed by both EAG and ERG, producing large outward currents, that then rapidly inactivate (Trudeau et al., 1999). This inactivation mechanism is similar to that of ERG, but shifted to more positive potentials, accounting for the delayed inactivation upon depolarization (Engeland et al., 1998). Finally, ELK1 also gives rise to a slowly activating potassium current accompanied with slow deactivation kinetics. In fact, ELK1 activates too slowly ($\tau_{activation}$ of 676 ms at 0 mV) to affect the shape of the action potential (Shi et al., 1998), but could potentially lengthen after-hyperpolarizations to slow action potential firing frequencies.

C2c. Sensory functions of EAG

In multicellular organisms, sensory perception relies on cells with specialized sensory receptors and transduction components that integrate those incoming signals so they can be directed into ascending pathways and allow for higher order neural processing. A role for EAG channels has been suggested in several sensory systems, including those involved in olfaction, hearing and phototransduction.

Ion channels are essential for odor transduction. These can be analyzed in patches of membrane from the cilia emanating from the distal end of the olfactory receptor neuron's single dendrite. Single-channel patch recordings of this membrane have shown

that a cyclic nucleotide-gated channel is the conductance pathway for the odor-elicited current underlying olfaction (Firestein et al., 1991). Due to the fact that EAG contains a cyclic nucleotide binding domain (cNBD), *Drosophila eag* mutants have also been examined for defects in olfaction. Three independent alleles of *eag* all showed reduced antennal responsiveness to a subset of common odorants having short aliphatic side chains (Dubin et al., 1998). Focal application of high K^+ saline to sensillae alters the excitability of the majority of neurons from wild-type, but not *eag*, antennae, suggesting that EAG may have a dendritic localization in olfactory neurons. Because *eag* also is expressed in the olfactory bulb of rats, a role for EAG in olfaction may be conserved among species (Ludwig et al., 1994).

EAG channels may also contribute to auditory transduction in the cochlea. The inner ear's receptor organ, where mechanically sensitive hair cells are located, is the organ of Corti. A positive endocochlear potential and a high K^+ concentration (150-180 mM) in the endolymph surrounding this structure is essential to sound transduction. This high K^+ gradient has been thought to be produced by a collaboration of the Na^+-K^+-ATPase and gap junctions found in tissue near this organ (Crouch et al., 1997). However, *eag* is also expressed in cochlear regions and, therefore, may also contribute to K^+ cycling. Rat *eag* mRNA is detectable in the organ of Corti and in the fibrocytes of the spiral ligament but not in the spiral prominence or stria vascularis (Lecain et al., 1999). The expression pattern of the rat *eag* transcript in the spiral ligament is complementary to the Na^+-K^+-ATPase distribution in the cochlear lateral wall, indicating that *eag* may be expressed in the corresponding cells. Although no genetic deafness or other hearing impairments have yet been linked to the human *ea*g gene, the expression pattern of *eag*

suggests that additional studies may uncover a role for this channel in auditory transduction.

Along with odor and sound transduction, *eag* also may play a role in phototransduction. In rod photoreceptors, the depolarizing current, also known as the dark-current, is carried by Na^+ ions and flows into a photoreceptor cell when unstimulated. This dark-current is mediated by cGMP-gated cation channels. Completing this current loop is another channel that carries an outward K^+ current, named I_{Kx}, which figures prominently in setting the dark resting potential and accelerates the voltage response to small photocurrents (Beech and Barnes, 1989). I_{Kx} is a non-inactivating K^+-selective current that is activated at potentials positive to -50 mV, very similar to EAG currents. *In situ* hybridization of bovine retinal tissue localizes two EAG channel transcripts (*beag1* and *beag2*) to photoreceptors and retinal ganglion cells (Frings et al., 1998). Comparison of bEAG currents with I_{Kx} reveals an intriguing similarity, suggesting that EAG polypeptides are involved in the formation of K^+ channels mediating the outward dark-current of photoreceptors. Small differences in heterologously expressed current profiles, such as faster deactivation in bEAG channels than in I_{Kx}, suggest the existence of unknown endogenous auxiliary subunits that may change EAG gating properties in native retinal cells.

C2d. EAG as a signaling molecule

The phenotypes of mutants and functional *in vivo* properties of EAG channels all support the argument for a classical role in neuronal function through ion conduction. However, there is growing evidence that EAG also may have a role in cell-cycle

regulation and proliferation. Although the role of EAG in these processes has typically been interpreted in terms of the K^+ current generated by EAG channels, findings by myself and others in the Wilson lab suggest that some of these effects may be mediated a conductance-independent effect of EAG on intracellular signaling pathways (presented in Chapter IV and the Appendix). Here I intend to relate: i) how other ion channels can influence the cell cycle, ii) EAG's effect on proliferation and the cell cycle, and iii) the initial *in vitro* observation of a conductance-independent effect of EAG on intracellular signaling pathways.

C2d.i. Other channels that influence cell cycle. Several classes of ion channel have been found to regulate cell proliferation (Allen et al., 1997; Cahalan et al., 2001; Kaczmarek, 2006). However, it appears that predominantly K^+ channels have been implicated in contributing to the control of cell cycle progression of both normally proliferating (e.g., lymphocytes, Schwann cells and glia) and abnormally proliferating (transformed) cell types (Chandy et al., 2004; Pardo, 2004; Vautier et al., 2004; Wilson and Chiu, 1993). Inhibition of some K_v channels through the use of blockers efficiently decreases proliferation in immune cells and cancer cells (Wonderlin and Strobl, 1996; Guo et al., 2005). For example, the activity of $K_v1.3$ in T-lymphocytes is responsible for the initiation of cell cycle progression in response to antigen presentation (Price et al., 1989; Freedman et al., 1992; Lin et al., 1993). Although other types of K^+ channels are involved in sustaining lymphocyte proliferation, $K_v1.3$ is highly expressed in these cells, and its activation is considered a key step in the immune response (Ullrich, 1999; Chandy et al., 2004; Lewis and Cahalan, 1995). There are also numerous examples of K^+ channels associated with the proliferation of transformed cells. K2p9.1 is expressed in

approximately 40% of breast cancers (Mu et al., 2003), K_v10.1 (the mammalian EAG homolog) expression is elevated in neuroblastoma, melanoma, breast carcinoma and cervical cancer cells (Farias et al., 2004; Meyer and Heinemann, 1998; Meyer et al., 1999; Pardo et al., 1999), and K_v11.1 is found in endometrial tumors, leukemias, and colon cancer (Cherubini et al., 2000; Lastraioli et al., 2004; Pillozzi et al., 2002). Although an exact molecular identification has not been made, suppression of a K_v channel with 4-aminopyridine (4-AP), barium and TEA inhibited both EGF- and insulin-stimulated myeloblastic leukemia ML-1 cell proliferation (Xu et al., 1996; Wang et al., 1997; Guo et al., 2005). Both MAPK/ERK and Akt pathways are stimulated in this growth phenotype and treatment of ML-1 cells with 4-AP potently prevents phosphorylation of Erk1/2 and Akt. This suggest that a 4-AP-sensitive K^+ channel plays an important role in controlling proliferation of ML-1 cells by affecting the activation of multiple insulin-dependent signal transduction processes (Guo et al., 2005). Although less sensitive to 4-AP than other K_v channels, a candidate molecule underlying this cell-cycle regulation may be EAG.

C2d.ii.EAG's affect on cell cycle and proliferation. The induction of differentiation in human myoblasts is partially controlled by the expression of two different hyperpolarizing currents, one of which is carried by EAG (Bauer and Schwarz, 2001). Undifferentiated myoblasts have a resting membrane potential of about -10 mV, which upon onset of differentiation it driven to about -30 mV by the transient expression of a non-inactivating K^+ current $I_{K(ni)}$, carried by human EAG1 channels (Bijlenga et al., 1998; Occhiodoro et al., 1998; Liu et al., 1998). Subsequently, as myoblasts reach fusion EAG1 expression decreases and the resting membrane potential is further hyperpolarized

by inwardly-rectifying K^+ channels to about -70 mV. This transient expression of EAG current partially explains why EAG is not found in adult skeletal muscle and indicates transient EAG expression is a cell cycle-related phenomenon, since myoblast fusion is commiserate with irreversible cell-cycle arrest (Bauer and Schwarz, 2001).

The example above illustrates that EAG currents can control cell-cycle processes. Conversely, cell-cycle progression also affects EAG current. When EAG is heterologously expressed in *Xenopus* oocytes, which are physiologically arrested in G2 during the first meiotic division, subsequent activation of mitosis-promoting factor (MPF) both relieves this arrest and reverses the rectification properties of EAG currents (Bruggemann et al., 1997). Under these conditions, at membrane potentials greater than +40 mV, EAG current starts to inwardly rectify. This unusual effect is due to intracellular Na^+ block of the channel pore, similar to an effect observed during the M phase in mammalian cells (Pardo et al., 1998). The application of nocodazole or colchecine, drugs that disrupt microtubules, similarly affect the rectification of EAG in inside-out patches (Camacho et al., 2000), suggesting that interactions with cytoskeletal elements during the M phase may underlie EAG's involvement in proliferation (Pardo et al., 2005).

Further support for a role of EAG in cell growth and differentiation, has been obtained in experiments showing that faulty regulation of *eag* expression leads to detrimental effects. Although preferentially expressed in the nervous system (Ludwig et al., 1994; Ludwig et al., 2000), *eag* also is observed in many human somatic cancers, while absent from the corresponding healthy tissues. These include breast carcinoma lines (MCF7, EFM-19 and BT-474), cervical carcinoma (HeLa) and neuroblastomas

(Pardo et al., 1999; Meyer and Heinemann, 1998), melanomas (Meyer et al., 1999), and gliomas (Patt et al., 2004). In addition, when expressed in some mammalian cell lines, human EAG (hEAG) confers oncogenic properties such as loss of contact inhibition, substrate independence, and increased proliferation (Pardo et al., 1999). Moreover, *eag*-transfected CHO cells result in tumor growth when transplanted into immune-suppressed mice. These findings have made EAG a promising target for novel cancer drugs, as well as a potential marker for early tumor detection and diagnosis (Pardo et al., 2005).

The apparent proliferative/cell-cycle functions associated with EAG channels may be conserved in other EAG sub-family members since the related channel hERG also appears to be correlated with cell-cycle regulation. hERG channels are overexpressed in primary cultures of myeloid leukemia, endometrial tumors and colon cancer cells (Cherubini et al., 2000; Pillozzi et al., 2002; Lastraioli et al., 2004). hERG current is detected in numerous tumor cell lines from human and murine sources, including neuroblastoma, adenocarcinoma, pituitary tumors, monoblastic leukemia and insulinoma β-cells (Bianchi et al., 1998). The resting potential of cycling neuroblastoma cells shifts in response to changes in voltage-dependence of activation for hERG channels (Arcangeli et al., 1995; Meyer and Heinemann, 1998) and inhibition of hERG decreases proliferation of neuroblastoma cells (Crociani et al., 2003). Tumor cells expressing hERG may have a selective advantage in surviving the ischemic environment that is typical of tumors. hERG may be contributing to oncogenesis by maintaining hyperpolarized resting potentials and enhancing proliferation (Bianchi et al., 1998). Another study suggests that hERG affects tumor growth by promoting the membrane

surface expression of tumor necrosis factor receptor 1 (TNFR1), which enhances TNFα-stimulated tumor proliferation (Wang et al., 2002a).

C2d.iii. A conductance-independent effect of EAG on intracellular signaling pathways. The traditional manner in which ion channels are believed to influence cellular properties is through their function of ion conduction. However, there is growing evidence that ion channels have important functions that are independent of their conduction properties. These multifunctional channel subunits include: TRP channels, voltage-gated Ca^{2+} channels, voltage-gated K^+ channels, K^+ channel subunits ($K_v\beta1$, $K_v\beta2$, MPS-1, Slob, KChIP1-4) and Na^+ channel subunits β1-β4 (Kaczmarek, 2006). Work by Andrew Hegle and myself from the Wilson lab (presented in Chapter IV and Appendix) indicates that EAG also has a role, independent of conduction, of an upstream regulator of intracellular signaling pathways.

Initial indications that EAG might directly regulate intracellular signaling pathways came from experiments showing that transfection of NIH 3T3 fibroblasts with *Drosophila eag* resulted in a significant increase in proliferation, as measured by cell counts and 5-bromo-2'-deoxyuridine (BrdU) incorporation. Expression of Sh, the prototypical K_v channel, did not increase proliferation, suggesting that the effect is specific to EAG. Previous studies have reported that K^+ channels are able to indirectly influence intracellular signaling by changing the membrane potential, thereby controlling Ca^{2+} influx through voltage-dependent Ca^{2+} channels and leading to activation of several intracellular signaling pathways (Sheng et al., 1990; Rosen et al., 1994; Lewis and Cahalan, 1995). However, extracellular application of EGTA, a Ca^{2+} chelator, did not affect EAG-stimulated proliferation, suggesting the effect is not due to altered Ca^{2+}

influx. More importantly, transfection with *eag-F456A*, a non-conducting EAG channel containing a point mutation in its selectivity filter (Heginbotham et al., 1994), caused the same amount of proliferation as observed following transfection of the *wild type* channel, further indicating that the EAG effect was not a secondary effect of K^+ flux.

Because the proliferative effect of EAG is independent of the conduction of K^+ ions, changes in extracellular K^+ concentrations ($[K^+]_o$) should have no effect on EAG-induced proliferation. Contrary to this expectation, however, Hegle, et. al. (2006) found that small increases in $[K^+]_o$ inhibited EAG-induced proliferation, while having little effect on vector-transfected controls. This observation led to the hypothesis that the voltage sensor of EAG channels regulates the interaction of EAG with intracellular signaling pathways. The hypothesis was tested using mutations that shifted the voltage-dependence of EAG channels. Two mutants, EAG-TATSSA (T449S/K460S/T470A) and EAG-HTEE (H487E/T490E), which when coupled with the F456A selectivity filter mutation increase the proportion of channels in the open state, both inhibited the proliferative effect of EAG channels. Together, these results suggested a novel role for the voltage sensor of EAG channels in an interaction of the channel with intracellular signaling pathways. Further investigations of this role of EAG presented in this thesis include: mapping the domain by which EAG regulates this signaling pathway, identifying the binding proteins that initiate the pathway, and characterizing the *in vivo* function of EAG-induced signaling.

C3. Distribution and localization of EAG

Proper tissue and cellular localization is essential for the correct function of proteins, including ion channels. *Drosophila* EAG is expressed in the axons and terminals of motor nerves innervating larval body wall muscle fibers and also is widely expressed in the larval and adult nervous system as indicated by immunocytochemistry (Wang et al., 2002b; Sun et al., 2004). When tissue from 3rd instar larvae is stained using an anti-EAG antibody, EAG channels are primarily found in neuropil and axonal tracts (Sun et al., 2004). In the ventral ganglion, EAG is specifically localized to neuronal synapses, as determined by comparison to the expression pattern of transgenic synaptobrevin. This is confirmed by further immunostaining studies of EAG channels at the NMJ (Wang et al., 2002b). When probed using a phosphospecific antibody, EAG is clearly seen in the axon and terminal arborizations of larval motor neurons.

Another method in determining EAG distribution is probing phenotypic changes after expressing dominant-negative EAG in *Drosophila* (Broughton et al., 2004). When a cytosolic fragment of EAG, which is thought to block proper EAG channel assembly, is expressed under the control of several Gal4 drivers, altered courtship behaviors are exhibited by flies. For example, the MJ286 and MJ164 drivers express in the dorsal region of the lateral protocerebrum and the MJ63 driver express in the ventral and posterior regions. Dominant-negative expression of EAG in these regions affects behaviors such as courtship initiation and duration. This strongly suggests that these regions likely express EAG channels and that lack of endogenous EAG function there causes specific behavioral defects. Importantly, however, the means by which this EAG fragment exerts its effects is not clear. The fragment used has not been verified to have a

direct dominant-negative effect on EAG current (Broughton et al., 2004), thus these findings may be due to loss of EAG current, or due to some other unknown mechanism.

In mammals there are two *eag* genes: *eag1* and *eag2* (also known as KCNH1 and KCNH5, respectively). The distributions of these two genes, as determined by Northern blotting and *in situ* hybridization in rat tissue, are similar but not entirely overlapping (Ludwig et al., 2000; Saganich et al., 2001). *eag* mRNA is absent from lung, kidney, liver, muscle and heart tissue, however, it is strongly expressed in brain. Rat *eag1* and *eag2* are both highly expressed in the olfactory bulb, neocortex, hypothalamus and hippocampus. *eag* is absent or only slightly expressed in a few regions such as the substantia nigra and trapezoid body. Other portions of the brain are enriched for either one or the other *eag* transcripts. *eag1* is preferentially expressed in the basal ganglia and granule cell layer of the cerebellum, while *eag2* is comparatively enriched in the thalamus, inferior colliculus and many lower brainstem nuclei (Ludwig et al., 2000; Saganich et al., 2001).

Using antibodies directed against individual EAG proteins, EAG expression in the hippocampus has been examined at the cellular and subcellular level. Both *eag1* and *eag2* are expressed in the stratum pyramidal layer of the CA3 region of rat hippocampal slices, which corresponds to the cell bodies of principal neurons (Saganich et al., 2001; Jeng et al., 2005). EAG1 channels are found in both hippocampal somas and neuropils (the regions of unmyelinated neuronal axonal and dendritic processes); suggesting EAG1 is broadly expressed throughout neuronal cells. On the other hand, EAG2 is largely localized to the soma of hippocampal cells, with few EAG2 channels found in the neuropil. Using axonal and dendritic markers, it has been shown that both EAG1 and

EAG2 are only found in somatodendric compartments and not in axons of rat hippocampal neurons. Moreover, the dendritic staining of EAG1 is specifically localized to glutamatergic, and not GABAergic, synapses (Jeng et al., 2005). This suggests that rat EAG1 K^+ channels may modulate the postsynaptic signaling of glutamatergic synapses. Conversely, immunohistochemical staining for EAG at the *Drosophila* larval NMJ (also a glutamatergic synapse) indicates EAG is expressed in the axon and terminal boutons of motor neurons (Wang et al., 2002b). Therefore, EAG may have different physiological roles in different species.

C4. Pharmacology of EAG

In the absence of a specific pharmacological blocker for EAG channels, the most distinguishing characteristic permitting identification of EAG channels, is their slowed current activation in response to negative prepulses (Ludwig et al., 1994; Robertson et al., 1996). This phenomenon is termed a Cole-Moore shift, after the properties affecting K^+ currents found in the squid giant axon (Cole and Moore, 1960) and is not known to be present in any other K_v channel. This voltage-dependent effect on activation kinetics is enhanced by increasing extracellular Mg^{2+} or H^+ concentrations (Terlau et al., 1996). The divalent cations Mn^{2+} and Ni^{2+} can also substitute for Mg^{2+} in altering voltage-dependent kinetics of EAG, but with differing effective concentrations (two-fold more and 30-fold less, respectively) (Meyer and Heinemann, 1998; Silverman et al., 2004). The binding site for Mg^{2+} has been mapped to negatively charged side chains within S2 and S3 that appear to also coordinate the charged residues with the S4 voltage-sensor as it passes through the membrane during activation (Silverman et al., 2000). The effect of

differing Mg^{2+} concentrations on kinetic properties suggests that each subunit of the putative tetrameric channel binds a Mg^{2+} ion (Frings et al., 1998). This binding has been shown to affect the cooperativity of the S4 sensors that leads to opening of the channel gate.

Channel blockers have been quite useful in identifying the genes underlying currents *in vivo* and in investigating the biophysical characteristics of K^+ channels. Investigation of isolated currents and blocked transitions allow for better models of channel kinetics and structure. There are two types of blockers of voltage-gated K^+ channels that act extracellularly: positively charged organic compounds and peptide toxins (Pongs, 1992). Among the most widely used organic blockers are the quaternary ammonium blockers. For example, tetraethyl-ammonium (TEA) binding blocks Sh channels and slows its C-type inactivation (MacKinnon and Yellen, 1990; Andalib et al., 2004). Quaternary ammonium blockers can also block K^+ channels intracellularly by interacting with distinct pore residues unrelated to the external binding sites. This type of blocker includes TEA, 4-aminopyridine (4-AP), quinine and quinidine. Unlike most known K^+ channels, EAG channels are comparatively resistant to 4-AP (IC_{50} of >100 mM compared to Sh, IC_{50} 5.5mM) (Bruggemann et al., 1993). There are no known EAG-selective toxins or agents that are able to completely block EAG currents that would allow for pharmacological isolation of EAG currents from other K^+ currents. However, although its affect on EAG channels has not been studied, the scorpion toxin CnErg1 is capable of a high-affinity partial block of the hERG channel (Corona et al., 2002; Hill et al., 2007).

EAG currents are also sensitive to other compounds, ions, and drugs that can

affect ion channels. The divalent cations Ba^{2+} and Zn^{2+} inhibit EAG currents by enhancing inactivation (Terlau et al., 1996; Ludwig et al., 1994). The tricyclic antidepressant imipramine and the antihistamine astemizole block the *C. elegans* homolog of EAG, EGL-2 (Weinshenker et al., 1999) as well as hEAG1 channels. In culture, these compounds can reduce the proliferative effects of EAG currents in cancer cells (Gavrilova-Ruch et al., 2002; García-Ferreiro et al., 2004). The non-specific antiarrythmic drugs clofilium and LY97241 are able to block EAG currents in a time-, use- and voltage-dependent manner, characteristics of open-channel blockers (Gessner and Heinemann, 2003). This mechanism is also supported by functional assays from EAG channels with mutated pore sites for other blockers such as MK-499, terfenadine, quinidine, and tetrabutylammonium (Gessner et al., 2004).

The antiarrhythmic drug dofetilide has little effect on EAG currents, but dofetilide does display high affinity binding to hERG. The gating properties of EAG can be altered by point mutations within the pore that make bovine EAG function more like hERG (Ficker et al., 2001). These mutations also confer dofetilide sensitivity onto bEAG channels, suggesting that the structures involved in gating also contribute to the pharmacological sensitivity of the channel. Importantly, a homologous mutation in the pore region (TAT/SSA) was used to alter *Drosophila* EAG channel activation to study the voltage-dependence of EAG signaling (Hegle et al., 2006), although the effects on dofetilide sensitivity have not been investigated. Additionally, EAG current in both heterologous and native tissue can be blocked by increases in intracellular Ca^{2+} concentrations (Stansfeld et al., 1996; Meyer et al., 1999), due to a C-terminal interaction between EAG and Ca^{2+}-bound CaM (Schonherr et al., 2000; Ziechner, 2006). This

interaction is essential to the regulation of EAG channel and is discussed in detail later.

D. MODULATION OF EAG

Although basic properties of EAG and other ion channels can be best understood by reductionist experiments, in order to fully appreciate the role they play in intercellular communication it is important to investigate how they are regulated and modulated by other proteins, especially those that are activity-dependent. The molecular mechanisms underlying learning and memory are believed to involve plasticity of synaptic connections. At the functional level, this is accomplished when: synaptic contacts are either strengthened or weakened by changing presynaptic activity, neurotransmitter release is modified, or postsynaptic receptivity and the resulting neuronal responses are altered. At the structural level, long-term changes typically involve the addition or retraction of synaptic contacts between neurons. In short, synaptic transmission is dynamic and tightly regulated by activity-dependent processes.

D1. Types of synaptic plasticity

Several types of synaptic plasticity have been identified and characterized. These include facilitation, post-tetanic potentiation (PTP), long-term potentiation (LTP), long-term depression (LTD), and homeostasis. Prior activity can enhance (i.e., facilitation, PTP, LTP), reduce (LTD), or maintain (homeostasis) the level of communication between neurons. Both pre- and postsynaptic changes underlie plasticity; which mechanism predominates depends on the specific neurons under investigation. Because

ion channels are essential to neuronal transmission, here I describe several ways in which channel modulation contributes to these types of plasticity.

D1a. Facilitation

Synaptic strength is highly dependent on the presynaptic pattern of activity. Due to synaptic plasticity, multiple presynaptic actions do not necessarily result in identical neurotransmitter release (Xu-Friedman and Regehr, 2004). Several distinct mechanisms contribute to presynaptic plasticity including facilitation and presynaptic depression. Facilitation enhances the postsynaptic current evoked by the second of two closely spaced presynaptic action potentials. Facilitation persists for about 100 ms, but exponential fitting of facilitation decay suggests that it may best be described as a rapid phase lasting tens of milliseconds, followed by a slower phase lasting hundreds of milliseconds (Zucker and Regehr, 2002). Facilitation is produced by the build-up of Ca^{2+} in the presynaptic terminal during synaptic activity (Delaney and Tank, 1994). Ca^{2+} levels are raised as the first stimuli opens voltage-gated Ca^{2+} channels, causing Ca^{2+}-dependent release of neurotransmitter (Xu et al., 2007). However, residual Ca^{2+} persists at the terminal, and when a second action potential arrives, this Ca^{2+} enhances the probability of neurotransmitter release.

Along with facilitation there are other similar phenomena that increase presynaptic output. In response to a high frequency train of stimuli, enhanced synaptic strength can occur for durations lasting from seconds to even minutes (Zucker and Regehr, 2002). These have been termed augmentation and post-tetanic potentiation (PTP), with the duration of augmentation being shorter than PTP. These processes can be

differentiated by differing rates of Ca^{2+} reuptake and vesicular turnover (Stevens and Wesseling, 1998). Both of these mechanisms appear to be caused by the same residual Ca^{2+} that is responsible for facilitation, the difference coming from different exocytotic replenishment and recovery processes (Gomis et al., 1999; Narita et al., 2000).

Even short term alterations in synaptic plasticity, such as facilitation, have been associated with defects in learning and memory. The *Drosophila* mutants *rut* and *dnc* have defects in learning, as well as NMJ synaptic transmission and cAMP metabolism (Zhong and Wu, 1991). Compared to controls, these mutants show increased excitatory junctional current (EJC) amplitudes in response to single stimuli, indicating a presynaptic effect. Also, repetitive stimulation does not increase the amplitude of subsequent EJCs, indicating impaired facilitation. Tetanus protocols in these mutants do not elicit persistent responses, implying PTP is defective as well. How cAMP and its effects on facilitation at the NMJ are involved in plasticity is not clearly understood, but almost certainly these defects are related to the plasticity necessary at central synapses important for learning and memory (Davis, 1996).

K^+ channels have been shown to influence facilitation in differing ways. Pharmacological inhibitors used to block K^+ channel currents can affect facilitation at the *Drosophila* NMJ (Wu et al., 1989). On the other hand, other channels, such as the $K_v2.1$ channel, appear to modulate facilitation by interacting with the secretory protein syntaxin, and facilitation occurs even after disruption of pore function (Singer-Lahat et al., 2007). Here, direct association of $K_v2.1$ with syntaxin promotes exocytosis and facilitation. Interestingly, motor end-plates of *Sh* larvae lack post-tetanic potentiation (PTP), but facilitation is not impaired (Delgado et al., 1994).

D1b. Long-term potentiation and long-term depression

Hebbian theory of learning and memory proposes that an increase in synaptic efficacy arises from the presynaptic cell's repeated and persistent stimulation of the postsynaptic cell (Hebb, 1949). This increase in activity enhances the effectiveness of subsequent stimuli and strengthens the circuit. One cellular corollary of this model which is thought to contribute to learning and memory formation is long-term potentiation (LTP). In 1973 Blis and Lømo found that each of the major pathways in the hippocampus (perforant, mossy fiber, and Schaffer collateral) is very sensitive to the history of previous stimuli (Bliss and Lømo, 1973). A brief, high-frequency train of stimuli to any of the three pathways increases the amplitude of the EPSPs in the target hippocampal neurons. The mechanisms causing this are different in each pathway, but this enhancement of synaptic transmission in each has been entitled LTP.

LTP has different phases, depending on the strength of the stimuli. Early LTP lasts for one to three hours and is believed to be caused by immediate pre- or postsynaptic changes such as a change in the mode of glutamate release, an increase in the number of vesicles released, increased kinase activity, addition of active glutamate receptors and formation of new synapses (Lisman and Raghavachari, 2006). Stronger stimuli can induce the more persistent phase of late LTP that lasts for at least 24 hours. Late LTP activates the cAMP-PKA-MAPK-CREB signaling pathway resulting in the synthesis of new mRNA and protein (Lüscher et al., 2000). Both of these phases establish a stronger

synapse in response to increased activity, suggesting LTP may model learning operations at the molecular level (Malenka and Bear, 2004; Barco et al., 2006).

LTP is believed to increase synaptic efficacy. Conversely, other mechanisms, such as external Ca^{2+} depletion, vesicle depletion, postsynaptic receptor desensitization and long-term depression (LTD), weaken synaptic transmission. Of these, LTD, studied as a complement to LTP, has been of most interest to investigators. LTD was first identified in CA1 hippocampal slices when previously established LTP was effectively reversed with 1-5 Hz low-frequency stimulation (Lynch et al., 1977; Barrionuevo et al., 1980). Although this type of depotentiation may be different than other forms of LTD, it showed that synaptic connections can be weakened by reduced neuronal activity. Mechanisms of LTD differ, depending on the CNS region in which it occurs, but LTD is known to depend on the involvement of differing NMDA receptor subtypes, cannabinoids, and physiological stress (Massey and Bashir, 2007). One model of the LTD process requires NMDA receptor activation, postsynaptic Ca^{2+} influx and activation of a serine/threonine phosphatase cascade (Mulkey et al., 1994). LTD may have an independent role in learning and memory, or it may serve as an adjunct to LTP by enhancing the signal-to-noise ratio, renormalizing synaptic weights after LTP, or by deleting previously stored information (Massey and Bashir, 2007). Importantly, I have described these phenomena only as homosynaptic contacts; inhibitory interneurons or multiple synapses also contribute to the formation of LTP and LTD. As the intricacies of *in vivo* neuronal architecture are considered and included, the complexity of these models must also be increased appropriately.

D1c. Homeostasis

Counterbalancing the Hebbian forms of synaptic plasticity discussed above is an emerging narrative of synaptic stabilization, or homeostasis. Homeostatic forms of plasticity act to steady the activity of a neuron or neuronal circuit in response to perturbations, such as changes in cell size, synaptic numbers, or synaptic strength, which can alter excitability (Turrigiano, 2007). In the developing nervous system this is important; as new synapses are initiated, destabilizing mechanisms constantly change electrical activity and increase protein turnover (Turrigiano and Nelson, 2004). Regulating overall activity is essential in these possibly highly-active, forward feeding, recurrent circuits.

In central neurons, synaptic homeostasis has been described as "synaptic scaling." Scaling either increases or decreases the strength of all of a neuron's synaptic inputs as a function of activity, whereas other mechanisms of synaptic plasticity are synapse specific When the activity of cortical neurons is blocked in culture, the amplitude of miniature excitatory postsynaptic currents (mEPSCs) increases to compensate for the decreased input (Turrigiano et al., 1998). Conversely, blocking GABA (γ-aminobutyric acid)-mediated inhibition initially raises firing rates, but eventually mESPC amplitudes and firing rates return to normal. These changes are due to postsynaptic alterations in the response to glutamate and affect each synapse in proportion to its initial strength. Synaptic scaling helps to ensure that firing rates do not become saturated, and operates during developmental changes in the number and strength of synaptic inputs, as well as during potentiation and depression (Turrigiano et al., 1998). Scaling has also been observed at cortical synapses *in vivo* following sensory deprivation and is

developmentally regulated (Maffei et al., 2004), suggesting that it is important in regulating cortical excitability during activity-dependent development.

Homeostatic plasticity has been described in a variety of systems, however, the molecular signaling mechanisms have not been well identified (Turrigiano, 2007). For homeostatic plasticity, neurons need to sense activity, integrate this measure over time, compare the activity to a set point, and then adjust synaptic properties to re-establish the set point. This type of negative feedback is common to many biological processes (Davis, 2006), but how it is implemented in synaptic plasticity is unknown. Nonetheless, one of the best examples of synaptic homeostasis is illustrated at the *Drosophila* NMJ.

Initial observations at the NMJ found that reductions in glutamate receptor function or chronic hyperpolarization of the muscle lead to compensatory increases in neurotransmitter release (Paradis, et al., 2001). The time scale of the compensatory changes was initially believed to be in durations of days. However, more recent experiments show that increased neurotransmitter release can be initiated within minutes of pharmacological blockade of glutamate receptors and is independent of new protein synthesis (Frank et al., 2006). Interestingly, large depolarizations are not required, but rather a change in the efficacy of spontaneous quantal release events (mEPSPs) is sufficient to trigger the induction of synaptic homeostasis. Also, induction and expression of synaptic homeostasis are blocked by mutations in presynaptic voltage-gated Ca^{2+} channels (Frank et al., 2006). This strongly argues in favor of a retrograde or transsynaptic signal from the postsynaptic muscle to the presynaptic motorneuron in regulating homeostasis.

D2. Ca^{2+}-dependent regulatory mechanisms

Activity dependent changes in intracellular Ca^{2+} appear to be a necessary first step underlying most types of plasticity. Intracellular Ca^{2+} can be increased either by influx through voltage-gated Ca^{2+} channels or by release from intracellular stores. The level of Ca^{2+} within extracellular fluid is typically in the range of 1 mM. By contrast, the resting concentrations of intracellular free Ca^{2+} (~100 nM) is 10^4 times lower than that outside cells, providing the potential for the ready movement of Ca^{2+} into cells. Ca^{2+} can bind to effector proteins directly or its effects can be mediated by a variety of intracellular messengers, including CaM and CaMKII, which are discussed below. Ca^{2+} has a multitude of targets; differences in concentration requirements and temporal mechanisms underlying Ca^{2+}-dependent modulation appear to determine which effect predominates at a particular site.

D2a. Calmodulin

CaM is the best studied and prototypical example of the E–F-hand family of Ca^{2+}-sensing proteins. CaM senses increases in Ca^{2+} by binding the ions in one or all four of its EF-hand motifs. Two of each these domains are located in the N- and C-termini, each pair with differing binding affinities to Ca^{2+}. Depending on the Ca^{2+}-dependent conformation of CaM, it can interact with and modulate the activity of a large number of target proteins, including enzymes and ion channels (Chin and Means, 2000; Levitan, 2006). A common feature of the interaction of CaM with many ion channels is constitutive binding; this allows for the fast transduction of a change in Ca^{2+} into a modulatory effect upon the channel (Levitan, 1999).

Channels that CaM is known to interact with include cyclic nucleotide-gated channels, NMDA receptors, SK and IK Ca^{2+}-activated K^+ channels, Ca^{2+} channels, and Na^+ channels (Levitan, 2006). CaM participates in the Ca^{2+}-dependent inactivation of both voltage-gated Ca^{2+} channels and NMDA receptors. Because both of these channels conduct Ca^{2+}, by mediating their inactivation CaM acts as a negative feed back regulator of Ca^{2+} permeability (Lee et al., 1999). A similar result occurs when CaM binds to and activates SK and IK K^+ channels, a hyperpolarization that decreases Ca^{2+} influx (Fanger et al., 1999). On the other hand, there are also examples of CaM enhancing neuronal activity. Bound CaM participates in the facilitation of certain voltage-gated Ca^{2+} channels and produces both Ca^{2+}-dependent and Ca^{2+}-independent shifts in the voltage dependence of activation and inactivation of voltage-gated Na^+ channels (Zühlke et al., 1999; Young and Caldwell, 2005). Therefore, depending on the changing Ca^{2+} concentrations and the CaM-sensitive proteins present, this dynamic role of CaM has important implications for neuronal physiology.

Like the ion channels discussed above, *Drosophila* EAG also binds and is regulated by CaM (Chapter III). Consistent with its important role in neuronal function, *Drosophila Cam* mutants have behavioral and neuromuscular defects (Arredondo et al., 1998). Even though the gene encoding for a particular mutant of CaM protein (CaM^{3cl}) has decreased affinity for Ca^{2+} it can still activate CaMKII and other CaM-activated signaling proteins. Because CaM^{3cl} mutants have defective neurotransmitter release, CaM may have protein targets that affect NMJ excitability distinct from CaMKII. One strong possible candidate is EAG. CaM binding was first described for human EAG channels. *In vitro* binding assays show CaM can specifically bind to and inhibit human

EAG1 in a Ca^{2+}-dependent manner (Schönherr et al., 2000). Additionally, stoichiometric recordings, from inside-out patches of *Xenopus* oocytes expressing EAG, indicate that one CaM molecule binding to EAG is sufficient to inhibit current through the channel. Schönherr et al. found a relatively low binding affinity (K_D of 480 nM Ca^{2+}) of CaM for EAG. Since this value is greater than the physiological intracellular concentration of Ca^{2+}, they concluded that CaM was not constitutively bound and that modulation of human EAG is mainly controlled by binding and release of Ca^{2+}-bound CaM. Ca^{2+}-dependent CaM binding is likely to underlie the inhibitory effects of increased Ca^{2+} first reported for rat EAG channels (Stansfeld et al., 1996).

D2b. CaMKII

CaMKII is a serine/threonine kinase formed from 8 to 12 subunits and has a broad range of substrates (GuptaRoy and Griffith, 1996). The high abundance of CaMKII in the nervous system makes it an unusual enzyme, because most catalytic molecules are present in relatively low amounts (Griffith, 2004a). CaMKII is a key Ca^{2+}-sensing signal transducer in neurons and other cells. The CaMKII protein consists of three distinct domains: (from N- to C-terminus) the catalytic, autoregulatory and association regions. During low levels of Ca^{2+}, the autoregulatory domain acts as a pseudo-substrate and interacts with the catalytic domain, blocking kinase function. In response to increased levels of internal Ca^{2+}, Ca^{2+} complexed to CaM binds the autoregulatory domain of CaMKII and activates the kinase (Smith et al., 1990; Fong and Soderling, 1990; Barria et al., 1997). This frees the catalytic domain to bind ATP and substrate, and promotes kinase activity. Within the autoregulatory domain of CaMKII is T287, which can be

autophosphorylated and promotes constitutive activity of the kinase. The activity of T287 phosphorylated CaMKII is independent of Ca^{2+}/CaM binding, and amounts to approximately 10% of the maximal Ca^{2+}-stimulated activity. If Ca^{2+} levels drop and lead to dissociation of CaM form CaMKII additional phosphorylation sites in the CaM binding domain become available. If the kinase is active, it can autophosphorylate at T305 and T306, which prevents rebinding of CaM and makes the kinase insensitive to Ca^{2+}/CaM (Griffith, 2004b).

The discovery of an abundant neuronal protein with activity-dependent "switch"-like properties lead investigators to investigate CaMKII as a candidate memory molecule (Miller and Kennedy, 1986). Indeed, CaMKII activity is required for induction of long-term potentiation (LTP) in the CA1 region of the hippocampus of mice (Malenka et al., 1989; Silva et al., 1992a; Lisman et al., 2002) and animals that lack CaMKII show defects in spatial learning (Silva et al., 1992b). Additionally, contextual fear conditioning can induce autophosphorylation of CaMKII in amygdala synapses, indicating this molecule may be important for learning in many memory paradigms (Rodrigues et al., 2004). Like CaM, CaMKII has numerous targets, including ion channels such as NMDA glutamate receptors and the *C. elegans* homolog of ERG, *unc-103* (Colbran, 2004; Reiner et al., 1999; LeBoeuf et al., 2007).

Similar to learning defects found in mammals, transgenic *Drosophila* with impaired CaMKII also show deficiencies in behavioral plasticity and learning (Griffith et al., 1993; 1994). Important to my thesis, the defective physiological and behavioral phenotypes associated with altered CaMKII activity are similar to those found in *eag* mutants (Griffith et al., 1994). This nonallelic genetic heterogeneity posits CaMKII as a

possible candidate for a genetic relationship with *eag*. CaMKII is highly concentrated at glutamatergic synapses, including the *Drosophila* NMJ (Soderling, 1993). In addition to defects in learning, transgenic inhibition of CaMKII activity reproduces the main features of the eag phenotype at the larval NMJ, namely a high frequency of spontaneous activity and increased amplitude of evoked EJPs. Most importantly, crosses of CaMKII-inhibited flies with *eag* mutants result in non-additivity of these phenotypes, namely the defects observed are no more severe than those observed for the individual mutants (Griffith et al., 1994). The similarity and non-additivity of the electrophysiological phenotypes at the NMJ led to the discovery of a role for *eag* in learning.

Consistent with the similar phenotypes observed in *Drosophila*, CaMKII functions to modulate the channel by phosphorylating a C-terminal threonine in EAG (EAG-T787) which increases EAG current (Wang et al., 2002b). This finding suggested that the similarity and non-additivity of the phenotypes of *eag* mutants and CaMKII-inhibited flies was due to a decrease in EAG current in both conditions. Recently, however, it has been demonstrated that CaMKII can directly bind to EAG and that, *in vitro*, binding can regulate kinase activity (Sun et al., 2004). The CaMKII binding domain of EAG shows high similarity to the CaMKII autoregulatory domain. This suggests EAG binds to the catalytic domain, analogous to the autoregulatory domain of the kinase. Mutations of single residues in the EAG domain (EAG -R784L, Q785L) almost completely eliminate binding to the kinase. Moreover, mutation of an amino acid (I206K) in the catalytic domain of CaMKII that is important for autoregulatory binding also abolishes EAG binding. Importantly, although the initial binding of EAG to CaMKII requires Ca^{2+}, the association, once established persists in the absence of Ca^{2+}

(Sun et al., 2004). Under these conditions the bound kinase is constitutively active, retaining 5 to 10 % of the maximal Ca^{2+}-stimulated activity. Given these multiple interactions, the degree to which the similar phenotypes of *eag* mutants and CaMKII-inhibited flies are due to the disruption of either EAG or CaMKII function is unclear. (These uncertainties are advanced in Chapter IV.) In addition, since CaMKII is so abundant in neurons, targeting the kinase to proper intracellular and substrate locations is necessary to enhance the signal-to-noise ratio of Ca^{2+}/CaM-dependent phosphorylation (Griffith, 2004a; Schulman, 2004). Independent of the direct binding of EAG to CaMKII, another protein present at the larval NMJ synapse, CMG, functions as a signaling module by recruiting CaMKII to EAG. This adaptor protein, and its modulation of EAG, is a further subject of my thesis (Chapter II).

D3. Signaling modules

Cells respond to various intracellular and extracellular cues by eliciting specific responses that are mediated by a complex array of signaling networks. These signaling networks, consisting of distinct as well as overlapping signaling pathways, involve distinct ligands, receptors, G proteins, small guanosines triphosphatases, kinases and transcription factors. In many instances, the same or similar signaling molecules are used to elicit distinctly different functional responses by these signaling pathways (Hunter, 2000). In spite of such high use of the same reoccurring signaling molecules, signaling networks are precisely regulated with minimal crosstalk with adjacent signaling pathways by means of signaling and scaffolding modules (Dhanasekaran et al., 2007).

These macromolecular complexes can contribute to the localization and function of ion channels. Ion channels are near ideal members of signaling modules since they are localized at the plasma membrane, able to respond quickly to synaptic and perisynaptic signals and can in turn alter membrane properties. Most, and perhaps all, ion channels are substrates for protein kinases and phosphoprotein phosphatases (Levitan, 2006) which can modulate channel expression, stability, and function. Ion channels can also bind integrin receptors, which mediate adhesion of the cell to the extracellular matrix and regulate cell motility, proliferation, differentiation and apoptosis (Arcangeli and Becchetti, 2006).

D3a. Scaffolding proteins

One particularly important signaling molecules in biology is cAMP-dependent protein kinase (PKA), which is involved ubiquitously in numerous signaling cascades ranging from odorant transduction, to glycogen breakdown, to cell death (Zhang et al., 2006). To harness this important kinase and tame its promiscuous behavior, scaffolding proteins such as A kinase anchoring proteins (AKAPs) can bind to the regulatory subunit of PKA and target the enzyme to a particular cellular compartment or specific substrate. Many different AKAPs have been discovered, including ones that appear to be specific for targeting PKA to ion channels (Wong and Scott, 2004). This type of regulation is very common; AKAPS are known to modulate voltage-gated Ca^{2+}, Na^{+} and K^{+} channels (Altier et al., 2002; Tibbs et al., 1998; Potet et al., 2001; Levitan, 2006). AKAPs can not only bind to PKA and target substrates but also to other protein kinases and phosphatases, indicating the complexity of AKAP scaffolding modules can be quite high (Klauck et al.,

1996; Wong and Scott, 2004). AKAPs are of additional interest to this work due to preliminary observations that EAG may be phosphorylated and regulated by PKA. This interaction may be mediated by a yet unknown AKAP, capable of binding EAG and PKA.

Another important class of scaffolding proteins that regulate ion channels is the membrane-associated guanylate kinases (MAGUK). MAGUKs play important roles in targeting, anchoring, and signaling of ion channels at synapses and in regulation of neural activity. MAGUKs are characterized by various evolutionarily conserved domains (PDZ, SH3, HOOK and GUK) involved in protein-protein interactions (Anderson, 1996; Hata et al., 1996). One of the better known MAGUKs is PSD-95, which can form multimeric protein structures at the post-synaptic density of neurons. PSD-95 can bind to and regulate numerous ion channels including AMPA and NMDA glutamate receptors and Sh-type K^+ channels. It can organize glutamate receptors and their associated signaling proteins and determines the size and strength of synapses. PSD-95 can also function in the dynamic trafficking of synaptic proteins by assembling cargo complexes for transport by molecular motors (Kim and Sheng, 2004).

The mammalian scaffolding protein calcium/calmodulin-dependent serine protein kinase (CASK) is another MAGUK important for neuronal function. CASK molecular composition differs slightly from other MAGUKs in that it has fewer PSD domains and in their place is a region with high homology to CaMKII. Importantly, however, this region does not show any kinase activity (Hata et al., 1996; Cohen, et al., 1998). CASK is expressed mostly in neuronal tissue and an insertional mutation caused by targeted knockout of the CASK gene results in lethality in mice within 1-2 days after birth

(Laverty and Wilson, 1998). Although the reason for lethality is not clear, these findings suggest that CASK is important in development (Hseuh, 2006).

In the nervous system CASK binds presynaptically to the membrane spanning protein neurexin which interacts postsynaptically with neuroligin, leading to the correct alignment of the pre- and postsynaptic machinery (Butz et al., 1998; Tabuchi et al., 2002). CASK is also present outside the nervous system, where it is involved in tight junction formation and maintenance (Irie et al., 1999). In *C. elegans,* mutations of the nematode homolog of this protein cause alterations of EGF receptor localization in vulval epithelial cells, leading to vulva malformations and reduced egg laying (Kaech et al., 1998). CASK also associates with, and in some cases target, several proteins, including N-type Ca^{2+}-channel β-subunits and amyloid precursor protein (Hata et al., 1996; Hoskins et al., 1996; Borg et al., 1998; Maximov et al., 1999). CASK has also been proposed as a co-activator of TRB1, a transcription factor involved in brain development through the activation of genes with T-element-containing promoters (Hsueh et al., 2000).

D3b. Camguk and modulation of EAG

The *Drosophila* homolog of mammalian CASK is Camguk (CMG), sometimes also referred to as Caki (Martin and Ollo, 1996). In *Drosophila* adults, CMG is expressed in the visual brain regions of flies (Martin and Ollo, 1996). In the larval CNS, CMG is expressed in synaptic regions of the ventral ganglion and brain lobes and in the pre- and postsynaptic region of the NMJ (Lu et al., 2003). Adult *cmg* mutants are characterized by a reduced locomotor behavior (Martin and Ollo, 1996) and show altered

courtship conditioning, indicating associative and non associative memory defects (Lu et al., 2003). Electroretinographic responses of *cmg* to single and continuous repetitive stimuli are abnormal and optomotor behavior is also defective (Zordan et al., 2005). In the absence of CMG, recordings from the indirect flight muscle fibers of adults show an increase in the frequency of miniature endplate potentials, with little change in quantal amplitude (Zordan et al., 2005). These phenotypes strongly support the involvement of CMG in synaptic and, more generally, nervous system function.

Like CASK, no catalytic activity has been detected for the CaMKII-like domain of CMG (Hata et al., 1996; Lu et al, 2003) even though the amino acid identities of the kinase (41%) and CaM-binding domains (61%) between CMG and CaMKII are high. Importantly, however, the CaMKII-like domain of CMG mediates a direct interaction with CaMKII (Lu et al., 2003). The interaction between CMG and CaMKII is regulated, and is established only in the presence of ATP and Ca^{2+}/CaM. Addition of a peptide consisting of the CaMKII autoregulatory domain disrupts the CMG-CaMKII interaction, suggesting that CMG interacts with either the autoregulatory domain or the region of the catalytic domain that normally binds to the autoregulatory domain of the kinase.

The functional effect of CMG binding to CaMKII is also regulated by the cellular level of Ca^{2+}/CaM. Experiments have shown that when CMG is complexed to CaMKII in conditions with Ca^{2+}/CaM, CaMKII becomes constitutively active via autophosphorylation of T287 and independent of further Ca^{2+}/CaM regulation (Lu et al., 2003). In the absence of Ca^{2+}/CaM, CMG bound to CaMKII leads to autophosphorylation of residue T306. Phosphorylation of T306, which is in the CaM binding site of CaMKII, results in kinase inactivation and dissociation of the CMG-

CaMKII complex. Inhibition of the kinase via T306 phosphorylation is only reversed by subsequent PP2A phosphatase activity. Thus, at low levels of Ca^{2+}, CMG complexed to CaMKII results in an inactive pool of kinase. In summary, Ca^{2+}/CaM levels, phosphatase activity, and CMG binding all contribute, in an inter-related way, to CaMKII modulation.

The effect of CMG on CaMKII function also has been studied *in vivo* (Lu et al., 2003). CMG and CaMKII are expressed both pre- and postsynaptically at the NMJ. Overexpression of CMG in postsynaptic larval muscle increased the amount of CaMKII inactivated by T306 phosphorylation. This indicates CMG can cause lowered levels of CaMKII activity. On the other hand, when CMG is expressed at elevated levels in the innervating motor neuron there is no measurable change in T306 phosphorylation. Although, the reason for this difference is not clear, other proteins present in the motor neuron may compete with CMG for the CaMKII binding site or, alternatively, interactions with other proteins may stabilize the complex preventing inactivation and release of the kinase. One plausible candidate for this is EAG. In this thesis I provide additional evidence for a functional relationship between these three proteins. My experiments (Marble et al., 2005; Chapter II) suggest that CMG enhances the interaction between EAG and CaMKII, possibly by forming a tripartite complex. Coexpression with CMG increases phosphorylation of T787 leading to more EAG channels at the plasma membrane and enhanced EAG current.

D4. Other EAG-interacting proteins

In addition to CaM, CaMKII, and CMG, several other EAG-interacting proteins have been identified, including Hyperkinetic, epsin, KCR1, and Slob. EAG subunits also

may interact directly with other voltage-gated channel subunits forming heteromultimeric channels. In most cases, the function and *in vivo* significance of these interactions remains speculative, and is largely based on other functions associated with these proteins.

D4a. Hyperkinetic

One of the first K^+ channel β-subunits to be characterized, *Drosophila* Hyperkinetic (Hk), was identified on the basis of a mutant leg-shaking phenotype similar to that observed for *Sh* and *eag* mutants (Kaplan and Trout, 1969). In heterologous expression systems, EAG has been shown to interact with Hk (Wilson et al., 1998). Hk, and its mammalian orthologs, $K_v\beta1$ and $K_v\beta2$, are primarily thought to be a subunit for the Sh subfamily of α-subunits, and show a strong homology with the aldo-keto reductase family of enzymes. Although enzymatic activity has not yet been established for Hk or $K_v\beta1$, the structurally similar $K_v\beta2$ has recently been shown to have aldo-keto reductase activity. UV absorption spectroscopy reveals that $K_v\beta2$ converts bound NADPH to $NADP^+$ when presented with aldehyde substrates (Weng et al., 2006). $K_v\beta2$-mediated oxidation occurs independently of $K_v1\alpha$-subunits, but when expressed with the $K_v1.4$ channel, the reaction modulates channel current (Weng et al., 2006). Like $K_v\beta1$, $K_v\beta2$ slightly increases rates of inactivation of $K_v1.4$ channels, attenuating K^+ current, but as the bound β-subunit catalyzes an oxidative reaction this effect on kinetics disappears (Rettig et al., 1994). These results demonstrate a functional link between channel gating and enzymatic activity, with the implication that K_v1 channels are modulated in response to oxidative stress. However, this association also suggests the possibility that channel

gating could reciprocally affect the oxidizing activity of the α-subunit, influencing redox pathways during prolonged depolarization.

Hk coimmunoprecipitates with EAG, and produces an increase in activation kinetics and amplitude of EAG current (likely through more channels at the membrane) when coexpressed in oocytes (Wilson et al., 1998). Hk also enhances mEAG, hERG and Sh channels, in agreement with the predominant effect on other Kv1 channels, although the increased inactivation caused by $K_v\beta1$ and $K_v\beta2$ upon $K_v1.4$ is not observed (Rettig et al., 1994; Chouinard et al., 1995). These results suggest a possible promiscuous role for Hk in the modulation of different K_v channels. Although it is not known whether EAG and Hk interact *in vivo*, there are phenotypic similarities that suggest this might be the case, including leg-shaking behavior and repetitive nerve firing and increased postsynaptic response (Kaplan and Trout, 1969; Stern and Ganetzky,1989).

D4b. Epsin

Another protein that interacts with EAG channels is the membrane-associated EH domain-binding protein epsin. In a binding overlay screen Piros et al. purified a 95-kDa protein from rat brain membranes that binds to EAG (Piros et al., 1999). When this protein, now identified as epsin, was co-expressed in mammalian cell lines it coimmunoprecipitated with EAG. Epsin affects the gating of EAG channels: it slows activation, shifts the voltage-dependence of activation to more positive potentials, and slows deactivation (Piros et al., 1999). What makes this interaction with EAG intriguing is the other known functions of epsin. Epsin plays a role in endocytosis, by virtue of binding to both Eps15 and to the α-adaptin subunit of AP-2, epsin drives the curvature of

clathrin-coated pits (Ford et al., 2002). Epsin is also homologous to the *Xenopus* mitotic protein MP90 which is heavily regulated by phosphorylation during cell division (Stukenberg et al., 1997). This raises the possibility that epsin could couple cell cycle regulation to the modulation of EAG. Indeed, in *Xenopus* oocytes expressing rat EAG, mitosis promoting factors induce a reduction of EAG current amplitude (Brüggemann et al., 1997). Epsin also is enriched in presynaptic nerve terminals and is involved in endocytotic processes, including synaptic vesicle recycling, nutrient uptake, and removal of receptors and ion channels from the cell membrane (Ford et al., 2002). Thus, epsin may regulate EAG gating kinetics or surface expression in a cell cycle- or activity-dependent manner.

D4c. KCR1

Another protein that associates with and modulates EAG channels is the integral membrane protein KCR1 (K^+ channel regulator 1). An interaction between KCR1 and EAG was discovered in a screen for genes that enhance the non-inactivating K^+ current found in cerebellar granule neurons $I_{K(ni)}$ (Hoshi et al., 1998). KCR1 was further examined if it could affect EAG channels because the $I_{K(ni)}$ current is similar to the non-/partially-inactivating current carried by EAG channels. It was found that KCR1 accelerates the activation of rat EAG channels when heterologously co-expressed. Far-Western blotting revealed that KCR1 and EAG proteins interact with each other by means of their C-terminal regions (Hoshi et al., 1998). KCR1 is a cerebellar protein with 12 putative transmembrane domains. It is also expressed in the heart where it can bind hERG and change the sensitivity of hERG to proarrhythmic drugs (Kupershmidt et al.,

2003). In addition, KCR1 functions as an α-1,2-glucosyltransferase, capable of adding *N*-linked oligosaccharides to substrate proteins. Although hERG itself is not a target for KCR1-mediated glycosylation, inhibition of KCR1 glycosylation function does alter its ability to modulate hERG's drug sensitivity (Nakajimi et al., 2007). It is not known if this effect is conserved and KCR1 similarly modulates the pharmacological characteristic of EAG channels, but this suggests a situation where enzymatic activity by KCR1 regulates EAG channels, or in turn, EAG binding could regulate glycosylation activity in KCR1.

D4d. Slob

The slowpoke-binding protein (Slob) is another multifunctional protein that interacts with EAG channels and may regulate cellular processes. Slob was initially identified using a yeast two-hybrid screen for binding partners of the *Drosophila* Ca^{2+}-activated, large conductance K^+ channel Slopoke (dSlo) (Schopperle et al., 1998). This study also showed Slob specifically interacts with EAG within a co-immunoprecipitating complex. *In vitro*, Slob has kinase activity and weakly phosphorylates itself and histone substrates. However, this activity is greatly enhanced when the protein is pretreated with the catalytic subunit of PKA (Zeng et al., 2004). Mutation of a candidate serine residue in Slob abolishes the effect, which can be restored by the introduction of a phospho-mimic aspartate residue, suggesting that PKA phosphorylation regulates Slob kinase activity (Zeng et al., 2004). Investigations of Slob have focused on its role within the dSlo complex. Slob binds to the carboxy-terminal domain of dSlo and leads to an increase in channel activity by increasing open probability (Schopperle et al., 1998).

Slob also recruits the scaffolding protein 14-3-3 to the dSlo complex, which can itself modulate channel function in a manner dependent on the phosphorylation of Slob by CaMKII (Zhou et al., 1999). The 14-3-3/Slob/dSlo complex is localized at presynaptic boutons in larval NMJs and transgenically expressed constitutively activated CaMKII enhances the Slob/14-3-3 interaction, demonstrating that the interaction of Slob and 14–3–3 is not static but can be influenced rapidly by changes in CaMKII activity in the fly.

The intricate regulation of dSlo activity by its associated proteins obviously speaks to the dynamic regulation of the channel complex. It is not known if similar properties exist for the EAG/Slob complex, but it is intriguing considering the numerous roles Slob and 14-3-3 play *in vivo*, such as the circadian and signaling pathways. Slob expression in photoreceptors and pars intercerebralis (PI) neurons cycles in tandem with light/dark entrainment and other circadian-regulated proteins (Jaramillo et al., 2004). Also, different Slob transcripts bind differentially to 14-3-3 and dSlo depending on circadian rhythms. 14-3-3 proteins are ubiquitous proteins known for binding many signaling proteins such as kinases, phosphatases and membrane receptors and are essential for cell proliferation and have a role in determining the timing of mitosis (Reuther et al., 1994). Because 14-3-3 also binds various nuclear signaling proteins, including Raf, a key component of mitogen-activated protein kinase (MAPK) signaling pathways (Fu et al., 1994), it is interesting to consider the potentially central role for the EAG/Slob complex involved in these pathways in *Drosophila*.

D4e. Multimerization

Although there is no K^+ current in larval muscle that shares the features of heterologously expressed EAG, mutations in the *Drosophila eag* gene affect all four identified K^+ currents in larval muscle, including the fast, transient voltage-dependent I_A current mediated by Sh channels (Connor and Stevens**,** 1971**;** Zhong and Wu, 1991). This led some investigators to hypothesize that EAG and Sh may heteromultimerize. Even though antibodies fail to detect full-length EAG in the plasma membrane of larval muscle fibers (Wang et al., 2002b), and even though heterologous expression of Sh largely replicates the properties of the I_A current in muscle (Timpe et al., 1988; Iverson et al., 1988), there is some evidence suggesting that EAG and Sh may interact. This possibility was first investigated by Zhong and Wu who found novel phenotypes expressed in *eag*;*Sh* double mutants that depended on specific allele combinations (Zhong and Wu, 1993). These phenotypes are different than the only additive defects found in other combinations of K^+ channels such as *Sh*;*Slo* flies. This genetic evidence suggesting an interaction between EAG and Sh channels is also supported by heterologous expression of EAG and Sh channels. When EAG and Sh are co-expressed in *Xenopus* oocytes EAG accelerates the N-type inactivation and slows the recovery from inactivation of the transient Sh current (Chen et al., 1996). These effects are opposite of what one may expect from simple additive properties of EAG and Sh currents. A chimera made of the N-terminal cytoplasmic and pore domains of Sh combined with the C-terminal domain of EAG shows that last half of EAG is crucial for the modulatory affects on Sh currents (Chen et al., 1996). In conclusion, although it currently seems

more likely that EAG exerts its effect on the K^+ currents in larval muscle by an indirect, activity-dependent mechanism, EAG and Sh could interact in other tissues.

E. THESIS GOALS AND HYPOTHESIS OF EAG REGULATION

In spite of the numerous K^+ channels now identified, EAG remains one of the few K^+ channels with a demonstrated role in learning. Because EAG currents share many basic properties with other K_v currents, a central theme underlying my thesis work has been that the unique role of EAG in learning is, in part, a result of the mechanisms that regulate EAG. To this end, I have characterized several Ca^{2+}-dependent mechanisms that regulate EAG, including interactions with the CMG adaptor protein (Chapter II), CaM (Chapter III), and CaMKII (Chapters II, III, and IV).

EAG is regulated by CaMKII phosphorylation (Wang et al., 2002b), as well as direct CaMKII binding to EAG (Sun et al., 2004). The adaptor protein CMG binds to CaMKII and EAG and modulates kinase activity (Lu et al., 2003). Therefore, it was hypothesized that a signaling module, consisting of EAG, CMG, and CaMKII, existed in *Drosophila*, and that these proteins functioned together to regulate EAG activity in presynaptic terminals. The experiments of Chapter II show that the adaptor protein CMG interacts directly with EAG *in vivo*, and that CMG increases EAG current by increasing phosphorylation at a CaMKII consensus phosphorylation site. Increased phosphorylation leads to greater EAG expression at the plasma membrane. Also, a non-canonical SH3 binding motif is identified in EAG when the EAG-CMG interaction is mapped for each protein.

Because EAG is regulated by CaMKII, and CaMKII is regulated by Ca^{2+}/CaM, by the transitive property, EAG is indirectly regulated by Ca^{2+}/CaM. Indeed, increases in Ca^{2+}/CaM lead to phosphorylation of EAG (Wang et al., 2002b). However, as shown in Chapter III, CaM also acts directly upon EAG by binding in a Ca^{2+}-dependent manner resulting in inhibition of EAG currents, not unlike previously observed for mammalian EAG channels (Stansfeld et al., 1996; Schönherr et al., 2000; Ziechner et al., 2006).

Chapter IV extends the previous description of the EAG-CaMKII interaction (Sun et al., 2004; Hegle et al., 2006), by showing that full length EAG regulates CaMKII activity in a voltage-dependent manner and that EAG-CaMKII interaction is essential for the voltage-dependent, conductance-independent signaling activity of EAG

Finally, because the experiments using heterologous expression systems suggest that regulation by Ca^{2+}-dependent mechanisms and EAG signaling can result in paradoxically opposing effects, a determination of their *in vivo* effects seemed essential to an understanding of the relative contributions of these mechanisms to EAG and neuronal function. To this end, I transgenically expressed four constructs, including the CaM binding mutant (*eag*-FFSS), the CaMKII binding mutant (*eag* -LAKK), the CaMKII phosphorylation site mutant (*eag*-T787A), and the non-conducting mutant (*eag*-F456A), and examined their ability to rescue the NMJ phenotypes observed in eag^{sc29} larvae (Chapters III and IV). Ca^{2+}-dependent CaM binding, which inhibits EAG currents in heterologous systems, is hypothesized to increase motorneuron and synaptic activity, whereas CaMKII phosphorylation of EAG, which increases EAG current by increasing the surface expression of EAG, is expected to limit motorneuron and synaptic activity. Because the effects of CaM binding are readily reversible, whereas the effects of CaMKII

phosphorylation on surface expression are not, the temporal differences in mechanism suggested that the effects of CaM regulation would be acute, and the effects of phosphorylation by CaMKII would be more protracted. However, the relative Ca^{2+} concentration requirements, the spatial and temporal characteristics of Ca^{2+} influx, and the possible contributions of other, as yet unidentified, proteins and signaling pathways *in vivo* might alter the outcomes of regulation by these mechanisms. Disruption of CaMKII binding to EAG could affect both EAG phosphorylation and decreased K^+ currents and non-conducting EAG signaling properties. These possibilities could be distinguished by analysis of the non-conducting version of EAG.

My results indicate that transgenic larvae expressing *eag* mutants that cannot bind CaMKII have defects in spontaneous NMJ activity, not unlike *eag* null mutants, suggesting that EAG regulation of CaMKII activity plays a role in limiting activity levels even at basal Ca^{2+} concentrations. In contrast, the role of EAG current, assessed by transgenic expression of non-conducting *eag*-F456A, appears limited to the regulation of EJP/EJC amplitudes. As predicted above, CaM binding to EAG functions acutely and reversibly to regulate EAG currents, with Ca^{2+} requirements that are high enough such that the effect is restricted to synaptic facilitation. CaM binding to EAG does not affect either basal EJC amplitudes or spontaneous activity. Finally, none of the features of the eag^{sc29} phenotype were rescued by transgenic expression of *eag*-T787A, indicating that phosphorylation of EAG has a crucial role even at basal levels of Ca^{2+}. Phosphorylation appears to affect both EAG signaling and current, as might be expected given that phosphorylation increases the surface expression of EAG up to 6-fold in heterologous expression studies.

CHAPTER II

CAMGUK/CASK ENHANCES ETHER À GO-GO K^+ CURRENT BY A PHOSPHORYLATION-DEPENDENT MECHANISM

A. ABSTRACT

Signaling complexes are essential for the modulation of excitability within restricted neuronal compartments. Adaptor proteins are the scaffold around which signaling complexes are organized. Here, we demonstrate that the Camguk (CMG)/CASK adaptor protein functionally modulates *Drosophila* Ether à go-go (EAG) potassium channels. Coexpression of CMG with EAG in *Xenopus* oocytes results in a more than twofold average increase in EAG whole cell conductance. This effect depends on EAG-T787, the residue phosphorylated by calcium/calmodulin-dependent protein kinase II (Wang et al., 2002b). CMG coimmunoprecipitates with wild type and EAG-T787A channels, indicating that T787, although necessary for the effect of CMG on EAG current, is not required for the formation of the EAG-CMG complex. Both CMG and phosphorylation of T787 increase the surface expression of EAG channels, and in COS-7 cells, EAG recruits CMG to the plasma membrane. The interaction of EAG with CMG requires a non-canonical Src homology 3-binding site beginning at position R1037 of the EAG sequence. Mutation of basic residues, but not neighboring prolines, prevents binding and

prevents the increase in EAG conductance. Our findings demonstrate that membrane-associated guanylate kinase adaptor proteins can modulate ion channel function; in the case of CMG, this occurs via an increase in the surface expression and phosphorylation of the EAG channel.

B. INTRODUCTION

Ether à go-go (EAG), the *Drosophila* ortholog of KCNH1, is the founding member of a family of potassium (K^+) channels identified by the presence of domains with homology to the PAS (Per, Arnt, Sim) and cyclic nucleotide binding domains of other proteins (Drysdale et al., 1991; Guy et al., 1991; Morais Cabral et al., 1998; Warmke et al., 1991). *eag* larvae exhibit spontaneous action potentials in the motor nerve and excitatory junctional potentials in muscle that are broadened compared to those of wild type larvae (Ganetzky and Wu, 1985). EAG is present in the axons and terminals innervating the larval body-wall musculature (Wang et al., 2002b) and is localized with synaptobrevin in the central nervous system (Sun et al., 2004).

In addition to hyperexcitability at the neuromuscular junction, *eag* mutants also exhibit defects in associative learning (Griffith et al., 1994). Intriguingly, there is substantial similarity in the electrophysiological and learning phenotypes of *eag* mutants and transgenic *Drosophila* expressing an inhibitory peptide of calcium and calmodulin (Ca^{2+}/CaM)-dependent protein kinase II (CaMKII) (Griffith et al., 1994), and phosphorylation of EAG by CaMKII results in a dramatic increase in current (Wang et al., 2002b). Recent work has demonstrated that *Drosophila* CaMKII interacts with the Camguk (CMG) adaptor protein (Lu et al., 2003). CMG is a member of the membrane-

associated guanylate kinase (MAGUK) family of adaptor proteins and the *Drosophila* ortholog of CASK and Lin-2 (Butz et al., 1998; Dimitratos et al., 1997; Hata et al., 1996; Hoskins et al., 1996). CMG/CASK/Lin-2 is unique in that the N-terminus (NT) displays considerable homology to CaMKII. The kinase domain of CMG, although appearing nonfunctional as a kinase, associates with CaMKII in an ATP- and Ca^{2+}/CaM-dependent fashion (Lu et al., 2003). Once Ca^{2+} levels decline, CMG downregulates cellular CaMKII activity by releasing the kinase in a form that must be dephosphorylated before it can be activated by subsequent increases in Ca^{2+}.

Given the regulation of EAG function by CaMKII, we sought to determine whether CMG also associates with EAG. Intriguingly, the interaction of CMG with EAG promoted an increase in whole cell conductance and alterations in inactivation kinetics that were reminiscent of the changes in current observed as a consequence of phosphorylation by CaMKII. Indeed, mutation of EAG-T787, the site phosphorylated by CaMKII, prevented the effects of CMG without affecting immunoprecipitation of the complex. Moreover, CMG increased EAG surface expression, whereas mutation of T787 decreased EAG surface expression, indicating that CMG and phosphorylation affect channel function by the same mechanism. One possible model that could account for these findings is that CMG may locally increase kinase efficiency by ensuring that only active kinase is in the vicinity of the channel.

C. RESULTS

C.1. CMG modulates EAG current

To determine whether the CMG adaptor protein might regulate EAG function, we examined EAG channels expressed in *Xenopus* oocytes either alone or together with an excess of CMG. Figure 2.1, A and B, shows examples of EAG current traces and average current-voltage relations obtained from a representative batch of oocytes. In response to test pulses to +60 mV (holding potential, -80 mV), co-expression with CMG resulted in peak currents that were increased 2.7-fold over control values (Fig 2.1B). CMG produced increases in current in 19 of 21 batches of oocytes examined. The increase averaged 2.3-fold above EAG controls and was significant ($p < 0.0001$) when tested using a two-way ANOVA with oocyte batch and CMG as variables. When CMG was coexpressed with *Shaker*, another *Drosophila* potassium channel, no increase in Shaker current was observed (data not shown). The average peak Shaker currents in response to test pulses to +60 mV (holding potential, -100 mV) were 12.5 ± 0.6 μA (n = 8) and 10.7 ± 0.8 μA (n = 10) in the absence and presence of CMG, respectively.

The primary effect of CMG was on EAG current amplitudes. Analysis of the voltage-dependence of EAG currents in an extracellular solution containing 25 mM KCl to enhance tail currents revealed little change in either the slope or midpoint of activation when EAG was coexpressed with CMG (Fig 2.1C). Scaled representative traces for the two conditions are shown in Figure 2.1D, *top*. Examination of activation and inactivation kinetics revealed only a modest increase in the inactivation time constant and a decrease in the percentage of inactivation (Fig 2.1D, *bottom*). The CMG-mediated decrease

Figure 2.1: CMG increases EAG current and conductance.
(A) Coexpression with CMG increases EAG current amplitudes in *Xenopus* oocytes. Macroscopic currents recorded in two electrode voltage clamp from representative oocytes in response to depolarizing voltage steps from -100 to 80 mV in 20 mV increments (holding potential, -80 mV). Linear leakage and capacitative components have been subtracted. Calibration bars apply to both sets of traces. **(B-G)** Dark symbols and bars represent measurements obtained in the presence of CMG. **(B)** Comparison of the average current-voltage relationships obtained for one batch of oocytes (batch refers to oocytes obtained from the same frog) injected with RNA encoding *eag* (n = 7) or *eag* together with an excess of *cmg* (n = 10) as indicated. Currents were elicited by a series of voltage steps from -100 to 80 mV (holding potential, -80 mV). Leak subtraction was performed using a P/4 protocol with pulses of opposite polarity preceding each test pulse (holding potential, -80 mV). **(C)** Normalized conductance-voltage (GV) relations for wild type EAG channels, alone (n = 9) or in the presence of CMG (n = 16). For each oocyte, conductance was determined using the relation $G = I_{tail} / (V_{tail} - E_K)$ and normalized to the maximum conductance. Measurements were made in an extracellular solution containing 25 mM KCl to enhance tail currents. E_K was experimentally determined for each oocyte. Boltzmann functions fit to the averaged data had a midpoint and slope of -12.2 mV and 10.3 for EAG, and a midpoint and slope of -13.6 mV and 9.2 for EAG in the presence of CMG. **(D)** *Top*, Scaled representative traces obtained for EAG alone (I_{peak} = 3.0 μA) or together with CMG (I_{peak} = 4.8 μA). Currents were elicited by a 400 ms pulse to 40 mV from a holding potential of -80 mV. *Bottom*, Kinetics of EAG currents in the absence and presence of CMG. Three batches of oocytes with a mean fold increase in current amplitude that approximated the mean for all oocytes were selected for kinetic analysis. For each oocyte, activation (*left*) and inactivation (*middle*) taus were obtained by fitting two exponentials plus a constant to the first 200 ms of the response to a 400 ms test pulse to 40 mV (holding potential, -80 mV). The percentage of inactivation (inact) was determined by dividing the mean current obtained during the final 10 ms of the pulse by the peak current observed during the pulse. N = 26 and 28 for EAG and EAG with CMG, respectively. The effect of CMG was analyzed using a two way ANOVA with oocyte batch and CMG as variables (* $p < 0.05$; *** $p < 0.001$; N.S., not significant). **(E)** CMG fails to affect EAG-T787A. Experiments performed as in (b). n = 9 and 9 in the absence or presence of CMG, respectively. **(F)** GV relations for EAG channels expressed alone or together with CMG. Currents shown in (b) were converted to conductance using the relation $G = I_{test} / (V_{test} - E_K)$. E_K was assumed to be -80 mV. **(G)** CMG increases the average whole cell conductance in oocytes expressing the wild type, but not mutant, channel. Fold increase in the whole cell conductance for the oocytes described in (d) and three batches of oocytes expressing EAG-T787A alone or with CMG. Conductances were determined as described in (f) in response to a test pulse to 60 mV (holding potential, -80 mV). To normalize for variation in channel expression across different batches of oocytes, the mean conductance in the presence of CMG was normalized to the mean conductance obtained for that batch of oocytes expressing EAG or EAG-T787A alone. The number of oocytes examined for each condition is indicated above each bar. The effect of CMG was statistically analyzed as described in (d). Error bars represent SEM.

FIGURE 2.1

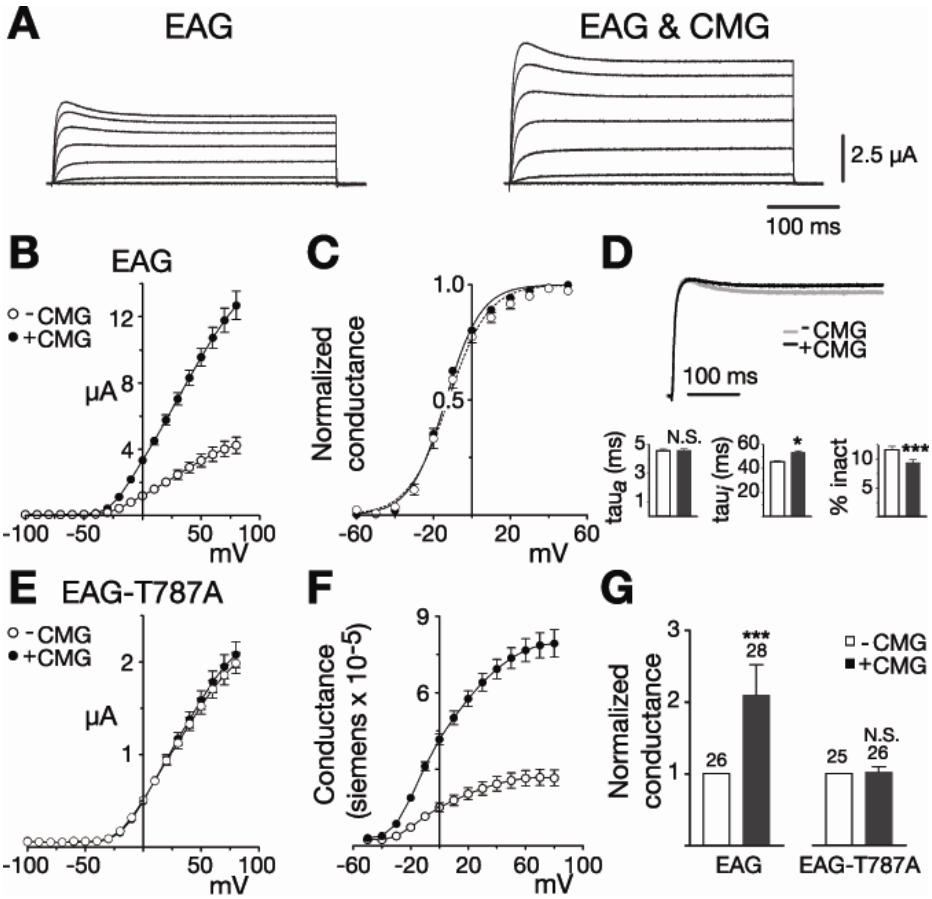
A
EAG
EAG & CMG
2.5 µA
100 ms
B
EAG
-CMG
+CMG
µA
mV
C
Normalized conductance
mV
D
-CMG
+CMG
100 ms
N.S.
*
***
E
EAG-T787A
F
Conductance (siemens x 10-5)
mV
G
Normalized conductance
-CMG
+CMG
***
N.S.
EAG
EAG-T787A

in inactivation was observed even when comparing oocytes with similar current amplitudes, suggesting that the effect on kinetics was not caused by a decreased efficiency of the voltage clamp for larger currents.

Many adaptor proteins affect the function of associated proteins by colocalizing the proteins with other modulators. Previous work has shown that EAG is phosphorylated by CaMKII activity endogenous to the oocytes even at basal Ca^{2+} levels (Wang et al., 2002b). Both the increase in current amplitude and the changes in inactivation in the presence of CMG are reminiscent of the changes in current observed as a consequence of phosphorylation. Because CaMKII has been shown to associate with CMG in the presence of ATP and Ca^{2+}/CaM (Lu et al., 2003), we sought to determine whether the effect of CMG on EAG currents could be mediated by phosphorylation. As shown in Figure 2.1E, the effect of CMG was dependent on EAG-T787, the residue previously shown to be phosphorylated by CaMKII *in vitro* and *in vivo*. When threonine at position 787 was replaced by alanine (EAG-T787A), CMG failed to increase current or affect inactivation.

The increase in current observed for wild type channels in the presence of CMG is most likely a result of an increase in the number of active channels given the lack of an appreciable change in either voltage-dependence or kinetics. Figure 2.1F displays the change in EAG activity in terms of the whole cell conductance for the batch of oocytes examined in Figure 2.1B. Figure 2.1G summarizes and compares the effect of CMG on the whole cell conductance of oocytes expressing EAG and EAG-T787A for three representative oocyte batches. If changes in open probability or single channel conductance do not contribute to the effect of CMG on EAG current, the average increase

in conductance suggests a more than twofold increase in the number of functional channels at the plasma membrane.

C.2. EAG and CMG co-immunoprecipitate from oocyte extracts

When oocyte extracts were probed with EAG (CT) antisera (Fig 2.2A, top blot, left three lanes), two protein bands were clearly identified. The primary EAG band ranged between 180 and 200 kDa depending on the protein markers used (Fig 2.2A, *top*, lanes 2 & 3). The second, lower molecular weight, band was also reliably observed and is most likely an alternate modification of the protein or a degradation product. Both bands were absent in Western blots of extracts prepared from uninjected oocytes (Fig 2.2A, *top*, lane 1). Immunoprecipitation reactions indicated that, in oocytes, EAG and CMG are part of the same protein complex. Immunoprecipitations using anti-CMG, but not preimmune, sera coprecipitated the EAG protein (Fig 2.2A, *top*, lanes 3-4). The reverse immunoprecipitation reaction is shown in the bottom blot (right three lanes). Immunoprecipitations using anti-EAG (NT), but not preimmune, sera coprecipitated CMG, which was observed as a single band near the predicted molecular weight of 103 kDa.

C.3. CMG and phosphorylation regulate EAG surface expression

One possible explanation of the failure of CMG to enhance EAG-T787A currents in our electrophysiological experiments is that phosphorylation of T787 may be required for the association of CMG with EAG. As shown in Figure 2.2A (*top and bottom*, lanes 6 and 9), there was no appreciable difference in the ability to immunoprecipitate the

Figure 2.2: CMG associates with EAG and increases EAG surface expression and phosphorylation. (A) Coimmunoprecipitation of EAG and CMG from *Xenopus* oocyte extracts. Lanes 1-3 show oocyte extracts for comparison; lane 4, immunoprecipitation with pre-immune sera; lanes 5-6, immunoprecipitation with indicated antibody. CMG associates with both wild type and EAG-T787A channels. *Top* (lanes 5-6), immuno-precipitation with CMG antisera. *Bottom* (lanes 5-6), reverse immunoprecipitation with EAG (NT) antisera. Similar results were observed in five experiments. Respective loads were 5, 10 and 20 μl for extracts, immunoprecipitated and coimmunoprecipitated proteins, respectively (see Materials and Methods). **(B)** CMG and phosphorylation of EAG-T787 both increase EAG surface expression. *Top*, Oocytes were labeled with biotin for 30 min and then quenched with glycine as described in Materials and Methods before preparation of oocyte extracts. For each condition, 600 μl of extract obtained from 50 oocytes was used for immunoprecipitation with EAG (NT) antisera. Proteins were separated by SDS-PAGE, transferred to PVDF membranes, blotted with the indicated antisera, and processed with ECL. Gels were run in parallel with equal amounts of the precipitates. *Bottom*, streptavidin-labeled bands were quantified by densitometry and normalized to the intensity of the EAG band in each experiment; data are presented as the mean ± SEM; n = 3 (* $p \leq 0.05$; ** $p \leq 0.01$; *** $p \leq 0.005$). **(C)** CMG increases phosphorylation of EAG-T787. *Top*, EAG was immunoprecipitated from oocyte extracts with EAG (NT) antisera. Gels were run in parallel, proteins transferred to PVDF membranes, which were then probed with either EAG (CT) antisera (*top*) or antibody recognizing EAG phosphorylated at T787 (*bottom*) (Wang et al., 2002b). *Bottom*, EAG labeled by phospho-specific antibody. Bands were quantified by densitometry and normalized to the EAG(CT)-labeled band and the corresponding region of the uninjected oocyte lane for each experiment; data are presented as the mean ± SEM; n = 3; p values as in (c). IP, Immunoprecipitation.

FIGURE 2.2

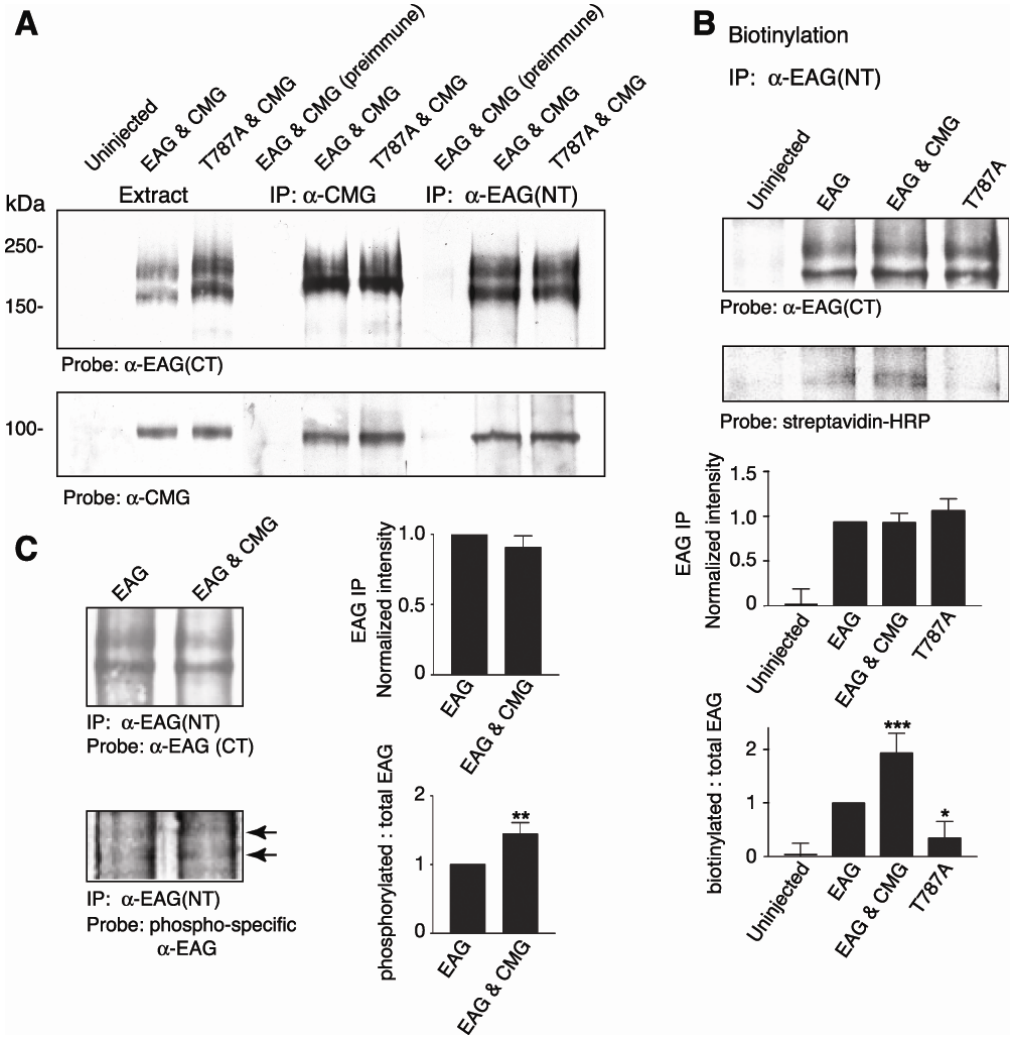
A
Uninjected
EAG & CMG
T787A & CMG
EAG & CMG (preimmune)
EAG & CMG
T787A & CMG
EAG & CMG (preimmune)
EAG & CMG
T787A & CMG
kDa
Extract
IP: α-CMG
IP: α-EAG(NT)
250-
150-
Probe: α-EAG(CT)
100-
Probe: α-CMG
B
Biotinylation
IP: α-EAG(NT)
Uninjected
EAG
EAG & CMG
T787A
Probe: α-EAG(CT)
Probe: streptavidin-HRP
EAG IP
Normalized intensity
1.5
1.0
0.5
0
Uninjected
EAG
EAG & CMG
T787A
biotinylated : total EAG
***
*
2
1
0
C
EAG
EAG & CMG
IP: α-EAG(NT)
Probe: α-EAG (CT)
IP: α-EAG(NT)
Probe: phospho-specific α-EAG
EAG IP
Normalized intensity
1.0
0.5
0
phosphorylated : total EAG
**
2
1
0

complex when EAG-T787A was expressed instead of the wild type channel, indicating that phosphorylation is not a prerequisite for formation of the complex. Either phosphorylation is required for CMG to exert an effect on EAG currents or, alternatively, the increase in current observed in the presence of CMG is the result of an increase in the efficiency of phosphorylation.

To begin to distinguish between these alternatives, we further investigated the mechanism underlying the effect of CMG on EAG current. Oocytes were surface labeled with biotin and, after biotin treatment, EAG was isolated by immunoprecipitation with EAG (NT) antisera (Fig 2.2B, top blot). As shown in Figure 2.2B (bottom blot) for a parallel blot of the immunoprecipitate probed with streptavidin, only the lower EAG band was detectably biotinylated. More importantly, compared with EAG channels expressed alone, there was a clear increase in the biotinylation of EAG when CMG was coexpressed (bottom blot, lanes 2 and 3). Finally, biotinylated EAG was lowest when expressing EAG-T787A (compare lanes 2 and 4). Semiquantitative comparisons of band intensities normalized to the intensity observed for wild type EAG indicated that the increases in biotinylation of EAG observed as a consequence of CMG and phosphorylation of EAG-T787 were significant (Fig 2.2B, *bottom*). The average increase in biotinylation observed for EAG in the presence of CMG was comparable with the increase in whole-cell conductance observed in oocyte recordings (Fig 2.1G). In addition, the decrease in biotinylation observed for EAG-T787A when compared with wild type EAG closely approximated the previously reported decrease in current observed when oocytes are injected with approximately equal concentrations of RNA (Wang et al., 2002b). A similar difference is observed in the experiments of Figure 2.1

(compare the current levels in B and E). These results suggest that CMG and phosphorylation of EAG-T787 increase EAG current by the same mechanism, namely by increasing the number of EAG channels in the plasma membrane.

C.4. CMG increases phosphorylation of EAG-T787

To determine whether the increase in current observed in the presence of CMG is the result of an increase in the efficiency of phosphorylation of EAG-T787, we immuno-precipitated EAG from oocyte extracts and probed the precipitate with an EAG antibody that specifically recognizes EAG phosphorylated at T787 (Wang et al., 2002b). As shown in Figure 2.2C (*left*), whereas there was no detectable difference in the overall level of EAG as a function of CMG (*top*), phosphorylation of T787 was increased when CMG was coexpressed (*bottom*). Comparisons of the level of phosphorylation averaged across multiple experiments (Fig 2.2C, *right*) indicated that the change in phosphorylation was significant. In summary, the enhancement of EAG current observed in the presence of CMG appears, at least in part, to be caused by an increase in the phosphorylation of T787. It remains unclear, however, whether phosphorylation is the sole mechanism underlying the increase in conductance and surface expression of EAG given the difference in the magnitudes of the effects. One possible explanation of this difference is that phosphorylation of EAG is more likely for channels in the membrane. Differences in the solubility of cytoplasmic versus membrane-associated channels may obscure differences in phosphorylation. Alternatively, the association with CMG and phosphorylation could have synergistic effects on the surface expression of EAG channels.

C.5. EAG recruits CMG to the plasma membrane in COS-7 cells

Additional indication of a functionally relevant interaction between EAG and CMG was obtained in COS-7 cells. Our ability to examine colocalization of EAG and CMG, as well as changes in the surface expression of EAG, was hampered by the fact that the primary epitope used by the only antibody, α-EAG(CT), that recognizes EAG in immunocytochemical experiments appears to be occluded when CMG is bound; in separate experiments α-EAG(CT) was the only anti-EAG antibody examined that failed to coprecipitate CMG from oocyte extracts (Marble and Wilson, unpublished observations). Although we were unable to examine changes in the localization of EAG, experiments in COS-7 cells suggested that the EAG-CMG complex may play a role in localizing CMG, in addition to its role in the modulation of EAG current. Changes in the localization of CMG as a function of coexpression with EAG were assessed using another binding partner, Tbr-1, a T-box transcription factor known to associate with the mammalian CMG homolog CASK (Hsueh et al., 2000). As shown in Figure 2.3A, little or no background labeling was observed when cells were mock-transfected with empty vector (*left top panel*). CMG expressed alone (*right top panel*) was localized to the cytoplasm and displayed a pattern consistent with a distribution to the endoplasmic reticulum as has been observed in the case of CASK (Hsueh et al., 2000). Also consistent with previous experiments, cotransfection with Tbr-1 shifted CMG into the nucleus (*right middle panel*). Most importantly, when EAG was coexpressed with CMG and Tbr-1, EAG successfully recruited a significant fraction of the CMG protein away from the nucleus to the cytoplasm and the plasma membrane (indicated by the arrows in the inset of the *left bottom panel*). In contrast, coexpression with the Shaker K^+ channel,

Figure 2.3: EAG-dependent translocation of CMG to the plasma membrane of COS-7 cells. COS-7 cells were transiently transfected with 0.4 μg of each of the cDNAs indicated below each panel. **(A)** The subcellular distribution of CMG as a function of co-expressed proteins was assessed by indirect immunofluorescence using antisera directed against CMG, followed by rhodamine-conjugated anti-guinea pig IgG. The *left top panel* shows the relative absence of CMG staining when cells were transfected with the empty pCDNA3 vector. The distribution of CMG shifts from the cytoplasm *(right top panel)* to the nucleus (*left middle panel*) when Tbr-1 is coexpressed as has previously been reported for the CMG homolog CASK (Hsueh et al., 2000). As shown in the *bottom left panel*, EAG competes with Tbr-1 to recruit a fraction of CMG to the plasma membrane, whereas Shaker fails to shift CMG from the nucleus. GW-CMV-Tbr-1 was a gift from M. Sheng (Massachusetts Institute of Technology, Cambridge, MA). Images were background subtracted for display using NIH Image software. Dashed boxes indicate the magnified areas displayed in the insets. Arrows within insets point to areas exhibiting particularly robust membrane staining. Scale bar, 10 μm. **(B)** Representative line scans of fluorescence intensity for key panels in (a). In each case, the scanned segment is the area between the two arrowheads. Intensity measurements were normalized to the highest intensity point of each image. **(C)** Averaged, normalized line scan data from three separate experiments examining the distribution of CMG to the cytoplasm, nucleus, and membrane for three expression conditions: CMG (C), CMG and Tbr-1 (CT), and CMG, Tbr-1, and EAG (CTE). Note that the bottom left panel of (a) was excluded from the analysis, given our inability to distinguish between the nucleus and cytoplasm. One-way ANOVA comparisons of fluorescence intensity are between C versus CT, and CT versus CTE conditions (* $p < 0.05$; ** $p < 0.01$; *** $p < 0.001$; N.S., not significant). Error bars represent SEM.

FIGURE 2.3

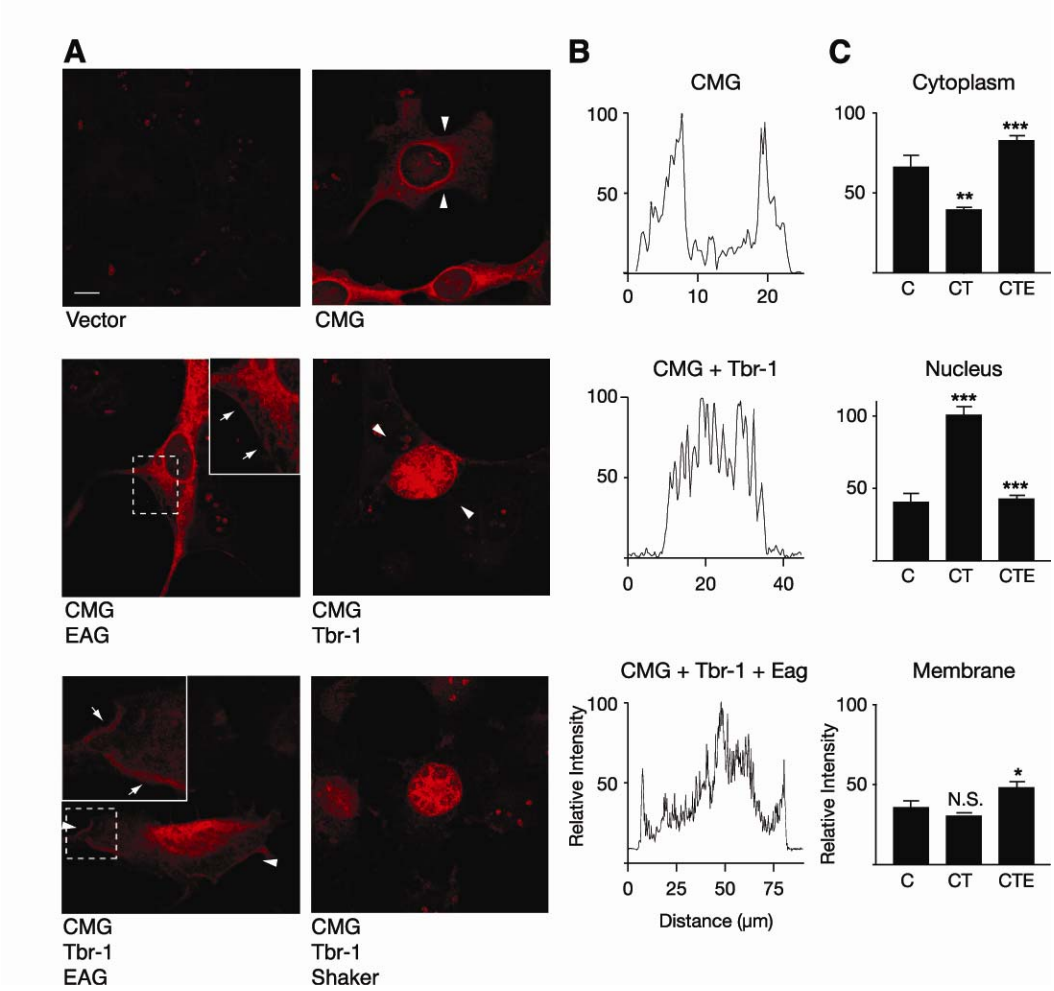
A
Vector
CMG
CMG
EAG
CMG
Tbr-1
CMG
Tbr-1
EAG
CMG
Tbr-1
Shaker
B
CMG
CMG + Tbr-1
CMG + Tbr-1 + Eag
Relative Intensity
Distance (μm)
C
Cytoplasm
Nucleus
Membrane
Relative Intensity
N.S.
C
CT
CTE

another MAGUK-interacting protein (Kim et al., 1995), failed to compete with Tbr-1 to alter CMG localization (*bottom right panel*). Finally, plasma membrane localization of CMG was also observed in the presence of EAG alone (indicated by the arrows in the inset in the *left middle panel*). Differences in CMG localization as a function of co-expression with Tbr-1 and EAG were quantified using line scans of fluorescence intensity normalized to the maximum fluorescence observed in each image examined. Figure 2.3B shows representative line scans, taken across the segments indicated by the arrowheads, for the panels shown in Figure 2.3A. Figure 2.3C displays line scan data for the cytoplasm, nucleus, and membrane averaged across three separate experiments. In each case, EAG produced a significant change in the localization of CMG when compared with the localization of CMG in the presence of Tbr-1 (see also Fig 2.6E).

C.6. EAG and CMG co-immunoprecipitate from *Drosophila* extracts

Immunoprecipitation reactions using protein extracts from wandering third-instar larvae indicated that EAG and CMG associate *in vivo*. In the experiment of Figure 2.4, CMG was immunoprecipitated and the precipitates separated by SDS-PAGE. Blotting with CMG antisera identified a single band near the molecular weight predicted for CMG, 103 kDa (Fig 2.4A), for immunoprecipitates from extracts of both wild type and *eag* null mutants (eag^{sc29}). More importantly, as shown in Figure 2.4B, EAG was observed in both extracts (*left panel*) and CMG immunoprecipitates (*right panel*) from wild type larvae, but was absent in eag^{sc29} larvae. As observed for oocytes, the primary EAG band was higher than the molecular weight predicted for EAG, but this band was identified by three antisera raised against different regions of the EAG protein (data not

FIGURE 2.4

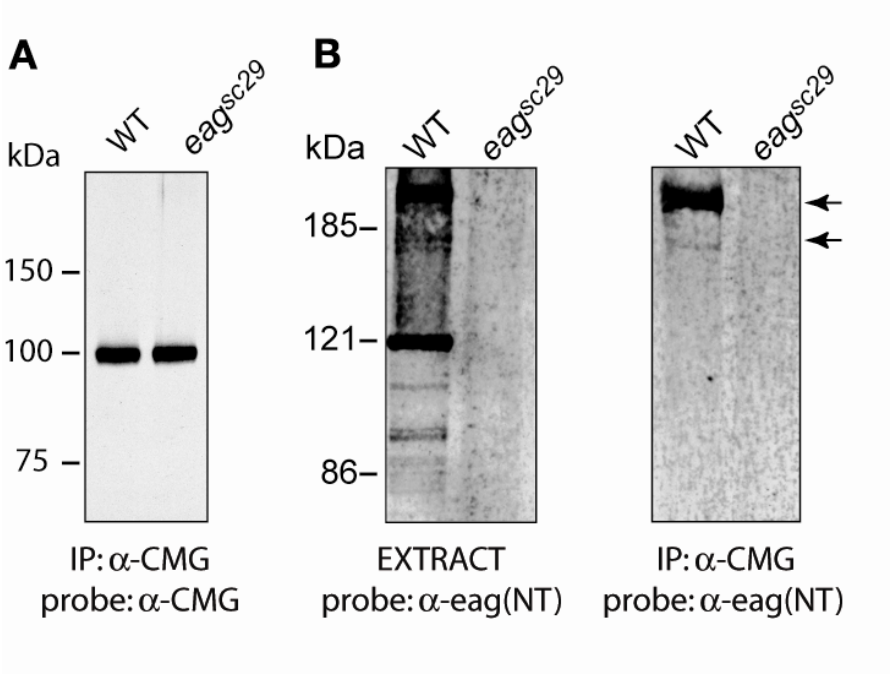

Figure 2.4: Native EAG and CMG coimmunoprecipitate from *Drosophila* extracts. Protein extracts were prepared from the nervous system, imaginal discs, and body muscle fibers of third instar larvae. CMG antisera were used to immunopreciptate CMG and associating proteins from extracts prepared from the indicated genotypes. Precipitated proteins were resolved by SDS-PAGE, transferred to nitrocellulose, and then probed with either CMG (A) or EAG (NT) antisera (B, *right*), followed by HRP-conjugated anti-guinea pig or anti-rabbit IgG, respectively. For comparison, input extract probed with EAG (NT) antisera is shown in the left panel of (b). Respective loads were 5, 10, and 20 µl for extracts, immunoprecipitated and coimmunoprecipitated proteins, respectively (see Materials and Methods). Similar results were obtained in five experiments. Bands were visualized using ECL. WT, Wild type; IP, Immunoprecipitation.

shown). The EAG-CMG complex also could be observed in immunoprecipitation reactions using membrane fractions prepared from adult fly heads (data not shown). In addition, reciprocal co-immunoprecipitation of CMG using α-EAG(NT) antisera was possible, but only when CMG was overexpressed using the Gal4-UAS system coupled with the neuron-specific C155-elav driver; this is presumably because of an observed decrease in EAG precipitation efficiency when using α-EAG(NT) versus α-EAG(CT) antisera (data not shown). These results suggest that EAG and CMG are part of a protein complex *in vivo*; however, neither these results nor our electrophysiological experiments in oocytes address whether the interaction between EAG and CMG is direct.

C.7. *In vitro* binding assays identify a direct interaction between EAG and CMG

A direct association of EAG and CMG was suggested by *in vitro* binding assays (Fig 2.5). In these assays, GST-tagged CMG or CMG domains were immobilized on glutathione sepharose beads and the ability to "pull-down" 6H-tagged EAG fragments assessed in Western blots using antibody directed against the MRSG-6H tag. The EAG and CMG fragments used to map the respective EAG- and CMG-binding sites are shown in Figure 2.5, A and B, together with a rating of their relative binding. As shown in Figure 2.5C for the EAG fragment 6H-$EAG_{869\text{-}1107}$, nearly all of the EAG available associated with GST-CMG (compare lanes 1 and 3). There was minimal background binding to the bead-immobilized GST tag, indicating that the association of EAG with CMG was not a result of a nonspecific effect.

Figure 2.5: A direct interaction between EAG and CMG adaptor protein in *in vitro* binding assays. (A) Schematic representation and respective binding for the EAG protein constructs used in mapping experiments. For comparison, full length EAG is shown at the top with the primary domains as indicated, including the six putative transmembrane domains, pore (P), and the region with homology to cyclic nucleotide binding domains (CNBD). The amino acid residues contained in each EAG construct are noted by the subscripted numbers on the left and the relative binding of each construct to full length CMG is indicated on the right. Note that the EAG C-terminal cytoplasmic domain contains six SH3 binding motifs as defined by the PxxP consensus sequence. The locations of these potential binding sites are indicated by asterisks. **(B)** Schematic representation and respective binding for the CMG constructs used in mapping experiments as described for (a). Binding to 6H-$EAG_{869\text{-}1107}$ is shown in C-F. This fragment was chosen for display because there was minimal degradation during purification. **(C)** 6H-$EAG_{869\text{-}1107}$ binding to full length CMG and CMG domains. GST-tagged CMG fragments immobilized on glutathione Sepharose beads were assayed for their ability to pull-down 6H-$EAG_{869\text{-}1107}$ as described in Materials and Methods. *Top*, western blot probed with MRGS-6H antibody to detect interacting EAG fragments. *Bottom*, bound 6H-$EAG_{869\text{-}1107}$ quantified by densitometry; data are presented as the mean ± SEM; n = 3. **(D)** 6H-$EAG_{869\text{-}1107}$ binding to GST-SH3 domain fusion proteins. *Top*, the ability of purified GST-SH3 domains, derived from the proteins indicated above each lane, to pull-down 6H-$EAG_{869\text{-}1107}$ was in immunoblots by comparing the relative amount of associating 6H-$EAG_{869\text{-}1107}$ to the amount available during the interaction experiment (*left lane*). As shown in lanes 2 and 3, there was little or no background binding to either glutathione Sepharose or immobilized GST tag. *Bottom*, bound 6H-$EAG_{869\text{-}1107}$ quantified by densitometry; data are presented as the mean ± SEM; n = 3. **(E)** Dose-response curves comparing the binding of CMG and the CMG SH3 domains to 6H-$EAG_{869\text{-}1107}$. Wells were coated overnight with 6H-$EAG_{869\text{-}1107}$, washed, and then incubated with the indicated concentrations of GST fusion protein. Bound protein was detected using anti-GST antibody, followed by alkaline phosphatase-conjugated secondary antibody and treatment with p-nitrophenylphosphate. Binding was determined by colorimetric reaction at 405 nm. Each concentration was assayed in quadruplicate. Data are presented as the mean ± SEM; n = 4. O.D., Optical Density. **(F)** Effect of salt concentration on the 6H-$EAG_{869\text{-}1107}$-CMG complex. Experiments examining the binding to GST-CMG were performed as described in Materials and Methods, with the exception that PBS buffer was modified to include the indicated NaCl concentrations. Complex formation was relatively unaffected in up to 1000 mM salt. *Bottom*, bound 6H-$EAG_{869\text{-}1107}$ quantified by densitometry; data are presented as the mean ± SEM; n = 3.

FIGURE 2.5

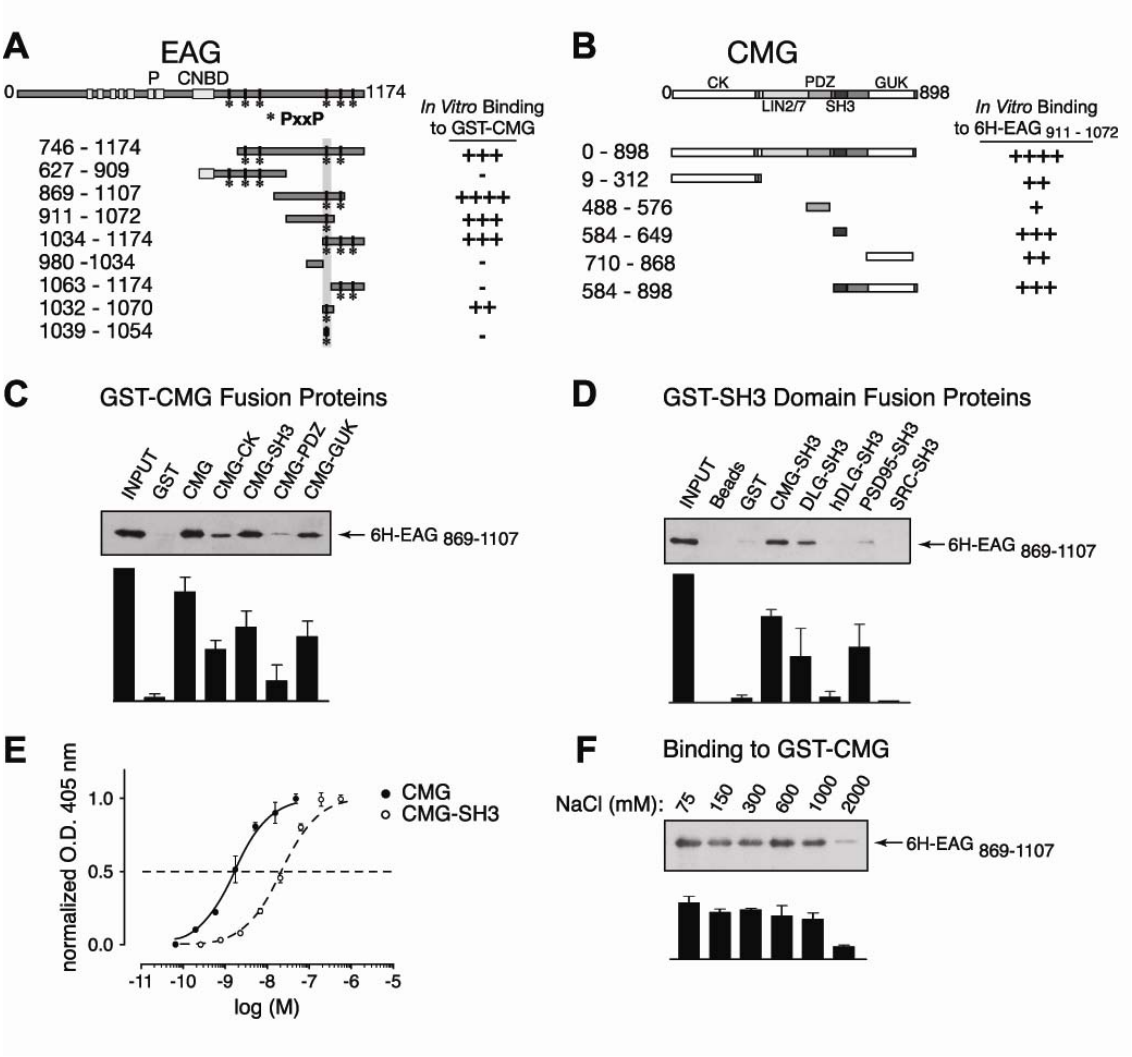
A
EAG
P CNBD
0
1174
* PxxP
In Vitro Binding to GST-CMG
746 - 1174 +++
627 - 909 -
869 - 1107 ++++
911 - 1072 +++
1034 - 1174 +++
980 -1034 -
1063 - 1174 -
1032 - 1070 ++
1039 - 1054 -
B
CMG
CK
PDZ
GUK
LIN2/7
SH3
0
898
In Vitro Binding to 6H-EAG 911 - 1072
0 - 898 ++++
9 - 312 ++
488 - 576 +
584 - 649 +++
710 - 868 ++
584 - 898 +++
C
GST-CMG Fusion Proteins
INPUT
GST
CMG
CMG-CK
CMG-SH3
CMG-PDZ
CMG-GUK
6H-EAG 869-1107
D
GST-SH3 Domain Fusion Proteins
INPUT
Beads
GST
CMG-SH3
DLG-SH3
hDLG-SH3
PSD95-SH3
SRC-SH3
6H-EAG 869-1107
E
normalized O.D. 405 nm
1.0
0.5
0.0
CMG
CMG-SH3
-11 -10 -9 -8 -7 -6 -5
log (M)
F
Binding to GST-CMG
NaCl (mM): 75 150 300 600 1000 2000
6H-EAG 869-1107

EAG C-terminal fragments associating with full length CMG associated most robustly with the SH3 and guanylate kinase (GUK) domains of CMG (Fig 2.5C). Although interactions with the GST-tagged CaMKII-like and PDZ [postsynaptic density-95 (PSD-95)/ DLG/zona-occludens-1] domains of CMG were also observed, the SH3 and GUK domains came closest to approximating the binding observed to the full length CMG protein. Recent structural studies have suggested that the SH3 domain of PSD-95, another MAGUK protein, requires the GUK domain for proper orientation of the SH3 domain-binding pocket (McGee et al., 2001). However, in our experiments, there was no additional increase in the association of EAG when using a larger CMG fragment including both the SH3 and GUK domains (Fig 2.5B, GST-$CMG_{584-898}$).

Additional experiments further characterized the interaction of EAG with CMG in regard to its specificity, affinity and mechanism. Figure 2.5D shows *in vitro* pull-down assays examining the binding of 6H-$EAG_{869-1107}$ to a selection of SH3 domains fusion proteins immobilized on glutathione Sepharose beads. The association of EAG with the CMG SH3 domain was specific because there was minimal binding to the SH3 domains of src and the human DLG ortholog (Fig 2.5D). Although EAG also bound to the SH3 domain of DLG, coexpression of EAG with DLG in oocytes failed to produce an increase in current (data not shown). In ELISAs (Fig 2.5E), full length CMG bound 6H-$EAG_{869-1107}$ with a K_d of 1-2 nM, whereas the CMG SH3 domain displayed a K_d of ~ 20 nM. Thus, interactions with other domains of CMG likely contribute to the affinity of the interaction. Finally, as shown in Figure 2.5F, the interaction between EAG and CMG was resistant to increases in salt concentration. Binding to CMG only decreased when

the salt concentration was increased to above 1 M, suggesting that binding is not solely mediated by electrostatic interactions.

C.8. Mapping the EAG interaction site identifies a noncanonical SH3 binding motif

Additional *in vitro* binding experiments were performed with the aim of mapping the primary interaction site in EAG. The C-terminal cytoplasmic domain of EAG contains six putative SH3 domain binding sites, as identified by the presence of a PxxP consensus sequence (Sparks et al., 1998). Indeed, as indicated on the right of Figure 2.5A, any EAG C-terminal fragment that contained the fourth putative SH3 binding motif directly associated with GST-tagged CMG. To determine whether this region was sufficient for the interaction, 38 amino acids spanning spanning the fourth SH3 motif (residues 1032 – 1070) were attached to a DHFR tag. Because DHFR-$EAG_{1032-1070}$ associated with CMG (Fig 2.5A), the fourth SH3 motif appears necessary and sufficient for the interaction.

Two strategies were employed to definitively establish the fourth SH3 binding motif as the site of the interaction with CMG. First, a peptide containing the fourth PxxP motif together with additional flanking amino acids ($EAG_{1039-1054}$) was synthesized, cross-linked to beads, and then examined for its ability to pull-down CMG SH3 domain that had been cleaved from the GST tag using thrombin. No association was observed even though a 16 amino acid peptide that has been used to investigate the specificity of binding to the Src SH3 domain (src peptide) (Sparks et al., 1998) associated with the Src SH3 domain under the same experimental conditions (data not shown). Second, rationalizing that the peptide may not have contained a sufficient number of flanking amino acids, we generated a point mutation in the first proline of the fourth SH3 binding

motif in the 6H-EAG$_{869-1107}$ fragment (P1045A). Little or no decrease in the association of this fragment with full length CMG was observed (Fig 2.6B, compare lanes 1 and 4).

Recent work has established that some SH3 domains interact with a noncanonical binding motif characterized by an RxxK consensus sequence (Harkiolaki et al., 2003; Liu et al., 2003). As shown in Figure 2.6A, this sequence also is present in EAG just four amino acids upstream of the fourth PxxP motif. Indeed, binding to CMG was substantially reduced when leucine was substituted for arginine at residue 1037 (Fig 2.6B, lane 2, R1037L$_{869-1107}$). Binding to the SH3 domain was eliminated when the other basic residue in this motif, lysine at position 1040, was replaced by methionine (Fig 2.6B, lane 3, K1040M).

To determine whether the above mutations were sufficient to disrupt the effect of CMG on EAG current, we returned to the oocyte expression system. As shown in Figure 2.6C, which compares scaled representative traces for wild type and EAG-R1037L/ K1040M channels, channel function was largely unaffected by mutations in the SH3 domain binding site. Figure 2.6D shows the result of coexpressing CMG with either wild type EAG, EAG-R1037L, EAG-K1040M, or the double mutant, EAG-R1037L/K1040M. As observed in our earlier experiments, CMG produced a more than twofold increase in the whole-cell conductance of wild type channels. The CMG-mediated increase was drastically reduced for EAG-R1037L and eliminated in EAG-K1040M and the double mutant. Finally, the SH3 binding motif also was required for the effect of EAG on CMG localization in COS-7 cells. As shown in Figure 6E, although wild type EAG produced the same changes in CMG localization observed in the experiments of Figure 2.3 (CTE-

Figure 2.6: A noncanonical SH3 binding motif in EAG mediates the EAG-CMG interaction. (A) Comparison of the amino acid sequence surrounding the fourth putative SH3-binding motif to the amino acid sequence of the noncanonical SH3-binding site in SLP-76, the Src homology 2 (SH2) domain containing a leukocyte protein of 76 kDa. Note that both proteins also contain prolines in the nearby sequence. **(B)** *In vitro* binding assays comparing the association of 6H-$EAG_{869\text{-}1107}$ and mutant EAG fragments (R1037L, K1040M, and R1037L/K1040M EAG) to GST-CMG, as indicated. *Top*, immunoblotting with MRGS-6H antibody to detect interacting EAG fragments. *Middle and Bottom*, Coomassie-stained gels showing the relative amounts of GST-CMG and EAG fragments present in each interaction experiment. **(C)** Scaled representative traces obtained for wild type and EAG-R1037L/K1049M channels. Currents were elicited by a 400 ms test pulse to +40 mV from a holding potential of -80 mV. Peak current amplitudes were 2.2 and 5.0 μA for EAG and EAG-R1037L/K1040M, respectively. **(D)** Mutations in the EAG binding site inhibit the effect of CMG on EAG conductance. Fold-increase in the whole-cell conductance as a function of CMG coexpression for oocytes expressing wild type, R1037L, K1040M, and R1037L/K1040M EAG channels. Conductances were determined as described in Figure 1G in response to a test pulse to 60 mV (holding potential, -80 mV). To normalize for normal variations in expression across different batches of oocytes, the mean conductance in the presence of CMG was normalized to the mean conductance obtained for oocytes expressing only EAG or the indicated EAG mutants. The SE and number of oocytes examined for each condition is indicated above each bar. The effect of CMG was statistically analyzed using a two way ANOVA with oocyte batch and CMG as variables (*** $p < 0.001$; N.S., not significant). WT, Wild type. **(E)** Disruption of the CMG binding site also disrupts the ability to compete with Tbr-1 and recruit CMG out of the nucleus of COS-7 cells. *Top*, Background subtracted images for three expression conditions: CMG and Tbr-1 (CT), CMG, Tbr-1, and EAG (CTE), and CMG, Tbr-1, and EAG-RL/KM (CTR). Arrowheads indicate the segments used for the line scans presented in the middle panels. Scale bar, 10 μm. *Middle*, Representative line scans obtained as described in Figure 3C. *Bottom,* Averaged, normalized line scan data from three separate experiments examining the distribution of CMG to the cytoplasm, nucleus and membrane for the three expression conditions. One-way ANOVA comparisons of fluorescence intensity between CT versus CTE and CTE versus CTR conditions were significant (*** $p < 0.001$). In contrast, there was no significant difference (N.S.) between the CT and CTR conditions. Error bars represent SEM.

FIGURE 2.6

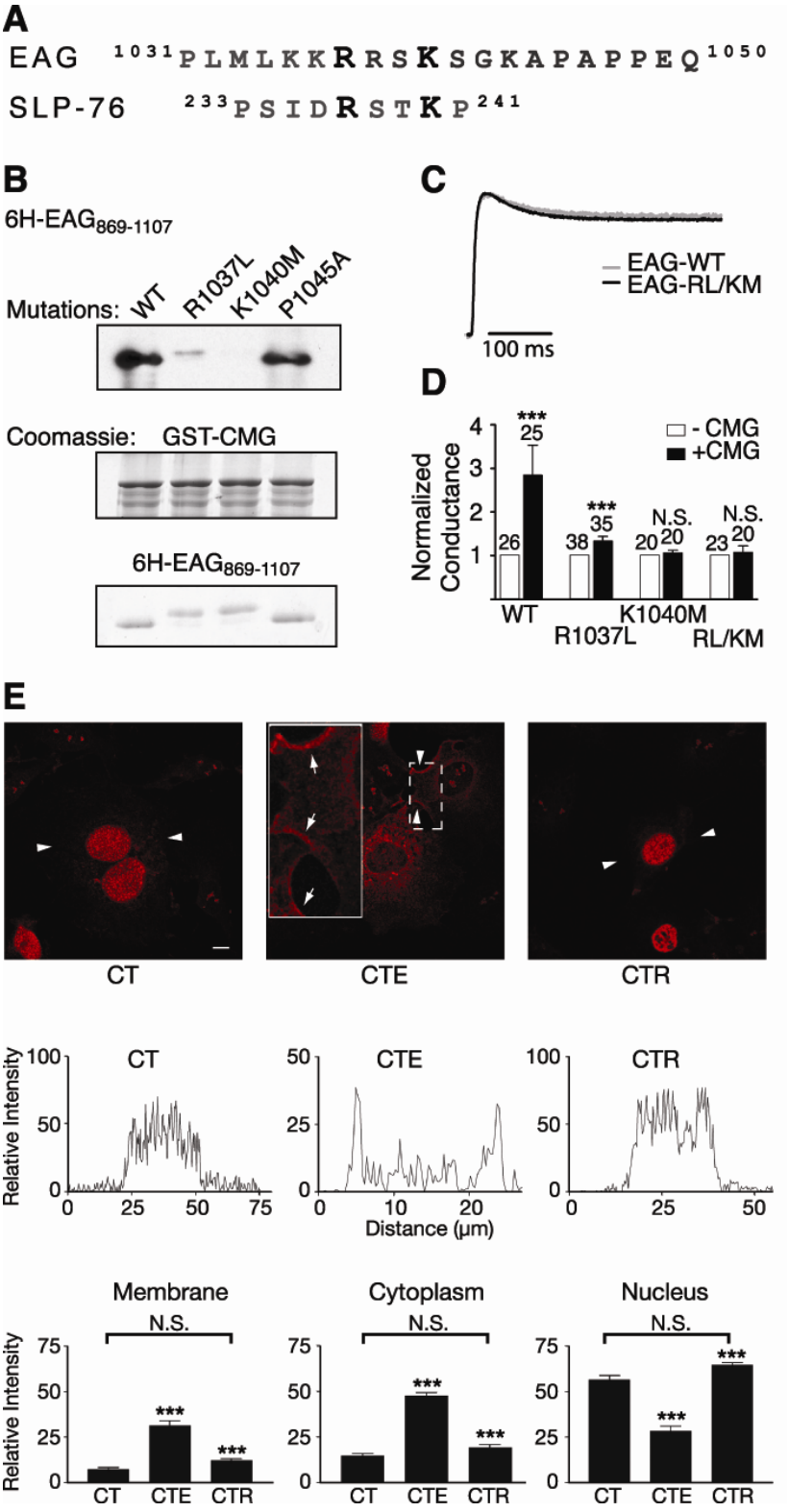
A
EAG 1031 P L M L K K R R S K S G K A P A P P E Q 1050
SLP-76 233 P S I D R S T K P 241
B
6H-EAG869-1107
Mutations: WT R1037L K1040M P1045A
Coomassie: GST-CMG
6H-EAG869-1107
C
EAG-WT
EAG-RL/KM
100 ms
D
Normalized Conductance
- CMG
+CMG
***
N.S.
WT
K1040M
R1037L
RL/KM
E
CT
CTE
CTR
Relative Intensity
Distance (μm)
Membrane
Cytoplasm
Nucleus
N.S.
***

labeled panels), EAG-R1037L/K1040M failed to compete with Tbr-1 (CTR-labeled panels). When statistically analyzed using a one-way ANOVA, there was no significant difference in the distribution of CMG to the membrane, cytoplasm, or nucleus when comparing averaged line scan data for the CMG and Tbr-1 (CT) and CMG, Tbr-1, and EAG-R1037L/K1040M (CTR) conditions. Together, these results indicate that a direct interaction between EAG and CMG is required for the effect EAG on the localization of CMG, as well as the effect of CMG on EAG current.

D. DISCUSSION

Our findings indicate that EAG is functionally regulated by an association with the CMG adaptor protein. The primary effect of CMG is to increase EAG current and whole-cell conductance, and this increase depends on a direct association between proteins, because mutations of the CMG binding motif in EAG prevent the effect. In addition, EAG successfully competes with another CMG/CASK-interacting protein to alter the localization of CMG. Thus, another distinct function of the EAG-CMG complex may be to localize CMG to the plasma membrane.

The mechanism primarily responsible for the increase in current appears to be an increase in the surface expression of EAG. Intriguingly, effects opposite those produced by CMG, namely decreased EAG current, decreased surface expression of EAG, and decreased inactivation, are observed when phosphorylation of EAG-T787 is prevented either by mutation of the phosphorylation site or by inhibition of CaMKII (Wang et al., 2002b). These findings suggest that the effect of CMG is produced by an increase in the phosphorylation of EAG-T787. In agreement, CMG increased the phosphorylation of

EAG-T787, and mutation of this site prevented the CMG-mediated increase in EAG current without disrupting formation of the EAG-CMG complex. These results suggest that the mechanism underlying the effect of CMG is indirect and point to a change in the localization or activity of either a kinase or phosphatase in the vicinity of the channel. In addition, however, the possibility that CMG also directly affects the surface expression of phosphorylated EAG has not been ruled out. Direct and indirect effects of CMG may additively affect the membrane association of EAG channels.

At present, the enzyme most likely responsible for mediating the effect of CMG is CaMKII. EAG-T787 has previously been shown to be phosphorylated by CaMKII, inhibition of CaMKII has been shown to decrease EAG current, and CaMKII directly associates with CMG (Lu et al., 2003; Wang et al., 2002b). However, it is not known whether other kinases such as protein kinase A can also phosphorylate T787, nor has the phosphatase responsible for dephosphorylating T787 been identified. Our results do not rule out the possibility that CMG may change the localization, activity or efficiency of another kinase or a protein phosphatase. Nonetheless, given that CMG interacts with CaMKII (Lu et al., 2003) and given that no interaction between CMG (or its orthologs) and other kinases or phosphatases has been identified, the most likely model accounting for the CMG effect on EAG is one in which a common association with CMG colocalizes EAG with CaMKII and increases the efficiency of phosphorylation.

Intriguingly, after decreases in Ca^{2+}, the association with CMG promotes phosphorylation of T306 of CaMKII, rendering the kinase inactive and then releasing it (Lu et al., 2003). CaMKII cannot be activated by subsequent increases in Ca^{2+} as long as phosphorylation of T306 persists. The creation of a pool of inactive kinase predicts that

CMG should have produced a decrease in EAG current, rather than the observed increase at basal Ca^{2+} levels. These observations can be reconciled, however, if the cytoplasm and the local membrane are considered as separate compartments. Because CMG only associates with active kinase, CMG, in addition to globally increasing the pool of inactive kinase, may ensure that only active kinase is in the vicinity of the channel. Alternatively, EAG may directly or indirectly change the effect of CMG on CaMKII. Assuming that the majority of EAG is normally localized at the membrane, either alternative would result in an increase in active kinase at the membrane versus the cytoplasm. The stability of the CMG/CaMKII complex may also be regulated by the activity history of the synapse. Ca^{2+} influx can cause T287 phosphorylation, which, in addition to making the kinase activity Ca^{2+}-independent, can decrease the off-rate of CaM by four orders of magnitude (Putkey and Waxham, 1996). CaMKII with "trapped" CaM would be resistant to deactivation by CMG even at low intracellular Ca^{2+}. EAG that was localized at a synapse that had been previously active then would be expected to be susceptible to CMG regulation.

The common association of CMG with EAG and CaMKII suggests that CMG acts as the central scaffold for the complex. However, EAG also directly associates with activated CaMKII (Sun et al., 2004), suggesting that EAG and CMG play equally important roles. The association between EAG and CaMKII constitutively activates the kinase and CaMKII remains associated with EAG even once Ca^{2+} returns to resting levels (Sun et al., 2004). Thus, the presence of EAG in the complex may alter the net effect of CMG on CaMKII activity. Finally, although phosphorylation of EAG-T787 is likely to occur via the constitutively active kinase, this constitutive activity is considerably lower

than that of the fully activated kinase (Sun et al., 2004). Indeed, in our experiments, the association with CMG further increased EAG currents and phosphorylation of the channel above and beyond the levels achieved by the CaMKII endogenous to oocytes. CMG may localize and then transfer CaMKII to EAG, or CaMKII holoenzyme, which has 12 subunits, may be able to bind to both EAG and CMG simultaneously. In addition, CMG may increase the number of CaMKII molecules in the vicinity of the channel, and interlocking all three proteins may further stabilize an EAG-CMG-CaMKII complex.

The clearest demonstration of the physiological importance of CMG/CASK/LIN-2, to date, has been obtained in *Caenorhabditis elegans*, in which a complex of proteins including LIN-2, LIN-7 and LIN-10 localizes the receptor tyrosine kinase LET-23 to the basolateral surface of vulval precursor cells. The absence of LIN-2, LIN-7 or LIN-10 results in mislocalization of LET-23 receptors, causing a vulvaless phenotype (Kaech et al., 1998). The LIN-2--LIN-7--LIN-10 complex appears evolutionarily conserved because a similar complex, consisting of CASK, Velis and the munc18-1 interacting protein Mint1, homologs of LIN-2, LIN-7 and LIN-10, respectively, has been observed in the mammalian central nervous system (Butz et al., 1998). These authors suggest that CASK is a scaffold for proteins involved in synaptic vesicle exocytosis and cell adhesion. The presynaptic complex may include not only Velis and Mint1, but also N-type Ca^{2+} channels and neurexins (Hata et al., 1996; Maximov et al., 1999). When combined with the previously demonstrated presynaptic localization of EAG, CMG and CaMKII (Lu et al., 2003; Sun et al., 2004; Wang et al., 2002b), our findings provide additional support for a role of CMG/CASK in presynaptic function *in vivo*.

E. MATERIALS AND METHODS

E.1. Plasmids and construction

For protein purification, plasmids containing DNA fragments spanning the indicated amino acids were generated by PCR using primers containing restriction sites and bases to maintain reading frame during subcloning. Glutathione S-transferase (GST) and 6Histidine (6H) fusion constructs were generated using the pGEX-4T1 or pGEX-KG vectors (Amersham Biosciences, Piscataway NJ) (Guan and Dixon, 1991) or the pQE30 vector series (Qiagen, Valencia CA), respectively. Where indicated, sequence encoding dihydrofolate reductase (DHFR) was subcloned into the pQE-*eag* construct to aid in the purification and identification of the small EAG fragment. PQE32-$eag_{869-1107}$ was a gift from B. Ganetzky (University of Wisconsin, Madision, WI). With the exception of the SH3 domains of CMG and *Drosophila* discs large (DLG), GST-SH3 domain fusion proteins were a gift from Brian Kay (Argonne National Laboratory, Argonne IL). Site-directed mutagenesis was performed using the PCR-based QuikChange mutagenesis kit (Stratagene, La Jolla CA).

For expression of EAG mutant constructs in *Xenopus* oocytes, *Sph* I and *Nae* I sites flanking the EAG SH3 domain binding site were used to subclone single site mutations from pQE-*eag* constructs into pGH19-*eag* (Wilson et al., 1998). A Kozak sequence was added to pGEX-*cmg* using PCR, and *cmg*, together with the Kozak sequence, was shuttled into pBluescript-KSM (a gift from W. Joiner and L.K. Kaczmarek, Yale University, New Haven, CT), which had been modified to contain the untranslated

regions of the *Xenopus* β-globin gene and a more flexible cloning site. All constructs were verified by sequencing.

E.2. Protein purification

GST-fusion proteins were purified according to manufacturer protocols (Amersham Biosciences). BL21 cells were freshly transformed with the construct of interest. Large-scale (1 L) cultures were grown in Luria Broth (LB) with ampicillin for 6 hrs and then induced for 6-12 hrs with isopropyl-β-D-thiogalactopyranoside. Bacteria were harvested by centrifugation, lysed, and cellular protein solubilized in buffer containing 150 mM NaCl, 20 mM Tris (pH 7.4) and 1% Triton X-100 in the presence of protease inhibitors (0.5 mM phenylmethanesulfonyl fluoride and 0.004 mg/ml each of aprotonin, pepstatin A, and leupeptin). In some cases GST-CMG was purified by incubation with 0.8 % N-lauroylsarcosine prior to solubilization and then neutralized with twice the concentration of Triton X-100. This increased the yield of CMG protein without affecting binding activity. Protein suspensions were centrifuged to remove insoluble material, and the supernatant incubated for 60-90 min with Glutathione-Sepharose 4B beads (Amersham Biosciences). Bead-immobilized proteins were extensively washed with 150 mM NaCl, 20 mM Tris (pH 7.4) and stored as a 50% slurry at 4 °C until use. 6H fusion proteins were purified similarly using nickel-nitrilotriacetic acid beads (Qiagen, Valencia CA) and a solubilization buffer containing 500 mM NaCl, 20 mM Hepes (pH 7.8) and 1% Triton X-100 in the presence of protease inhibitors. 6H fusion proteins were fractionally eluted from beads using successively increasing concentrations of imidazole ranging from 8 to 400 mM. Eluted fractions were checked for the presence of the desired protein using

SDS-PAGE, and fractions containing the protein were pooled and dialyzed overnight in PBS (consisting of the following, in mM: 136 NaCl, 2.7 KCl, 10 Na_2HPO_4, 1.8 KH_2PO_4, pH 7.4). Dialyzed protein was stored at 4°C or frozen at -20°C prior to use. Protein concentrations were determined by comparison to known concentrations of bovine serum albumin (BSA).

E.3. Peptides and antibodies

Peptides used for binding studies and immunization were synthesized by Open Biosystems (Huntsville, AL). An N-terminal peptide corresponding to amino acids 161-179 of the EAG sequence and a purified C-terminal (CT) fragment (6H-$EAG_{1034-1174}$) were used for immunization of rabbits according to standard procedures (Open Biosystems). Sera were screened against the antigens in ELISAs and in Western blots of purified N- or C-terminal EAG fragments as appropriate. Purified GST-$CMG_{152-897}$ was used for the immunization of guinea pigs as previously described (Dimitratos et al., 1997). Phosphospecific anti-EAG antibody was a gift from Leslie Griffith (Brandeis University, Waltham, MA).

E.4. *In vitro* binding assays

GST fusion proteins immobilized on Sepharose beads were mixed with 6H fusion proteins in PBS containing 0.5% Triton X-100 and protease inhibitors (EDTA-free Complete tablets; F. Hoffmann-LaRoche, Basel, Switzerland) and incubated with shaking for 2-3 hrs at 4 °C. Except where indicated otherwise, the protein concentrations used were 1-2 and 0.5-1 μM, respectively, in 100 μl buffer containing a constant 10 μl bead

bed volume. The beads were collected by centrifugation and then washed three times with PBS containing 0.1% Triton X-100, followed by three washes with 50 mM Tris, pH 8.0, 140 mM NaCl, 0.1% Triton X-100, and a final wash with 50 mM Tris, pH 8.0. The pellets, including beads and associated proteins, were resuspended in sample buffer and analyzed by SDS-PAGE and Western blotting. Blots were probed with MRGS-6H antibody (Qiagen) followed by horseradish peroxidase (HRP)-conjugated anti-mouse secondary and then visualized with ECL (Amersham Biosciences).

E.5. ELISAs

ELISAs were performed as described previously (Garcia et al., 1998; Muller et al., 1996) with minor modifications. GST-CMG fusion proteins were eluted from glutathione Sepharose according to manufacturer protocols (Amersham Biosciences). 6H-$EAG_{869-1107}$, at a concentration of 0.16 μg/ml in BBS (125 mM borate, 75 mM NaCl pH 8.5), was bound to the wells of Costar (Cambridge, MA) 96-well assay plates by overnight incubation (4°C). Plates were then washed extensively with BBS and blocked with BBS containing 1% bovine serum albumin (BBS-BSA) prior to addition of serially diluted CMG protein at the indicated concentrations (50 μl/well). Each concentration was assayed in quadruplicate. After overnight incubation (4°C), plates were washed four times and then incubated with anti-GST antibody (1:1000 in BBS-BSA). Plates were washed again and incubated with alkaline phosphatase-conjugated anti-rabbit IgG (1:1000 in BBS-BSA). After a final set of washes, binding to 6H-$EAG_{869-1107}$ was determined by treating wells with FAST p-Nitrophenylphosphate (Sigma-Aldrich, St. Louis MO) and measuring the colorometric reaction at 405 nm.

E.6. Immunocytochemistry

COS-7 cells were maintained at a subconfluent density at 37°C and 5% CO_2 in DMEM supplemented with 10% fetal bovine serum (FBS). Twenty-four hours before transfection, cells were plated and grown to 80% confluence on 12 mm poly-L-lysine coated glass coverslips (Becton-Dickinson, Franklin Lakes NJ). For transient transfection, each coverslip was washed twice with Opti-MEM (Invitrogen, Carlsbad CA) and incubated for 10 hrs in 350 µl Opti-MEM containing 0.4 µg of each of the indicated cDNAs and 1.5 µl LipofectAMINE reagent (Invitrogen, Carlsbad CA), followed by incubation in 1 ml of DMEM with 10% FBS for 12 hrs. Coverslips were washed with PBS and fixed with a 3:7 mixture of 50 mM glycine (pH 2.0) and absolute ethanol for 1 hr at room temperature (RT). After washing three times, cells were permeabilized with 0.1% Triton-X 100 in PBS for 20 min (RT) and blocked for 30 min in a blocking buffer consisting of 10 % horse serum and 0.1% BSA in distilled deionized water. Cells were then incubated with a 1:500 dilution of CMG antisera in blocking buffer for 1 hr at RT, washed with PBS, and incubated with a cyanine 2- or rhodamine-conjugated secondary antibody (Jackson ImmunoResearch, West Grove, PA) for 30 min at 37 °C. Coverslips were mounted on glass slides with Gelmount medium (Biomeda, Foster City, CA). Results were viewed with a Zeiss (Oberkochen, Germany) LSM 510 confocal microscope, and images were prepared for publication with Adobe Photoshop (version 7.0; Adobe Systems, San Jose, CA).

E.7. Immunoprecipitations

Body-wall muscle fibers and CNS tissue from third-instar larvae of the indicated genotypes were homogenized in radioimmunoprecipitation assay buffer (150 mM NaCl, 50 mM Tris pH 8.0, 0.1% SDS, 1% IGEPAL CA-630, 0.5% sodium deoxycholate) containing Complete protease inhibitor on ice and solubilized for 20 min. Cellular debris was removed by centrifugation (3000 x g, 5 min, 4 ^{o}C).

Fly head tissue was obtained from 15 ml of adult flies frozen in liquid nitrogen. Heads were collected by sieving and homogenized in ice cold HM buffer (1 mM EDTA, 5 mM HEPES, pH 7.4, and Complete protease inhibitor). Cell debris was removed by centrifugation, and supernatant was further centrifuged to separate membranes (15000 x g, 15 min). The heavy membrane pellet was solubilized in ice-cold buffer (HM buffer plus 100 mM NaCl and 1 % Triton X-100) for 20 min and supernatant was precleared with protein-A/G agarose beads (Santa Cruz Biotechnology, Santa Cruz CA).

For immunoprecipitations from *Xenopus* oocytes, 30 oocytes for each condition were homogenized in 1.5 ml 100 mM NaCl, 1 mM DTT, 0.5% Triton X-100, 20 mM Tris pH 7.4 and Complete protease inhibitor, and then solubilized on ice for 15 min. Homogenate was centrifuged 20000 x g, 4 ^{o}C, for 10 min and the supernatant collected.

Protein concentrations of homogenates were determined using Bradford assay (Bio-Rad, Hercules CA) and equilibrated across conditions by diluting homogenates to a concentration of 2 mg/ml. A volume of 600 µl of diluted extract was used for each immunoprecipitation reaction. CMG and EAG (NT) antisera were added to protein samples and incubated for 16 hrs at 4 ^{o}C. Immunocomplexes were precipitated with protein-A/G beads for 2 hrs at 4 ^{o}C and then washed 3 times in solubilization buffer and boiled for 10 min in sample loading buffer (250 mM Tris pH 6.8, 12.5% glycerol,

0.125% bromophenol blue, 1% SDS, 3% β-mercaptoethanol). After addition of sample buffer, 5, 10, and 20 μl were loaded in each lane for extracts, immunoprecipitated and co-immunoprecipitated proteins, respectively.

Immunoprecipitations and cellular extracts were resolved via SDS-PAGE (8% acrylamide, 250 mM Tris pH 6.8, 2.5% SDS) and transferred to polyvinylidene difluoride (PVDF) membrane for Western blotting. Blots were blocked (5% dry milk in TBS) and washed, probed with either CMG or EAG (CT) sera (1:1000 and 1:2000, respectively) followed by HRP-conjugated secondary antibody (1:2000) and visualized by ECL (Amersham Biosciences).

For experiments biotinylating surface membrane proteins, oocytes were washed in cold PBS then incubated for 30 min in 2 mM Sulfo-NHS-LC-Biotin (Pierce, Rockford, IL) in PBS. The labeling reaction was quenched with 3 washes of 100 mM glycine in PBS. Fifty oocytes were homogenized in 1 ml of Buffer H (100 mM NaCl, 0.5% Triton X-100, 20 mM Tris, pH 7.4) supplemented with Complete protease inhibitor, 1 mM orthovanadate, 1 mM benzamidine, 1% phosphatase inhibitor cocktail 1 (Sigma), 2 μM microcystin LR and 5 mM 2-glycerol-phosphate.

Volume intensities of protein bands were quantified using Quantity One software (Bio-Rad). Experimental values ($n \geq 3$) were corrected for background by subtracting values obtained for uninjected lanes, and then were normalized to the value obtained for immunoprecipitated wild type EAG in the absence of CMG.

E.8. Electrophysiology

For expression in *Xenopus* oocytes, plasmids were linearized and RNA transcribed using the appropriate RNA polymerase according to manufacturer instructions (Message Machine; Ambion, Austin TX). RNA concentrations were quantified with spectrophotometric readings using an average reading for three or four dilutions of RNA.

The follicular membrane of stage V-VI oocytes was removed by incubation in Ca^{2+}-free OR2 solution (containing the following, in mM: 82.5 NaCl, 2.5 KCl, 1 $MgCl_2$, 5 Hepes, pH to 7.6 with NaOH) containing collagenase (2 mg/ml; Type 1A Sigma) for ~2 h at RT with gentle agitation. Oocytes were injected with premixed stocks of *eag* and *cmg* RNA. Individual oocytes were injected with 0.1-0.2 ng *eag* RNA and an excess of *cmg* RNA. In some oocyte batches (oocytes from the same frog), the capacity of oocytes to translate the *eag* constructs was verified by performing parallel injections of a larger volume of the same RNA mix and observing a linear increase in EAG current amplitude. After RNA injections, oocytes were maintained in L-15 media (containing the following: 50% L-15, 15 mM Hepes, 50 mg/ml gentamycin, and 5 mg/ml BSA, pH to 7.4 with NaOH) at 18 ^{O}C for 3-5 days. Recordings were performed using a Turbo TEC-10C amplifier (NPI Electronics, Tamm, Germany) and pCLAMP8 software (Molecular Devices, Union City, CA). The extracellular recording solution contained the following (in mM): 140 NaCl, 2 KCl, 1 $MgCl_2$, 10 Hepes, pH 7.1 with NaOH. Pipettes were filled with 2 M KCl and had resistances of 0.3 - 0.6 MΩ. Experiments were performed at RT.

Amplitude measurements refer to the peak currents observed during test pulses to the indicated voltages. Activation and inactivation time constants were determined by fitting traces (excluding capacitative transients) with two exponentials and a steady state.

Unless otherwise noted, measurements were statistically compared using a two-way ANOVA. Data are presented as the mean ± SEM.

CHAPTER III

BI-DIRECTIONAL REGULATION OF *DROSOPHILA* ETHER-Á-GO-GO POTASSIUM CHANNELS BY CA^{2+}/CALMODULIN-DEPENDENT MECHANISMS

A. ABSTRACT

Ether á go-go (EAG) potassium (K^+) channels play a critical role in regulating synaptic activity in *Drosophila*. Because EAG channels are presynaptically localized, calcium (Ca^{2+})-dependent regulation of EAG current could serve as an excellent feedback mechanism for activity-dependent changes in synaptic strength. We have previously shown that Ca^{2+}/calmodulin (CaM)-dependent protein kinase type II (CaMKII) enhances EAG current by phosphorylation of EAG. Here, we show that Ca^{2+}/CaM also acts directly to modulate EAG currents and this modulation is independent of CaMKII regulation. *In vitro* binding assays and electrophysiological analysis in *Xenopus* oocytes indicate that Ca^{2+}-dependent binding of CaM to the C-terminus inhibits EAG current. The effects of CaM mutants suggest that the C-terminal lobe of CaM anchors CaM to EAG at low Ca^{2+} concentrations and that the N-terminal lobe of CaM mediates current inhibition at higher Ca^{2+}. To determine how the opposing effects of CaM and CaMKII affect synaptic currents *in vivo*, we recorded from the larval neuromuscular junctions (NMJs) of transgenic flies expressing *eag* with point mutations in either the CaM binding

or CaMKII phosphorylation site. We show that acute inhibition of EAG current by Ca^{2+}/CaM plays a critical role in frequency-dependent facilitation, whereas phosphorylation-dependent increases in EAG stabilize synaptic activity at basal levels of intracellular Ca^{2+}. Our results demonstrate how Ca^{2+}-dependent mechanisms, through divergent effects on a single target, can have opposing short-term and long-term effects, and suggest that EAG channels may be an important target for activity-dependent scaling at presynaptic sites.

B. INTRODUCTION

Drosophila EAG channels give rise to a voltage-dependent K^+ current that is critical for proper neuronal signaling.EAG is present along axons, where it presumably facilitates action potential repolarization, and at synaptic sites, where it can affect synaptic transmission (Wang et al., 2002; Sun et al., 2004). In recordings from larval NMJs, *eag* mutants exhibit a high level of spontaneous activity and an increase in the number and size of evoked excitatory junctional potentials (EJPs), features that are consistent with a loss of hyperpolarizing K^+ current (Ganetzky and Wu, 1983; Wu et al., 1983a; Griffith et al., 1994). In addition, a role in the CNS is indicated by the failure of *eag* flies to learn in courtship conditioning assays (Griffith et al., 1994). In mammals, immunocytochemistry and in situ hybridization indicate that the homologs of EAG (EAG1/KCNH1 and EAG2/KCNH5) are enriched in the olfactory bulb, hippocampus, and layers II-VI of the cerebral cortex (Ludwig et al., 1994; Ludwig et al., 2000; Saganich et al., 2001; Jeng et al., 2005).

Many channels have evolved Ca^{2+}-dependent feedback mechanisms that ensure synaptic transmission is robust and capable of adaptation. In the case of EAG, we have shown that CaMKII phosphorylates the channel and that phosphorylation increases EAG current by increasing the surface expression of EAG channels (Wang et al., 2002; Marble et al., 2005). In contrast, currents of the human EAG homolog, EAG1, are inhibited by intracellular Ca^{2+} (Stansfeld et al., 1996; Meyer et al., 1999; Schonherr et al., 2000). This regulation of EAG1 is mediated via a direct interaction with calmodulin (CaM), but Ca^{2+}/CaM was not found to inhibit *Drosophila* EAG currents. Because the primary CaM-binding domain (CBD) of human EAG shares 44% amino acid identity and 69% amino acid similarity with the corresponding region of the *Drosophila* channel (Figure 3.1), we reinvestigated the effect of CaM on *Drosophila* EAG currents.

In this study, we found that Ca^{+2}-dependent binding of CaM inhibited *Drosophila* EAG currents, most likely via a depolarizing shift the voltage-dependence of the channel. Co-expression with mutant CaM constructs revealed that binding and the functional effects were differentially mediated by the C- and N-terminal lobes of CaM. Recordings at the NMJs of transgenic larvae expressing *eag* constructs with mutations in either the CaM binding or CaMKII phosphorylation site showed that modulation by CaM contributes to short-term synaptic plasticity, whereas modulation by CaMKII contributes to long-term stabilization of synaptic activity. Our results suggest that the opposing actions of Ca^{2+}/CaM and CaMKII operate on different timescales to promote synaptic stability while still allowing for short-term changes in synaptic strength.

FIGURE 3.1

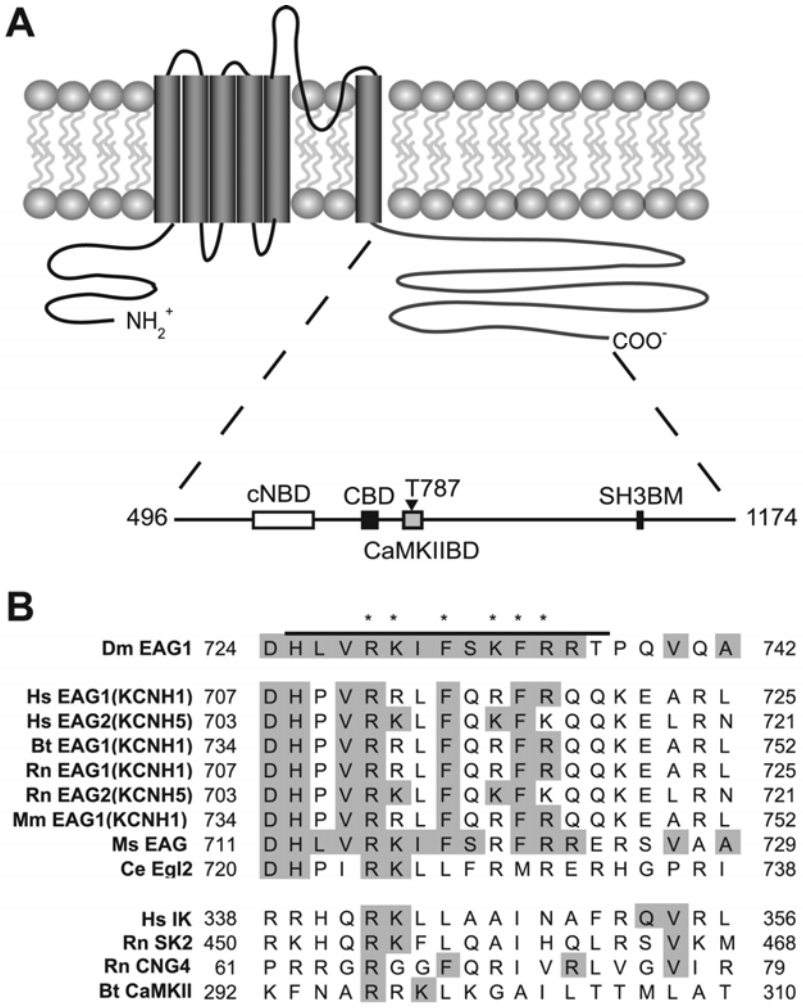

Figure 3.1: Schematic of the EAG K+ channel.
(A) Topology of a EAG K+ channel subunit in the plasma membrane with a schematic highlighting the intracellular C-terminal tail with several domains indicated: cNBD (region similar to cyclic-nucleotide binding domains but lacks nucleotide-binding activity, residue 593-665), CBD (putative CaM-binding domain, aa 725-737), the CaMKII phosphorylation site (aa T787, indicated by the inverted triangle, ref. 2), CaMKIIBD (CaMKII binding domain, aa 773-794, ref. 1), and the SH3BM (SH3 binding motif, aa 1032-1070, ref. 12). **(B)** Sequence alignment of the putative CaM-binding domain in EAG channels from Drosophila (Dm), human (Hs, accessions: NP_002229 and NP_647479), cow (Bt, accession NP_776797), rat (Rn, accessions NP_113930 and NP_598294), mouse (Mm, accession NP_034730), Tobacco Hawkmoth (Ms, M. sexta, accession AAQ09035), round worm (C. elegans, accession NP_503402) as well as human intermediate K+ channel (Hs IK, accession AF022150), rat small-conductance K+ channel (Rn SK2, accession U69882), rat cyclic-nucleotide-gated channel (Rt CNG4, accession X55519), and bovine CaMKII (Bt CaMKII, accession CAI25258).

C. RESULTS

C.1. Ca^{2+}/CaM binds to EAG in a Ca^{2+}-dependent manner

To determine whether CaM can bind to the putative CBD (aa725-740) of *Drosophila* EAG, we performed *in vitro* binding assays with a GST fusion protein containing approximately 80% of the intracellular C-terminus of EAG (GST-$EAG_{628-1174}$) (Figure 3.2A). Minimal CaM binding was detected in zero Ca^{2+} and 10 mM EGTA, but binding was readily apparent at 1 mM Ca^{2+}. In experiments mapping the interaction site, CaM failed to bind to the full-length C-terminal cytoplasmic domain of EAG, but small deletions at either end conferred binding (Figure 3.2B). Decreased binding to the full length C-terminal domain was also observed for previous studies with human EAG1 (Schonherr et al., 2000). In our experiments, the smallest fragments that conferred binding were 556-772 (Figure 3.2B) and 628-876 (Figure 3.2C), consistent with the CaM binding domain lying between amino acids 628 and 772. To verify that the observed CaM binding was mediated by the CBD, we mutated two phenylalanines (F731 and F734) critical for CaM-binding to human EAG1. As expected, mutating these phenylalanines to serines largely eliminated CaM-binding to GST-$EAG_{628-876}$ (Figure 3.2D) and GST-$EAG_{628-1174}$ (not shown).

C.2. Ca^{2+}/CaM inhibits EAG current

To determine the physiological effect of CaM binding, EAG channels were expressed in *Xenopus* oocytes. In recordings from excised inside-out patches, EAG currents exhibited considerable rundown even in aspartate-based recordings solutions, which have been reported to eliminate rundown of the mammalian EAG current (Schonherr et al.,

Figure 3.2: Ca^{2+}-dependent binding of CaM to EAG.
(A) *Left*, Representative blot of the results of *in vitro* binding assays showing that bovine CaM (17 kDa) binds immobilized GST-$EAG_{628-1174}$ in the presence of 1 mM $CaCl_2$, but largely fails to bind in a buffer containing 10 mM EGTA (0 μM $CaCl_2$. Binding is specific because CaM did not bind to glutathione sepharose beads (lane 1) or immobilized GST (lane 2) in the presence of 1 mM $CaCl_2$. CaM was detected on Western blots using a mouse monoclonal antibody and visualized by enhanced chemiluminescence (ECL). *Center,* Coomassie-stained gel of the result of the pull-down for each condition. Equal amounts of GST-$EAG_{628-1174}$ were present in the with and without Ca^{2+}. Lower molecular weight bands are degradation of the primary EAG band with runs slightly below 100 kD. *Right*, labeled bands were quantified by densitometry and normalized to the density observed in the corresponding area of the GST alone lane (minimum, lane 2) and the intensity of the EAG band (maximum, lane 3) for each experiment. Data are presented as the mean ± S.E.M, n = 2. Similar results also were observed in three experiments using the GST-$EAG_{628-876}$ fragment. **(B)** Mapping the CBD of EAG. The ability of CaM to bind to several C-terminal EAG deletion constructs was assessed in the presence of 1 mM $CaCl_2$, and binding (plus sign) or no binding (minus sign) indicated to the right of the construct. Representative binding results for several constructs are shown below. **C)** *Left*, Binding of CaM to wild type $EAG_{628-876}$ and $EAG_{628-876}$-F731S/F734S in the presence of 1 mM Ca^{2+}. As in (A) CaM was detected on Western blots using by a mouse monoclonal antibody. At the bottom we show a representative Coomassie-stained gel of the pull-down demonstrating that equal amounts of the wild type and mutant GST-$EAG_{628-1174}$ fragments were present. *Right*, binding data averaged across three experiments. Bands were quantified by densitometry and normalized as described in (A). The reduction in binding observed for $EAG_{628-876}$-F731S/F734S was significant ($p < 0.05$) when analyzed using a one way ANOVA.

FIGURE 3.2

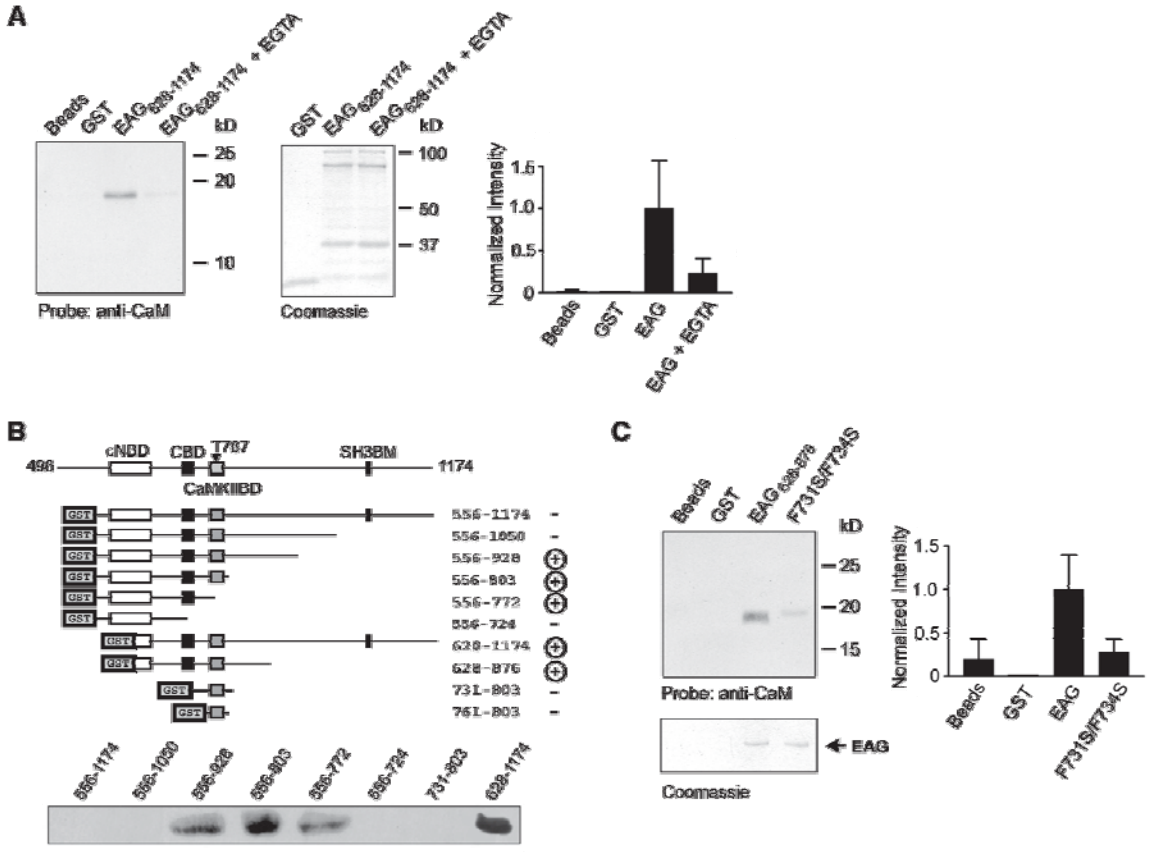
A
Beads
GST
EAG628-1174
EAG628-1174 + EGTA
kD
25
20
10
Probe: anti-CaM
GST
EAG628-1174
EAG628-1174 + EGTA
kD
100
50
37
Coomassie
Normalized Intensity
1.5
1.0
0.5
0
Beads
GST
EAG
EAG + EGTA
B
cNBD
CBD
T787
SH3BM
498
1174
CaMKIIBD
556-1174
556-1050
556-928
556-803
556-772
556-724
628-1174
628-876
731-803
761-803
556-1174
556-1050
556-928
556-803
556-772
556-724
731-803
628-1174
C
Beads
GST
EAG628-876
F731S/F734S
kD
25
20
15
Probe: anti-CaM
EAG
Coomassie
Normalized Intensity
1.5
1.0
0.5
0
Beads
GST
EAG
F731S/F734S

2000). In addition, transfection of mammalian cells lines with *Drosophila eag* results in currents that are barely distinguishable from endogenous outward currents (Zhou et al., 2001; Hegle et al., 2006). We therefore examined Ca^{2+}/CaM regulation of EAG using two-electrode voltage clamp (Figure 3.3). Ca^{2+} influx was stimulated with 10 μM ionomycin (IM), a cell-permeant Ca^{2+} ionophore, in a bath solution containing 2.5 mM $CaCl_2$ and DIDS (100 μM) to block the Ca^{2+}-activated chloride current endogenous to oocytes. Treatment with IM rapidly induced a significant decrease in EAG currents (Figure 3.3A, left). The traces show the currents before, during, and after IM application, and the plot below shows the time-dependence of the IM effect. The reduction of EAG current was typically observed within 10 s of the onset of IM treatment and currents decreased by an average of twenty percent.

The effect of IM on EAG currents could be due to either a direct interaction with Ca^{2+}/CaM or another Ca^{2+}-dependent process. To distinguish between these alternatives, we examined the effects of IM on EAG-F731S/F734S. As shown in Figure 3.3A, EAG-F731S/F734S currents were unaffected by IM. Moreover, IM failed to inhibit currents of two other CBD mutants, EAG-K733E/F734S/R735E and EAG-R728E/K729E, in which negatively charged glutamate residues were substituted for positively charged residues that likely promote electrostatic interactions between CaM and EAG. The block of inhibition is quantified in Figure 3.3B. Together, these results suggest that IM inhibits EAG via direct Ca^{2+}/CaM binding as opposed to other Ca^{2+}-dependent pathways.

Ca^{2+}/CaM-binding to KCNQ2/3 channels is critical for channel expression (Wen and Levitan, 2002). To examine the effect of the CBD mutations on EAG expression levels, we compared the current amplitudes of oocytes injected with increasing amounts of wild

Figure 3.3: Effects of Ca^{2+}/CaM on wild type and mutant EAG currents.
(A) Ca^{2+}-dependent inhibition of EAG currents requires a functional CaM-binding domain. *Left panel* shows representative traces of wild type and mutant EAG currents in response to voltage steps from –80 mV to 0 mV before, during, and after application of IM. Voltage-steps were applied every 5 sec (0.25 Hz). DIDS was used to block endogenous Ca^{2+}-activated Cl^- currents and had no effect on EAG currents (compare initial and recovery traces, obtained in the presence and absence of DIDS, respectively). The scale bar in all traces is 2 μA. *Right panel* plots the peak instantaneous current at 0 mV at each time point, showing the time-course of Ca^{2+}-dependent inhibition and the durations of drug exposure. No change in current was apparent in the absence of IM. **(B)** Summary of the percent inhibition induced by IM treatment for wild type and mutant EAG currents. N = 18, 8, 7, and 8 for wild type EAG, EAG- F731S/F734S, EAG-K733E/F734S/R735E, and EAG-R728E/K729E, respectively. **(C)** Peak current amplitudes of wild type EAG and F731S/F734S mutants in oocytes injected with different amount of RNA were normalized to the maximum amplitude of wild type EAG currents. Data were fit with the equation $I = I_{max}(1-e^{-bx})$, where x is the amount of RNA per oocytes and b is the rate constant. For wild type EAG, $I_{max} = 100 \pm 7\%$, $b = 4.06 \pm 0.88$; for F731S/F734S, $I_{max} = 94 \pm 5\%$ and $b = 1.59 \pm 0.21$. $N \geq 9$ for each data point. **(D)** The conductance – voltage (G-V) relationships of wild type and mutant EAG channels in untreated oocytes. An extracellular solution with 25 mM K+ was used to enhance tail currents. Conductance was determined for individual oocytes using the relation $G = I_p / V - V_r$, where I_p is the peak tail current observed following a voltage step to the indicated potential. The reversal potential, V_r, was determined for each oocyte. To allow comparison, G-V curves were normalized by dividing by the maximum conductance. The curves shown are theoretical Boltzmann distributions fit to the averaged data. N as in Table 1. **(E)** The averaged 10-90% rise times (ms) throughout the course of the experiments. N as in Table 3.1.

FIGURE 3.3

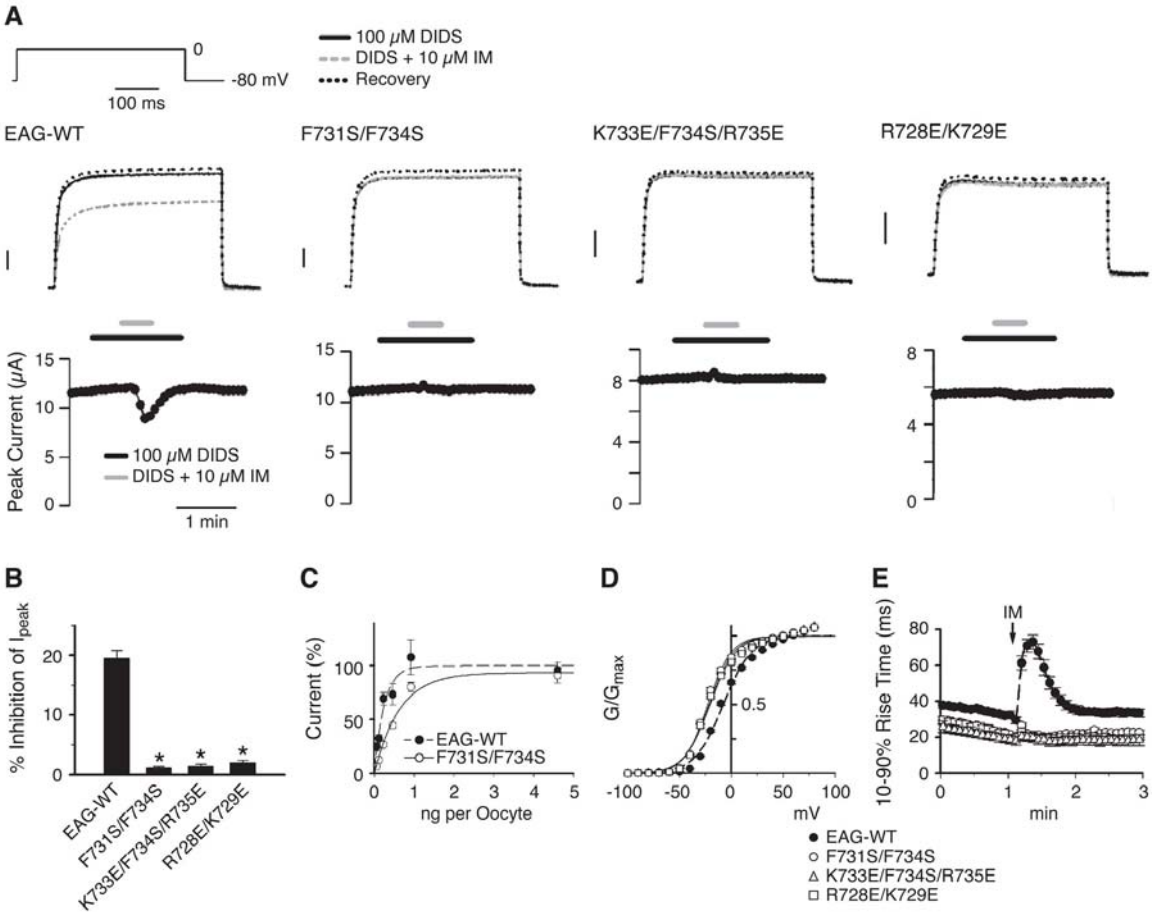
A
0
-80 mV
100 ms
100 μM DIDS
DIDS + 10 μM IM
Recovery
EAG-WT
F731S/F734S
K733E/F734S/R735E
R728E/K729E
Peak Current (μA)
100 μM DIDS
DIDS + 10 μM IM
1 min
B
% Inhibition of I peak
EAG-WT
F731S/F734S
K733E/F734S/R735E
R728E/K729E
C
Current (%)
EAG-WT
F731S/F734S
ng per Oocyte
D
G/G max
0.5
mV
E
IM
10-90% Rise Time (ms)
min
EAG-WT
F731S/F734S
K733E/F734S/R735E
R728E/K729E

type EAG and F731S/F734S RNA (Figure 3.3C). A fit of the relationship between RNA and current amplitudes shows that F731S/F734S mutants required 2.5-fold more RNA than wild type to reach 63% saturation. However, wild type and mutant current amplitudes and protein levels (not shown) were indistinguishable once saturation was reached. Thus, although the CBD mutations reduced the efficiency of expression, the CBD domain is not critical for expression in contrast to the findings for KCNQ2/3 channels.

Comparisons of the properties of wild type and CBD mutant currents revealed differences in the voltage-dependence of activation. At resting Ca^{2+} concentrations, the conductance-voltage relationships of EAG-F731S/F734S, -K733E/F734S/R735E, and -R728E/K729E were shifted to hyperpolarized potentials compared to those obtained for wild type EAG (Figure 3.3D, Table 3.1). For example, half-maximal activation of EAG-F731S/F734S occurred at –22.5 ± 0.97 mV compared to -7.7 ± 0.72 mV for wild-type channels. The difference in the voltage-dependence of activation is not due to a difference in expression, because it is also evident in oocytes with similar current amplitudes. Consistent with the changes in the voltage-dependence of activation, differences in kinetics were also observed (Table 3.1). Currents from channels with mutations in the CaM binding site activated and inactivated more rapidly than wild type currents, and mutant currents also inactivated more extensively than wild type currents. These changes in kinetics appeared to be accounted for by the shift in voltage-dependence when currents were measured at a voltage shifted by an amount corresponding to the shift in the midpoint of activation (not shown).

TABLE 3.1

	EAG	F731S/F734S	K733E/F734S/R735E	R728E/K729E
Voltage-dependence				
n	6	7	7	7
V50 (mV)	-7.7 ± 0.72	-22.5 ± 0.97	-20.4 ± 0.82	-21.2 ± 0.95
Slope (mV/e-fold)	13.65 ± 0.27	11.34 ± 0.37	12.57 ± 0.41	11.88 ± 0.33
Z (e)	-3.53 ± 0.38	-1.16 ± 0.06	-1.27 ± 0.05	-1.23 ± 0.06
Gmax (mS)	0.15 ± 03	0.13 ± 0.04	0.16 ± 0.01	0.10 ± 0.01
Kinetics				
n	16	21	12	21
Activation				
10-90% rise time (ms)	37.6 ± 1.6 (17)	29.3 ± 2.2 (8)	29.5 ± 1.8 (7)	25.8 ± 3.3 (8)
tau (ms)	3.6 ± 0.09	2.95 ± 0.09	2.79 ± 0.07	2.99 ± 0.06
Inactivation				
percent	10.1 ± 0.8	19.1 ± 1.7	18.9 ± 2.3	21.7 ± 1.3
tau (ms)	58.0 ± 2.0	55.5 ± 2.9	55.9 ± 2.9	49.7 ± 1.2

Table 3.1. Properties of wild type and EAG mutant currents.
The relationship between conductance and membrane potential was determined as described in Methods. The data were fit with a Boltzmann equation, and the resulting parameters are indicated above. The steepness of the G-V relationship is indicated as both the slope and equivalent gating charge (Z). Activation and inactivation time constants were obtained by fitting currents elicited in response to a +40 mV test pulse with two exponentials and a steady state. Measurements of rise times correspond to the data shown in Figure 3.3E and the N for each measurement is indicated inside the parentheses.

The shift in the voltage-dependence of the CaM binding mutants may be explained either by a change in channel structure caused by the mutations, or by Ca^{2+}/CaM-binding to wild type EAG at resting Ca^{2+} levels. The latter alternative is supported by the observation that mutations that eliminate CaM binding produce changes that are opposite to those observed in response to IM treatment. Specifically, the effect of IM on wild type EAG current amplitudes (Figure 3.3A) and kinetics (Figure 3.3E) is consistent with a depolarizing shift in the voltage-dependent activation upon Ca^{2+}/CaM binding. Moreover, little or no change in kinetics was observed for mutant channels in the presence of IM. Together, these results suggest that CaM can bind to the wild type channel at resting Ca^{2+} concentrations and that Ca^{2+}/CaM-binding stabilizes the closed state of EAG channels.

C.3. Lobe-specific effects of CaM on EAG current

The possibility that CaM may bind to EAG channels at rest prompted us to further examine the role of Ca^{2+} in CaM binding. CaM can bind some targets in the absence of Ca^{2+} and preassociation with Ca^{2+}-free CaM (ApoCaM) has been hypothesized as a mechanism that allows increases in Ca^{2+} to be more rapidly transduced. Preassociation has been most clearly demonstrated using a CaM mutant (CaM_{1234}) that is unable to bind Ca^{2+} due to aspartate to alanine substitutions at each of the four EF-hands (Xia et al., 1998). CaM_{1234} competes with wild type CaM for the Ca^{2+} channel binding site resulting in dominant negative suppression of Ca^{2+}/CaM-dependent inactivation of Ca^{2+} currents (Erickson et al., 2001; Pitt et al., 2001; Erickson et al., 2003). Similarly, if ApoCaM preassociates with EAG, CaM_{1234} should act as a dominant negative suppressor of IM inhibition. As shown in Figure 3.4, coexpression of CaM_{1234} with EAG did not alter the

FIGURE 3.4

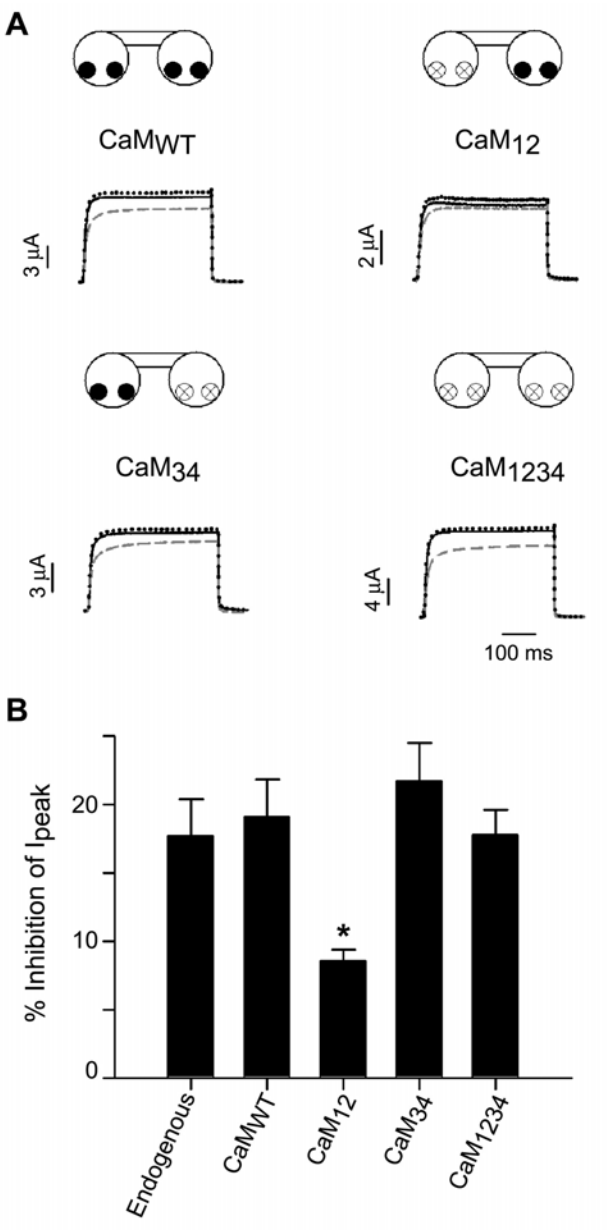

Figure 3.4 Lobe-specific effects of CaM on EAG.
(A) Current traces from oocytes coexpressing EAG and CaM_{wt}, CaM_{12}, CaM_{34}, or CaM_{1234} in response to IM. **(B)** Summary of the percent inhibition of peak instantaneous currents at +40 mV for wild type EAG coexpressed with the indicated constructs. Only CaM_{12} had a dominant negative effect on the Ca^{2+}-dependent inhibition of EAG currents by IM. N = 6 (Endogenous CaM), 6 (CaM_{wt}), 8 (CaM_{12}), 7 (CaM_{34}), 6 (CaM_{1234}).

amount of inhibition induced by IM compared to the inhibition observed in oocytes expressing EAG, either alone or with wild type CaM (CaM_{WT}). These results indicate that CaM does not bind EAG channels in its Ca^{2+}-free state.

The failure of ApoCaM to suppress the effects of IM on EAG current does not rule out a Ca^{2+}-dependent preassociation of CaM, which could be facilitated by low levels of Ca^{2+} present at rest. The N- and C-terminal lobes of CaM have different affinities for Ca^{2+} and can differentially affect some ion channels (Saimi and Kung, 2002). To explore whether CaM has lobe-specific effects on EAG currents, we examined the effects of overexpressing CaM_{12} and CaM_{34} in which the first two or last two EF-hands, respectively, are incapable of binding Ca^{2+}. As shown in Figure 3.4A, CaM_{12}, but not CaM_{34}, greatly reduced IM-dependent inhibition of EAG currents. The data for all CaM constructs are summarized in Figure 3.4B, and show that mutations in the N-terminal lobes of CaM (CaM_{12}) reduced the IM effect by 50% and that the other CaM constructs did not modify the inhibition produced by the CaM endogenous to oocytes. These data indicate that the low affinity N-terminal lobe is essential for the electrophysiological effects of Ca^{2+}/CaM. In addition, the most likely explanation of the differences in the effects of CaM_{12} and CaM_{1234} is that the C-terminal lobe must be able to bind to EAG in a Ca^{2+}-dependent manner in order for CaM_{12} to have a dominant negative effect. These results suggest that CaM can bind to EAG via its C-terminal lobe at resting levels of intracellular Ca^{2+}. However, if the *in vitro* dissociation constant of Ca^{2+}/CaM and EAG channels is higher than the resting Ca^{2+} concentration, only a small fraction of CaM_{12} would be bound to EAG at rest. CaM_{12} would then predominantly exert its dominant negative effect by binding to EAG during the initial rise in Ca^{2+}.

C.4. Ca^{2+}/CaM and CaMKII modulate EAG independently

As shown previously (Wang et al., 2002b), phosphorylation of EAG by CaMKII enhances EAG currents. Ca^{2+}/CaM is thus paradoxically capable of both inhibiting EAG currents by direct binding to EAG and potentiating currents via activation of CaMKII. The proximity of the minimal CaM- and CaMKII-binding domains (aa 725-744 and 773-794, respectively) and the regulatory phosphorylation site (T787) raised the question of whether these sites might interact. Previous studies (Sun et al., 2004) demonstrated binding of CaM to EAG was not required for either the binding of CaMKII to the channel or for phosphorylation of T787. To determine if CaMKII binding or phosphorylation modulated the ability of EAG to bind CaM, we examined the ability of various GST-EAG fusion proteins to bind CaM. As shown above (Figure 3.2), the full length C-terminus of EAG (556-1174) does not support direct CaM binding, although fusion proteins lacking either the first 72 or the last 246 aa can directly bind CaM. To determine if binding of CaMKII could relieve the inhibitory influences of either the proximal or distal C-terminus, we compared the ability of GST-$EAG_{556-1174}$ to bind CaM to that of GST-$EAG_{556-1174}$ bound to either wild type or a constitutively active CaMKII mutant (T287D/T306D/T307D). T287D/T306D/T307D CaMKII binds to EAG constitutively (Sun et al., 2004), but does not itself bind CaM. Immunoblotting for CaM demonstrates that CaM associates with GST-$EAG_{556-1174}$ only when wild type CaMKII is bound to the fusion protein (Figure 3.5A). This CaM is presumably bound indirectly to the complex via CaMKII, because EAG complexed to the triple mutant kinase, which cannot bind CaM, has no associated CaM. We also investigated the possibility that phosphorylation of T787 could relieve the distal C-terminal inhibition of CaM binding. CaM binding to WT

FIGURE 3.5

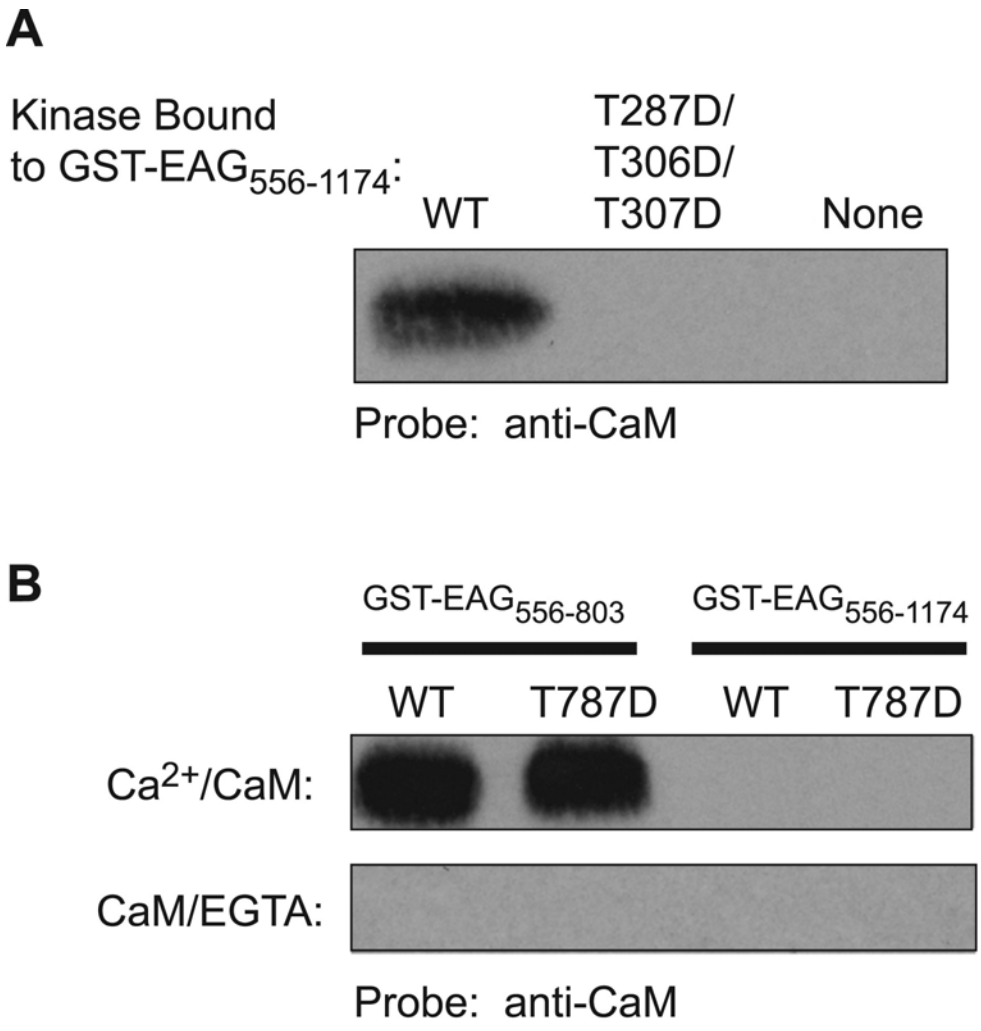

Figure 3.5 CaMKII binding and phosphorylation do not relieve distal C-terminal inhibition of CaM binding to EAG. (A) Wild type CaMKII or T287D/T306D/T307D CaMKII (which binds EAG constitutively but does not bind CaM (Sun et al., 2004)) or buffer alone were incubated with glutathione sepharose beads conjugated to GST-$EAG_{556-1174}$ in the presence of Ca^{2+}/CaM, and washed with Ca^{2+} buffer. Bound CaM was detected by immunoblotting. $N \geq 2$ for all experiments, and representative data are shown. **(B)** Phosphomimic mutation of the CaMKII phosphorylation site of EAG does not affect its CaM binding ability. CaM was incubated with glutathione sepharose beads conjugated to GST-$EAG_{556-803}$, GST-$EAG_{556-1174}$ or T787D mutants of the two fusion proteins in the presence of Ca^{2+}/CaM or CaM/EGTA, and washed with buffers containing Ca^{2+} or EGTA correspondingly. Bound CaM was detected by immunoblotting.

and T787D phosphomimic mutants of GST-$EAG_{556-1174}$ and GST-$EAG_{556-803}$ was tested. Immunoblotting showed that only GST-$EAG_{556-803}$ bound CaM, and the phosphorylation state of T787 did not matter (Figure 3.5B). We conclude that occupancy of the CaMKII-binding site and phosphorylation of T787 do not influence the ability of EAG to bind CaM.

The above experiments suggest that the ability to bind CaM is not modulated by phosphorylation, but they did not rule out an effect on the kinetics of CaM association. Phosphorylation of the regulatory domain of CaMKII at a site near its CaM-binding domain has been shown to decrease the off rate of CaM by over three orders of magnitude, trapping CaM on the phosphorylated kinase (Meyer et al., 1992). To determine if phosphorylation of T787 in the EAG C-terminal altered the kinetics of CaM binding and release, we used fluorescence anisotropy to measure the association of acrylodan-labeled CaM to WT, T787A and T787D GST-$EAG_{556-803}$. In all cases, the on rate of CaM was very fast and no difference could be accurately measured. The off rate was much slower (1×10^{-3}/s for WT GST-$EAG_{556-803}$) and could be measured after addition of an excess of unlabelled CaM. The off rates of T787A and T787D GST-$EAG_{556-803}$ were not significantly different from WT (0.5×10^{-3}/s and 1.5×10^{-3}/s respectively). The similarity in off rate suggests that phosphorylation of T787 does not alter the kinetics of CaM release from EAG.

Although the biochemical interactions of CaM and CaMKII with EAG occur independently, it remains possible that these processes interact to alter the outcome of regulation. Several possibilities exist. First, CaM binding could regulate the effects of T787 phosphorylation. This is unlikely to be the case since the effects of modulation of

T787 are seen in the absence of Ca^{2+} influx (Wang et al., 2002b). However, to more rigorously look at the role of CaM in the phosphorylation-mediated increase in EAG current, we measured the effect of KN93, a CaMKII inhibitor, on wild type and F731S/F734S EAG. Application of KN93 decreased the current amplitudes of wild type and mutant channels equivalently (Figure 3.6A). This is consistent with the basal CaMKII activity in oocytes previously observed (Wang et al., 2002b) and demonstrates that CaM binding is not required for the phosphorylation-mediated regulatin of current amplitude. A second possibility is that CaMKII phosphorylation could modulate the inhibitory effect of CaM binding. To investigate this issue we looked at the ability of IM to inhibit wild type and EAG-T787A currents. The level of inhibition of EAG-T787A was indistinguishable from that for wild type channels (Figure 3.6B) demonstrating that phosphorylation does not affect the ability of CaM to regulate the channel.

C.5. *In vivo* roles of Ca^{2+}-dependent modulation

To determine the contributions of CaM and CaMKII to EAG function *in vivo*, we transgenically expressed *eag* constructs containing point mutations in either the CaM binding (*eag*- F731S/F734S) or CaMKII phosphorylation sites (*eag*-T787A) in the eag^{sc29} null background using the Gal4/UAS system (Brand and Perrimon, 1993). Because *eag* is predominantly expressed in neurons (Wang et al., 2002; Sun et al., 2004), UAS-*eag* expression was driven using the pan-neuronal *elav* driver (*elav5147*-Gal4). Rescue of the eag^{sc29} phenotype was assessed relative to the rescue obtained using wild type *eag* (*eag*-WT) in recordings of synaptic activity at the larval NMJ. As previously observed for other *eag* mutants (Ganetzky and Wu, 1983; Wu et al., 1983a; Griffith et al., 1994),

FIGURE 3.6

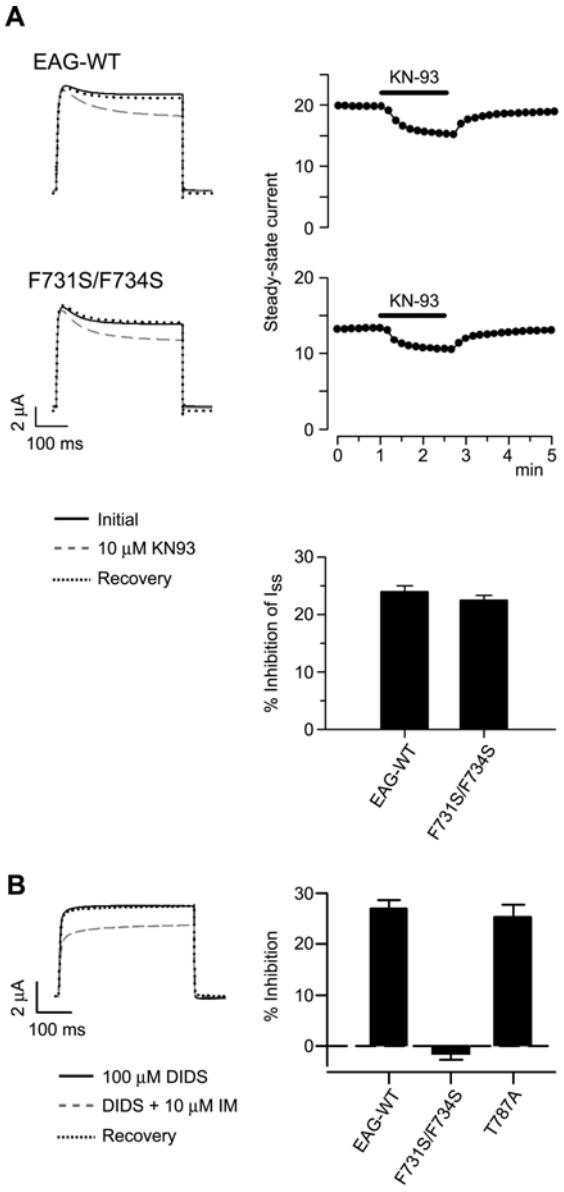

Figure 3.6 CaM and CaMKII independently modulate EAG current.
(A) Current traces *(left)* from oocytes expressing wild type and F731S/F734S mutant EAG channels in response to a depolarizing step from –80 mV to +40 mV before, during, and after perfusion with 10 µM KN-93, a CaMKII-specific inhibitor, in normal extracellular bath solution. Voltage steps were applied every 10 s (0.1 Hz). The time course of drug application and inhibition of steady-state current at +40 mV is indicated to the *right*. Average percent inhibition of steady-state current by KN-93 ($n \geq 5$) is shown in the *right panel, bottom.* **(B)** Current traces from EAG-T787A channels before, during and after the response to IM (*left)*. The protocol was identical to that described in Figure 3.3. Summary of percent inhibition for wild type, F731S/F734S, and T787A EAG peak currents in response to IM from the same recording day ($n \geq 7$) is shown in the *right panel*.

eag^{sc29} larvae exhibited a high level of spontaneous activity (Figure 3.7A, left) and an increase in the amplitudes of excitatory junctional currents (EJCs) evoked by stimulation of the motor nerve (Figure 3.7B, left). All three chromosomal insertions of *eag*-WT (Rescue 1-3) restored these properties to levels that were statistically indistinguishable from wild type larvae (Figure 3.7A,B), although some larvae transgenically expressing the wild type channel displayed a residual level of spontaneous activity (Figure 3.7A, left).

If the resting Ca^{2+} in presynaptic terminals is high enough, disruption of CaM binding in *eag*-F731S/F734S would be expected to have a hyperpolarizing effect by increasing EAG current. Although recordings from muscle fibers only indirectly assess presynaptic currents, an increase in EAG current might be detected as a more complete elimination of spontaneous activity, a change in the stimulation threshold required to evoke a muscle response, or smaller evoked EJCs due to curtailment of the presynaptic action potential. *eag*-F731S/F734S appeared no more effective than the wild type construct at eliminating spontaneous activity (Figure 3.7A) and there was no obvious difference in stimulus threshold. In addition, the amplitudes of EJCs evoked in *eag*-F731S/F734S larvae were indistinguishable from the amplitudes observed in transgenic larvae expressing the wild type channel (Figure 3.7B). Together, these results suggest that CaM normally does not inhibit EAG current at resting Ca^{2+} concentrations and that the kinetics of CaM inhibition are slow enough not to play a role during the rise in Ca^{2+} produced by a single action potential.

To determine whether CaM inhibition of EAG current plays a role when intracellular Ca^{2+} is elevated by activity, we examined facilitation of EJP amplitude. Facilitation was

Figure 3.7 CaM binding to EAG is necessary for proper synaptic function. (A) *Left*, representative traces showing spontaneous activity of 3rd-instar wild type (WT), eag^{sc29}, and transgenic *eag*-WT (Rescue) and *eag*-F731S/F734S larvae. Each of the three traces shown for each genotype is from a different larva. Spontaneous EJPs of different amplitude represent EJPs from Type 1a or 1b boutons, or both summed. Events smaller than 5 mV were judged to be miniature endplate potentials because they are insensitive to block by tetrodotoxin (Wilson, unpublished observations) and, therefore, were excluded from determinations of EJP frequency. *Right*, Average frequency of spontaneous EJPs recorded from WT, eag^{sc29}, three *eag*-Rescue lines and two *eag*-F731S/F734S lines. **(B)** *Left*, representative EJC traces evoked by stimulation of the motor nerve using a suction electrode. For amplitude determinations the stimulus was set at 0.5 V above the minimum stimulus required to reliably evoke a response. *Right*, average EJC amplitudes for the indicated genotypes. Amplitudes were normalized to the average amplitude observed in wild type larvae. **(C)** *Left*, Representative examples of facilitation observed in response to stimulation at 20 Hz. Facilitation is disrupted in eag^{sc29} even when spontaneous activity is low (second trace). *Right*, Averaged facilitation for the indicated genotypes at stimulus frequencies ranging from 5 to 40 Hz. eag^{sc29} larvae show a defect in facilitation at stimulus frequencies of 10 Hz or greater, which corresponds to the frequency at which Ca^{2+} begins to accumulate in the motor nerve terminal (Macleod et al., 2002). Data points are averaged measurements from 5-31 muscles. Statistical significance is shown for responses to stimulation at 40 Hz. In A and B, gray background boxes indicate the transgenic insertion line to which all post-hoc comparisons were made, which was chosen to be the transgenic *eag*-WT line showing the least amount of rescue. In A – C, NS = not significant, * $p< 0.05$, ** $p<0.01$, *** $p<0.001$ in a one way ANOVA.

FIGURE 3.7

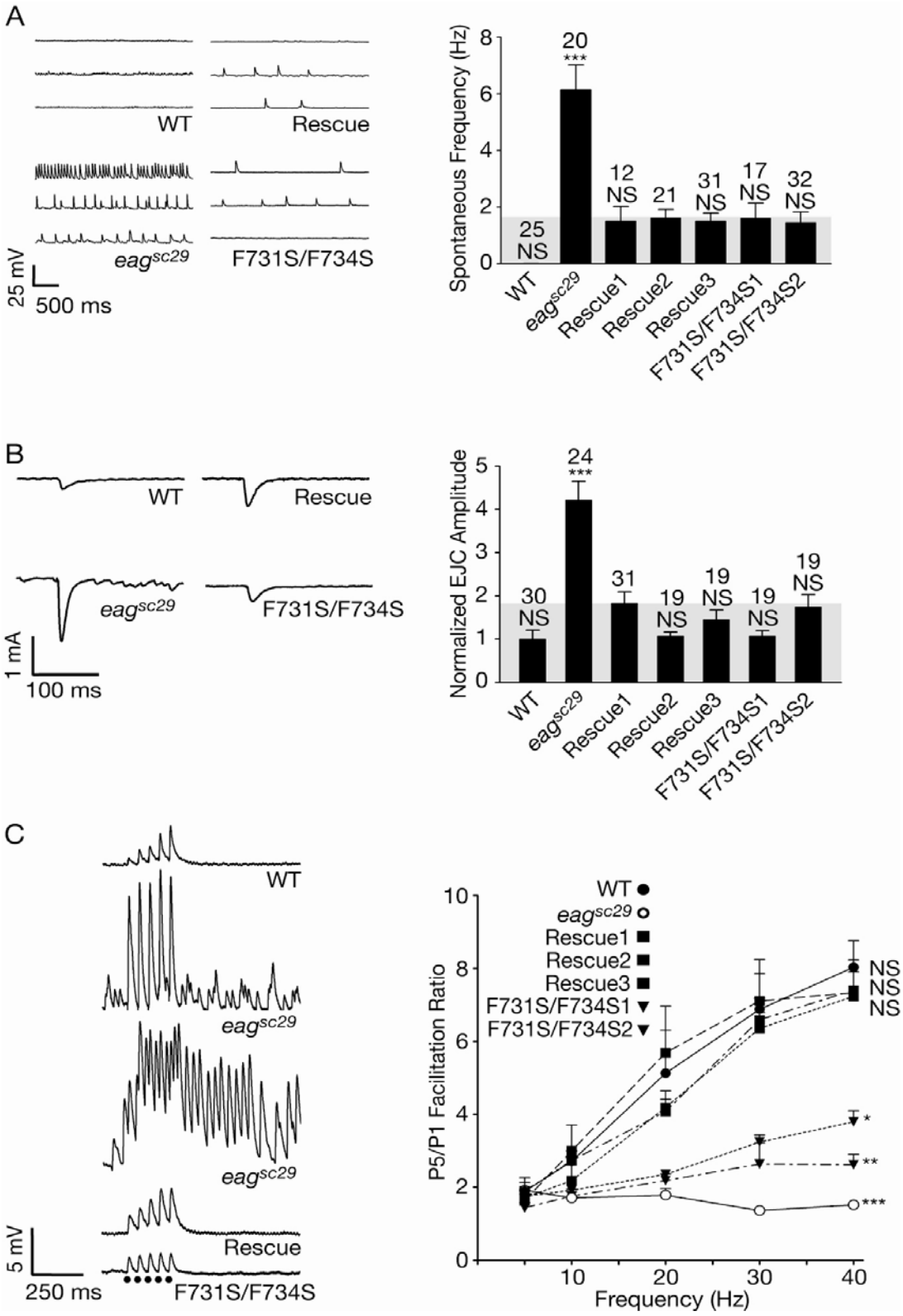
A
WT
Rescue
eag^sc29
F731S/F734S
25 mV
500 ms
Spontaneous Frequency (Hz)
20
***
12
NS
21
31
NS
17
NS
32
NS
25
NS
WT
eag^sc29
Rescue1
Rescue2
Rescue3
F731S/F734S1
F731S/F734S2
B
WT
Rescue
eag^sc29
F731S/F734S
1 mA
100 ms
Normalized EJC Amplitude
24
***
30
NS
31
19
NS
19
NS
19
NS
19
NS
C
WT
eag^sc29
eag^sc29
Rescue
F731S/F734S
5 mV
250 ms
P5/P1 Facilitation Ratio
WT
eag^sc29
Rescue1
Rescue2
Rescue3
F731S/F734S1
F731S/F734S2
NS
NS
NS
*
**
***
Frequency (Hz)

assessed using five pulses, administered at the indicated frequencies, and evaluated by dividing the amplitude of the response to the fifth stimulus by the amplitude of the response to the first. In wild type larvae, facilitation clearly increases as the stimulus frequency increases (Figure 3.7C, *right*). Facilitation has not previously been examined in *eag* mutants, because hyperexcitability causes irregular firing in many instances. However, as shown in Figure 3.7C, facilitation was disrupted in eag^{sc29} larvae for stimulus frequencies above 10 Hz, and was disrupted even in larvae exhibiting low levels of spontaneous activity (Figure 3.7C *left*, second and third traces) suggesting that disrupted facilitation is not solely due to the fact that presynaptic Ca^{2+} levels have already been elevated by prior activity. Most importantly, the defect in facilitation was completely rescued by transgenic expression of wild type *eag*, whereas *eag*-F731S/F734S failed to rescue facilitation even though spontaneous activity levels and EJC amplitudes were restored. Thus, CaM inhibition of EAG current makes a critical contribution to facilitation at the larval NMJ.

We also investigated the role of phosphorylation by CaMKII in the regulation of EAG in recordings from larvae expressing the phosphorylation site mutant, *eag*-T787A. In contrast to *eag*-WT and *eag*-F731S/F734S, *eag*-T787A failed to rescue all aspects of the eag^{sc29} phenotype, including spontaneous activity (Figure 3.8A), EJC amplitude (Figure 3.8B), and frequency-dependent facilitation (Figure 3.8C). The failure to rescue did not appear to be due to disruption of other genes or variations in protein expression that can occur depending on the point of insertion of the transgene, because it was observed in three independent transgenic lines. In addition, there was no difference in the expression of EAG protein for transgenic lines expressing the different constructs that

Figure 3.8 Phosphorylation of EAG is necessary for synaptic modulation. (A) Representative traces *(left)* and average frequencies (*right*) of spontaneous EJP activity for lines transgenically expressing *eag*-WT (Rescue) and *eag*-T787A, compared to the data for wild type and eag^{sc29} larvae. Each of the three traces shown for each genotype is from a different larva. **(B)** Representative EJC traces *(left)* and average *(right)* EJC amplitudes for the genotypes described above. Average amplitudes are normalized to that of wild type larvae. **(C)** Representative examples of facilitation at 20 Hz (*left*) and averaged facilitation (*right*) for the indicated genotypes at stimulus frequencies ranging from 5 to 40 Hz. Data points are averaged measurements from 5-31 muscles. Statistical significance is shown for responses to stimulation at 40 Hz. In A and B, gray background boxes indicate the transgenic insertion line to which all post-hoc comparisons were made. In A – C, NS = not significant, * $p< 0.05$, ** $p<0.01$, *** $p<0.001$ in a one way ANOVA.

FIGURE 3.8

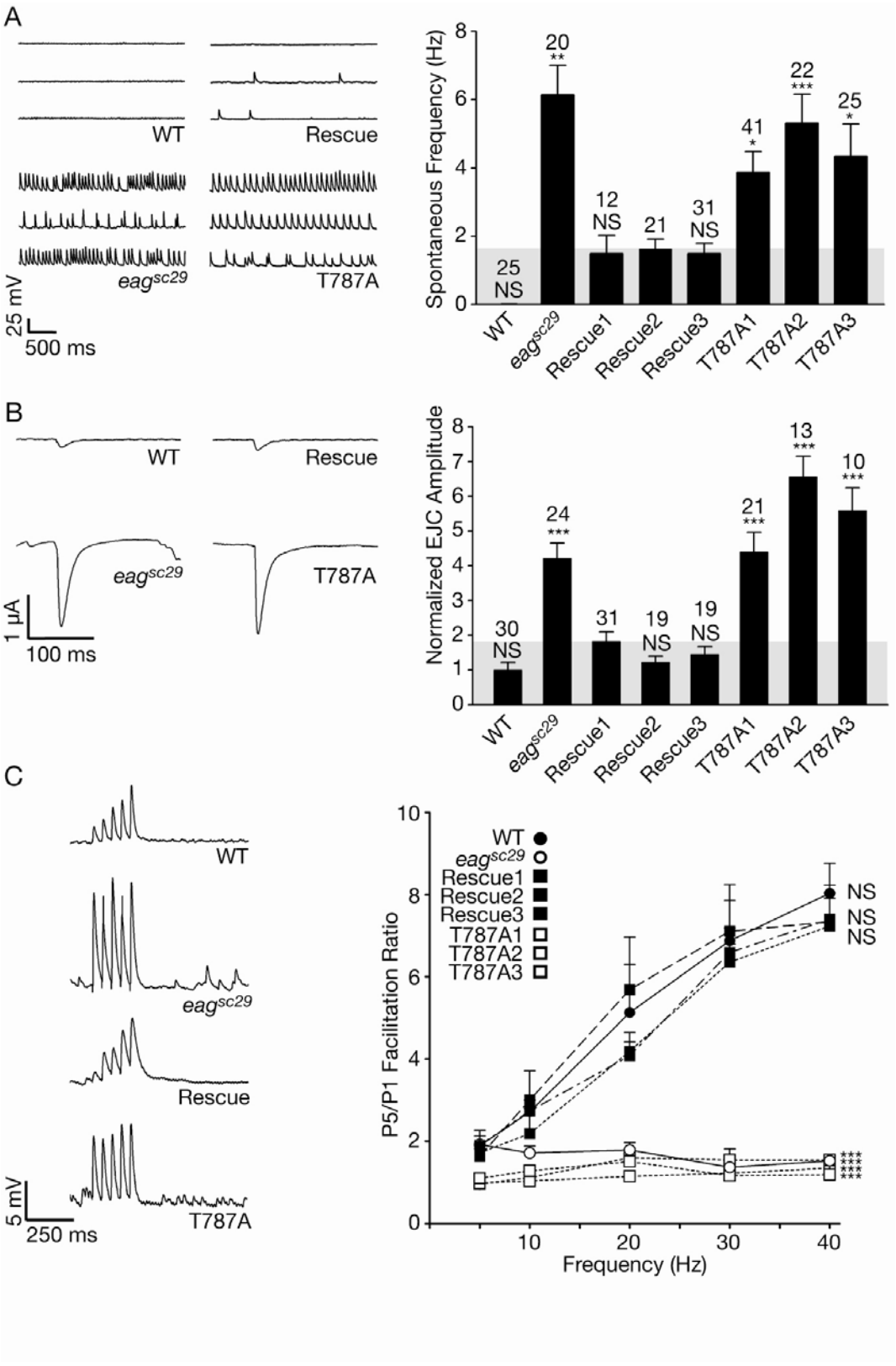
A
WT
Rescue
eag^sc29
T787A
25 mV
500 ms
Spontaneous Frequency (Hz)
20
**
12
NS
21
31
NS
41
*
22
***
25
*
25
NS
WT
eag^sc29
Rescue1
Rescue2
Rescue3
T787A1
T787A2
T787A3
B
WT
Rescue
eag^sc29
T787A
1 µA
100 ms
Normalized EJC Amplitude
30
NS
24
***
31
19
NS
19
NS
21
***
13
***
10
***
C
WT
eag^sc29
Rescue
T787A
5 mV
250 ms
P5/P1 Facilitation Ratio
Frequency (Hz)
NS
NS
NS

could explain the failure of *eag*-T787A to restore normal electrophysiological properties (*not shown*). Given that phosphorylation of T787 can increase the surface expression of EAG by as much as 6-fold in *Xenopus* oocytes (Marble et al., 2005), we conclude that phosphorylation of T787 makes a significant contribution to the presence of EAG at the plasma membrane even at basal levels of activity. Either resting Ca^{2+} levels are sufficient to result in phosphorylation or the activity of the relevant phosphatase is sufficiently low to prevent dephosphorylation over an extended time period. The change in surface expression appears to affect both the conduction and non-conduction, signaling functions of EAG (Hegle et al., 2006; Chapter IV).

D. DISCUSSION

The results of the present study demonstrate that Ca^{2+}/CaM regulates *Drosophila* EAG, not only by activating CaMKII, but also by direct binding to the channel. Binding and phosphorylation have opposite effects; Ca^{2+}/CaM binding inhibits EAG current, whereas Ca^{2+}/CaM-mediated phosphorylation increases it. In *Xenopus* oocytes, the inhibitory effect of CaM is readily reversible, whereas the increase in EAG current mediated by CaMKII is not because dephosphorylation is required to reverse the effect. These observations led us to predict that, *in vivo*, the effects of CaM would be acute, whereas the effects of phosphorylation by CaMKII would be more protracted. A more prolonged effect of phosphorylation also was predicted by the fact that phosphorylation increases EAG surface expression (Marble et al., 2005) and by the possibility that CaMKII bound to EAG may be constitutively active (Sun et al., 2004). These predictions were tested in recordings at the NMJs of larvae transgenically expressing mutant *eag*

constructs in the *eag*^{sc29} null background. In larvae expressing *eag* with a defective CaM binding site (*eag*-F731S/F734S), only frequency-dependent facilitation remained disrupted suggesting that the inhibitory effects of CaM occur only when Ca^{2+} levels are elevated by activity. In contrast, transgenic *eag*-T787A larvae retained all the electrophysiological features of the *eag*^{sc29} phenotype, indicating that phosphorylation of this site plays a critical role in limiting activity at this synapse. Our results suggest that phosphorylation plays a role even at basal Ca^{2+} levels, which have been estimated to be in the range of 20-30 nM in larval motor nerve terminals (Macleod et al., 2002).

By transgenically expressing channels with point mutations in the binding and phosphorylation sites, these experiments avoided confounding effects of CaM and CaMKII on other targets. However, the possibility that other Ca^{+2}-binding proteins and kinases may act on these sites has not been ruled out. In this regard, transgenic inhibition of CaMKII recapitulates the high spontaneous activity and increased EJP amplitude observed in *eag* mutants (Griffith et al., 1994). The results for CaM are less clear, because homozygous *Cam*^{null} alleles are larval lethals. *Cam*^{null}/*Cam*^{3cl} larvae exhibit defective neurotransmitter release (Heiman et al., 1996; Nelson et al., 1997; Arredondo et al., 1998), but defects in facilitation have not been reported, possibly due to the fact that the protein produced by the *CaM*^{3cl} allele still can activate CaMKII and other CaM-activated signaling proteins.

A previous study (Schonherr et al., 2000) suggested that Ca^{2+}/CaM inhibits human but not *Drosophila* EAG currents. This conclusion was based on the indirect observation that melanoma cell lysates reduced the currents of human, but not *Drosophila*, channels in a small number of inside-out patches (Schonherr et al., 2000). Because of the rundown

of current observed for *Drosophila* EAG in excised patches, we re-examined Ca^{2+}/CaM regulation using intact oocytes and the Ca^{2+} ionophore, IM. The observation that mutations in the primary CBD abolished the inhibitory effect of IM, combined with the ability of CaM mutants to disrupt the effect, indicate that Ca^{2+}/CaM modulation is conserved in *Drosophila* EAG. Ca^{2+}/CaM completely inhibited human EAG currents but inhibited *Drosophila* EAG currents by a maximum of thirty-two percent. This difference in efficacy could be species-specific but is more likely due to differences in experimental conditions: the concentration of endogenous CaM nor the effective Ca^{2+} concentration in oocytes treated with IM could not be precisely controlled. Oocytes might also contain other endogenous Ca^{2+} binding proteins (Pongs et al., 1993; Cox et al., 1994), which could either modulate the effective Ca^{2+} concentration or bind to EAG but be incapable of inducing Ca^{2+}-dependent inhibition.

CaM resembles a dumbbell with two Ca^{2+}-binding EF-hand domains in both the N-terminal (I, II) and C-terminal (III, IV) lobes. Previous studies have shown that the two lobes of CaM can mediate separate functions in which one lobe is responsible for initial binding to the target protein, while the other effects a change in protein activity (Xia et al., 1998; Keen et al., 1999; Peterson et al., 1999; DeMaria et al., 2001; Erickson et al., 2001; Pitt et al., 2001; Schumacher et al., 2001; Saimi and Kung, 2002; Erickson et al., 2003; Gamper and Shapiro, 2003; Tang et al., 2003; Gamper et al., 2005). Because the N-terminal lobe has a lower affinity for Ca^{2+} (Kd ~ 1 μM) than the C-terminal lobe (Kd ~ 100 nM) (James et al., 1995), the N-terminal lobe has been suggested to be more responsive to large, local increases in intracellular Ca^{2+}, while the C-terminal lobe is more sensitive to small, global changes in Ca^{2+} (DeMaria et al., 2001). Our results

suggest that the C-terminal lobe of CaM preassociates with EAG, either at resting Ca^{2+} levels or during the initial rise in Ca^{2+}, and that Ca^{2+} binding to the N-terminal lobe of CaM mediates inhibition of EAG current. The resting Ca^{2+} concentration in oocytes has been estimated to be ~ 100 nM (Lechleiter and Clapham, 1992; Girard and Clapham, 1993),

Unlike the tethering of ApoCaM to Ca^{2+} channels, ApoCaM does not appear to associate with EAG as indicated by the inability of CaM_{1234} to reduce IM inhibition. The above interpretation is consistent with recent results for human EAG (Ziechner et al., 2006), which demonstrated that CaM constructs with mutations in the C-terminal lobes (CaM_{34} and CaM_{1234}) failed to interact with EAG channels in binding assays and failed to inhibit EAG current in recordings from excised patches. Results regarding mutations in the N-terminal lobe of CaM also are in agreement: CaM_{12} produced 57 ± 3.6% (n = 8) and 37 ± 11% (n = 4) reductions in Ca^{2+}/CaM inhibition of *Drosophila* and human EAG currents, respectively. The competitive approach used in our experiments offers the additional insight that binding to the C-terminal lobe is likely to be a requisite step preceding the inhibitory effects of the N-terminal lobe of CaM. Thus, modulation of EAG is in many ways similar to that observed for several other ion channels, including L- and P/Q- type Ca^{2+} channels and small conductance Ca^{2+}-activated and KCNQ K^+ channels (Peterson et al., 1999; DeMaria et al., 2001; Erickson et al., 2001; Pitt et al., 2001; Schumacher et al., 2001; Saimi and Kung, 2002; Erickson et al., 2003; Tang et al., 2003), with the primary difference lying in the Ca^{2+}-dependence of the preassociation of the C-terminal lobe.

Facilitation of neurotransmitter release is the most well-characterized presynaptic form of plasticity and is largely attributable to an activity-dependent increase in the Ca^{2+} concentration in presynaptic terminals (Zucker and Regehr, 2002). Increased Ca^{2+} can occur by accumulation when the influx of Ca^{2+} during presynaptic spikes exceeds the capacity of Ca^{2+} clearing mechanisms, by a broadening of the presynaptic action potential, or by a combination of these mechanisms. Spike broadening through a reduction in presynaptic K^+ current has been shown to contribute to facilitation at some synapses (Aldrich et al., 1979; Augustine, 1990; Jackson et al., 1991; Qian and Saggau, 1999; Klyachko et al., 2001; Felmy et al., 2003). The fact that such examples remain limited is likely to be a function of the electrophysiological inaccessibility of most nerve terminals. At mossy fiber boutons, dendrotoxin-sensitive, fast-inactivating K^+ channels contribute to facilitation through a mechanism thought to rely on channel inactivation (Felmy et al., 2003), whereas in pituitary nerve terminals, a cGMP-dependent enhancement of large-conductance Ca^{2+}-activated K^+ current is thought to contribute via a complex mechanism involving decreased inactivation of Na^+ channels (Klyachko et al., 2001). Our results indicate that short-term inhibition of EAG current, through a Ca^{2+} dependent interaction with calmodulin (or related protein) can be a major determinant of presynaptic facilitation. When combined with previous work showing that at the larval NMJ Ca^{2+} begins to accumulate at stimulus frequencies greater than 10 Hz (Macleod et al., 2002), our results further suggest that the interplay between spike broadening and increases in presynaptic Ca^{2+} concentration can be a dynamically regulated positive feedback loop affecting neurotransmitter release. Finally, differences in the Ca^{2+} requirements for CaM binding and phosphorylation of EAG may have important

implications for homeostatic mechanisms of plasticity. Our results indicate that the opposing actions of Ca^{2+}/CaM operate on different timescales to promote stability, while still allowing for short-term changes in synaptic strength. Thus, EAG channels may be an attractive locus for mechanisms underlying activity-dependent scaling of neurotransmission (Davis, 2006; Turrigiano, 2007).

E. MATERIALS & METHODS

E.1. Molecular biology

Glutathione S-transferase (GST) tagged constructs were generated by subcloning cDNA fragments spanning the indicated amino acid sequence into pGEX-4T1 (Amersham Biosciences, Piscataway NJ). cDNA fragments were generated by PCR and/or restriction digests using pGH19-EAG (Wilson et al., 1998) as the template. Mutant EAG constructs were created with the QuikChange Site-Directed mutagenesis kit (Stratagene, LaJolla, CA, USA) using oligonucleotides containing base changes necessary to change the amino acid sequence and introduce or remove restriction enzyme sites. For transgenic expression, mutant *eag* fragments were subcloned into pPUAST-*eag*. All constructs were verified by restriction digests followed by DNA sequencing. CaM_{WT}, CaM_{12}, CaM_{34}, and CaM_{1234} constructs were a gift from David Yue (Johns Hopkins University School of Medicine, Baltimore, MD).

E.2. *In vitro* binding assays

GST-fusion constructs were grown and purified as previously described (Marble et al., 2005). Equal amounts GST or EAG protein, as determined in protein assays, were

present for each condition of a given interaction experiment. Bovine CaM (EMD Biosciences Inc., La Jolla, CA) (0.5 μM) was incubated for 1 hr at 4°C with 1 μM of the indicated GST-EAG fragments immobilized on Sepharose beads with 0.5% Triton-X100 in PBS (in mM: 137 NaCl, 2.7 KCl, 10 Na_2HPO_4, 1.76 KH_2PO_4, pH 7.4) containing protease inhibitors and either 1 mM $CaCl_2$ or 10 mM EGTA. Sample volume was 100 μl with a bead bed volume of 10 μl. Beads were collected by centrifugation and washed six times with PBS containing 0.1% Triton X-100 and either 1 mM $CaCl_2$ or 10 mM EGTA. Pellets, including beads and associated proteins, were analyzed using 12% SDS-PAGE gels and Western blotting. Blots were incubated with a 1:1000 dilution of mouse anti-CaM primary antibody overnight at 4°C, then washed twice with TBS-T (TBS with 0.05% Tween, 0.2% Triton X-100) and once with TBS, before incubation with a 1:2,000 dilution of horseradish perodixase (HRP)-conjugated goat anti-mouse secondary antibody. After four washes in TBS-T, bound CaM was visualized by enhanced chemiluminescence (ECL) (Amersham Biosciences, Piscataway NJ). Volume intensities of protein bands were quantified using Quantity One software (Bio-Rad, Hercules CA). For each blot, measurements were corrected for background by subtracting values obtained in the corresponding region of the lane for glutathione sepharose controls, and then normalizing to the value obtained for wild type EAG fusion protein.

E.3. Electrophysiology

Oocytes were surgically removed from *Xenopus laevis* frogs (Xenopus I, Ann Arbor, MI) as described previously (Marble et al., 2005). RNA was transcribed using T7 mRNA mMessage mMachine (Ambion, Austin, TX) and 46.5 nl of RNA was injected per

oocyte. Oocytes were incubated in ND96 media (containing in mM: 96 NaCl, 2 KCl, 1 MgCl2, 5 HEPES, pH 7.4 and antibiotics) for 1-5 d before recording using a Turbo TEC-10C amplifier (NPI Electronics, Tamm Germany) and pCLAMP8 software (Molecular Devices-Axon Instruments, Union City CA) as previously described (Marble et al, 2005). Normal extracellular bath solution contained (in mM): 140 NaCl, 2 KCl, 2 $MgCl_2$, 10 HEPES, pH 7.4. For ionomycin experiments, the bath contained (in mM): 100 mM Na-Aspartate, 2 KCl, 2.5 $CaCl_2$, 1 $MgCl_2$, 10 HEPES, pH 7.4. DIDS (4,4'-diisothiocyanatostilbene-2,2'-disulfonic acid), dissolved to a stock concentration of 100 mM in DMSO, was included at a final concentration of 100 μM to block endogenous Ca^{2+}-activated Cl^- channels. DIDS was used because flufenamic acid, another commonly used Ca^{2+}-activated Cl^- channel blocker, accelerated inactivation of EAG currents (data not shown). A high K^+ solution was used for determining G-V relations and contained (in mM): 117 NaCl, 25 KCl, 1 $MgCl_2$, 10 HEPES, pH 7.4. The holding potential was –80 mV unless otherwise specified.

Recordings from body wall muscle fibers 6 and 7 of WT, *eag*^{sc29} and transgenic 3rd-instar larvae were performed using a modified HL3 saline (Stewart et al., 1994) containing (in mM): 70 NaCl, 5 KCl, 4 $MgCl_2$, 10 $NaHCO_3$, 5 trehalose, 115 sucrose and 5 Hepes (pH 7.1), with either 0.4 mM $CaCl_2$ for recordings of spontaneous activity, or 0.15 mM $CaCl_2$ for responses evoked by stimulation of the motor nerve cut free from the ventral ganglion. Data were collected and analyzed using an AxoClamp 2B and pCLAMP9. For evoked activity, the intensity of the stimulus was set to 0.5 V above threshold. Excitatory junctional currents were elicited from a holding potential of –70 mV. Facilitation was assessed using five pulses at the indicated frequency, averaging the

responses across a minimum of three trials, and then normalizing the average amplitude of the fifth EJP to the average amplitude of the first. A minimum of ten seconds was allowed between trials. Experiments were performed at room temperature.

E.4. Measurements of off-rates by steady-state fluorescence

Labeling of CaM (C75) with Acrylodan was performed according to (Waxham et al., 1998). Slow off-rates were measured at 25 °C in a Hitachi F-4010 spectrofluorimeter. Fluorescence excitation and emission maxima for CaM(C75)ACR were 370 and 470 nm, respectively. Slit widths were 10 nm for both excitation and emission. Addition of components was done manually to a cuvette with a 0.5 ml volume. The standard buffer for fluorescence experiments was 25 mM MOPS, pH 7.0, 150 mM KCl, 0.1 mM EGTA, 0.1 mg/ml bovine serum albumin and 1 mM $CaCl_2$. CaM(C75)ACR was used at a concentration of 0.2 μM. Eag-$C1_{(556\text{-}803)}$ and its mutants were all used at 0.5 μM . A 50-fold excess of unlabeled CaM was added to the cuvette to initiate dissociation. A cuvette containing the same sample but lacking excess CaM served as a monitor for photobleaching and variations in lamp intensity in each of these experiments. All such measurements were performed at least two times, and the data were fit with a single exponential function to determine the value of k_{off} for CaM.

E.5. *Drosophila* transgenics

pPUAST-*eag* constructs were injected along with the Δ2,3 recombinant helper plasmid into w^- embryos and positive transformants identified by the w^+ phenotype in F1. To verify expression of EAG protein, the resulting transgenic lines were crossed to a

Gal4-heat shock driver and induced for three hours at 37 ^{o}C over a ten hour period. Extracts were probed with antisera directed against the carboxy terminal of EAG as previously described (Marble et al., 2005). Only lines resulting in significant inducible expression of EAG were employed in electrophysiological experiments. To assess rescue of the null phenotype at the larval neuromuscular junction, UAS-*eag* constructs were expressed using a pan-neuronal (elav5147-Gal4) driver and crossed into the eag^{sc29} null background (eag^{sc29}; *elav-Gal4*; *UASeag*).

CHAPTER IV

A CAMKII BINDING DOMAIN UNDERLIES VOLTAGE-DEPENDENT CONDUCTANCE-INDEPENDENT SIGNALING BY EAG POTASSIUM CHANNELS

A. ABSTRACT

Voltage-gated ion channels regulate cell signaling and neuronal excitability by regulating ion movement across cell membranes. Recent studies suggest that channels also can affect biochemical events by mechanisms that do not rely on ion conduction. Here we identify a domain that underlies the ability of nonconducting ether à go-go (EAG) K^+ channels to regulate intracellular signaling pathways and show that the activity of Ca^{2+}/calmodulin-dependent protein kinase II (CaMKII) depends on channel conformations associated with the position of the voltage sensor. *In Drosophila*, signaling deficient channels failed to rescue the high levels of spontaneous activity characteristic of *eag* mutants, suggesting that voltage-dependent, conductance-independent EAG signaling plays a role in the homeostatic regulation of neuronal activity. Our results identify a novel function for voltage sensing and suggest this mechanism may serve as a direct link between neuronal activity and the state of intracellular messengers.

B. INTRODUCTION

Recent studies suggest that voltage-gated ion channels can affect cell signaling and neuronal function by mechanisms that do not require ion flux (Kaczmarek, 2006; Runnels et al., 2001; MacLean et al., 2003; Dolmetsch et al., 2001; Gomez-Ospina et al., 2006; Malhotra et al., 2000). The voltage-gated K^+ channel EAG was originally implicated as a possible bifunctional channel in studies showing a role for human EAG in cell cycle progression and oncogenesis (Pardo et al., 1999; Meyer and Heinemann, 1998; Farias et al., 2004; Patt et al., 2004). In studies of the *Drosophila* ortholog expressed in NIH 3T3 cells, we have shown that EAG acts independently of conductance as an upstream regulator of intracellular signaling and proliferation (Hegle et al., 2006, see appendix). Notably, mutations that increase the proportion of channels in the open state inhibit the proliferation induced by non-conducting channels, suggesting that conformations associated with the position of the voltage sensor are a switch for the signaling activity of EAG.

Because the above findings were largely obtained using heterologous expression systems, it remains unclear whether EAG signaling is operational in neurons, where both fly and mammalian channels are predominantly expressed (Saganich et al., 2001; Ludwig et al., 2000; Ludwig et al., 1994; Sun et al., 2004; Jeng et al., 2005). In recordings at the neuromuscular junctions (NMJs) of *Drosophila* larvae, loss of *eag* results in a high level of spontaneous activity and an increase in the amplitudes of evoked excitatory junctional potentials (EJPs), effects that have been generally assumed to be the result of a reduction in neuronal K^+ current (Ganetzky and Wu, 1983; Wu et al., 1983; Griffith et al., 1994).

In addition, loss of *eag* produces defects in learning suggesting that EAG plays an important role in the adult CNS (Griffith et al., 1994).

Here we present evidence that the signaling activity of *Drosophila* EAG channels is mediated via voltage-dependent regulation of Ca^{2+}/calmodulin- dependent protein kinase II (CaMKII), and that this mechanism is conserved in mammalian EAG. Mutation of key residues in the EAG carboxyl-terminal CaMKII binding domain abolished EAG-mediated signaling, and phosphorylation assays using mutations that shift the voltage-dependence of EAG suggest that membrane-associated CaMKII activity is modulated by voltage-driven conformational changes in EAG. In recordings from the larval NMJs of transgenic *Drosophila*, EAG channels with mutations in the CaMKII binding domain failed to rescue the high levels of spontaneous activity characteristic of *eag* mutants, whereas non-conducting EAG channels rescued spontaneous activity with an efficiency nearly overlapping that observed for wild type channels. These results suggest that the signaling and conductance functions of EAG are phenotypically separable, and that, *in vivo*, voltage-dependent, conductance-independent signaling plays a key role in the homeostatic regulation of neuronal activity.

C. RESULTS

C.1. CaMKII binding domain is required for EAG signaling

To determine the domain and mechanism underlying the signaling activity of EAG, we examined the effects of deletions and mutations in the cytoplasmic tails using 5-bromo-2'-deoxyuridine (BrdU) assays of NIH 3T3 cell proliferation. Figure 4.1A compares the effects of wild type and non-conducting channels (EAG-F456A) with the

effects of truncated channels that lack the cytoplasmic N- or C-terminal domains. As observed previously (Hegle et al., 2006), incorporation of BrdU, a fluorescent indicator of cell proliferation, was significantly increased over control levels ($p < 0.01$, $n = 6$) for coverslips transfected with wild type EAG and EAG-F456A (Fig 4.1C). Although the N-terminal deletion (EAG-ΔNT, containing amino acids 213-1174), which lacks the PER-ARNT-SIM (PAS) dimerization domain (Crews and Fan, 1999), failed to disrupt EAG-induced proliferation ($n = 3$), the C-terminal deletion (EAG-ΔCT, containing amino acids 1-514) decreased proliferation to a level comparable to vector-transfected controls ($p < 0.05$ in comparison to EAG, $n = 3$; Fig 4.1A,C). These results suggest that a key domain underlying EAG-induced proliferation resides in the cytoplasmic C-terminal tail of EAG.

The EAG C-terminus is nearly twice as long as that of Shaker channels and contains several domains that could mediate the signaling activity of EAG. In addition to a domain with homology to the cyclic nucleotide-binding domains of other channels (Guy et al., 1991), it contains a functional CaMKII binding domain with high similarity to the autoinhibitory domain of the kinase (Hanks et al., 1988; Sun et al., 2004), a functional calmodulin (CaM) binding domain (Schonherr et al., 2000), three putative nuclear localization signals (NLS), and a series of putative Src-Homology 3 (SH3) motifs, one of which is known to interact with the Camguk/CASK (CMG) adapter protein (Marble et al., 2005, see Chapter II). To identify the domain(s) contributing to the signaling activity of EAG, we generated mutations in candidate domains, including the CaMKII (EAG-LAKK), CaM (EAG-FFSS), and CMG (EAG-RLKM) binding domains, the CaMKII phosphorylation site (EAG-T787A), and two putative NLS domains (EAG-NLS-1 and -2). The third putative NLS overlaps with the CMG binding domain and should also be

Figure 4.1: The EAG CaMKII binding domain is essential for signaling.
(A) The C-terminal domain is required for EAG signaling. Representative scans showing BrdU labeling of coverslips transfected with the pCS2 vector, pCS2-*eag*, pCS2-*eag*-F456A, and N- and C-terminal deletion mutants. **(B)** Representative scans showing BrdU labeling of coverslips transfected with *eag* CaMKII binding domain mutants as indicated. **(C)** Average fluorescence intensities for coverslips examining the role of the N- and C-terminal cytoplasmic domains normalized to the level of vector-transfected controls, indicated by the gray shaded background ($p = 0.0034$ overall; $p < 0.01$ for individual comparisons of WT-EAG and EAG-F456A to vector controls, $n = 6$; $p < 0.05$ for comparison of the CT-deletion to wild type EAG, $n = 3$). **(D)** Average fluorescence intensities of coverslips transfected with domain mutations, including those shown in (b), normalized to vector-transfected controls (overall $p = 0.0167$, $n = 5$). **(E)** Representative blots showing total expression and surface expression of wild type and mutant channels, with actin as the loading control. **(F)** Average surface expression from blots as in (e). For each experiment, bands were quantified by densitometry and normalized to the band for wild type EAG in the extract, prior to determining the ratio of EAG in the streptavidin precipitate to total EAG (overall $p = 0.4623$, $n = 3$). **(G)** Representative recordings from oocytes expressing wild type EAG or EAG-LAKK. Oocytes were stepped from -100 to +60 mV in 10 mV increments (holding potential, -80 mV); every other trace is shown. Capacitative and leak currents were subtracted using a P/4 protocol. Scale bars, 5 μA and 100 ms. **(H)** Average conductance-voltage (GV) relations obtained for WT-EAG ($n = 9$) and EAG-LAKK ($n = 4$). Conductances were calculated from currents using the relation $G = I_{peak}/ (V_{test} - E_K)$, with E_K was assumed to be -100 mV, and then normalized to the maximum conductance observed. Boltzmann fits had midpoints of 1.2 ± 0.4 and 2.8 ± 3.2 mV and slopes of 16.1 ± 0.3 and 19.9 ± 2.9, for EAG and EAG-LAKK, respectively. Scale bars = 10 μm for these and all scans in subsequent figures. Data are presented as the mean ± SEM. N.S., not significant; * = $p < 0.05$ in comparisons to wild type EAG; WT, wild type; Ctrl, control.

FIGURE 4.1

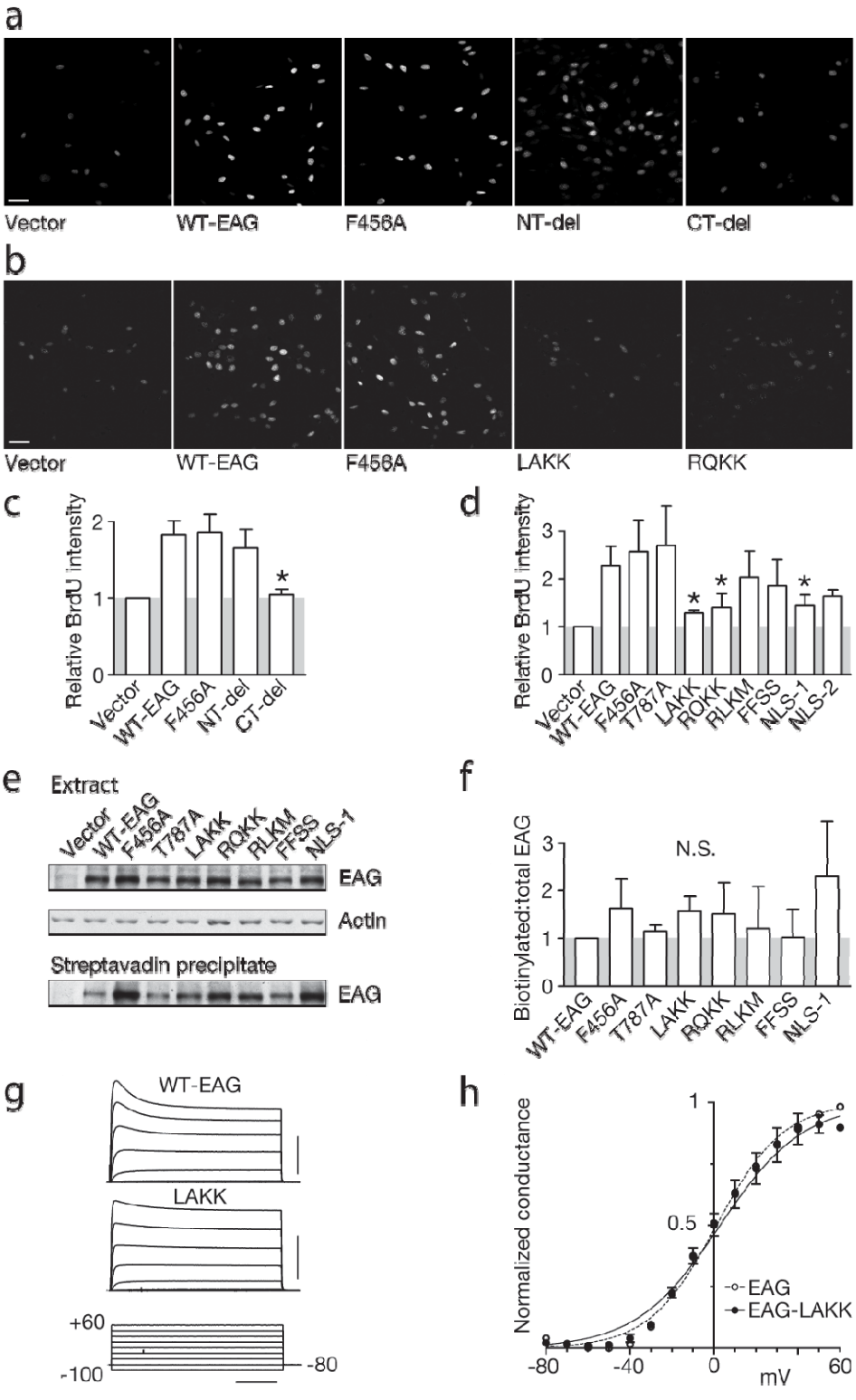
a
Vector
WT-EAG
F456A
NT-del
CT-del
b
Vector
WT-EAG
F456A
LAKK
RQKK
c
Relative BrdU intensity
Vector
WT-EAG
F456A
NT-del
CT-del
d
Relative BrdU intensity
Vector
WT-EAG
F456A
T787A
LAKK
RQKK
RLKM
FFSS
NLS-1
NLS-2
e
Extract
Vector
WT-EAG
F456A
T787A
LAKK
RQKK
RLKM
FFSS
NLS-1
EAG
Actin
Streptavadin precipitate
EAG
f
Biotinylated:total EAG
N.S.
WT-EAG
F456A
T787A
LAKK
RQKK
RLKM
FFSS
NLS-1
g
WT-EAG
LAKK
+60
-100
-80
h
Normalized conductance
EAG
EAG-LAKK
mV

disrupted by the RLKM mutation. Assays of BrdU incorporation revealed that the most predominant inhibition was produced by the CaMKII binding domain mutation, EAG-LAKK (Fig 4.1B,D; $p < 0.05$ in comparison to wild type EAG, $n = 5$). The proliferation observed using EAG-LAKK was statistically indistinguishable from that observed for vector-transfected controls (Fig 4.1D). Further verification of the importance of the CaMKII binding domain was obtained using EAG-RQKK, in which residues neighboring LA were replaced with lysines. EAG-RQKK also significantly inhibited proliferation (Fig. 4.1B,D; $p < 0.05$, $n = 5$).

The reduced proliferation observed with mutations in the CaMKII domain could not be explained by changes in surface expression, because precipitation of biotinylated cell extracts revealed no significant difference in surface expression for the various C-terminal domain mutations (Fig. 4.1E,F). Furthermore, when expressed in *Xenopus* oocytes, EAG-LAKK and EAG-RQKK exhibited outward currents comparable to those observed for wild type EAG, although, as shown for EAG-LAKK (Fig. 4.1G), inactivation was slower and less extensive. In addition, comparison of normalized conductance-voltage (GV) relationships revealed no detectable difference in the voltage-dependence of EAG-LAKK and wild type channels (Fig. 4.1H). Together, these data suggest that the CaMKII binding domain is essential for EAG-mediated proliferation; however, they do not rule out possible contributions of other regions of the channel. In particular, a mutation in the first putative NLS (NLS-1) also inhibited proliferation, but surface expression of this construct was quite variable (Fig 4.1D-F).

C.2. Voltage-dependent conformations regulate CaMKII activity

The most notable feature of EAG-mediated proliferation is that EAG signaling is regulated by conformations associated with the position of the voltage sensor. Specifically, mutations in the sixth transmembrane domain that shift the voltage-dependence of activation to more negative potentials (EAG-HTEE and EAG-TATSSA) disrupt EAG-mediated proliferation when coupled with the F456A mutation to render channels non-conducting (referred to as EAG-HFA and EAG-TFA, respectively). By short-circuiting the negative feedback effect of ion conduction on membrane potential, EAG-HFA and EAG-TFA channels are forced into a predominantly open conformation and, in this state, EAG-mediated proliferation is inhibited (Hegle et al., 2006). If CaMKII is the most immediate downstream target of EAG signaling, then either CaMKII activity or localization also should be regulated by voltage-dependent conformations of EAG. Recent *in vitro* studies suggest that kinase activity may be regulated, because CaMKII associated with the C-terminal cytoplasmic tail of EAG retains 5-10% of its maximal activity when the complex is washed in Ca^{2+}-free buffer (Sun et al., 2004). This constitutive activity is distinct from that mediated by phosphorylation of T287 of the kinase, although T287 can still be autophosphorylated.

To determine whether EAG regulates CaMKII in a voltage-dependent manner, we probed extracts of cells transfected with EAG-HTEE, EAG-TATSSA or their non-conducting counterparts for phosphorylated kinase, given that autophosphorylation is an indicator of kinase activity (Hudmon and Schulman, 2002). As shown in Figure 4.2A, in extracts the ratio of phosphorylated to total CaMKII was uniform for the different EAG constructs. In contrast, however, when the membrane fraction was isolated using

FIGURE 4.2

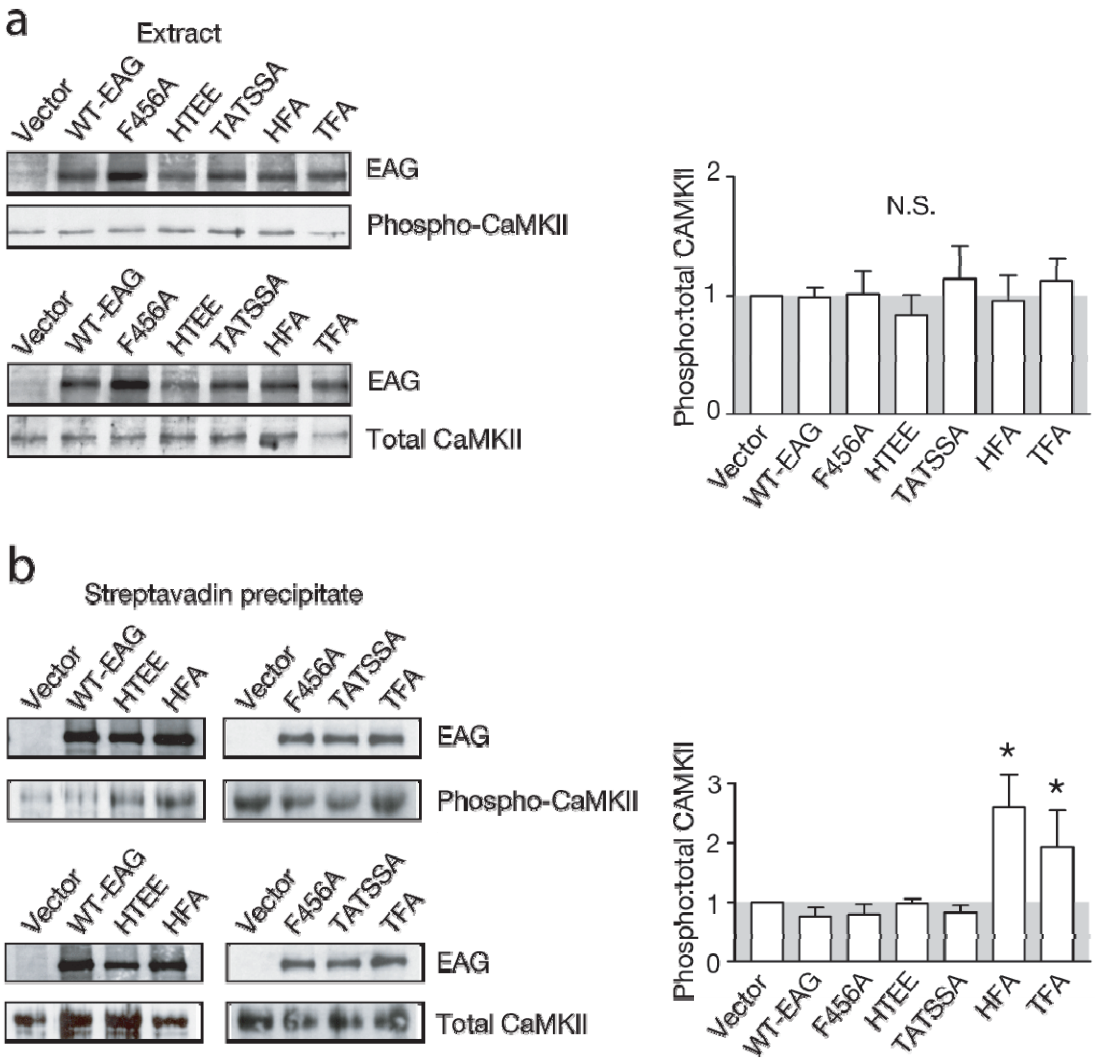

Figure 4.2: EAG regulates membrane-associated CaMKII activity.
(A) *Left*, Representative blots showing EAG, phospho-CaMKII and total CaMKII in extracts of NIH 3T3 cells expressing the indicated constructs. *Right*, Averaged densitometric quantification of CaMKII activity, shown as the ratio of phospho:total CaMKII and normalized to the activity observed for vector-transfected controls (overall $p = 0.8314$, $n = 4$). **(B)** Membrane-associated CaMKII activity. Biotinylation and precipitation were performed as described in Methods. *Left*, Representative blots. *Right*, Average ratio of phospho:total CaMKII analyzed as described in (a). Overall $p = 0.0028$, $n = 4$. In both (a) and (b), equal amounts of either extracts or precipitates were separated by SDS-PAGE and probed with EAG (CT), phospho-CaMKII or CaMKII antisera.

biotinylation and precipitation with streptavidin, there was an approximate two-fold increase in membrane-associated kinase activity for the EAG-HFA and EAG-TFA conditions when compared to controls (Fig 4.2B, $p < 0.05$, $n = 4$). In addition, there appeared to be a small decrease in CaMKII activity for EAG constructs that induce proliferation. A local decrease in CaMKII activity, or a shift in localization to different membrane-associated complexes, could explain why mutations in the CaMKII binding domain inhibit the proliferation response. Together, these results suggest that the effect of EAG on CaMKII activity depends on voltage-dependent conformations of the channel and, further, that EAG-mediated increases in kinase activity negatively regulate the proliferation pathway.

In previous experiments (Hegle et al., 2006), both wild type EAG and the non-conducting selectivity filter mutant (EAG-F456A) increased the activity of p38 MAPK (p38), and p38 inhibitors blocked the proliferation induced by either channel. If p38 is downstream and inhibited by CaMKII in the proliferation pathway, then regulation of p38 activity by EAG should also be voltage-dependent (Supplementary Fig. 4.S1A). However, we failed to detect voltage-dependent regulation of p38 in either cell extracts or membrane-associated fractions (data not shown). Either the effects on p38 are limited to molecules in close proximity to EAG or voltage-dependent regulation affects the localization of p38 to a compartment that is not adequately represented by the membrane fraction. Lastly, CaMKII may regulate a step that is downstream of p38 to inhibit proliferation (Supplementary Fig. 4.S1B). This latter possibility would imply that EAG regulates two distinct signaling pathways.

C.3. EAG signaling is conserved in mouse channels

Further support for the role of the CaMKII binding domain in EAG-induced proliferation was obtained in experiments examining the conservation of EAG signaling in mouse EAG (mEAG) channels. As with *Drosophila eag*, transfection of either wild type or non-conducting (F466A) *meag* resulted in a significant increase in BrdU incorporation (Fig. 4.3A; $p < 0.05$ and 0.001 for mEAG and mEAG-F466A, respectively, $n = 4$). Recordings from NIH 3T3 cells expressing mEAG revealed a robust outward current (Fig. 4.3B), which exhibited voltage-dependent activation kinetics reminiscent of the Cole-Moore shift as expected for EAG channels (Ludwig et al., 1994; Cole and Moore, 1960) (Supplementary Fig. 4.S2A). In contrast, the outward currents observed in cells transfected with mEAG-F466A overlapped with the currents observed in vector-transfected controls (Fig. 4.3B), and, in both cases, changes in prepulse voltage had an effect on kinetics that was opposite that observed for currents recorded from cells transfected with the wild type channel (Supplementary Fig. 4.S2A).

The mEAG C-terminal cytoplasmic tail contains a stretch of amino acids with homology to the CaMKII binding domain in the *Drosophila* channel, as well as the CaMKII autoinhibitory domain (Fig. 4.3C). To examine whether this domain is also required for mEAG-mediated proliferation, two mutants, mEAG-RQEE and mEAG-QKEE, were generated based on homology to key residues in the other sequences. Both constructs produced an outward current that was comparable to that observed for the wild type channel in amplitude and voltage-dependence, although activation was slower (Supplementary Fig. 4.S2B,C). Coverslips transfected with either mutant exhibited substantially reduced BrdU incorporation compared to coverslips transfected with wild

Figure 4.3: CaMKII-dependent signaling is conserved in mammalian EAG.
(A) *Left*, Representative scans showing BrdU labeling of coverslips transfected with vector, *meag* or *meag*-F466A. *Right*, Average fluorescence intensities for the indicated conditions normalized to vector-transfected controls (overall $p = 0.0105$; $n = 4$; in individual post-hoc comparisons to vector levels, indicated by gray shading, * = $p < 0.05$; ** = $p < 0.01$). **(B)** Averaged currents elicited by ~160 ms ramps from -100 to +100 mV for NIH 3T3 cells transfected with wild type mEAG (——; n = 16), mEAG-F466A (----; n = 6), or empty vector (••••; n = 4). Capacitative and leak currents were subtracted using a P/8 protocol. **(C)** Alignment of the autoinhibitory domain of CaMKII with homologous regions of *Drosophila* EAG and mEAG. Conserved residues shaded in gray. Outlined box identifies *Drosophila* EAG and mEAG residues mutated in this study. **(D)** *Left*, Representative scans showing BrdU labeling of coverslips transfected with *meag* CaMKII-binding domain mutants, as indicated. *Right*, Average fluorescence intensities, normalized to vector-transfected controls (overall $p = 0.0113$, $n = 3$; in individual comparisons to vector, * = $p < 0.05$). **(E)** *Left*, Proliferation-Voltage (PV) curve generated using the voltages estimated for different K^+ concentrations based on the data in Supplementary Fig. 3d,e. The mEAG GV curve and corresponding Boltzmann fit have been added for comparison (midpoint -9.2 ± 1.4 mV, slope 22.5 ± 1.3; Supplementary Fig. 3c). Note that one interpretation of the steeper slope of the PV curve is that all four subunits may need to be in a closed conformation for proliferation to occur. *Right*, Proliferation induced by mEAG and the CaMKII binding mutant mEAG-RQEE at K^+ concentrations predicted to result in membrane potentials of -52 and -16 mV. Only proliferation induced by the wild type channel is regulated by the membrane potential, in spite of the fact that mEAG-RQEE channels are as efficient as mEAG in driving the membrane potential to more negative values. In paired two-tailed t-tests, $p = 0.0109$ for mEAG and 0.5069 for mEAG-RQEE, $n = 4$.

FIGURE 4.3

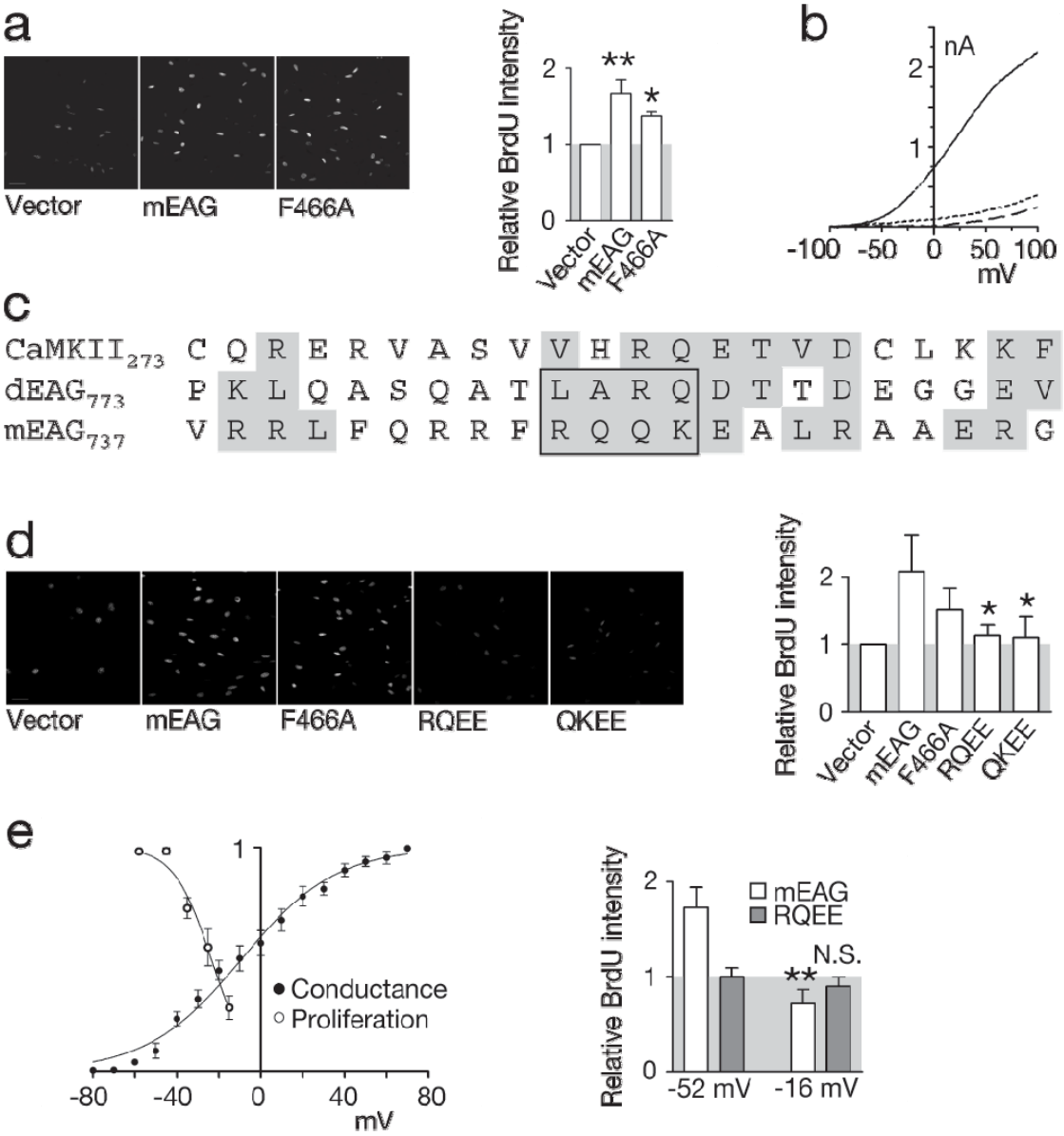
a
Vector
mEAG
F466A
Relative BrdU Intensity
2
1
0
**
*
Vector
mEAG
F466A
b
nA
2
1
-100 -50 0 50 100
mV
c
CaMKII273 C Q R E R V A S V V H R Q E T V D C L K K F
dEAG773 P K L Q A S Q A T L A R Q D T T D E G G E V
mEAG737 V R R L F Q R R F R Q Q K E A L R A A E R G
d
Vector
mEAG
F466A
RQEE
QKEE
Relative BrdU intensity
2
1
0
*
*
Vector
mEAG
F466A
RQEE
QKEE
e
1
Conductance
Proliferation
-80 -40 0 40 80
mV
Relative BrdU intensity
2
1
0
mEAG
RQEE
N.S.
**
-52 mV
-16 mV

type *meag* ($p < 0.05$, n = 3; Fig. 4.3D), indicating that the CaMKII binding domain plays a critical role in the proliferation induced by both mouse and fly channels.

Voltage-dependent proliferation also was conserved in mEAG channels (Fig. 4.3E). In keeping with the observation that mEAG currents were more robust than those generated by *Drosophila* EAG, the membrane potentials of mEAG expressing cells also were substantially more hyperpolarized (-52.5 ± 2.7 mV, n = 15) than the ~ -12 mV average membrane potential reported using the *Drosophila* channel (Hegle et al., 2006). The increased working range allowed us to examine the voltage-dependence of mEAG signaling using iso-osmotic substitution of K^+ for Na^+ in the media. The effect of K^+ on membrane potential was first determined in current clamp recordings during perfusion of a range of concentrations (Supplementary Fig. 4.S2D). Averaged membrane potentials for each concentration were well-approximated using the Goldman equation, assuming a permeability ratio of 1.0:0.67 for K^+ to Cl^-, respectively (Supplementary Fig. 4.S2E).

The above measurements allowed us to estimate the resting potentials of cells in proliferation assays at each K^+ concentration. Figure 4.3E (*left*) depicts the resulting 'proliferation-voltage' (PV) curve, in which normalized BrdU intensity is plotted as a function of voltage. The PV curve was well-fit by a Boltzmann function with half maximal activation (V_{50}) at -23.5 mV and a slope of -8.9. Comparison of the PV and GV curves suggests that that proliferation is maximal when the channels are predominantly closed, as previously suggested for the *Drosophila* channel (Hegle et al., 2006). The voltage-dependence of the proliferation induced by mEAG channels accounts for the decreased effectiveness of non-conducting mEAG-466A (Fig. 4.3A,D), given that the average resting potential for cells expressing mEAG-F466A was -10.7 ± 2.4 mV (n = 14).

Finally, voltage-dependent proliferation was not observed for the CaMKII binding domain mutant, mEAG-RQEE, in spite of its ability to shift the membrane potential (-49.7 ± 4.4 mV, n = 6; Fig. 4.3E, *right*).

C.4. Regulation of neuronal activity

To investigate the role of EAG signaling *in vivo*, we used the GAL4-UAS system (Phelps and Brand, 1998) to express various channel constructs in the null, eag^{sc29}, background. As observed in mammals (Ludwig et al., 1994; Jeng et al., 2005; Saganich et al., 2001), *Drosophila* EAG is largely neuron-specific: EAG is expressed throughout the brain and optic lobes, and, in larvae, is enriched in the axons and terminals of motor neurons that synapse on the body wall muscle fibers (Sun et al., 2004; Wang et al., 2002b). We therefore used the neuron-specific *elav* promoter to drive EAG expression. The two primary defects observed at the larval neuromuscular junctions (NMJs) of *eag* mutants are a high frequency of spontaneous excitatory junctional potentials (EJPs) and increased amplitudes of both spontaneous and evoked excitatory junctional currents (EJCs) (e.g., eag^{sc29}, Fig. 4.4). In extracellular recordings of motor nerve activity, these defects are readily seen to reflect hyperexcitability of the motor nerve and/or terminals (Ganetzky and Wu, 1985) and have led to the suggestion that EAG current normally contributes to the maintenance of the resting potential, in addition to the repolarization of evoked action potentials.

Figure 4.4: EAG signaling contributes to synaptic function *in vivo.*
(a) *Left*, Representative EJCs elicited by electrical stimulation of the motor nerve for w^- males (WT) and homozygous eag^{sc29} larvae, compared to EJCs observed for heterozygous wild type (WT-rescue), eag^{LAKK}, and eag^{F456A} constructs transgenically expressed using the neuron-specific *elav* promoter. Recording solution contained 0.15 mM Ca^{2+}. This low concentration of Ca^{2+} enhances amplitude differences presumably by minimizing evoked neurotransmitter release. Bars, 0.5 μA and 100 ms. *Right*, Averaged EJC amplitudes for w^- male (WT) and eag^{sc29} larvae compared to transgenics expressing the indicated *eag* constructs. Statistical comparisons are to the rescue condition indicated by the gray background shading, overall $p < 0.0001$, n indicated inside each bar. **(b)** *Left*, Representative recordings of spontaneous EJP activity in wild type and eag^{sc29} larvae compared to transgenic larvae expressing either wild type or LAKK channels. Each of the 3 traces shown is a recording from a different fiber. HL3 saline contained 0.4 mM Ca^{2+}. Bars, 20 mV and 500 ms. *Right*, Average data for the indicated genotypes. Overall $p < 0.0001$. Note: In both (a) and (b) only data from muscle fibers 6 and 7 were included. For individual comparisons to wild type rescue: * $p < 0.05$; *** $p < 0.001$; N.S., not significant.

FIGURE 4.4

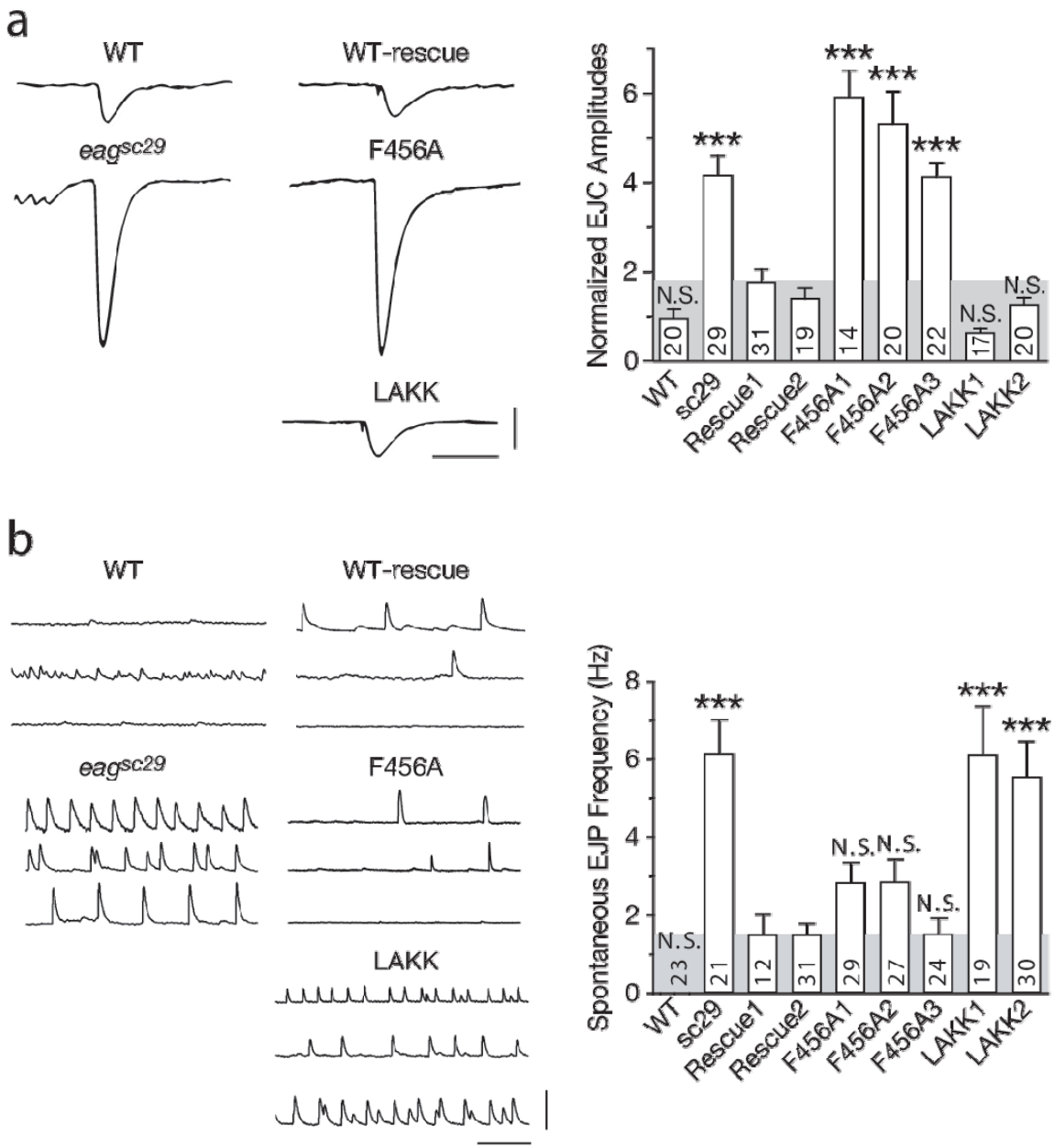
a
WT
WT-rescue
eagsc29
F456A
LAKK
Normalized EJC Amplitudes
***
***
***
***
N.S.
N.S.
N.S.
20
29
31
19
14
20
22
17
20
WT
sc29
Rescue1
Rescue2
F456A1
F456A2
F456A3
LAKK1
LAKK2
b
WT
WT-rescue
eagsc29
F456A
LAKK
Spontaneous EJP Frequency (Hz)
***
***
***
N.S.
N.S.
N.S.
N.S.
23
21
12
31
29
27
24
19
30
WT
sc29
Rescue1
Rescue2
F456A1
F456A2
F456A3
LAKK1
LAKK2

In comparisons of transgenic lines expressing wild type, signaling- (*eag*-LAKK), and conductance- (*eag*-F456A) deficient EAG, both wild type and signaling-deficient channels restored evoked EJC amplitudes to levels statistically indistinguishable from the amplitudes observed for wild type larvae (Fig. 4.4A), whereas non-conducting channels failed to rescue this defect. These results suggest that *eag*-LAKK is reasonably expressed and that EAG current plays the predominant role in repolarizing the motor neuron action potential. In contrast, whereas lines expressing non-conducting EAG reduced the frequency of spontaneous activity to levels comparable to that observed using wild type EAG, the spontaneous activity observed in *eag*-LAKK expressing larvae remained high, at levels comparable to those observed in the absence of EAG (Fig. 4.4B). The observed phenotypes were consistent regardless of the point of insertion for each transgene, indicating that the effects were not due to disruption of another gene. These results indicate that EAG signaling, not current, plays the predominant role in maintaining a stable level of motorneuron activity, and, further suggest that EAG signaling may be a key player in the homeostatic regulation of this synapse. These results also may account, in part, for the phenotypic similarities observed for *eag* mutants and transgenic *Drosophila* expressing the autoinhibitory domain of CaMKII (Griffith et al., 1994). A high level of spontaneous activity is the feature that most clearly distinguishes *eag* mutants from mutants of other K^+ channel genes such as *Shaker* (Ganetzky and Wu, 1983; Wu et al., 1983).

D. Discussion

The EAG signaling mechanism described here suggests a novel function for the voltage sensors of ion channels that is distinct from the regulation of ion flux. Signaling depends on voltage-dependent conformations of the channel: proliferation is highest when non-conducting EAG is predominantly in a closed conformation and membrane-associated CaMKII is inhibited. A pore-independent function for voltage sensors also has been indicated in studies of the recently identified *Ci*-VSP, a protein that contains a transmembrane voltage sensor linked to a functional phosphatase (Murata et al., 2005), and the VSOP (voltage-sensor only proteins)/Hv1 proteins, which lack a conventional channel pore, but conduct protons through a pathway in the voltage sensing domain (Ramsey et al., 2006; Sasaki et al., 2006). In this regard, it is important to note that non-conducting EAG channels do not produce a detectable proton current when a pH gradient is imposed (Wilson, unpublished observations). Thus, regulation of CaMKII must occur via voltage-dependent conformational changes in the channel. Our data support a model in which the suppression of CaMKII activity by closed EAG conformations relieves downstream inhibition of p38, by changing either the localization or activity of a component of this pathway (Supplementary Fig. 4.S1). This cascade also may underlie the oncogenic potential of abnormally expressed human EAG (Pardo et al., 1999; Meyer and Heinemann, 1998; Farias et al., 2004; Patt et al., 2004).

Direct voltage- or activation- dependent regulation of enzyme activity is likely to occur in other ion channels that interact directly with enzymes. However, because CaMKII is nearly ubiquitous, mechanisms that limit accessibility to substrates and extend or restrict the conditions during which enzyme activation can occur are likely to be

particularly important to the function of this kinase. Both the α_{1C} subunits of L-type Ca^{2+} channels and the NR2B subunits of NMDA receptors contain carboxyl terminal regions that successfully compete with the autoinhibitory domain to bind to CaMKII (Bayer et al., 2001; Hudmon and Schulman, 2005). In both cases, Ca^{2+} influx is required for initial binding, because Ca^{2+}/calmodulin promotes the dissociation of the autoinhibitory domain and exposes binding sites that reside in the catalytic region of the kinase. However, once the interaction is established, it persists even when Ca^{2+} returns to basal levels. For NR2B subunits, binding has been reported to result in constitutive kinase activity as observed for EAG (Sun et al., 2004 whereas for α_{1C} subunits bound kinase appears to remain dependent on Ca^{2+}/calmodulin for activation. It remains to be seen, however, whether conformations associated with the activation state of either NMDA receptors or L-type Ca^{2+} channels directly affect kinase activity. Intriguingly, an initial requirement for increased Ca^{2+}, followed by Ca^{2+}-independence and a more direct regulation through the activation state of associating ion channels are features expected for a molecular tag of prior activity (Martin, 2002) and would be expected to result in an increase in the temporal and spatial efficiency of CaMKII.

Although the signaling activity of EAG channels was initially identified by an increase in proliferation, proliferation and growth may only be affected when EAG is abnormally expressed. Indeed, no growth related phenotype has been reported for *eag* mutants, and under normal circumstances, EAG is predominantly expressed in neurons in both flies and mammals. Importantly, in mammals, *in situ* hybridization and immunostaining suggest that EAG is enriched in hippocampus and cortex (Jeng et al., 2005; Saganich et al., 2001), however, currents mediated by EAG in these neurons have

yet to be identified. Our results suggest the possibility that signaling, not current, may be the relevant functional output of EAG.

CaMKII is well-established as a key component of synaptic plasticity and learning in a number of systems, including *Drosophila* and mammals (Silva et al., 1992a; Griffith et al., 1993; Silva et al., 1992b). Although our experiments do not address the identity of downstream target(s) of EAG-CaMKII signaling in either NIH 3T3 fibroblasts or *in vivo*, through the regulation of small GTPases such as Ras, CaMKII activity regulates MAPK pathways that activate nuclear transcription factors, such as the cAMP response element binding protein (CREB), that control the transcription of activity-dependent genes (Thomas and Huganir, 2004). Specifically, Ras-mediated activation of p42/44 MAPK contributes to facilitation and long-term potentiation (LTP) (Bolshakov et al., 2000; Zhu et al., 2002), whereas p38 regulates long-term depression (LTD) (Zhu et al., 2002; Thomas and Huganir, 2004; Guan et al., 2003). CaMKII activity also contributes to p38 inactivation through the regulation of ASK1 and SynGAP (Takeda et al., 2004; Krapivinsky et al., 2004). It is therefore not unreasonable to hypothesize that EAG signaling through CaMKII may influence plasticity pathways via downstream regulation of MAPKs that mediate potentiation, depression, and learning. Because our results suggest that EAG signaling plays a critical role in maintaining a low basal level of excitability, and because factors that affect basal activity alter the set-point on which incoming signals must be processed (Davis, 2006; Turrigiano and Nelson, 2004), EAG signaling through CaMKII appears to be a likely candidate for the homeostatic regulation of neuronal activity.

E. Materials and Methods

E.1. Molecular biology and transgenics

eag was subcloned into pCS2 and pPUAST vectors using EcoRI and XbaI sites flanking the coding sequence. A Cavener initiation sequence (Cavener, 1987) was added to *eag* via PCR as a 5' extension on an oligonucleotide primer. All mutant constructs, including *eag*-F456A, *eag*-T787A, *eag*-L782K/A783K (LAKK), *eag*-R784K/Q785K (RQKK), *eag*-R1037L/K1040M (RLKM), *eag*-F731S/F734S (FFSS), *eag*-K663A/R664A (NLS1), *eag*-R698A/R699E (NLS-2), *eag*-H487E/T490E (HTEE), *eag*-T449S/A460S/T470A (TATSSA), *eag*-HTEE-F456A (HFA), *eag*-TATSSA-F456A (TFA), *meag*-F466A, *meag*-R746E/Q747E (RQEE) and *meag*-Q748E/K749E (QKEE), were generated by site-directed mutagenesis using QuikChange (Stratagene). *Eag*-ΔCT was generated by introducing a stop codon at E511. *Eag*-ΔNT was constructed using PCR by replacing the first 212 N-terminal residues with a short sequence (MRLHVWRV) to allow proper S1 membrane insertion. pCDNA3 and the pCDNA3-*meag* construct were gifts from Yi Zhou, University of Alabama at Birmingham. All constructs were verified by sequencing. pPUAST-*eag* was co-injected along with the Δ2,3 recombinant helper plasmid into w^- *Drosophila* and transformants were scored for the w^+ phenotype in F1. To assess rescue of neuronal activity, UAS-*eag* was expressed using the pan-neuronal (elav5147-Gal4) driver and crossed into the eag^{sc29} null background.

E.2. Immunocytochemistry and proliferation assays

NIH 3T3 fibroblasts were maintained at 37°C and 5% CO_2 in Dulbecco's modified Eagle's medium (DMEM, Invitrogen) supplemented with 10% fetal bovine serum (FBS)

as previously described (Chouinard et al., 1995). For transfection, coverslips were incubated for at least 5 hrs in DMEM containing 1.6 μg of the indicated cDNAs and 4 μl LipofectAMINE-2000 (Invitrogen). Coverslips were then washed and incubated in standard media for 12 hrs. Cell density at the time of transfection was critical to allow effective expression while minimizing cell loss due to dissociation of cells from coverslips during subsequent growth. Experiments using increased concentrations of KCl were performed by equimolar substitution of KCl for NaCl in DMEM prepared according to standard formula. For BrdU labeling, 10 μM BrdU was added to each well for 3 hrs. For quantification of BrdU incorporation using NIH ImageJ software, we scanned the regions of each coverslip with the highest cell densities; this likely underestimates EAG-induced proliferation. Scans were background subtracted, and the intensity of all pixels above background was summed across the total area of each scan. Total intensities were averaged across all scans for each condition before normalizing to the average intensity for controls. Normalized data were then averaged across experiments.

E. 3. Biochemistry

Cells grown on culture plates were transfected with 8μg of the indicated cDNAs and 20 μl of LipofectAMINE-2000 (Invitrogen). Cells were dissociated with trypsin-EDTA 48 hrs after transfection, washed and resuspended in PBS. Biotinylation and precipitation of EAG was performed as described (Marble et al., 2005). Briefly, cell suspensions were incubated in 2 mM sulfo-NHS-LC-biotin (Pierce) and the reaction was quenched by washing with 100 mM glycine in PBS. Cells were lysed in PBS supplemented with 1% IGEPAL CA-630, 0.5% sodium deoxycholate, 0.1% SDS, 1 mM DTT and protease

inhibitors, and the homogenate was centrifuged twice for 10 min at 20,000 x *g*. Protein concentrations of supernatants were determined by Bradford assay and diluted to ~ 0.5 mg/ml. Surface proteins were precipitated with streptavidin agarose and the precipitate washed extensively before addition of sample loading buffer. Blots were probed with antisera directed against the carboxyl-terminal domain of EAG (EAG (CT); 1:2000) in blocking buffer, followed by horseradish peroxidase (HRP)-conjugated secondary antibody (1:2000), and visualized with ECL (Amersham Biosciences). Assays of CaMKII and p38 MAP kinase activity were performed using extracts prepared in buffer containing the following (in mM): 20 Tris (pH 7.4), 100 NaCl, 50 NaF, 1 Na_3V0_4, 1 EDTA, 1 DTT, 1 benzamidine, and 0.005 microcystin-LR with 1% IGEPAL CA-630, 0.5% sodium deoxycholate, 0.1% SDS, and protease inhibitors. For CaMKII activity blots, antisera were directed against phospho-Thr-286 (1:200) or total CaMKII (1:1000) (Santa Cruz). For p38 MAPK activity blots, antisera were directed against phospho-Thr180/Tyr182 (1:250) or total p38 MAPK (1:500) (Cell Signaling Technologies). Protein bands were quantified using ImageJ.

E.4. Electrophysiology

For studies in *Xenopus* oocytes, performed as previously described (Marble et al., 2005), mutant constructs were subcloned into pGH19-*eag* (Wilson et al., 1998). Oocytes were injected with 0.1-0.2 ng of RNA, except for non-conducting constructs, which were injected at 1-2 ng. The recording solution contained the following (in mM): 140 NaCl, 2 KCl, 1 $MgCl_2$ and 10 Hepes (pH 7.1 with NaOH). For recordings from NIH 3T3 cells, cells maintained on plates were co-transfected with pCDNA3-EGFP and the indicated constructs, and were replated onto coverslips prior to recording as previously described

(Hegle et al., 2006). Unless otherwise noted, the extracellular solution contained the following (in mM): 40 sodium aspartate, 100 NaCl, 4 KCl, 1.5 $MgCl_2$, 1 $CaCl_2$, 2 glucose and 10 Hepes (pH 7.4 with NaOH). The pipette solution contained the following (in mM): 35 potassium aspartate, 110 KCl, 2 MgATP, 1 NaATP, 3 sodium phosphocreatine, 0.1 NaGTP, 8 EGTA and 10 Hepes (pH 7.4 with KOH). Larval recordings were obtained from body wall muscle fibers 6 and 7 in 3rd instar WT, eag^{sc29} and transgenic larvae using HL3 media containing (in mM): 70 NaCl, 5 KCl, 4 $MgCl_2$, 10 $NaHCO_3$, 5 trehalose, 115 sucrose and 5 Hepes (pH 7.1) with either 0.4 or 0.15 mM $CaCl_2$. Data were collected and analyzed using an AxoClamp 2B and pClamp9 software. All experiments were performed at room temperature.

E.5. Statistics

Unless otherwise noted, data were analyzed using one-way analysis of variance (ANOVA) with Bonferroni post-hoc analysis for selected conditions. The repeated measures ANOVA was used for proliferation and biochemical assays. Data are presented as the mean ± SEM.

FIGURE 4.S1

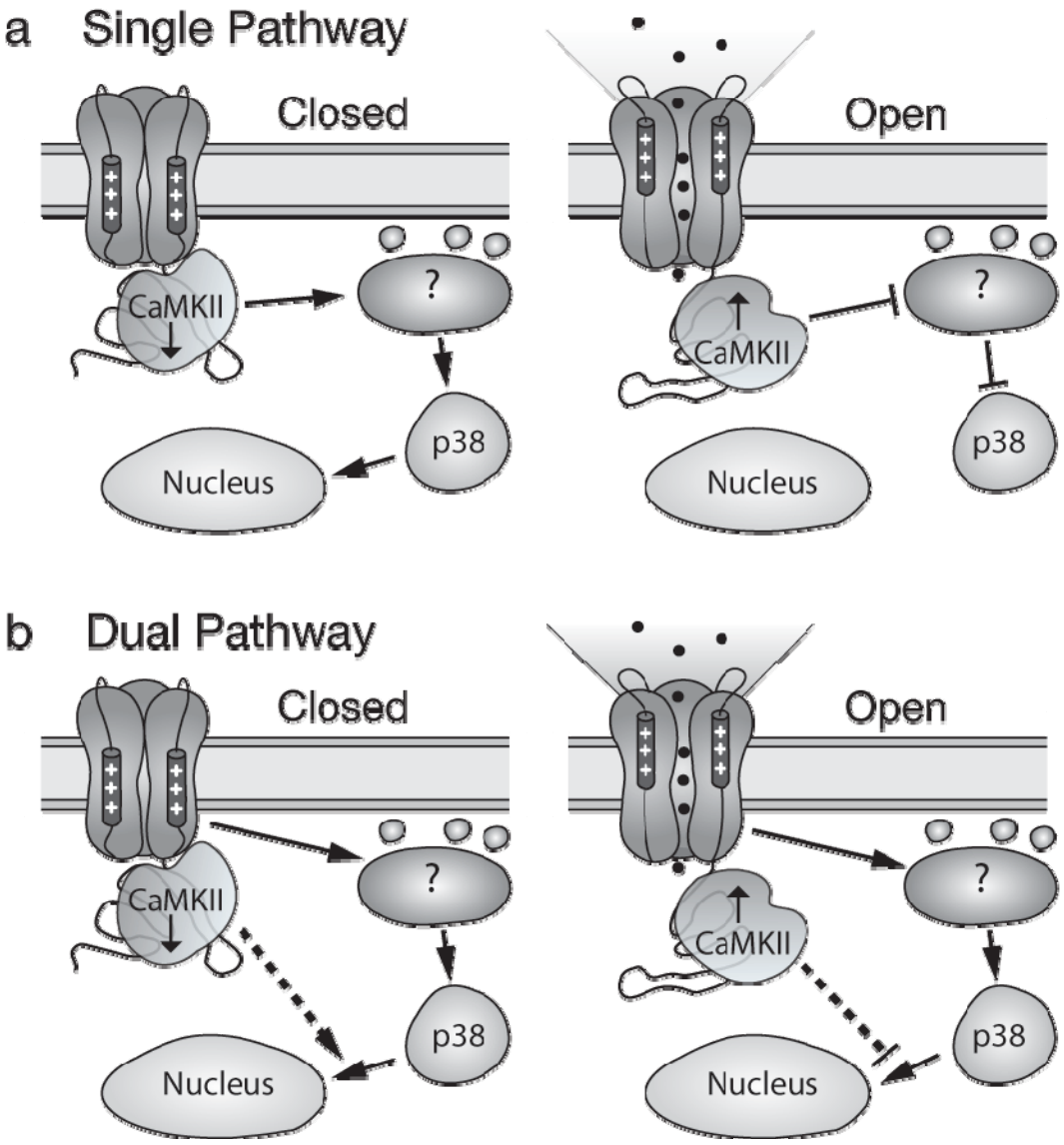

Supplementary Figure 4.S1: Model of EAG signaling via CaMKII
(A) The signaling activity of EAG results in proliferation of NIH 3T3 fibroblasts when channels are in a predominantly closed conformation (*left*). When EAG channels are open, CaMKII activity is increased, resulting in downregulation of proliferation. **(B)** An alternative model of EAG signaling that takes into account the fact that p38 activity was consistently increased for all EAG constructs examined. In this model, EAG regulation of CaMKII activity affects a step that is downstream of p38 MAPK to inhibit proliferation.

FIGURE 4.S2

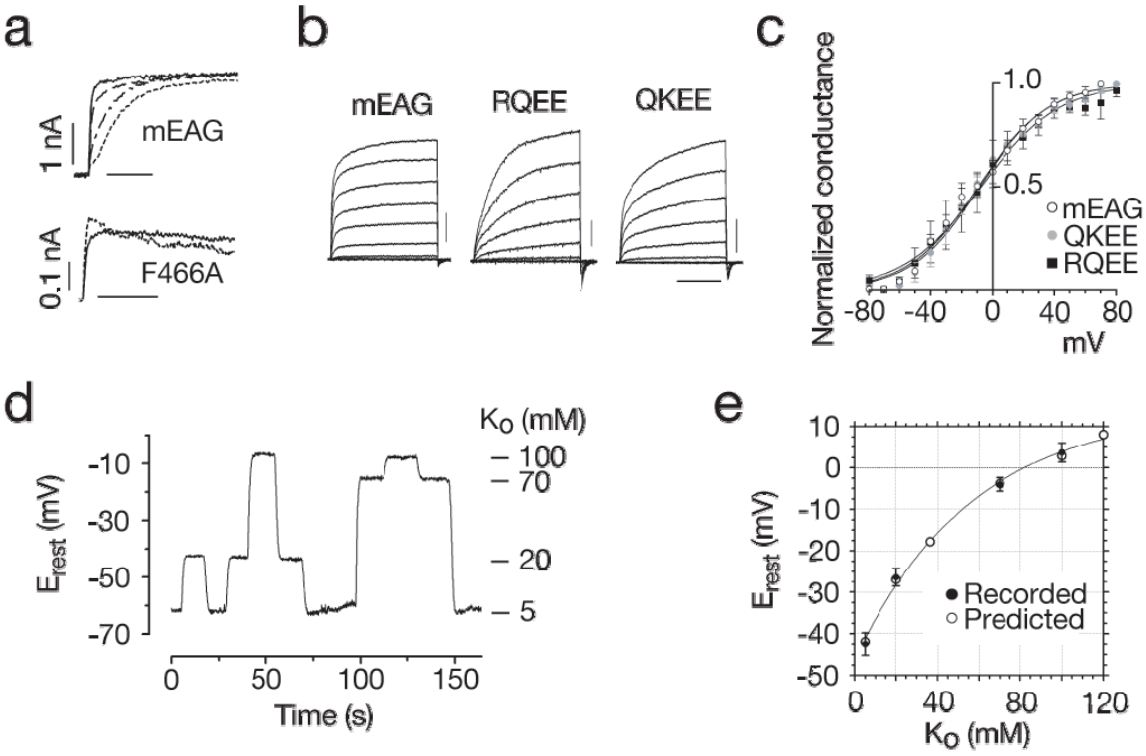

Supplementary Figure 4.S2: Electrophysiological characterization of cells expressing mEAG. (A) Prepulse regulation of the kinetics of mEAG current. Currents elicited with steps to +40 mV were preceded by a 500 ms prepulse to the following potentials: for mEAG, -120 (••••), -100 (-•-•-), -80 (----) and -60 mV (——) in 10 mV increments; for mEAG-F466A, -120 (••••) and -70 mV (solid ——). (Bars, 100 ms and 50 ms for mEAG and mEAG-F466A respectively.) **(B)** Representative currents from NIH 3T3 cells expressing wild type mEAG, mEAG-RQEE or mEAG-QKEE. Cells were stepped from -80 mV to voltages ranging from -90 to +70 mV in 10 mV increments; every other trace is shown. (Bars, 1 nA and 100 ms.) **(C)** Normalized G-V relations obtained for mEAG (n = 5), mEAG-RQEE (n = 3) and mEAG-QKEE (n = 3) obtained from tail currents enhanced using a recording solution containing 20 mM KCl. GV curves were generated using the relation $G = I_{peak}/ (V_{tail} - E_K)$, where E_K was assumed to be -100 mV. Conductances were normalized to the maximum conductance observed. Boltzmann fits had midpoints of -9.2 ± 1.4, -8.2 ± 1.4 and -7.4 ± 1.5 mV and slopes of 22.5 ± 1.3, 21.9 ± 1.2 and 25.1 ± 1.3, for mEAG, EAG-QKEE and EAG-RQEE, respectively. **(D)** Representative recording showing the changes in membrane potential observed during perfusion with solutions containing the indicated K^+ concentrations. **(e)** Averaged membrane potentials (n equals at least 8 for each concentration) compared to the values estimated using the Goldman equation.

CHAPTER V

DISCUSSION

Since their discovery, voltage-gated ion channels have steadily been more appreciated for their elegant complexity in contributing to neuronal function. Early measurements of neuronal properties suggested there were biological mechanisms for sensing and propagating electrical impulses (Cole and Curtis, 1939; Cole and Hodgkin, 1939). When K^+ channels were first cloned, organized, charged residues in their sequence explained how they might be capable of responding to changes in electric potential (Papazian et al., 1987; Tempel et al., 1987). However, regions found in channels that are not directly involved in voltage-sensing or ion conduction suggested other mechanisms of modulation and regulation of channel function (Tempel et al., 1988; Rehm et al., 1989; Demo and Yellen, 1991). Later, many of these modulatory functions were confirmed by experimentation (Chung et al., 1991; Levitan, 2006).

In this thesis I investigate the function of the *Drosophila* K^+ channel EAG. Using various *in vitro* and heterologous expression methods I investigate the modulatory action of other neuronal proteins on EAG function, as well as the role EAG has on influencing important cellular activities. These reductionist interactions confirm EAG does associate with individual binding partners, kinases, etc., but what adds strength to this evidence is *in vivo* analysis of neuronal properties. Those results suggest that EAG is indeed an

important subject of modulation and is keenly involved in fundamental neuronal function, which almost certainly plays a significant role in learning and memory. Many other researchers have contributed to the work presented here, however, much of my individual research centered on the *in vivo* results of EAG properties. Therefore, the majority of conclusions discussed here also will focus on the *in vivo* consequences of EAG function and regulation.

A. SUMMARY OF RESULTS

In Chapter II of this thesis I investigated the role of the adaptor protein CMG on the localization and function of the EAG K^+ channel. Previous experiments indicated that EAG is regulated by CaMKII phosphorylation (Wang et al., 2002b), as well as direct CaMKII binding to EAG (Sun et al., 2004). CMG also binds to CaMKII and modulates its kinase activity (Lu et al., 2003). I investigated the possibility of a complex consisting of EAG, CMG, and CaMKII, which functioned together to regulate EAG activity. I found that CMG interacts directly with EAG in numerous contexts including *in vitro* protein binding, heterologous expression, and *in vivo* immunoprecipitation experiments. CMG modulated channel function by enhancing EAG activity via increased phosphorylation at a CaMKII consensus site, leading to greater EAG expression at the plasma membrane. Additionally, the binding domains of each protein were elucidated, identifying a non-canonical SH3 binding motif in EAG necessary for binding CMG.

Chapter III explored the role of phosphorylation and Ca^{2+}/CaM binding in channel function. *Drosophila* and mammalian homologs of EAG were known to be influenced by changes in the concentration of Ca^{2+} (Stansfeld et al., 1996; Schönherr et al., 2000; Wang

et al., 2002b; Ziechner et al., 2006). In this thesis I demonstated that increases in Ca^{2+}/CaM have multiple, opposing effects upon EAG current. Increased levels of Ca^{2+}/CaM lead to CaMKII phosphorylation of EAG, enhancing current (Wang et al., 2002b), and CaM directly binds to EAG in a Ca^{2+}-dependent manner, causing inhibition of current. Furthermore, I investigated the effects CaMKII and CaM have on synaptic plasticity. I showed that defects in the phosphorylation of EAG are consistent with lowered numers of functional EAG channels at the synaptic membrane and that CaM binding to EAG is necessary for normal synaptic properties such as facilitation.

Growing evidence has shown that the EAG K^+ channel may have important functions other than simple ion conduction in neurons (Pardo et al., 2005; Hegle et al., 2006; Kaczmarek, 2006). These include an influence on kinase signaling, proliferation, and oncogenesis. A mechanism that may explain these effects is explored in Chapter IV. When studied in a heterologous expression system, disruption of CaMKII binding to EAG abolishes EAG-mediated signaling (see Appendix). This signaling appears to play a role in *Drosophila*, as transgenic mutants of EAG that cannot bind CaMKII have defects in spontaneous NMJ activity, similar to *eag* null mutants. Therefore, it seems that some of the behavioral and electrophysiological phenotypes exhibited by *eag* mutants may be caused by this voltage-sensitive, conduction-independent, function of EAG channels.

B. EAG IS A TARGET OF MODULATION

What distinguishes neurons from other cells is their excitability and ability to generate action potentials; excitable cells have a nonlinear membrane response to

depolarizations, causing amplification and propagation of the depolarization (Hille, 2001). This can cause an action potential which leads to a chain of events resulting in intercellular communication. All excitable cells depend on voltage-gated ion channels for this purpose; ion channels are the work-horses of neuronal and other communication. Ion channels are capable of quickly detecting changes in cell activity and converting that information into a response on a time scale of milliseconds. Therefore, mechanisms that modify their response, even in minor ways, can have dramatic effects on overall neuronal excitability.

C. MULTI-DIRECTIONAL MODULATION OF EAG

Activity-dependent regulation of channel function is a common theme among ion channels (Yu and Catterall, 2004; Levitan, 2006) and EAG is no exception. What makes EAG interesting is that the same activity-dependent molecule, in this case CaM, both enhances and inhibits EAG current, albeit through differing mechanisms. Other types of ion channels also respond to activity- and Ca^{2+}-dependent modulation, but in most cases where there is both up- and down-regulation, the molecules responsible for it are dissimilar. For example, phosphorylation of $Ca_V1.2$ L-type Ca^{2+} channels is promoted by AKAP79/150 that target PKA (Oliveria et al., 2007). PKA-mediated enhancement increases L-type channel activity in dendrites and dendritic spines of hippocampal pyramidal neurons. The complex consisting of $Ca_V1.2$, AKAP79/150, and PKA also includes the Ca^{2+}/calmodulin-activated phosphatase calcineurin (CaN). Co-targeting of PKA and CaN by AKAP79/150 confers bi-directional regulation of L-type current amplitude both in transfected HEK293 cells and hippocampal neurons.

This bi-directional mechanism of channel regulation is similar to that of CaM/CaMKII upon EAG. However, in EAG's case the action differs in at least two features. First, the manner in which Ca^{2+} bi-directionally modulates EAG can be considered less complicated than that of certain Ca^{2+} channel complexes, such as $Ca_V1.2$. The kinase that phosphorylates EAG is directly regulated by Ca^{2+}/CaM and CaM modulates EAG by direct binding. In comparison, in order for Ca^{2+}/CaM to modify $Ca_v1.2$ channels it must first either increase or decrease adenylate cyclase (AC) activity (it can do both, depending on AC isoform (Hanoune and Defer, 2001; Ostrom et al., 2003)), which changes cAMP levels that regulate PKA activity. Also, CaM must exploit the phosphatase CaN to balance the PKA effects. These multiple layers of action of cAMP, PKA and CaN may cause a time-lag in response to an initial signal, but result in a more robust and persistent response (Oliveria et al., 2007). Therefore, in comparison, the bi-directional effect of CaM on EAG currents is much more direct (although PKA may also be involved as well) (Fig. 5.1). This may mean there are possibly fewer steps in this pathway in which the activity levels of signaling molecules can be further regulated, but the *relative* directness may suggest a faster, more focused response to Ca^{2+} concentration and activity changes.

The mechanism of EAG modulation differs in a second way from this common kinase/phosphatase antagonism. In the example of $Ca_V1.2$ the bi-directional effect of Ca^{2+}/CaM modulates the channel via the same PKA/CaN phosphorylation/phosphatase sites. Unlike $Ca_V1.2$ which can either be in a phosphorylated state or a dephosphorylated state, EAG can be in either state and still be modulated by CaM. Therefore, EAG can in

FIGURE 5.1

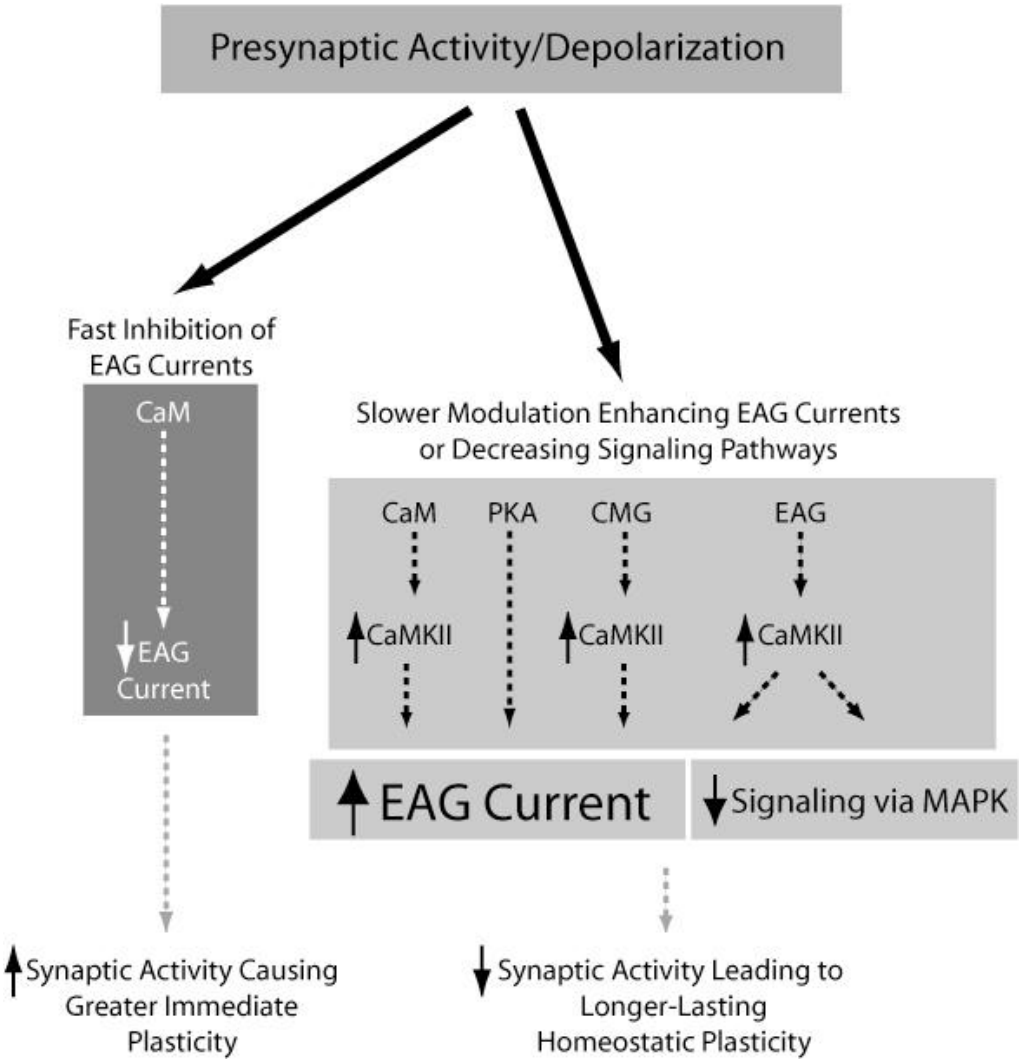

Figure 5.1: Model of EAG regulation, and influence on signaling pathways, in response to synaptic activity.
Left, In response to synaptic activity and rapid Ca^{2+} influx, CaM binds to and inhibits EAG currents. Following subsequent depolarizations, this causes enhanced facilitation which may lead to Hebbain mechanisms strengthening the synapse. *Right*, Relatively slower, and perhaps longer lasting, mechanisms such as phosphorylation of EAG by CaMKII (in response to Ca^{2+}/CaM) or PKA, and enhanced by CMG, would also be caused by elevated levels of synaptic activity. This would result in higher EAG currents and decreases in further synaptic activity. EAG can also respond to depolarizations by increasing CaMKII activity, which may have two results. First, this may again enhance EAG phosphorylation and more directly lower activity. Second, CaMKII may regulate other signaling molecules, which may be responsible for the regulation of spontaneous neuronal firing or other unknown cellular functions. In both of these cases, the result would decrease neuronal activity in a homeostatic fashion.

fact be in multiple regulatory states, not just simply up- or down-regulated. In this regard, the EAG complex is more like the KCNQ channel protein complex, which, along with KCNQ2/3 channel subunits, contains AKAP150/yotiao, PKC, CaM, CaN, PSD-95, PKA and casein kinase 2 (Marx et al., 2002). In this complex CaM modulates K^+ current indirectly via regulating kinase and phosphatase activity, but also through direct binding to the channel (Gamper and Shapiro, 2003). No endogenous phosphatases have yet been identified for EAG phosphorylation sites, but this leaves open the possibility of further regulation of EAG channels. Because CMG is a scaffolding protein with multiple protein binding sites it would not be surprising it may coordinate many more members within the EAG complex.

D. EAG CONTRIBUTES TO SYNAPTIC PLASTICITY

The larval neuromuscular junction (NMJ) is the only preparation in *Drosophila* suitable for quantitative analysis of synaptic transmission at identifiable synapses (Guo and Zhong, 2006). It has been used extensively to study the molecular basis of synapse development, synaptic plasticity, synaptic vesicle release, and functions of genes involved in learning and memory. For these reasons it was chosen to examine the role of EAG on synaptic plasticity.

One way of discussing the activity-dependent regulation of EAG channels is to make a distinction based on the effective EAG-dependent response. Depending on the mechanism of modulation, EAG responds to activity/depolarizations and contributes to either increases or decreases in activity (Fig. 5.1). EAG responses that work to further depolarize the neuron could play a part in Hebbian mechanisms that strengthen the

synapse and enhance intercellular neurotransmission. On the other hand, modulatory effects upon EAG that counteract changes in activity may contribute to homeostatic mechanisms within the cell. Depending on the strength and duration of a neuronal stimulus, or the state of other modulatory proteins within the neuron, either of these forms of synaptic plasticity may be favored.

For the sake of organization, I will focus my discussion on the consequences of neuronal input favoring depolarization and the resultant effects on EAG-dependent changes in neuronal excitability. However, one could conversely frame the following descriptions in response to hyperpolarization and decreases in activity, and reach similar general conclusions. In an attempt to understand how these differing roles of EAG influence neuronal activity I plan to discuss first how EAG contributes to short-term plasticity, followed by possible contributions to homeostatic properties

D.1 EAG contributes to short-term plasticity

Various forms of short-term synaptic plasticity at the NMJ have been demonstrated, including facilitation, augmentation, posttetanic potentiation, and depression (Jan and Jan, 1978; Zhong and Wu, 1991; Broadie et al., 1997; Delgado et al., 2000; Wu et al., 2005). These forms of plasticity are disrupted in a number of mutants with defective intracellular signal transduction pathways and impaired learning and memory (Zhong and Wu, 1991; Rohrbough et al., 1999, Rohrbough et al., 2000). Few mutants of *Drosophila* K^+ channels have been linked to defects in learning and memory (Gasque et al., 2006); however, EAG is one of them. It is technically difficult to actually measure many synaptic properties of *eag* mutants, especially the eag^{SC29} null mutation, due to its strong

hyperexcitable phenotype. For example, the induction of facilitation and potentiation are believed to require basal levels of synaptic Ca^{2+}, which after an initial depolarization, increase and enhance subsequent vesicle release. In *eag* mutants, due to their high levels of spontaneous activity, synapses may already be potentiated. Therefore, mutating specific modulatory sites within EAG allows me to evaluate how it contributes to synaptic plasticity using transgenic EAG hypomorphs. Using this technique it was found that EAG does specifically control facilitation at the *Drosophila* NMJ.

When the CaM binding site in EAG is mutated (EAG-FF/SS) to disrupt this interaction, transgenic larvae expressing this channel show low levels of facilitation at a simulating frequency of 5 Hz, similar to that found in wild type or EAG-Rescue larvae. However, unlike these controls, EAG-FF/SS transgenics do not demonstrate facilitation at higher frequencies (up to 40 Hz). The best explanation of how EAG is responsible for regulating facilitation at the NMJ is its effect upon the action potential. This suggests a mechanism in which CaM already bound to EAG (via its C-terminal lobe, at resting levels of Ca^{2+}) responds quickly to an initial depolarization through Ca^{2+} binding to the N-terminal lobe and causes a conformational shift inhibiting EAG current. This decrease in outward K^+ flux may broaden the action potential effect at the presynaptic terminal and allow higher residual Ca^{2+} that would enhance postsynaptic responses upon further depolarization.

A way to investigate this mechanism would be through direct measurement of activity in the NMJ presynaptic bouton. Extracellular recordings from segmental nerves can detect the presence of action potentials but the method is not sensitive enough to measure the magnitude and kinetics of presynaptic activity (Ganetzky and Wu, 1985). Given this

limitation, recording synaptic currents from varicosities using extracellular macropatch electrodes may be more informative (Budnik et al., 1990; Mallart et al., 1991, Wong et al., 1999; Cheung et al., 1999). This focal extracellular recording technique permits quantification of synaptic transmission from individual nerve-ending varicosities and would show changes in action potential profiles and changes in membrane potential due to Ca^{2+}-dependent EAG modification. However, the best way to determine Ca^{2+}-dependent functions of EAG may be through direct Ca^{2+} imaging in the NMJ.

Changes in $[Ca^{2+}]_i$ can be measured in *Drosophila* larvae motor terminals by loading calcium indicators into neuronal terminals through cut axons (Macleod et al., 2002). Using this technique, researchers have characterized the Ca^{2+} kinetics of presynaptic boutons. The rapid decay of the calcium signal following a single action potential (< 60 ms) is primarily produced by fast calcium extrusion mechanisms present in motor neuron terminals. This permits sustained physiological processes during high rates of impulse activity which drive locomotor activity (Lnenicka et al., 2006). If the changes in internal Ca^{2+} levels caused by EAG do regulate facilitation, imaging could be able to detect it. Also, if EAG affects resting $[Ca^{2+}]_i$, this could similarly be measured.

Little is known how CaM binding to EAG structurally confers inhibition upon the channel. The comparisons between wild type and mutant EAG currents made in Chapter III suggest that CaM stabilizes the closed state, causing a depolarizing shift in the conductance-voltage relationship and a slowing of kinetics. Similar to EAG, the CaM domain in voltage-gated Ca^{2+} channels is located too far in primary sequence from the pore to postulate a simple model for how Ca^{2+}/CaM effects gating. However, recent X-ray crystallographic work on these channels has somewhat revealed how CaM binds to

and may affect gating of Ca^{2+} channels, which may translate to other channels (Petegem and Minor, 2006). One interesting finding is that a cytosolic subunit, $Ca_v\beta$, and the CaM domain collaborate to affect the movement of a common element in the pore. This may suggest accessory proteins in the EAG complex may be necessary for proper CaM inhibition of EAG channels. Also, again like EAG, Ca_v channels have a large cytoplasmic region that makes multiple intermolecular contacts with the CaM-binding motif. Therefore, further defining the interactions and conformational changes between these domains and their relationship to the CaM binding domain and other complex partners are at the heart of determining how CaM-dependent ion channels such as EAG work.

Other efforts investigating the effect of CaM on Ca^{2+} channel kinetics have found that CaM can support inactivation and facilitation at the same CaM binding site (Zühlke et al., 1999; Lee et al., 1999). Point mutations in the CaM binding domain of the channel indicate a strong facilitation that is usually masked by Ca^{2+}-dependent inactivation. This bimodal regulation of channel activity is reminiscent of EAG, and may shine light on the mechanism by which CaM regulates the K^+ channel. As opposed to disrupting the CaM-EAG interaction, as shown in this thesis, one could further examine CaM function upon EAG by instead enhancing CaM affinity for Ca^{2+} or screening for mutations in EAG that enhance CaM inhibition (Rashid et al., 2004; Shifman et al., 2006). If these approaches were studied in vivo, EAG may in fact cause spontaneous NMJ activity or increases in facilitation above wild type. It would be interesting to determine what effects that would have behaviorally.

In summary, transgenic EAG-FF/SS larvae, which cannot directly bind CaM, show defects in synaptic plasticity. Quite remarkably, this suggests that not only is EAG *necessary* for facilitation, but that only two point mutations in the CaM binding domain of EAG are necessary to completely abolish this type of synaptic plasticity. This strongly implicates EAG as an essential component in presynaptic function at the NMJ.

D.2 EAG may contribute to synaptic homeostasis

One of the better understood examples of synaptic homeostasis occurs at the NMJ where changes in presynaptic function lead to compensatory changes in postsynaptic excitability. The same holds true for presynaptic responses caused by postsynaptic changes (Davis and Bezprozvanny, 2001). Examples at the NMJ include increased receptor expression in response to decreased neurotransmitter release and the reciprocal result, higher transmitter release in response to decreased receptor sensitivity (Paradis, et al., 2001). However, a homeostatic system is defined as having a constant output; therefore, homeostatic responses do not necessarily need to be trans-synaptic (Davis, 2006). In the case of the EAG K^+ channel, it appears to regulate neuronal homeostasis predominantly through presynaptic mechanisms.

The finding that defects in CaM binding to EAG remove presynaptic facilitation indicates that short-term synaptic plasticity is greatly regulated by EAG function. The kinetics of this modulation are in the millisecond time scale, suggesting the channel has an important influence on coincidental stimulation and high frequency neuronal transmission. In contrast to this short-term Hebbian mechanism that enhances neuronal communication; EAG also functions to counter-balance increases in activity by lowering

synaptic output. This opposing EAG effect appears to work on a longer time scale, therefore depending on the strength and duration of stimuli, either or both mechanisms could be favored in this model.

D.3 Long-term activity enhances EAG current

There are two distinct ways EAG contributes to synaptic homeostatic regulation. The first is through its voltage-sensitive, non-conducting regulation of the CaMKII/p38 signaling pathway which promotes inhibition of spontaneous neuronal firing (this will be discussed more below). This pathway may result in changes in gene expression and protein synthesis, and may result in true long-term changes to synaptic processes. The second way EAG influences homeostasis in response to activity is through higher K^+ conductance caused by phosphorylation of the channel. This response may occur through differing routes, including Ca^{2+}/CaM-dependent phosphorylation by CaMKII, enhanced CaMKII activity by CMG, or phosphorylation by PKA. Although distinct in mechanism, these proteins appear to act upon EAG current all through the same function -- increasing EAG channels present at the plasma membrane. The time scale for this action is not known, but if due to higher recruitment of peri-synaptic channels, it may be intermediary, falling between that of the short-term CaM inhibition of EAG channels and longer-term kinase signaling affects that may require gene transcription and translation.

D.4 Ca^{2+}/CaM-dependent CaMKII phosphorylation of EAG

Mutation of T787 abolishes the ability of CaMKII to phosphorylate EAG, which causes decreased EAG currents and faster inactivation kinetics of the channel (Wang et

al., 2002b). In Chapter II, I show that this decreased current is caused by fewer EAG channels present at the plasma membrane. Therefore, at synapses where high levels of activity increase intracellular levels of Ca^{2+}/CaM, which stimulates CaMKII kinase activity, the number of EAG channels phosphorylated and targeted to the plasma membrane will act to decrease neuronal activity. This homeostatic mechanism utilizes EAG to moderate excessive neuronal activity (or conversely, low levels of activity could decrease EAG current causing higher levels of activity).

A key characteristic of homeostatic mechanisms is the establishment of a set point, to which activity levels return after synaptic perturbations. In practice, the molecular specification of a set point has been difficult to precisely define in any system (Davis, 2006). One theory that could explain how the initial levels are registered is that a set point could be genetically specified as part of cellular identity. This may be specified by the precise abundance of each ion channel trafficked to the surface (Prinz et al., 2003; Mee et al., 2004). However, both theoretical and experimental efforts demonstrate that ion channel numbers are free parameters that can be varied by homeostasis to retarget activity to the set point (Prinz et al., 2003). In fact, there is a strong likelihood that set points are functions of entire signaling systems, rather than being encoded by a small subset of proteins (Davis, 2006). This possibility argues in favor of the EAG-CaMKII signaling pathway in its control of neuronal activity. Many unknown steps in this pathway could regulate and influence the signaling output.

D.5 CMG enhances CaMKII phosphorylation of EAG

Among the EAG adaptor/interacting proteins Hk, KCR1, Slob, and epsin, the only one known to be directly involved in activity-dependent regulation of EAG channels is CMG. In Chapter II I show that CMG enhances phosphorylation at the CaMKII site causing higher EAG currents, greater numbers of EAG channels expressed at the plasma membrane, and slower inactivation kinetics. These properties are all consistent with a model of a complex consisting of EAG, CMG, and CaMKII, with CMG, by binding both other proteins, enhancing kinase activity upon the channel. CMG can increase phosphorylation in at least two ways. First, CaMKII anchored to EAG via CMG effectively increases kinase concentration near its substrate. Second, since CMG only binds CaMKII when it is in its active state, CMG bound to CaMKII in the presence of Ca^{2+}/CaM can provide a source of specifically *active* kinase (Lu et al., 2003). Therefore, CMG functions to enhance the homeostatic control of CaMKII over EAG during times of high activity. Also, EAG in turn may serve to keep CaMKII bound to CMG, keeping the kinase active. Importantly, CMG can also down-regulate CaMKII and hence EAG currents in response to low levels of activity. The association of CMG to CaMKII, after decreases in activity and Ca^{2+} levels, promotes phosphorylation of T306, rendering the kinase inactive (Lu et al., 2003). If this results in an eventual lower amount of phosphorylated EAG, this is another way that this complex homeostatically responds to decreases in activity by perhaps inhibiting EAG current and increasing subsequent activity.

This effect on EAG phosphorylation/current by Ca^{2+}-dependent regulation of kinase activity by CMG has yet to be investigated. Future experiments that measure the effect

on EAG due to CMG binding and unbinding to CaMKII may further explain EAG's role in homeostasis. Another possible experiment that might help explain the modulatory role of CMG upon EAG channels could be screening for other yet unknown members of the channel complex. The reasons for this suggestion are many. First, the stoichiometry of the complex has not been evaluated; therefore multiple CMG proteins could interact with all four EAG subunits. Second, other members of the MAGUK family are known to multimerize; therefore multiple CMG components also could be present on each EAG subunit (Kim and Sheng, 2004). Third, CMG has multiple protein binding domains (PDZ, SH3, HOOK, GUK and CaMKII-like), of which the function of many has yet to be determined (Martin and Ollo, 1996; Hata et al., 1996; Cohen, et al., 1998). Therefore, it is very possible many other yet discovered proteins contribute to the EAG complex. Binding screens for proteins capable of interacting with EAG or CMG domains may result in the identification of other proteins such as phosphatases and β-subunits that could regulate complex function.

D.5 PKA enhances phosphorylation of EAG and CMG binding

In addition to phosphorylation by CaMKII, preliminary experiments indicate EAG is a substrate for phosphorylation by PKA (data not shown). Inhibition of PKA activity decreases heterologously expressed EAG currents, and point mutations at two PKA phosphorylation consensus sites in the C-terminus of EAG abolish this effect. Importantly, one site is T787, which is phosphorylated by CaMKII, and the other is within the SH3 binding motif (S1039) that mediates CMG binding. Electrophysiological assays in *Xenopus* oocytes suggest that prior phosphorylation by PKA may be required

for the association with CMG. These findings suggest that, *in vivo*, PKA may regulate synaptic activity via modulation of EAG surface expression.

Much is known about the roles of cAMP PKA in mammals during LTP and memory formation (Martin and Morris, 2002; Wang et al., 2004). Several types of synaptic plasticity depend on cAMP signaling, including Schaffer collateral/CA1, mossy fiber and cerebellar parallel fiber LTP. Studies of transgenic mice have also demonstrated that adenylyl cyclase activity is required for hippocampus-dependent memory formation. Mice lacking Ca^{2+}-stimulated adenylyl cyclase activity learn normally and have short-term memory but lack contextual and spatial memory and long-term memory for passive avoidance (Wong et al., 1999b; Wang et al., 2004).

In *Drosophila*, memory mutants associated with defects in cAMP/PKA signaling predominantly affect the function of proteins involved in mobilization and release of synaptic vesicles (Cheung et al., 2006). For example, *dunce* and *rutabaga*, exhibit abnormal levels of synaptic vesicles cycling from the reserve pool of vesicle to the active exo-/endocytotic recycling pool (Zhong and Wu, 1991; Kidokoro et al., 2004). However, another important way PKA affects neuronal plasticity is through phosphorylation of presynaptic ion channels (Kandel and Schwartz, 1982; Levitan, 2006). Because *eag*, *dnc*, and *rut* mutants all show similar defects in facilitation at the NMJ, and given the possibility that PKA may regulate EAG, the phenotypes observed in the cAMP/PKA mutants may, in part, be due to decreased phosphorylation of EAG. Although *eag* and *dnc* mutants also show similar morphological changes at the NMJ, such as increased axonal branches over the muscles and the number of varicosities on the neuritis (Budnik et al., 1990; Schuster et al., 1996; Budnik, 1996), no epistatic analysis of *eag/dnc*, *eag/rut*

or *eag/PKA* double mutants has been performed. Future investigations into the connection between PKA activity and EAG channels *in vivo* may begin with determination if there are, or are not, additive phenotypes between any of these mutant pairs.

From observations made from heterologously expressed EAG channels, the result of phosphorylation by either CaMKII or PKA appear to be similar. However, the effect of PKA phosphorylation of S1039, which is within the CMG-binding motif of EAG, adds the possibility of further regulation of the channel. Specifically, my results suggest that phosphorylation of T787 regulates EAG surface expression at basal levels of activity. Activity-dependent phosphorylation of S1039 could result in an additional regulation of EAG surface expression that is activity-dependent. With some exceptions (Pokorska et al., 2003) it is generally believed that increased levels of synaptic activity cause an increase cAMP levels and enhanced PKA activity (Chetkovich et al., 1991; Bading, 2000). This pathway is also consistent with the homeostatic mechanism described for CMG, since the phospho-mimic mutation of S1039D supports CMG binding and thus increased EAG currents. Further analysis of this association may include: *in vitro* phosphorylation assays to prove that indeed PKA does phosphorylate EAG, screening for possible PKA-anchoring proteins within the EAG complex or physiological analysis of the effects of altered CMG-binding using S1039A and S1039D transgenic larvae.

E. PHYSIOLOGICAL SIGNIFICANCE OF EAG SIGNALING

The EAG-dependent signaling (here, this "signaling" refers to the non-conducting, voltage-sensitive effects of EAG channels, associated with CaMKII activity and other

unknown molecules) identified by the Wilson lab is an unconventional role for voltage-gated K^+ channels. How this mechanism works, as well as its function in modulating cell processes, has been under investigation. The biophysical and cellular mechanisms of EAG signaling including: kinetics of EAG-dependent proliferation, how CaMKII may be activated by the EAG voltage-sensor, and possible roles in oncogenesis, have been elaborated upon elsewhere (Hegle, 2007). Here, I focus on the *in vivo* function of EAG signaling and the possible down-stream targets of EAG-CaMKII signaling.

Elevated spontaneous motor neuron firing observed in *eag* larvae suggests EAG channels are important to neuronal function. EAG conduction may contribute to the control of spontaneous firing by several classic mechanisms, including: setting the resting membrane potential, increasing action potential repolarization and after-hyperpolarization of the membrane potential. However, evidence presented in Chapter IV suggests that EAG conduction is not necessary to inhibit spontaneous firing and that EAG influences this attribute by a different process, one associated with CaMKII-dependent signaling. Transgenic *eag*-LAKK larvae (in which CaMKII binding is eliminated) display a defect in spontaneous firing similar to that observed in *eag* mutants (Fig. 4.4). One possible explanation for this is that disruption of CaMKII binding results in lower amounts of phosphorylated EAG, similar to the findings for *eag*-T787A larvae (Fig 3.8). However, *eag*-LAKK larvae display wild type EJC amplitudes (Fig. 4.4), suggesting the channels function normally, in contrast to *eag*-T787A. In addition, spontaneous activity is rescued by non-conducting *eag*-F456A channels, indicating that the elevated firing associated with *eag*-LAKK larvae is independent of EAG K^+ conduction, and instead is regulated by the EAG signaling (see Chapter IV, Appendix). These findings fit together well with

observations made in flies expressing the CaMKII inhibitory peptide *ala* (Griffith et al., 1994). Transgenic *ala* larvae exhibit elevated spontaneous activity similar to that seen in *eag* mutants and *eag*-LAKK transgenics. CaMKII most likely has other functions that may result in the phenotypes seen in *ala* transgenics, but the evidence presented here suggests the defects in spontaneous activity are associated with EAG-dependent signaling.

The many roles of cellular signaling by EAG channels proposed in this thesis, ranging from regulation of proliferation, differentiation, and tumor progression to influences on synaptic homeostasis and LTD, suggest significant contribution to possibly many signaling pathways (Kaczmarek, 2006; Pardo et al., 1999; Thomas and Huganir, 2004; Zhu et al., 2002; Guan et al., 2003). A major unanswered question concerns the identity of downstream effectors regulated by EAG-associated CaMKII activity. Known cellular targets of CaMKII phosphorylation are numerous, numbering over 60 (Yoshimura et al., 2000; Knebel, 2003), therefore finding all the specific substrates of EAG-dependent phosphorylation may be difficult. However, one signaling protein that has been identified as a probable, if indirect, downstream target of EAG-dependent signaling is the MAPK p38 (Fig. A.2E). The pathway between EAG and p38 is not known, but known intermediates between CaMKII and p38 in the MAPK signaling pathway include the synaptic GTPase-activating protein (SynGAP) and the apoptosis-signal regulating kinase (ASK1), a known substrate of CaMKII that also influences p38 MAPK activity (Krapivinsky et al., 2004; Takeda et al., 2004). Also, the subcellular location of signaling molecules may make a difference on the activity of CaMKII (Figure 4.S1). If the activity of the kinase depends on if it is bound to EAG or CMG at the plasma membrane (Lu et

al., 2003; Sun et al., 2004) then the identity of downstream partners may differ depending on location of the kinase.

One benefit of using *Drosophila* as model organism is the ability to use its genetic properties to find components of signaling pathways (Baker, 2007; Jacob and Lum, 2007). To date, there have been no large scale screens for suppressors or enhancers of *eag* phenotypes in Drosophila. However, there are a few genes, primarily structural proteins, known to suppress electrophysiological phenotypes associated with *eag* (Hurd et al., 1996, Schuster et al., 1996). Since the only identified phenotype of *eag* specific to its role in signaling is the high spontaneous firing found at the NMJ (Fig. 4.4), screens for mutants that suppress this phenotype may elucidate possible downstream targets of EAG signaling. It is possible that the characteristic high levels of leg shaking found in adult *eag* mutants is caused by the same signaling-dependent spontaneous activity found in larvae. If so, screens for suppressors of *eag* leg shaking may identify other signaling components. However, because other ion channel mutants (Kaplan and Trout, 1969) also show high levels of leg shaking, this phenotype may not be specific to EAG-dependent signaling. Also, screening larvae for their ability to suppress the larval NMJ phenotype would be impractical due to the throughput limits of the measurement on candidates. Because EAG affects growth of cells in heterologous expression systems, a growth or proliferation phenotype associated with *eag* mutants or *eag* over-expression in non-neuronal tissues could be possible. If such a phenotype is identified, this could facilitate discovery of other members of the EAG signaling pathway.

F. EAG SIGNALING MAY PLAY A ROLE IN SYNAPTIC PLASTICITY

Because it is voltage-dependent, the effect of EAG signaling is likely to depend on the level of neuronal activity. EAG signaling may contribute to synaptic activity by at least two mechanisms (Fig. 5.1, *right*), namely through direct effects on EAG function and through effects on other intracellular signaling pathways. First, voltage-sensitive enhancement of CaMKII activity by EAG may lead to larger number of EAG channels phosphorylated, increasing EAG current. Although this modulation is not responsible for regulating spontaneous synaptic firing (since the F456A mutation rescues this phenotype), it could accentuate EAG functions caused by other activity-dependent mechanisms, such as phosphorylation by CaMKII or PKA and CMG binding (Wang et al., 2002b, Chapter II). This would result in lower amounts of synaptic activity in response to depolarizations. Second, as previously discussed, depolarization causing shifts of EAG to the open state may also enhance the EAG-dependent CaMKII signaling mechanism that inhibits spontaneous firing. Both of these mechanisms can cause decreased synaptic output in response to high levels of neuronal activity. Although the time scales of action may differ, both of these mechanisms are homeostatic in nature. Similarly, if CaMKII levels are enhanced long enough by CaM or constitutive activity, this may result in promotion of the EAG-dependent signaling pathway and lead to long-term homeostatic changes in the activity levels of neurons.

A role in synaptic plasticity and learning in flies and mammals has been well established for CaMKII (Griffith et l., 1993; Silva et al., 1992a; Silva et al., 1992b). CaMKII utilizes GTPases such as Ras to regulate MAPK pathways that activate nuclear transcription factors (CREB) that control transcriptional control of activity-dependent

genes (Thomas and Huganir, 2004). Depending on the circumstances of activity and which pathway is activated, CaMKII activity contributes to differing forms of plasticity (Chapman et al., 1994). In the mammalian hippocampus, activation of p42/44 MAPK causes greater glutamate receptor insertion during facilitation and LTP (Bolshakov et al., 2000; Zhu et al., 2002). Conversely, p38 signaling can induce both short-term synaptic depression and LTD through removal of glutamate receptors (Shu, et al., 2002; Guan et al., 2003; Thomas and Huganir, 2004). Given the largely conserved function of these pathways in learning and memory, CaMKII-dependent EAG signaling may affect neuronal function via these mechanisms.

A model has been proposed to explain the possible role of EAG signaling on synaptic potentiation and depression (Hegle, 2007). At rest, predominantly closed EAG channels would inhibit CaMKII activity, leading to increased p38 MAPK activity and sustaining synaptic depression (Fig 4.S1). In response to subthreshold depolarizing events, some EAG channels would begin to open, increasing CaMKII activity and lowering p38 activity. This would permit downstream plasticity mechanisms to respond to changes in membrane potential even without Ca^{2+} influx caused by action potential generation.

G. ROLES FOR EAG IN MAMMALS

The multiple roles for EAG discussed in the thesis (CaM-dependent short-term facilitation, homeostatic mechanisms via CaM, CaMKII, PKA, CMG, and signaling, learning and memory, etc.) suggest that EAG is an important regulator of neuronal function in *Drosophila*. However, the function of EAG channels in mammalian cells is less well known. In non-neuronal cells, cases for EAG's involvement in differentiation,

cell cycle progression, and oncogenic potential have been made (Stansfeld et al., 1996; Occhiodoro et al., 1998; Pardo et al., 1998; Meyer et al., 1999; Pardo et al., 1999; Camacho et al., 2000; Farias et al., 2004). In neuronal cells all previous research has dealt with either vertebrate sensory functions (Beech and Barnes, 1989; Firestein et al., 1991; Frings et al., 1998; Lecain et al., 1999) or channel expression and localization (Saganich et al., 1999; Ludwig et al., 2000; Saganich et al., 2001). Also, there has been no mouse or human mutation identified that affects the *eag1* or *eag2* genes. Therefore, in mammals, the physiological roles of EAG in neurons are mostly unknown.

Given this lack of information, it is difficult to translate the growing amount of knowledge based upon research done in invertebrates into possible functions in mammals. Nonetheless, EAG channels are expressed widely in the brain, including in the neocortex, hypothalamus and hippocampus (Ludwig et al., 2000; Saganich et al., 2001). Jeng et al. have shown that both EAG1 and EAG2 are only found in somatodendric compartments and not in axons of rat hippocampal neurons, although this has yet to be confirmed by the use of multiple antibodies (Jeng et al., 2005). This dendritic staining of EAG1 is specifically localized to glutamatergic, and not GABAergic, synapses. This suggests rat EAG1 K^+ channels may modulate the postsynaptic signaling of glutamatergic synapses and contribute to postsynaptic mechanisms of plasticity. Importantly, *Drosophila* EAG domains, such as those necessary for CaM and CaMKII binding, are conserved and functional in mammalian *eag* (Ludwig et al., 1994; Schonherr et al., 2000; Fig. 3.1; Fig. 4.3), strongly implying they may serve similar purposes in higher organisms.

Roles for the function of mammalian EAG can be proposed by analogy to other somatodendritically localized K+ channels. $K_v2.1$ is a major component of somatodendritic I_K in regulating somatodendritic excitability in hippocampal and cortical pyramidal neurons (Colbert and Pan, 2002). Somatodendritic $K_v2.1$ channels in pyramidal neurons function in regulating excitability and Ca^{2+} influx during periods of repetitive high frequency firing. Activity-dependent dephosphorylation of neuronal Kv2.1 channels at one site yields hyperpolarizing shifts in their voltage-dependent activation and homoeostatic suppression of neuronal excitability. Also, activity-dependent hyperphosphorylation at the same site causes the opposite effect (Misonou et al., 2006). In this case, distinct regulation of an individual phosphorylation site allows for graded and bidirectional homeostatic regulation of $K_v2.1$ functions. The time course of this mechanism has not been investigated, but this is reminiscent of the bi-directional effect Ca^{2+}/CaM has on EAG currents which may function in the same way in hippocampal neurons.

Similarly, another activity-dependent bidirectional effect on hippocampal synaptic plasticity is regulated by CaMKII and PKA. Pharmacological stimulation of NMDA receptors that produces chemical long-term depression can induce a brief dephosphorylation of the translation factor cytoplasmic polyadenylation element-binding protein (CPEB) (Atkins et al., 2004). This dephosphorylation is regulated by a PKA-dependent phosphatase. Conversely, modest LTP induction results in a transient phosphorylation of CPEB by CaMKII, and stronger stimulation, known to induce protein synthesis-dependent late phase-LTP, elicited a prolonged phosphorylation of CPEB by CaMKII. Therefore, bi-directional regulation of CPEB phosphorylation by CaMKII and

protein phosphatases may serve as a mechanism to convert early phase-LTP into protein synthesis-dependent late phase-LTP by stimulating protein synthesis and stabilizing synaptic enhancement (Atkins et al., 2004).

These examples suggest at least three points concerning possible roles of EAG and CaMKII in mammalian neurons. First, these are further illustrations of how complex regulation of synaptic activity can be. Similar to the numerous ways EAG is regulated, and how its function may affect downstream plasticity changes, $K_v2.1$ and CaMKII are both tightly controlled to result in the desired neuronal outcome. There may be even more modulators and partners of EAG channels found in mammalian cells than in *Drosophila*. Second, depending on the strength of stimulation, differing responses may result. Like the different CaMKII phosphorylation levels of CPEB, the activity of CaMKII depends on numerous factors. From the example of CaMKII bound to EAG, kinase activity may depend on Ca^{2+}/CaM concentration, constitutive activity, autophosphorylation, whether it is bound to EAG/CMG or not, or its subcellular localization. Third, CaMKII is necessary for numerous kinds of synaptic plasticity, including both LTP and LTD (Silva et al., 1992b; Griffith, 2004; Hansel et al., 2006). Therefore, like the EAG-signaling model in *Drosophila*, multiple pathways may be activated in mammalian neurons resulting in synaptic plasticity ranging from facilitation, potentiation, and short-term depression to LTP, LTD, and homeostasis.

H. FUTURE DIRECTIONS

The findings presented here help to explain how the EAG K^+ channel is regulated by activity-dependent mechanisms, how that regulation affects EAG function, and how

channels can influence signaling pathways independent of ion conduction. There are, however, several open questions that could be addressed by future experiments.

As mentioned in the previous section, the role EAG channels plays in mammals in not well understood, especially in terms of EAG's effects on behavior and memory. One way to address this would be create of a mouse genetic knockout of the *eag1* and *eag2* homologs of *eag* (Table 1.1). Analysis of resultant phenotypes may explain more about the function of EAG. In comparison, knockouts of other K^+ channels have helped develop models of neurological defects such as benign familial neonatal convulsions. For example, mice lacking the voltage-gated Shaker-like potassium channel $K_v1.1$ α-subunit develop recurrent spontaneous seizures early in postnatal development (Rho et al., 1999). This type of information has lead to better understanding of the causes of epilepsy and other diseases.

Some knockout genes cause mortality during early development, making it difficult to assess phenotypes. If this is the case for *eag*, then conditional knockouts that remove expression from specific tissues may be of more use (McHugh et al., 1996; Tsien et al., 1996; Tang et al., 1999). In particular, the neurological aspects of EAG function could be dissected by excluding expression from regions such as the hippocampus. If EAG channels do contribute to synaptic plasticity, its affect on phenomena such as facilitation, LTP, or LTD could be assayed. Also, since learning and memory defects are highly associated with *Drosophila eag*, behavioral experiments could be performed to see if those functions are conserved among different species.

Slightly more pragmatic future experiments to understand the function of EAG might be further investigations in the *Drosophila* model. Since the transgenic flies with

regulatory mutations I made all show defects in synaptic transmission, including some with plasticity defects such as facilitation, it would be of interest to determine if these also result in learning and memory defects. At this stage it should be fairly straight forward to test if there are differences observed in assays such as courtship conditioning or olfactory recognition and discrimination (Siegel and Hall, 1979**;** Griffith et al., 1993; Carlson, 1996).

It may be of particular interest to determine if the *eag*-LAKK lines exhibit learning defects. Such experiments could provide additional evidence supporting a role for EAG in the regulation of intracellular signaling pathways. Also, because EAG is highly regulated by CaMKII, one could hypothesize that transgenic *eag*-LAKK, and *ala* flies would exhibit similar learning phenotypes. A learning phenotype would be particular useful in screens aiming to identify downstream components of the EAG signaling pathway. Also, to determine if EAG does contribute to homeostatic regulation at the NMJ, one could block neuronal activity either with TTX or postsynaptic responses with glutamate receptor inhibitors and induce an increase in compensatory transmitter release. It would be of interest if this homeostasis is disrupted by *eag*-LAKK.

As previously mentioned, the complex consisting of EAG channels and adaptors/regulators may contain numerous proteins. To date, about a dozen have been shown to directly bind EAG or EAG fragments. Some small screens have been made to identify proteins with SH3 binding domains that interact with EAG (Fig. 2.5D; G. Wilson, unpublished results), but this excludes many possible interactions with other classes of proteins. It might be valuable to perform a large protein interaction screen such as a yeast one-hybrid screen using the intracellular N- and C-termini as bait. This

may identify other complex partners such as phosphatases or AKAPs capable of localizing PKA activity to the channel.

I. CONCLUSIONS

These studies show that the EAG K^+ channel is an important component of activity-dependent regulation of neuronal function and can directly translate voltage changes into modulation of intracellular messenger pathways. Specific proteins including CaM and CMG are newly identified as modulators of *Drosophila* EAG current and their interacting domains have been mapped. CaM and CaMKII associated with EAG are also shown to regulate specific electrophysiological properties, both short- and longer-term, of the larval NMJ, indicating that the channel is a key hub in several activity dependent pathways. These may influence resultant neuronal functions such as synaptic plasticity, synaptic stability and neurotransmitter release. It is hoped that these studies will motivate further investigation of the roles of ion channels and their contributions to diverse cellular and system functions including proliferation, excitability, learning and memory.

APPENDIX A

A VOLTAGE-DRIVEN SWITCH FOR ION-INDEPENDENT SIGNALING BY ETHER À GO-GO K^+ CHANNELS

A. ABSTRACT

Voltage-gated channels maintain cellular resting potentials and generate neuronal action potentials by regulating ion flux. Here, we show that Ether à go-go (EAG) K^+ channels also regulate intracellular signaling pathways by a mechanism that is independent of ion flux and depends on the position of the voltage sensor. Regulation of intracellular signaling was initially inferred from changes in proliferation. Specifically, transfection of NIH 3T3 fibroblasts or C2C12 myoblasts with either wild type or non-conducting (F456A) *eag* resulted in dramatic increases in cell density and BrdU incorporation over vector- and *Shaker*-transfected controls. The effect of EAG was independent of serum and unaffected by changes in extracellular calcium. Inhibitors of p38 mitogen-activated protein (MAP) kinases, but not p44/42 MAP kinases (extracellular signal-regulated kinases), blocked the proliferation induced by non-conducting EAG in serum-free media, and EAG increased p38 MAP kinase activity. Importantly, mutations that increased the proportion of channels in the open state inhibited EAG-induced proliferation, and this effect could not be explained by changes in the surface expression

of EAG. These results indicate that channel conformation is a switch for the signaling activity of EAG and suggest a novel mechanism for linking channel activity to the activity of intracellular messengers, a role that previously has been ascribed only to channels that regulate calcium influx.

B. INTRODUCTION

Voltage-gated ion channels generate neuronal action potentials, the primary units of information transfer in the brain, by regulating ion flux (Hille, 2001). Effects of ion channels on synaptic connectivity, transmitter release, plasticity, and other cellular processes are generally assumed to be a secondary consequence of ion flux. Specifically, changes in membrane potential and action potentials alter Ca^{2+} influx and Ca^{2+} regulates multiple intracellular signaling pathways (Catterall, 2000; Deisseroth et al., 1998; Dineley et al., 2001; Dolmetsch et al., 2001; Hardingham and Bading, 2003; Sutton et al., 1999). Several recent studies, however, have indicated that some voltage-gated ion channels are bifunctional proteins (Dolmetsch et al., 2001; MacLean et al., 2003; Malhotra et al., 2000; Runnels et al., 2001; Wang et al., 1999). These studies show that voltage-gated channels can contribute to transcriptional regulation, protein scaffolding, cell adhesion, and intracellular signaling, and the effects appear largely independent of ion conduction.

Recent studies of Ether à go-go (EAG, KCNH1) voltage-dependent K^+ channels suggest that EAG may also be bifunctional. First, a region of *Drosophila* EAG with similarity to the autoinhibitory domain of Ca^{2+}/calmodulin-dependent protein kinase II (CaMKII) can associate with activated, Ca^{2+}/CaM-bound, CaMKII. *In vitro* assays

indicate that once Ca^{2+} levels decline, EAG-bound kinase retains five to ten percent of its maximum Ca^{2+}-stimulated activity (Sun et al., 2004). Second, human EAG has been implicated in cell cycle regulation and cancer: transfection can induce oncogenic transformation, EAG is present in some cancer cell lines but absent in the corresponding healthy tissues, and implanting EAG-expressing cells into immune-suppressed mice results in tumor progression (Farias et al., 2004; Pardo et al., 1999). These studies implicate EAG as a component of one or more intracellular signaling pathways.

Our investigation of the involvement of EAG in intracellular signaling was prompted by experiments in which we observed an increase in NIH 3T3 fibroblast density following transient transfection with *Drosophila eag*. Our findings indicate that conformational changes of EAG associated with the position of the voltage-sensor may be an alternative mechanism, independent of ion flux, by which ion channels can affect intracellular signaling.

C. RESULTS

C.1. Transfection with EAG stimulates proliferation

Figure A.1A shows a representative experiment demonstrating an increase in NIH 3T3 cell density following transfection with *eag*. Cell density was significantly higher for coverslips transfected with *eag* than for controls transfected with empty vector ($p < 0.01$; similar results obtained for two other experiments). To determine the mechanism underlying this increase, cells were labeled with BrdU, a marker for proliferation. Coverslips transfected with *eag* displayed substantial increases in BrdU incorporation when compared to vector-transfected controls (Fig 2.1B; $p < 0.0001$, $n = 3$). In

FIGURE A.1

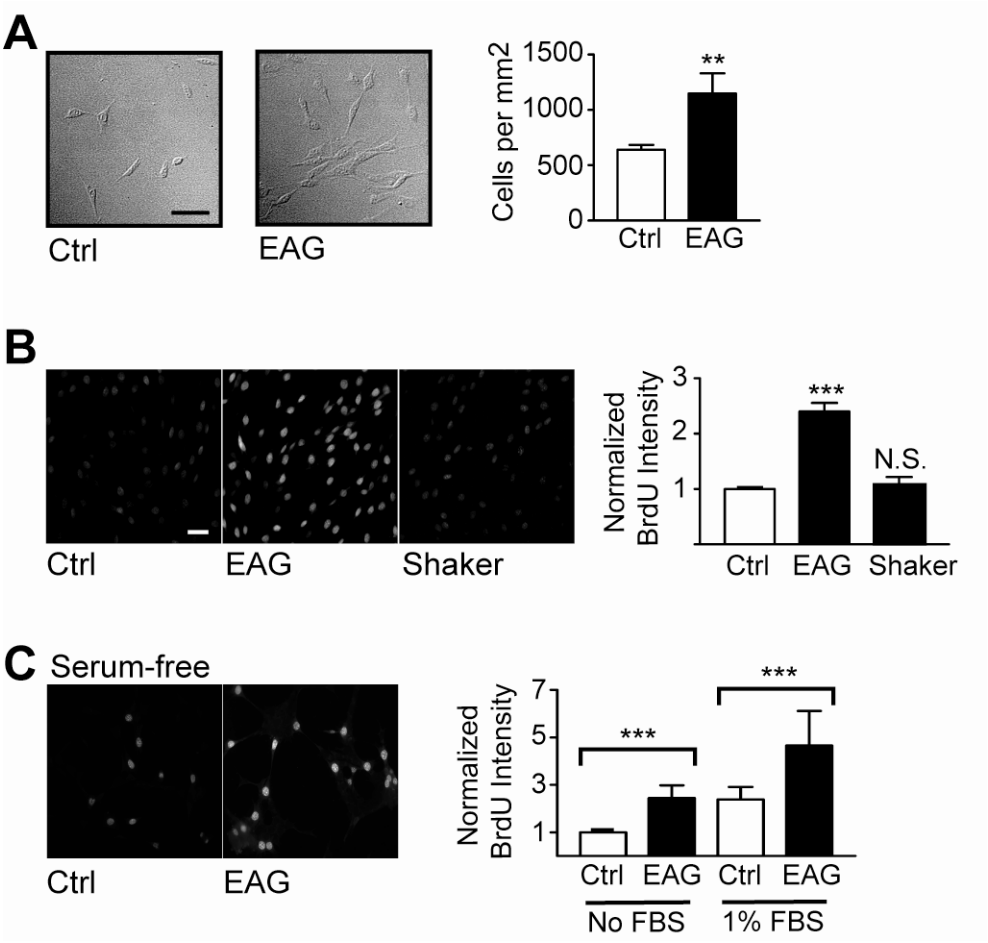

Figure A.1: EAG stimulates proliferation of NIH 3T3 fibroblasts.
(A) Differential interference contrast microscopy images and cell densities for coverslips transfected with pCS2-*eag* or vector alone. For each condition, cell numbers were averaged across at least 6 visual fields (0.05 mm^2 / field). Similar results were documented for two additional experiments. **(B)** *Left*, representative scans showing BrdU labeling of cells transfected as indicated. BrdU labeling was detected by using secondary antibody conjugated to a fluorescent indicator. *Right*, Average fluorescence intensities normalized to vector-transfected controls (n = 3). Compared with fluorescence intensity measurements, the percent of BrdU-positive versus total cells was 14.0 ± 4.9, 47.1 ± 4.1 and 18.3 ± 2.0, for vector-, *eag*-, and *Shaker*- transfected coverslips, respectively.
(C) *Left*, BrdU incorporation in cells deprived of FBS. *Right*, Normalized fluorescence intensities for three experiments. (Scalebar = 10 μm.) Data are presented as the mean ± SEM. * $p < 0.05$; ** $p < 0.01$, *** $p < 0.0001$; N.S., not significant (ANOVA); Ctrl, control.

contrast, transfection with the gene encoding Shaker, another voltage-dependent K^+ channel, resulted in BrdU incorporation that was indistinguishable from control levels, indicating that the effect was specific to EAG. Increased proliferation also was observed by using phospho-histone labeling, another marker for proliferation (data not shown). These results indicate that proliferation accounts, at least in part, for the observed increase in cell density. EAG-induced proliferation was not limited to NIH 3T3 cells because EAG also increased proliferation in C2C12 myoblasts (data not shown). Finally, increased proliferation was also observed in response to EAG when cells were "synchronized" in serum-free media before reintroduction of fetal bovine serum (FBS). However, proliferation was increased even in the complete absence of FBS (Fig A.1C; $p < 0.0001$, $n = 3$); thus, the growth factors present in serum were not required for the effect of EAG on signaling.

C.2. EAG-induced proliferation is independent of ion flux

K^+ currents are essential for the proliferation of numerous cell types, including T-lymphocytes and Schwann cells (DeCoursey et al., 1984; Wilson and Chiu, 1993). The roles of K^+ channels in proliferation, as well as other cellular processes, is generally assumed to be indirect. K^+ channels alter the membrane potential to modulate Ca^{2+} influx through voltage-dependent Ca^{2+} channels, which, in turn, affects numerous intracellular messenger pathways (Lewis and Cahalan, 1995; Rosen et al., 1994). However, in the present experiments, ion conduction was not required for the effect of EAG on proliferation. Figure A.2A shows recordings from *Xenopus* oocytes expressing wild type EAG, myc-tagged EAG or EAG-F456A, which contains a point mutation in the

Figure A.2: EAG-mediated signaling is independent of K^+ conductance.
(A) Representative currents and average current-voltage relations for oocytes injected with *eag* (n = 10), myc-*eag* (n = 4), *eag*-F456A (n = 8), or water (n = 7) as indicated. Currents were elicited by using steps from -110 to +60 mV (holding potential of -120 mV), and peak currents were plotted as a function of voltage. **(B)** *Left,* Non-conducting channels increased BrdU incorporation similar to wild type EAG. *Right*, Normalized fluorescence intensities (n = 3). **(C)** SB-203580 (20 μM), an inhibitor of p38 MAP kinase, inhibits proliferation induced by non-conducting EAG in the absence of serum. *Right*, average data (n = 3). (Scalebar, 10 μm.) **(D)** Average data for the "p38 MAP kinase inhibitor" (25 μM, n = 3), the control compound SB-202474 (25 μM, n = 2), and PD-98059 (40 μM, n = 3) effects on EAG-F456A-induced proliferation in serum-free media. **(E)** EAG increases p38 MAP kinase activity. *Left*, Representative blots of NIH 3T3 cell extracts run out in parallel were probed with antibodies for total p38 (1:500), phosphorylated (active) p38 (1:100), and actin, followed by anti-rabbit HRP-conjugated secondary antibody. *Right*, average data (n = 4). Asterisks and error bars as in Figure 1.

FIGURE A.2

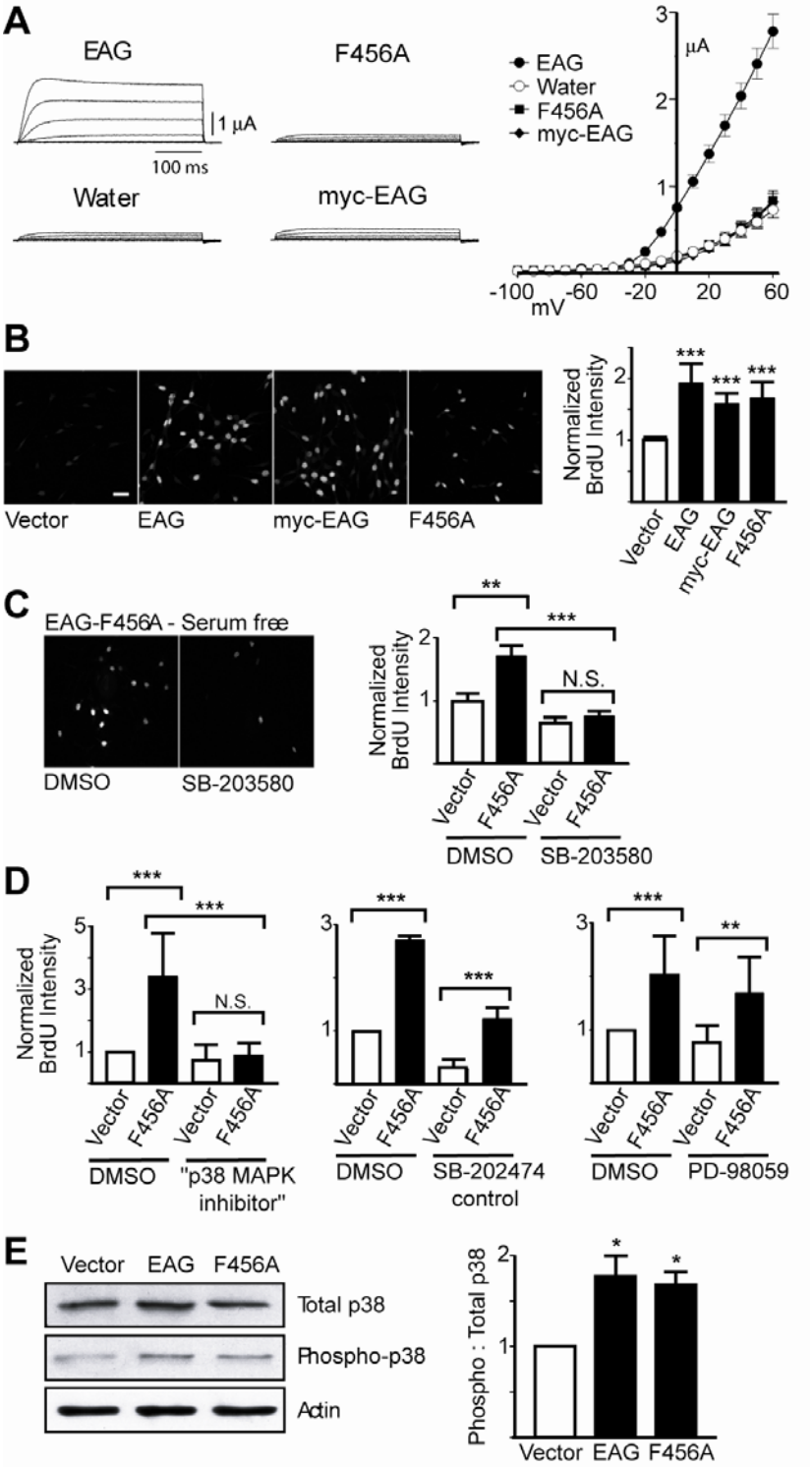
A
EAG
F456A
1 µA
100 ms
Water
myc-EAG
EAG
Water
F456A
myc-EAG
µA
mV
B
Vector
EAG
myc-EAG
F456A
Normalized BrdU Intensity
C
EAG-F456A - Serum free
DMSO
SB-203580
Normalized BrdU Intensity
N.S.
D
Normalized BrdU Intensity
N.S.
DMSO
"p38 MAPK inhibitor"
SB-202474
control
PD-98059
E
Vector EAG F456A
Total p38
Phospho-p38
Actin
Phospho : Total p38

selectivity filter of the channel pore. The selectivity filter sequence is conserved in all K^+ channels (Doyle et al., 1998) and point mutations in this sequence eliminate conduction in Shaker, as well as numerous other K^+ channels (Heginbotham et al., 1994; MacLean et al., 2003; Preisig-Muller et al., 2002). Both myc-EAG and EAG-F456A failed to produce the outward currents characteristic of the wild type channel. Comparison of current-voltage relations (Fig A.2A, *right*) revealed little difference between myc-EAG and EAG-F456A currents and currents recorded from water-injected controls, which are carried by channels endogenous to oocytes. Although the mechanism underlying the absence of current in myc-EAG is unclear, both myc-EAG and EAG-F456A produced detectable gating currents (data not shown), indicating that defects in the folding or trafficking of EAG cannot wholly account for the absence of K^+ current.

Myc-EAG and EAG-F456A increased proliferation to a degree similar to wild type channels (Fig A.2B). The increases in BrdU incorporation were significant in comparisons to vector-transfected controls ($p < 0.0001$; $n = 3$). Moreover, the effects of myc-EAG and EAG-F456A were not significantly different from the effect of the wild type channel. In short, changes in K^+ flux, and the changes in membrane potential and Ca^{2+} influx that are presumed to result, cannot account for the proliferation induced by EAG. Additional evidence that the signaling mechanism of EAG does not include an indirect effect on Ca^{2+} influx was obtained by incubating cells in EGTA-buffered media prior to and during incubation of cells with BrdU. EAG-induced proliferation in the presence of EGTA (1 mM, 5 hrs) was 90.1 ±11.2% and 95.1 ± 3.7% of the proliferation in standard Ca^{2+}-containing media for wild type EAG and EAG-F456A channels respectively ($n = 3$, not significant). Higher concentrations of EGTA caused cells to

detach and, therefore, were not assessed.

C.3. EAG-induced proliferation requires the p38 MAP kinase pathway

MAP kinase signaling is central to proliferation in numerous cell types and in response to a variety of signals (Pearson et al., 2001). To determine whether the proliferation induced by non-conducting EAG channels requires this pathway, cells were treated with inhibitors of MAP kinase signaling in serum-free media. The p38 MAP kinase inhibitor SB-203580 [4-(4-fluorophenyl)-2-(4-methylsufinylphenyl)-5-(4-pyridyl)-1*H*-imidazole] (20 μM) blocked the proliferation observed in response to EAG-F456A (Fig 2.2C; $p < 0.0001$, $n = 3$), reducing proliferation to levels that were no different from the proliferation observed for controls ($p > 0.05$, $n = 3$). Similar results were obtained by using the "p38 MAP kinase inhibitor" [2-(4-chlorophenyl)-4-(4-fluorophenyl)-5-pyridin-4-yl-1,2-dihydropyrazol-3-one] (Fig A.2D, *left*). In contrast, although the control compound, SB-202474, [4-ethyl-2(*p*-methoxyphenyl)-5-(4'-pyridyl)-1*H*-imidazole] reduced the overall level of proliferation in both vector- and *eag*-F456A-transfected conditions, it failed to inhibit the EAG-specific increase (Fig A.2D, *center*; $p < 0.0001$, $n = 2$). Finally, although PD-98059 [2'-amino-3'-methoxyflavone], an inhibitor of the p44/42 extracellular signal-regulated kinases, reduced proliferation in the presence of FBS (data not shown), PD-98059 (40 μM) had little effect on the increase in proliferation specifically induced by non-conducting EAG in serum-free media (Fig A.2D, *right*; $p < 0.01$, $n = 3$). These results suggest that p38, but not p44/42, MAP kinase signaling is required for the proliferation stimulated by non-conducting EAG-F456A channels.

To determine whether EAG affects p38 MAP kinase activity, we immunoblotted NIH 3T3 cell lysates with antibodies that detect either total p38 MAP kinase or, specifically, the phosphorylated, active kinase. As shown in Figure A.2E, p38 phosphorylation nearly doubled in the presence of either wild type or non-conducting EAG (Fig A.2E; $p < 0.05$, $n = 4$) and the magnitude of the effect appeared to approximate the average increase in BrdU incorporation (Fig A.2 B,C).

C.4. EAG-induced proliferation is regulated by the position of the voltage-sensor

The observation that the signaling activity of EAG does not depend on ion conduction predicts that changes in extracellular K^+ concentration ($[K^+]_o$) should not affect EAG-induced proliferation. However, although increased $[K^+]_o$ increased proliferation in vector-transfected controls, increasing $[K^+]_o$ by 10 mM inhibited EAG-induced proliferation, returning proliferation to control levels. Specifically, at 15 mM $(K^+]_o$, EAG-induced proliferation was 93.9 ± 1.5 % of controls compared to 151.4 ± 7.3 percent in normal 5.3 mM $[K^+]_o$. (Measurements were normalized to vector-transfected controls in 5.3 mM; $p < 0.001$). Similar results were observed in two additional experiments. Because increases in $[K^+]_o$ will depolarize the membrane and shift the position of the voltage sensor even in non-conducting EAG channels, we hypothesized that the signaling activity of EAG might depend on voltage-sensitive conformations of the channel. Specifically, the $[K^+]_o$ experiments predict that increases in the proportion of channels in the open state should decrease EAG signaling activity.

To explore the possibility that the signaling activity of EAG might be regulated by the position of the voltage sensor, we examined the effects of EAG channels containing

mutations in the sixth transmembrane segment that shifted their voltage-dependence of activation. Figure A.3A shows representative currents obtained for the wild type channel and two mutants, EAG-TATSSA (T449S/K460S/T470A) and EAG-HTEE (H487E/T490E), when expressed in *Xenopus* oocytes. Comparison of the conductance-voltage (GV) relations (Fig A.3B) reveals that the predominant effect of both mutations was to produce hyperpolarizing shifts in the midpoints of activation from 8.0 ± 1.1 mV (wild type, n = 6) to -10.8 ± 1.2 mV (n = 9) and -31.6 ± 2.0 mV (n = 7) for EAG-TATSSA and EAG-HTEE channels, respectively. In addition, the TATSSA and HTEE mutations also produced changes in kinetics; however, these changes were in opposite directions (Fig A.3A). Comparison of the average resting potentials of oocytes expressing EAG channels (Fig A.3C) revealed that the resting potentials closely followed the changes in the V_{10} for activation (the voltage at which 10% of channels are activated; Fig A.3D). This would be expected if EAG is the major channel contributing to the membrane potential. Wild type EAG produced only a small shift in the resting potential from -44.5 ± 2.8 to -52.8 ± 1.9 mV. In contrast, EAG-TATSSA and EAG-HTEE shifted the resting potential to -82.8 ± 1.1 and -90.7 ± 0.9 mV, respectively. It is important to note that, given that K^+ channel conformation and membrane potential act as a negative feedback loop, the proportion of channels in the closed state should be similar in each case, provided that each of the constructs contributes to the membrane potential to a similar extent.

The above EAG constructs were used to address whether the signaling activity of EAG is regulated by channel conformation. As shown in Figure A.4A, there was an approximately 2-fold increase in the proliferation of NIH 3T3 cells regardless of whether

FIGURE A.3

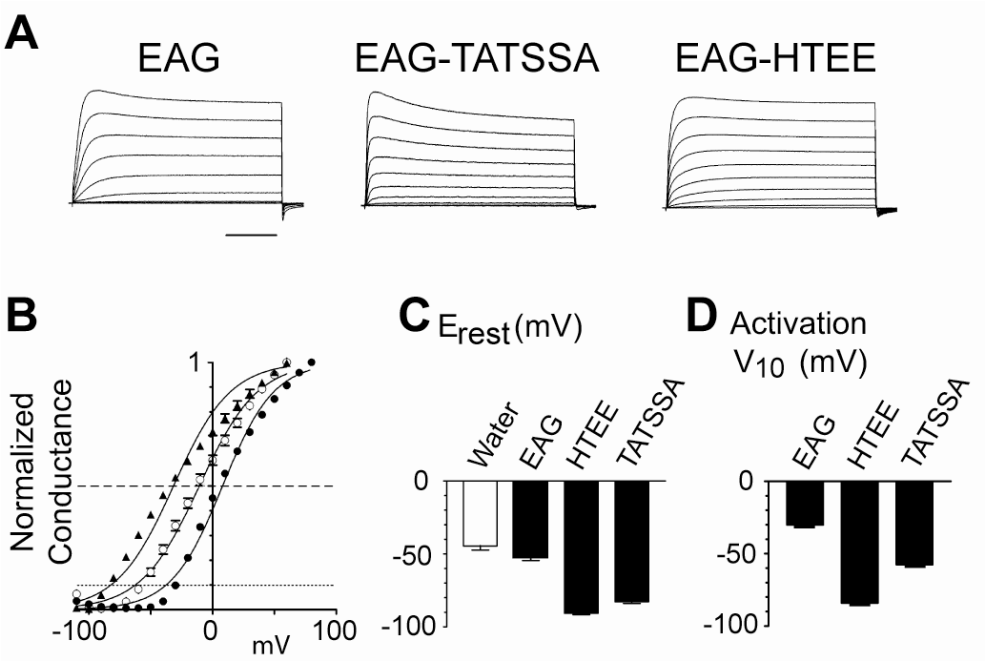

Figure A.3: Comparison of the properties of wild type and mutant EAG channels. **(A)** Recordings from oocytes expressing EAG constructs as indicated. Voltages were stepped from -110 to +80 mV (holding potential of -120 mV). (Bar, 100 msec.) **(B)** Normalized G-V relations obtained for EAG (●), EAG-TATSSA(○) and EAG-HTEE (▲). GV curves were generated using the relation $G = I_{peak}/ (V_{test} - E_K)$, where E_K was assumed to be -120 mV. Conductances were normalized to the maximum conductance observed. Boltzmann fits to the data had slopes of 20.7 ± 0.9 and 23.5 ± 1.0 for EAG and EAG-TATSSA, respectively. For EAG-HTEE, the slope was constrained to 23. Horizontal dotted and dashed lines represent 10% and 50% maximal activation, respectively. **(C)** Averaged resting potentials for the same oocytes. **(D)** Average V_{10} for activation obtained from GV curves.

wild type *eag*, *eag*-TATSSA or *eag*-HTEE were used. Given the negative feedback of conducting EAG channels on channel conformation, these results suggest that proliferation depends on the position of the voltage sensor of EAG channels rather than on a specific resting membrane potential. Indeed, measurement of the resting potentials of NIH 3T3 cells transfected with these constructs indicated that, although EAG channels contributed to the membrane potential to a lesser degree than in oocytes, each construct shifted the resting potential closer to the respective activation threshold (Fig A.4B).

Additional evidence in support of the hypothesis that channel conformation is a "switch" for the signaling activity of EAG was obtained using *eag*-TATSSA and *eag*-HTEE constructs that had been rendered non-conducting by including the F456A mutation, in effect short-circuiting the negative feedback function of EAG. As expected, the resting potentials of cells expressing these double mutants were similar to the resting potentials of vector-transfected controls (Fig A.4B). The shifted voltage-dependence of these channels, combined with their inability to shift the resting potential, should result in a larger proportion of TATSSA-F456A and HTEE-F456A channels in the open conformation. On the basis of the prediction above, increasing the proportion of channels in the open state should decrease EAG-induced proliferation. As predicted, both EAG-TATSSA/F456A and EAG-HTEE/F456A failed to increase proliferation above control levels (Fig A.4A). In contrast, as observed in our earlier experiments, proliferation was robust for EAG-F456A. Finally, neither changes in expression level or changes in the surface expression of EAG (Fig A.4C) could account for the changes in proliferation observed with the double-mutant constructs. Together, these results suggest that the signaling activity of EAG depends on voltage-sensitive conformations of the channel.

FIGURE A.4

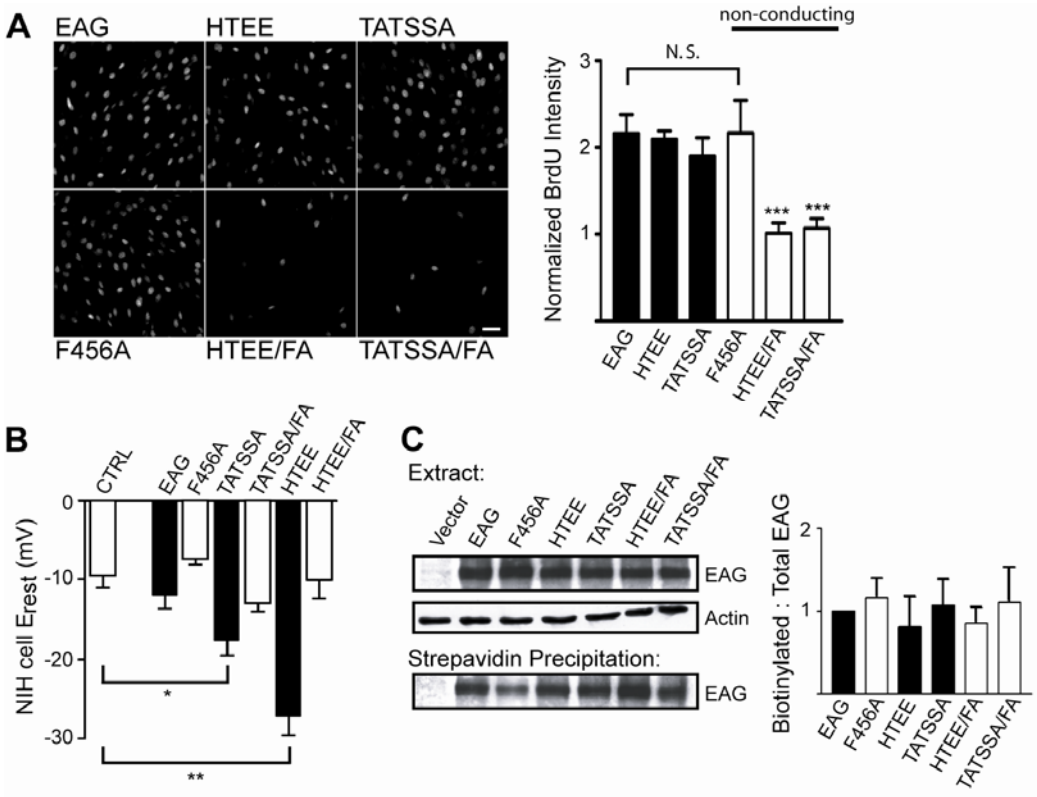

Figure A.4: EAG-mediated signaling is regulated by channel conformation. **(A)** *Left*, BrdU labeling for EAG, EAG-HTEE or EAG-TATSSA (upper panels) and corresponding non-conducting mutants (lower panels). *Right*, Proliferation is inhibited when EAG is predominantly open but non-conducting (n = 3). (Scalebar = 10 μm.) Asterisks and error bars as in Figure 1. **(B)** Whole recordings of NIH 3T3 cell resting potentials. Individual isolated cells were selected for recordings on the basis of EGFP fluorescence. Resting potentials were more depolarized than observed in oocytes, presumably because of the presence of channels, in particular Ca^{2+} channels, endogenous to NIH 3T3 cells (Chen et al., 1988; Pemberton et al., 2000). The number of oocytes examined for each condition were, from left to right, 16, 13, 8, 12, 11, 13, and 8. **(C)** Total expression and surface expression of wild type and mutant EAG channels. *Left*, Representative blots. *Right*, average data for three experiments. Before preparation of extracts and precipitation with streptavidin agarose, cells were labeled with biotin and then quenched with glycine as described in Methods. Equal amounts of either the extract (upper panels) or the precipitates (lower panels) were separated by SDS-PAGE and probed with EAG (CT) or actin antisera. Bands were quantified by densitometry and normalized to the band observed for wild type EAG in each experiment.

D. DISCUSSION

Our results indicate that EAG is a bifunctional protein that not only regulates K^+ flux, but also regulates intracellular signaling pathways. The effect of EAG on intracellular signaling was evident as an increase in proliferation of NIH 3T3 cells and did not appear to be due to an indirect effect of K^+ ions because it was observed even with non-conducting channels. To date, other examples of bifunctional channels include α1C Ca^{2+} channels whose carboxyl-terminal regions regulate transcription (Dolmetsch et al., 2001), a member of the TRP family of cation channels (TRP-PLIK) that contains a functional kinase domain (Runnels et al., 2001), and voltage-gated sodium channels whose β-subunits not only modulate channel function but also act as cell adhesion molecules (Malhotra et al., 2000). EAG appears to differ from the above channels in that signaling activity is linked to channel conformations determined by the position of the voltage sensor. The signaling function of EAG is a novel mechanism that may link channel gating to intracellular messenger pathways. This role has typically been ascribed only to channels that regulate Ca^{2+} influx. Recently, however, *Ci*-VSP, a novel protein containing a transmembrane voltage sensor linked to a functional cytoplasmic phosphatase and tensin (PTEN) domain, has been reported to regulate phosphoinositide turnover in a voltage-dependent manner (Murata et al., 2005).

The signaling activity of EAG characterized in the present study appears negatively correlated with the proportion of channels in the open state or, at the single channel level, the magnitude of the single channel open probability (p_o). It is tempting to speculate that EAG-induced signaling is limited to channels in a specific conformation, presumably one of two previously characterized EAG closed states (Schonherr et al., 2002; Tang et al.,

2000). Comparison of NIH 3T3 cell resting potentials (Fig A.4B) to the GV curves obtained in oocytes (Fig A.3B) predicts that > 50% of the channels must be closed or that the single channel p_o must be < 50% of the maximum for a significant increase in proliferation to occur. However, given the reduced effect of EAG on the NIH 3T3 cell versus oocyte resting potentials, this correlation appears to break down for more quantitative comparisons. For example, at the mean resting potentials of -12, -18, and -28 mV for cells expressing wild type, TATSSA, and HTEE channels (Fig A.4B), the GV curves indicate that approximately 68, 56, and 49% of channels will be closed, respectively. This observation predicts that proliferation response should be highest for wild type channels and lowest for EAG-HTEE, a trend that is not observed in our data. There are several possible explanations of this discrepancy. First, the resting potentials measured in NIH 3T3 cells may not accurately reflect the resting potentials of cells in our proliferation assays given that the cells are treated differently. Secondly, the GV curves obtained in oocytes may not be representative of channel behavior in NIH 3T3 cells. Unfortunately, EAG current could not be effectively isolated from the other outward currents endogenous to NIH 3T3 cells to address this concern. Third, it is possible that proliferation is not as sensitive an indicator of voltage-dependence as the GV curve. GV curves, which are continuous functions, represent the average behavior of a million or more channels, whereas proliferation, which is a step function, represents the average behavior of hundreds of cells at best. Fourth, EAG-induced proliferation may be limited by the availability or activity of downstream components of the affected signaling pathway. Finally, voltage-dependent enzymatic activity or protein-protein interactions may require that channels occupy a given conformation for a specific duration. Although

channel conformation may serve as a switch for the signaling activity of EAG, the domain underlying signaling remains under investigation. Possibilities include an amino-terminal PER-ARNT-SIM (PAS) domain, several putative nuclear localization signals in the carboxy-terminal domain, and a region with homology to the autoinhibitory domain of CaMKII that has been shown recently to regulate kinase activity in *in vitro* assays (Wang et al., 2002b).

The proliferation induced by EAG was unaffected by changes in extracellular Ca^{2+}, suggesting that increased Ca^{2+} influx is not an essential downstream component of EAG-induced signaling. Nonetheless, our experiments do not address intracellular Ca^{2+} concentrations or the possible role of Ca^{2+} released from intracellular stores. Moreover, although Ca^{2+} influx may not be a downstream component of the EAG-induced pathway, our results suggest that any mechanism that regulates EAG surface expression or voltage-dependence may be an upstream regulator of EAG signaling. Indeed, Ca^{2+}/calmodulin binding to EAG decreases EAG current by shifting channel activation to more positive potentials (Chapter III) and, Ca^{2+}, by increasing CaMKII activity and phosphorylation of EAG, increases EAG surface expression (Marble et al., 2005). Thus, both of these Ca^{2+}-dependent mechanisms could act upstream of EAG to increase EAG signaling in an activity-dependent manner, and the role of Ca^{2+} should be further explored.

In the present study, the voltage-dependent signaling activity of EAG increased proliferation of NIH 3T3 cells and C2C12 myoblasts; however, it is unclear whether EAG-induced signaling normally regulates proliferation *in vivo*. No gross morphological defects have been observed in *Drosophila eag* mutants at any developmental stage. It should be noted, however, that a role for *Drosophila ras* in proliferation was only

uncovered by using overexpression of mutant *ras* constructs (Karim and Rubin, 1998), despite the well-established role of *ras* in proliferation in other systems. Although the developmental profile of EAG expression is unknown, EAG transcripts and protein appear most highly expressed in mature neurons in both *Drosophila* and mammals (Jeng et al., 2005; Ludwig et al., 1994; Saganich et al., 2001; Sun et al., 2004). Thus, there is little evidence to suggest that EAG regulates proliferation in normal tissues at present. However, abnormally expressed EAG may have a role in proliferation and transformation, given that human EAG has been suggested to have an oncogenic potential and EAG appears abnormally expressed in several tumor cell lines (Pardo et al., 1999; Patt et al., 2004).

Intracellular signaling pathways typically have a variety of possible roles; the output of a pathway in any given cell at any given developmental stage will depend on context and crosstalk between other pathways. In the present study, proliferation may simply be the "read-out" of a change in the activity of one or more intracellular signaling pathways. Given that EAG appears largely neuron specific and localized at synapses (Jeng et al., 2005; Sun et al., 2004; Wang et al., 2002b), and given that synaptic plasticity and memory acquisition are disrupted in *eag* mutants (Engel and Wu, 1998; Griffith et al., 1994), EAG signaling may normally regulate activity-dependent changes in neuronal function. Indeed, EAG-mediated proliferation was blocked by inhibitors of the p38 MAP kinase pathway, and transfection of EAG increased p38 MAP kinase activity. An important future question concerns whether the link between EAG and p38 activity is conserved in neurons. MAP kinase signaling is central to not only proliferation but also synaptic plasticity and learning (Sweatt, 2004; Thomas and Huganir, 2004).

E. MATERIALS & METHODS

E.1. Plasmids and construction

pCS2-myc-*eag* contains a myc tag added to the amino-terminus (Wang et al., 2002b). For the wild type construct, EcoRI and XbaI sites flanking the coding sequence were used to subclone *eag* (without the myc tag) into the pCS2 vector. A Kozak sequence (GCCACC) was added to improve channel expression. *Shaker* was subcloned into pCS2 by using *EcoRI* sites flanking the coding sequence of pGH19-*Shaker* (Chouinard et al., 1995). *Eag*-F456A, *eag*-H487E/T490E (HTEE), *eag*-T449S/A460S/T470A (TATSSA) and double mutants were generated by site-directed mutagenesis using QuikChange (Stratagene). For oocyte expression, mutant constructs were subcloned into pGH19-*eag* (Wilson et al., 1998). All constructs were verified by sequencing.

E.2. Immunocytochemistry and proliferation assays

NIH 3T3 fibroblasts were maintained at 37°C and 5% CO_2 in Dulbecco's modified Eagle's medium (DMEM, Invitrogen) supplemented with 10% fetal bovine serum (FBS) as previously described (Chouinard et al., 1995). For transfection, coverslips were washed with Opti-MEM and incubated for 8-10 hrs in 350 µl of Opti-MEM containing 0.4 µl of the indicated cDNAs and 1.5 µl of LipofectAMINE (Invitrogen). Coverslips were then washed and incubated in standard media for 12 hrs. For serum-free experiments, this was followed by incubation in FBS-free DMEM for 12 hrs, with 1% FBS added to a subset of wells as a positive control. MAP kinase inhibitors or control compounds were added following washout of LipofectAMINE.

For BrdU labeling, 10 μM BrdU was added to each well for ~ 60 min. Coverslips were washed with phosphate-buffered saline (PBS) and fixed with a 3:7 mixture of 50 mM glycine (pH 2.0)/100% ethanol for 1 hr at room temperature (RT), then denatured with 4 M HCl for 15 min. Cells were labeled with anti-BrdU fluorescein-conjugated antibody (Molecular Probes) for 45 min at 37 ^{o}C. Labeling was visualized using an Olympus BX51W1 microscope equipped with a Qimaging Retiga Exi camera and IPlab 3.6 software. Coverslips from the same experiment were viewed using identical settings, and multiple representative scans were taken for each coverslip. To quantify fluorescence, scans were background subtracted, and the intensity of all pixels above background was summed across the total area of each scan. Total intensities were averaged across all scans for each condition before normalizing to the average intensity for controls. Normalized data were then averaged across experiments (N). Data were analyzed using a two-way analysis of variance (ANOVA) with Tukey's post-hoc analysis with the condition and experiment number as variables (* $p < 0.05$, ** $p < 0.01$, *** $p < 0.0001$; N.S., not significant). Data are presented as the mean ± SEM. MAP kinase inhibitors were purchased from Calbiochem.

E.3. Biochemistry

Cells grown on culture plates were dissociated with trypsin-EDTA 48 hrs after transfection, washed and resuspended in PBS. Biotinylation and precipitation of EAG was performed as described (Marble et al., 2005). Briefly, cell suspensions were incubated in 2 mM sulfo-NHS-LC-biotin (Pierce) and the reaction was quenched by washing with 100 mM glycine in PBS. Cells were lysed in PBS supplemented with 1% IGEPAL CA-630, 0.5% sodium deoxycholate, 0.1% SDS, 1 mM DTT and protease

inhibitors, and the homogenate was centrifuged twice for 10 min at 20,000 x *g*. Protein concentrations of supernatants were determined by Bradford assay and diluted to ~ 0.5 mg/ml. Surface proteins were precipitated with strepavidin agarose and the precipitate washed extensively before addition of sample loading buffer. Blots were probed with antisera directed against the carboxyl-terminal domain of EAG (EAG (CT); 1:2000) in blocking buffer, followed by horseradish peroxidase (HRP)-conjugated secondary antibody (1:2000), and visualized with ECL (Amersham Biosciences). Protein bands were quantified by using Quantity One software (BioRad). Assays of p38 MAP kinase activity were performed by using extracts prepared in buffer containing the following: 20 mM Tris (pH 7.4), 100 mM NaCl, 50 mM NaF, 1 mM Na_3V0_4, 1 mM EDTA, 1 mM DTT, 1 mM benzamidine, and 0.001 mM microcystin-LR with 1% IGEPAL CA-630, 0.5% sodium deoxycholate, 0.1% SDS, and protease inhibitors.

E.4. Electrophysiology

Experiments using *Xenopus* oocytes were performed as described (Marble et al., 2005). Oocytes were typically injected with 0.1-0.2 ng of RNA; non-conducting constructs were injected at 1-2 ng. The recording solution contained the following: 140 mM NaCl, 2 mM KCl, 1 mM $MgCl_2$ and 10 mM Hepes (pH 7.1 with NaOH). Pipettes had resistances of 0.3 - 0.6 MΩ. Experiments were performed at RT. Leak and capacitative currents were subtracted using P/4 methods.

For NIH 3T3 cell recordings with an Axopatch200B amplifier, cells maintained on plates were co-transfected with pCDNA3-EGFP and the indicated constructs and were then replated onto coverslips. Pipette resistances ranged from 3 to 6 MΩ. The extracellular solution contained the following: 40 mM sodium aspartate, 100 mM NaCl, 4

mM KCl, 1.5 mM $MgCl_2$, 1 mM $CaCl_2$, 2 mM glucose and 10 mM Hepes (pH 7.4 with NaOH). The pipette solution contained the following: 35 mM potassium aspartate, 110 mM KCl, 2 mM MgATP, 1 mM NaATP, 3 mM sodium phosphocreatine, 0.1 mM NaGTP, 8 mM EGTA and 10 mM Hepes (pH 7.4 with KOH).

BIBLIOGRAPHY

Akhavan, A., Atanasiu, R., Noguchi, T., Han, W., Holder, N., and Shrier, A. (2005) Identification of the cyclic-nucleotide-binding domain as a conserved determinant of ion-channel cellsurface localization. J Cell Sci *118*, 2803-2812.

Aldrich, R. W., Getting, P. A., and Thompson, S. H. (1979) Mechanism of frequency-dependent broadening of molluscan neurone soma spikes. J Physiol *291*, 531-544.

Allen, D. H., Lepple-Wienhues, A., and Cahalan, M. D. (1997) Ion channel phenotype of melanoma cell lines. J Membr Biol *155*, 27-34.

Altier, C., Dubel, S. J., Barrere, C. Jarvis, S. E., Stotz, S. C., Spaetgens, R. L., Scott, J. D., Cornet, V., Waard, M. D., Zamponi, G.W., Nargeot, J., and Bourineta, E. (2002) Trafficking of L-type calcium channels mediated by the postsynaptic scaffolding protein AKAP79. J Biol Chem *277*, 33598–33603.

Andalib, P., Consiglio, J. F., Trapani, J. G., and Korn, S. J. (2004) The external TEA binding site and C-type inactivation in voltage-gated potassium channels. Biophys J *87*, 3148–3161.

Anderson, J. M. (1996) Cell signalling: MAGUK magic. Curr Biol *6*, 382-384.

Arcangeli, A., Bianchi, L., Becchetti, A., Faravelli, L., Coronnello, M., Mini, E., Olivotto, M., and Wanke, E. (1995) A novel inward-rectifying K+ current with a cell-cycle dependence governs the resting potential of mammalian neuroblastoma cells. J Physiol *489 (Pt 2)*, 455-471.

Arcangeli, A. and Becchetti, A. (2006) Complex functional interaction between integrin receptors and ion channels. Trends Cell Biol *16*, 631-639.

Arredondo, L., Nelson, H. B., Beckingham, K., and Stern, M. (1998) Increased transmitter release and aberrant synapse morphology in a Drosophila calmodulin mutant. Genetics *150*, 265–274.

Atkins, C. M., Davare, M. A., Oh, M. C., Derkach, V., and Soderling, T. R. (2005) Bidirectional regulation of cytoplasmic polyadenylation element-binding protein

hosphorylation by Ca2+/calmodulin-dependent protein kinase II and protein phosphatase 1 during hippocampal long-term potentiation. J Neurosci *25*, 5604-5610.

Augustine, G. J. (1990) Regulation of transmitter release at the squid giant synapse by presynaptic delayed rectifier potassium current. J Physiol *431*, 343-364.

Bading, H. (2000) Transcription-dependent neuronal plasticity. The nuclear calcium hypothesis. Eur J Biochem *267*, 5280-5283.

Baker, N. E. (2007) Patterning signals and proliferation in Drosophila imaginal discs. Curr Opin Genet Devel *17*, 287–293.

Barco, A., Bailey, C. H., and Kandel, E. R. (2006) Common molecular mechanisms in explicit and implicit memory. J Neurochem *97*, 1520-1533.

Barhanin, J., Lesage, F., Guillemare, E., Fink, M., Lazdunski, M., and Romey, G. (1996) KvLQT1 and IsK (minK) proteins associate to form the IKs cardiac potassium current. Nature *384*, 78-80.

Barria, A., et al. (1997) Regulatory phosphorylation of AMPA-type glutamate receptors by CaMKII during long-term potentiation. Science *276*, 2042-2045.

Barrionuevo, G., Schottler, F., and Lynch, G. (1980) The effects of repetitive low frequency stimulation on control and "potentiated" synaptic responses in the hippocampus. Life Sciences *27*, 2385-2391.

Bauer, C. K., and Schwarz, J. R. (2001) Physiology of EAG K+ channels. J Membr Biol *182*, 1-15.

Baumann, A., Frings, S., Godde, M., Seifert, R., and Kaupp, U. B. (1994) Primary structure and functional expression of a Drosophila cyclic nucleotide-gated channel present in eyes and antennae. EMBO J *13*, 5040-5050.

Bayer, K-U., De Koninck, P., Leonard, A. S., Hell, J. W., and Schulman, H. (2001) Interaction with the NMDA receptor locks CaMKII in an active conformation. Nature *411*, 801-805.

Beech, D. J. and Barnes, S. (1989) Characterization of a voltage-gated K+ channel that accelerates the rod response to dim light. Neuron *3*, 573-581.

Bhattacharjee, A. and Kaczmarek, L. K. (2005) For K+ channels, Na+ is the new Ca2+. Trends in Neurosci *28*, 423-428.

Bianchi, L., Wible, B., Arcangeli, A., Taglialatela, M., Morra, F., Castaldo, P., Crociani, O., Rosati, B., Faravelli, L., Olivotto, M., and Wanke, E. (1998) herg encodes a K+ current highly conserved in tumors of different histogenesis: a selective advantage for cancer cells? Cancer Res *58*, 815-822.

Bijlenga, P., Occhiodoro, T., Liu, J-H., Bader, C. R., Bernheim, L., and Fischer-Lougheed, J. (1998) An ether -`a-go-go K+ current, Ih-eag, contributes to the hyperpolarization of human fusion-competent myoblasts. J Physiol *512*, 317-323.

Bischofberger, J. and Jonas, P. (1997) Action potential propagation into the presynaptic dendrites of rat mitral cells. J Physiol *504*, 359-365.

Bliss, T. V. P. and Lømo, T. (1973) Long-lasting potentiation of synaptic transmission in the dentate area of the anaesthetized rabbit following stimulation of the perforant path. J Physiol *232*, 331-356.

Bolshakov, V. Y., Carboni, L., Cobb, M. H., Siegelbaum, S. A., and Belardetti, F. (2000) Dual MAP kinase pathways mediate opposing forms of long-term plasticity at CA3-CA1 synapses. Nat Neurosci *3*, 1107-1112.

Borg, J. P., Straight, S. W., Kaech, S. M., de Taddeo-Borg, M., Kroon, D. E., Karnak, D. Turner, R. S., Kim, S. K. and Margolis, B. (1998) Identification of an evolutionarily conserved heterotrimeric protein complex involved in protein targeting. J Biol Chem *273*, 31633-31636.

Brand, A. H. and Perrimon, N. (1993) Targeted gene expression as a means of altering cell fates and generating dominant phenotypes. Development *118*, 401-415.

Broadie, K., Rushton, E., Skoulakis, E. M., and Davis, R. L. (1997) Leonardo, a Drosophila 14-3-3 protein involved in learning, regulates presynaptic function. Neuron *19*, 391-402.

Broughton, B. J., Kitamoto, T., and Greenspan, R. J. (2004) Excitatory and inhibitory switches for courtship in the brain of Drosophila melanogaster. Curr Biol *14*, 538–547.

Bruggemann, A., Pardo, L. A., Stuhmer, W., and Pongs, O. (1993) Ether-a-go-go encodes a voltage-gated channel permeable to both K+ and Ca2+ and modulated by cAMP. Nature 365, 445-448.

Bruggemann, A., Stuhmer, W., and Pardo, L. A. (1997) Mitosis-promoting factor-mediated suppression of a cloned delayed rectifier potassium channel expressed in Xenopus oocytes. Proc Natl Acad Sci U S A *94*, 537-542.

Butz, S., Okamoto, M., and Sudhof, T. C. (1998) A tripartite protein complex with the potential to couple synaptic vesicle exocytosis to cell adhesion in brain. Cell *94*, 773-782.

Budnik, V., Zhong, Y. and Wu, C-F. (1990) Morphological plasticity of motor axons in Drosophila mutants with altered excitability. J Neurosci *10*, 3754-3766.

Budnik, V. (1996) Synapse maturation and structural plasticity at Drosophila neuromuscular junctions. Curr Opin Neurobiol *6*, 858-867.

Cahalan, M. D., Wulff, H., and Chandy, K. G. (2001) Molecular properties and physiological roles of ion channels in the immune system. J Clin Immunol *21*, 235-252.

Camacho, J., Sanchez, A., Stuhmer, W., and Pardo, L. A. (2000) Cytoskeletal interactions determine the electrophysiological properties of human EAG potassium channels. Pflugers Arch *441*, 167-174.

Carlson, J. R. (1996) Olfaction in Drosophila: from odor to behavior. Trends Genet *12*, 175-180.

Catterall, W. A. (2000) Structure and regulation of voltage-gated Ca2+ channels. Annu Rev Cell Dev Biol *16*, 521-555.

Chandy, G. K., Wulff, H., Beeton, C., Pennington, M., Gutman, G. A., and Cahalan, M. D. (2004) K+ channels as targets for specific immunomodulation. Trends Pharmacol Sci *25*, 280-289.

Chapman, P. F., Frenguelli, B. G., Smith, A., Chen, C-M. and Silva, A. J. (1995) The α-Ca2+/calmodulin kinase II: A bidirectional modulator of presynaptic plasticity. Neuron *14*, 591-597.

Chen, M. L., Hoshi, T., and Wu, C. F. (1996) Heteromultimeric interactions among K+ channel subunits from Shaker and eag families in Xenopus oocytes. Neuron *17*, 535–542.

Chen, C., Corbley, M. J., Roberts, T. M., and Hess, P. (1988) Voltage-sensitive calcium channels in normal and transformed 3T3 fibroblasts. Science *239*, 1024-1026.

Cherubini, A., Taddei, G. L., Crociani, O., Paglierani, M., Buccoliero, A. M., Fontana, L., Noci, I., Borri, P., Borrani, E., Giachi, M., *et al.* (2000) HERG potassium channels are more frequently expressed in human endometrial cancer as compared to non-cancerous endometrium. Br J Cancer *83*, 1722-1729.

Chetkovich, D. M., Gray, R., Johnston, D., and Sweatt, J. D. (1991) N-methyl-D-aspartate receptor activation increases cAMP levels and voltage-gated Ca2+ channel activity in area CA1 of hippocampus. Proc Natl Acad Sci USA *88*, 6467-6471.

Cheung, U. S., Shayan, A. J., Boulianne, G. L., and Atwood, H. L. (1999) Drosophila larval neuromuscular junction's responses to reduction of cAMP in the nervous system. J Neurobiol 40, 1-13.

Cheung, U., Atwood, H. L., and Zucker, R. S. (2006) Presynaptic effectors contributing to cAMP-induced synaptic potentiation in Drosophila. J Neurobiol *66*, 273-280.

Chin, D. and Means, A. R. (2000) Calmodulin: a prototypical calcium sensor. Trends Cell Biol *10*, 322-328.

Cho, S. Y., Beckett, E. A., Baker, S. A., Han, I., Park, K. J., Monaghan, K., Ward, S. M., Sanders, K. M., and Koh, S D. (2005) A pH-snsitive potassium conductance (TASK) and its function in the murine gastrointestinal tract. J Physiol *565*, 243-259.

Chouinard, S. W., Wilson, G. F., Schlimgen, A. K., and Ganetzky, B. (1995) A potassium channel beta subunit related to the aldo-keto reductase superfamily is encoded by the Drosophila hyperkinetic locus. Proc Natl Acad Sci U S A *92*, 6763-6767.

Chung, S. K., Reinhart, P. H., Martin, B. L., Brautigan, D., and Levitan, I. B. (1991) Protein kinase activity closely associated with a reconstituted calcium-activated potassium channel. Science *253*, 560-562.

Cloues, R. K. and Sather, W. A. (2003) Afterhyperpolarization regulates firing rate in neurons of the suprachiasmatic nucleus. J Neurosci *23*, 1593–1604.

Cohen, A. R., Woods, D. F., Marfatia, S. M., Walther, Z., Chishti, A. H., and Anderson, J. M. (1998) Human CASK/LIN-2 binds syndecan-2 and protein 4.1 and localizes to the basolateral membrane of epithelial cells. J Cell Biol *142*, 129–138.

Colbert, C. M. and Pan, E. (2002) Ion channel properties underlying axonal action potential initiation in pyramidal neurons. Nat Neurosci *5*, 533-538.

Colbran, R. J. (2004) Protein phosphatases and calcium/calmodulin-dependent protein kinase II-Dependent synaptic plasticity. J Neurosci *24*, 8404-8409.

Cole, K. S., and Curtis, H. J. (1939) Electrical impedance of the squid giant axon during activity. J Gen Physiol *22*, 37-64.

Cole, K. and Hodgkin, A. (1939) Membrane and protoplasm resistance in the squid giant axon. J Gen Physiol *22*, 671-687.

Cole, K. S., and Moore, J. W. (1960) Potassium ion current in the squid giant axon: dynamic characteristic. Biophys J *1*, 1-14.

Connor, J. A. and Stevens, C. F. (1971) Voltage clamp studies of a transient outward membrane current in gastropod neural somata. J Physiol *213*, 21-30.

Cox, J.A., Durussel, I., Comte, M., Nef, S., Nef, P., Lenz, S. E., and Gundelfinger, E.D. (1994) Cation binding and conformational changes in VILIP and NCS-1, two neuron-specific calcium-binding proteins. J Biol Chem *269*, 32807-32813.

Crews, S. T., and Fan, C. M. (1999) Remembrance of things PAS: regulation of development by bHLH-PAS proteins. Curr Opin Genet Dev *9*, 580-587.

Crociani, O., Guasti, L., Balzi, M., Becchetti, A., Wanke, E., Olivotto, M., Wymore, R. S., and Arcangeli, A. (2003) Cell cycle-dependent expression of HERG1 and HERG1B isoforms in tumor cells. J Biol Chem *278*, 2947-2955.

Crouch, J. J., Sakaguchi, N., Lytle, C., and Schulte, B. A. (1997) Immunohistochemical localization of the Na–K–Cl co-transporter (NKCC1) in the gerbil inner ear. J Histochem and Cytochem *45*, 773–778.

Cui, J., Melman, Y., Palma, E., Fishman, G. I., and McDonald, T. V. (2000) Cyclic AMP regulates the HERG K+ channel by dual pathways. Current Biology *10*, 671–674.

Curran, M. E., Splawski, I., Timothy, K. W., Vincent, G. M., Green, E. D., and Keating, M. T. (1995) A molecular basis for cardiac arrhythmia: HERG mutations cause long QT syndrome. Cell *80*, 795-803.

Davis, G. W. and Bezprozvanny, I. (2001) Maintaining the stability of neural function: A homeostatic hypothesis. Annu Rev Physiol *63*, 847-869.

Davis, G. W. (2006) Homeostatic control of neural activity: From phenomenology to molecular design. Annu Rev Neurosci *29*, 307–323.

Deal, K. K., Lovinger, D. M., and Tamkun, M. M. (1994) The brain Kvl.1 potassium channel: in vitro and in vivo studies on subunit assembly and posttranslational processing. J Neurosci *14*, 1666-l676.

DeCoursey, T. E., Chandy, K. G., Gupta, S., and Cahalan, M. D. (1984) Voltage-gated K+ channels in human T lymphocytes: a role in mitogenesis? Nature *307*, 465-468.

Deisseroth, K., Heist, E. K., and Tsien, R. W. (1998) Translocation of calmodulin to the nucleus supports CREB phosphorylation in hippocampal neurons. Nature *392*, 198-202.

Delaney, K. R. and Tank, D. W. (1994) A quantitative measurement of the dependence of short-term synaptic enhancement on presynaptic residual calcium. J Neurosci *14*, 5885-5902.

Delgado, R., Latorre, R., and Labarca, P. (1994) Shaker mutants lack post-tetanic potentiation at motor end-plates. Eur J Neurosci *6*, 1160-1166.

Delgado. R., Maureira, C., Oliva, C., Kidokoro, Y., and Labarca, P. (2000) Size of vesicle pools, rates of mobilization, and recycling at neuromuscular synapses of a Drosophila mutant, shibire. Neuron *28*, 941-953.

DeMaria, C. D., Soong, T. W., Alseikhan, B. A., Alvania, R. S., and Yue, D. T. (2001) Calmodulin bifurcates the local Ca2+ signal that modulates P/Q-type Ca2+ channels. Nature *411*, 484-489.

Demo, S. D. and Yellen, G. (1991) The inactivation gate of the Shaker K+ channel behaves like an open-channel blocker. Neuron *7*, 743-753.

Dhanasekaran, D. N., Kashef, K., Lee, C. M., Xu, H., and Reddy, E. P. (2007) Scaffold proteins of MAP-kinase modules. Oncogene *26*, 3185–3202.

Dimitratos, S. D., Woods, D. F., and Bryant, P. J. (1997) Camguk, Lin-2, and CASK: novel membrane-associated guanylate kinase homologs that also contain CaM kinase domains. Mechanisms of Development *63*, 127-130.

Dineley, K. T., Weeber, E. J., Atkins, C., Adams, J. P., Anderson, A. E., and Sweatt, J. D. (2001) Leitmotifs in the biochemistry of LTP induction: amplification, integration and coordination. J Neurochem *77*, 961-971.

Dolmetsch, R. E., Pajvani, U., Fife, K., Spotts, J. M., and Greenberg, M. E. (2001) Signaling to the nucleus by an L-type calcium channel-calmodulin complex through the MAP kinase pathway. Science *294*, 333-339.

Doyle, D. A., Morais Cabral, J., Pfuetzner, R. A., Kuo, A., Gulbis, J. M., Cohen, S. L., Chait, B. T., and MacKinnon, R. (1998) The structure of the potassium channel: molecular basis of K+ conduction and selectivity. Science *280*, 69-77.

Drysdale, R., Warmke, J., Kreber, R., and Ganetzky, B. (1991) Molecular characterization of eag: a gene affecting potassium channels in Drosophila melanogaster. Genetics *127*, 497-505.

Dubin, A. E., Liles, M. M., and Harris, G. L. (1998) The K+ channel gene ether a go-go is required for the transduction of a subset of odorants in adult Drosophila melanogaster. J Neurosci *18*, 5603-5613.

Engel, J. E. and Wu, C-F. (1996) Altered habituation of an identified escape circuit in *Drosophila* memory mutants. JNeurosci *16*, 3486–3499.

Engel, J. E., and Wu, C. F. (1998) Genetic dissection of functional contributions of specific potassium channel subunits in habituation of an escape circuit in Drosophila. J Neurosci *18*, 2254-2267.

Engeland, B., Neu, A., Ludwig, J., Roeper, J., and Pongs, O. (1998) Cloning and functional expression of rat ether-a-go-go-like K+ channel genes. J Physiol *513 (Pt 3)*, 647-654.

Epstein, D. J., Martinu, L., Michaud, J. L., Losos, K.M., Fan, C-M., and Joyner, A. L. (2000) Members of the bHLH-PAS family regulate Shh transcription in forebrain regions of the mouse CNS. Development *127*, 4701-4709.

Erickson, M. G., Alseikhan, B. A., Peterson, B. Z., and Yue, D. T. (2001) Preassociation of calmodulin with voltage-gated Ca(2+) channels revealed by FRET in single living cells. Neuron *31*, 973-985.

Erickson, M. G., Liang, H., Mori, M. X., Yue, and D. T. (2003) FRET two-hybrid mapping reveals function and location of L-type Ca2+ channel CaM preassociation. Neuron *39*, 97-107.

Fanger, C. M., Ghanshani, S., Logsdon, N. J., Rauer, H., Kalman, K., Zhou, J., Beckingham, K., Chandy, K. G., Cahalan, M. D., and Aiyar, J. (1999) Calmodulin mediates calcium-dependent activation of the intermediate conductance KCa channel, IKCa1. J Biol Chem *274*, 5746-5754.

Farias, L. M., Ocana, D. B., Diaz, L., Larrea, F., Avila-Chavez, E., Cadena, A., Hinojosa, L. M., Lara, G., Villanueva, L. A., Vargas, C.*, et al.* (2004) Ether a go-go potassium channels as human cervical cancer markers. Cancer Res *64*, 6996-7001.

Felmy, F., Neher, E., and Schneggenburger, R. (2003) Probing the intracellular calcium sensitivity of transmitter release during synaptic facilitation. Neuron *37*, 801-811.

Ficker, E., Jarolimek, W., and Brown, A. M. (2001) Molecular determinants of inactivation and dofetilide block in ether a-go-go (EAG) channels and EAG-related K+ channels. Mol Pharmacol *60*:1343–1348.

Firestein, S., Zufall, F., and Shepherd, G. M. (1991) Single odor-sensitive channels in olfactory receptor neurons are also gated by cyclic nucleotides. J Neurosci *77*, 3565-3572.

Fong, Y. L. and Soderling, T.R. (1990) Studies on the regulatory domain of Ca2+/calmodulin-dependent protein kinase II. Functional analyses of arginine 283 using synthetic inhibitory peptides and site-directed mutagenesis of the αsubunit. J Biol Chem *265*, 11091-11097.

Ford, M. G. J., Mills, I. G., Peter, B. J., Vallis, Y., Praefcke, G. J. K., Evans, P. R., and McMahon, H. T. (2002) Curvature of clathrin-coated pits driven by epsin. Nature *419*, 361-366.

Frank, A. C., Kennedy, M. J., Goold, C. P., Marek, K. W., and Davis, G. W. (2006) Mechanisms underlying the rapid induction and sustained expression of synaptic homeostasis. Neuron *52*, 663-677.

Freedman, B. D., Price, M. A., and Deutsch, C. J. (1992) Evidence for voltage modulation of IL-2 production in mitogen-stimulated human peripheral blood lymphocytes. J Immunol *149*, 3784-3794.

Frings, S., Brull, N., Dzeja, C., Angele, A., Hagen, V., Kaupp, U. B., and Baumann, A. (1998) Characterization of ether-a-go-go channels present in photoreceptors reveals similarity to IKx, a K+ current in rod inner segments. J Gen Physiol *111*, 583-599.

Fu, H., Xia, K., Pallas, D. C. Cui, C., Conroy, K., Narsimhan, R. P., Mamon, H., Collier, R. J., and Roberts. T. M. (1994) Interaction of the protein kinase Raf-1 with 14-3-3 proteins. Science *266*, 126-129.

Gamper, N. and Shapiro, M. S. (2003) Calmodulin mediates Ca2+-dependent modulation of M-type K+ channels. J Gen Physiol *122*, 17–31.

Gamper, N., Li, Y., and Shapiro, M. S. (2005) Structural requirements for differential sensitivity of KCNQ K+ channels to modulation by Ca2+/calmodulin. Mol Biol Cell *16*, 3538-3551.

Ganetzky, B., Robertson, G. A., Wilson, G. F., Trudeau, M. C., and Titus, S. A. (1999) The eag family of K+ channels in Drosophila and mammals. Ann N Y Acad Sci *868*, 356-369.

Ganetzky, B., and Wu, C. F. (1983) Neurogenetic analysis of potassium currents in Drosophila: synergistic effects on neuromuscular transmission in double mutants. J Neurogenet *1*, 17-28.

Ganetzky, B., and Wu, C. F. (1985) Genes and membrane excitability in *Drosophila*. Trends Neurosci *8*, 322-326.

Garcia, E. P., Mehta, S., Blair, L. A., Wells, D. G., Shang, J., Fukushima, T., Fallon, J. R., Garner, C. C., and Marshall, J. (1998) SAP90 binds and clusters kainate receptors causing incomplete desensitization. Neuron *21*, 727-739.

Garcia-Ferreiro, R. E., Kerschensteiner, D., Major, F., Monje, F., Stuhmer, W., and Pardo, L. A. (2004) Mechanism of block of hEag1 K+ channels by imipramine and astemizole. J Gen Physiol *124*, 301-317.

Gasque, G., Labarca, P., Delgado, R., and Darszon, A. (2006) Bridging behavior and physiology: Ion-channel perspective on mushroom body-dependent olfactory learning and memory in Drosophila. J Cell Physiol *209*, 1046-1053.

Gavrilova-Ruch, O., Schonherr, K., Gessner, G., Schonherr, R., Klapperstuck, T., Wohlrab, W., and Heinemann, S. H. (2002) Effects of imipramine on ion channels and proliferation of IGR1 melanoma cells. J Membrane Biol *188*, 137-149.

Gessner, G., Zacharias, M., Bechstedt, S., Schonherr, R., and Heinemann, S. H. (2004) Molecular determinants for high-affinity block of human EAG potassium channels by antiarrhythmic agents. Mol Pharmacol *65*, 1120–1129.

Gessner, G. and Heinemann, S. H. (2003) Inhibition of hEAG1 and hERG1 potassium channels by clofilium and its tertiary analogue LY97241. Brit J Pharmacol *138*, 161-171.

Girard, S., and Clapham, D. (1993) Acceleration of intracellular calcium waves in Xenopus oocytes by calcium influx. Science *260*, 229-232.

Goldstein, S. A., Bockenhauer, D., O'Kelly, I. and Zilberberg, N. (2001) Potassium leak channels and the KCNK family of two-P-domain subunit. Nature Rev Neurosci *2*, 176-184.

Gomez-Ospina, N., Tsuruta, F., Barreto-Chang, O., Hu, L., and Dolmetsch, R. (2006) The C terminus of the L-type voltage-gated calcium channel Ca(V)1.2 encodes a transcription factor. Cell *127*, 591-606.

Gomez-Varela, D. de la Pena, P. Garcia, J. Giraldez, T. Barros, F. (2002) Influence of amino-terminal structures on kinetic transitions between several closed and open states in human erg K+ channels. J Membrane Biol *187*, 117-133.

Gomis, A., Burrone, J., and Lagnado, L. (1999) Two actions of calcium regulate the supply of releasable vesicles at the ribbon synapse of retinal bipolar cells. J Neurosci *19*, 6309–6317.

Griffith, L. C., Verselis, L. M., Aitken, K. M., Kyriacou, C. P., Danho, W., and Greenspan, R. J. (1993). Inhibition of calcium/calmodulin-dependent protein kinase in Drosophila disrupts behavioral plasticity. Neuron *10*, 501-509.

Griffith, L. C., Wang, J., Zhong, Y., Wu, C. F., and Greenspan, R. J. (1994) Calcium/calmodulin-dependent protein kinase II and potassium channel subunit eag similarly affect plasticity in Drosophila. Proc Natl Acad Sci U S A *91*, 10044-10048.

Griffith, L. C. (2004a) Calcium/calmodulin-dependent protein kinase II: An unforgettable kinase. J Neurosci *24*, 8391-8393.

Griffith, L. C. (2004b) Regulation of calcium/calmodulin-dependent protein kinase II activation by intramolecular and intermolecular interactions. J Neurosci *24*, 8394-8398.

Guan, Z., Kim, J. H., Lomvardas, S., Holick, K., Xu, S., Kandel, E. R., and Schwartz, J. H. (2003) p38 MAP kinase mediates both short-term and long-term synaptic depression in aplysia. J Neurosci *23*, 7317-7325.

Guillemin, K., and Krasnow, M. A. (1997) The hypoxic response: huffing and HIFing. Cell *89*, 9-12.

Guo, T. B., Lu, J., Li, T., Lu, Z., Xu, G., Xu, M., Lu, L., and Dai, W. (2005) Insulin-activated, K+-channel-sensitive Akt pathway is primary mediator of ML-1 cell proliferation. Am J Physiol Cell Physiol 289, C257-C263.

Guo, H-F. and Zhong, Y. (2006) Requirement of akt to mediate long-term synaptic depression in Drosophila. J Neurosci *26*, 4004–4014.

GuptaRoy, B. and Griffith, L. C. (1996) Functional heterogeneity of alternatively spliced isoforms of Drosophila Ca2+/calmodulin-dependent protein kinase II. J Neurochem *66*, 1282-1288.

Gutman, G. A. (2005) International Union of Pharmacology. LIII. Nomenclature and molecular relationships of voltage-gated potassium channels. Pharmacol Rev *57*,473–508

Guy, H. R., Durell, S. R., Warmke, J., Drysdale, R., and Ganetzky, B. (1991) Similarities in amino acid sequences of Drosophila eag and cyclic nucleotide-gated channels. Science *254*, 730.

Hanks, S. K., Quinn, A. M., and Hunter, T. (1988) The protein kinase family: conserved features and deduced phylogeny of the catalytic domains. Science *241*, 42-52.

Hanoune, J. and Defer, N. (2001) Regulation and role of adenylyl cyclase isoforms. Annu Rev Pharmacol Toxicol *41*, 145–174.

Hansel, C., de Jeu, M., Belmeguenai, A., Houtman, S. H., Buitendijk, G. H. S., Andreev, D., De Zeeuw, C. I., and Elgersma, Y. (2006) αCaMKII is essential for cerebellar LTD and motor learning. Neuron *51*, 835–843.

Hao, H-X., Cardon, C. M., Swiatek, W., Cooksey, R. C., Smith, T. L., Wilde, J., Boudina, S., Abel E. D., McClain, D. A., and Rutter, J. (2007) PAS kinase is required for normal cellular energy balance. Proc Natl Acad Sci USA *104*, 15466-15471.

Hardingham, G. E., and Bading, H. (2003) The Yin and Yang of NMDA receptor signalling. Trends Neurosci *26*, 81-89.

Harkiolaki, M., Lewitzky, M., Gilbert, R. J., Jones, E. Y., Bourette, R. P., Mouchiroud, G., Sondermann, H., Moarefi, I., and Feller, S. M. (2003) Structural basis for SH3 domain-mediated high-affinity binding between Mona/Gads and SLP-76. EMBO Journal *22*, 2571-2582.

Hata, Y., Butz, S., and Sudhof, T. C. (1996) CASK: a novel dlg/PSD95 homolog with an N-terminal calmodulin-dependent protein kinase domain identified by interaction with neurexins. Journal of Neuroscience *16*, 2488-2494.

Hausser, M., Stuart, G., Racca, C., and Sakmann, B. (1995) Axonal initiation and active dendritic propagation of action potentials in substantia nigra neurons. Neuron *15*, 637-647.

Hebb, D.O. (1949) The organization of behavior. (New York, Wiley)

Heginbotham, L., Lu, Z., Abramson, T., and MacKinnon, R. (1994) Mutations in the K+ channel signature sequence. Biophys J *66*, 1061-1067.

Hegle, A. P., Marble, D. D., and Wilson, G. F. (2006) A voltage-driven switch for ion-independent signaling by ether-a-go-go K+ channels. Proc Natl Acad Sci U S A *103*, 2886-2891.

Hegle, A. P., Marble, D. D., and Wilson, G. F. (submitted) A CaMKII binding domain underlies voltage-dependent conductance-independent signaling by EAG potassium channels.

Heiman, R. G., Atkinson, R. C., Andruss, B. F., Bolduc, C., Kovalick, G. E., and Beckingham, K. (1996) Spontaneous avoidance behavior in Drosophila null for calmodulin expression. Proc Natl Acad Sci U S A *93*, 2420-2425.

Hill, A. P., Sunde, M., Campbell, T. J., and Vandenberg, J. I. (2007) Mechanism of block of the hERG K+ channel by the scorpion toxin CnErg1. Biophys J *92*, 3915–3929.

Hille, B. (2001) Ion channels of excitable membranes, 3rd edn (Sunderland, MA, Sinauer Associates).

Hoffman, D. A., Magee, J. C., Colbert, C. M., and Johnston, D. (1997) K+ channel regulation of signal propagation in dendrites of hippocampal pyramidal neurons. Nature *387*, 869-875.

Hopkins, W. F., Demas, V., and Tempel, B. L. (1994) Both N- and C-terminal regions contribute to the assembly and functional expression of homo- and heteromultimeric voltage-gated K+ channels. J Neurosci *14*, 1385-1393.

Hoshi, T., Zagotta, W. N., and Aldrich, R. W. (1990) Biophysical and molecular mechanisms of Shaker potassium channel inactivation. Science *250*, 533-538.

Hoshi, N., Takahashi, H., Shahidullah, M., Yokoyama, S., and Higashida, H. (1998) KCR1, a membrane protein that facilitates functional expression of non-inactivating K+ currents associates with rat EAG voltage-dependent K+ channels. J Biol Chem *273*, 23080–23085.

Hoskins, R., Hajnal, A. F., Harp, S. A., and Kim, S. K. (1996) The C. elegans vulval induction gene lin-2 encodes a member of the MAGUK family of cell junction proteins. Development *122*, 97-111.

Hsueh, Y. P., Wang, T. F., Yang, F. C., and Sheng, M. (2000) Nuclear translocation and transcription regulation by the membrane-associated guanylate kinase CASK/LIN-2. Nature *404*, 298-302.

Hsueh, Y-P. (2006) The role of the MAGUK protein CASK in neural development and synaptic function. Curr Med Chem *13*, 1915-1927.

Hudmon, A. and Schulman, H. (2002) Neuronal Ca^{2+}/calmodulin dependent protein kinase II: Role of structure and autoregulation in cellular function. Ann Rev Biochem *71*, 473-510.

Hurd, D. D., Sternt, M., and Saxton, W. M. (1996) Mutation of the axonal transport motor kinesin enhances paralytic and suppresses Shaker in Drosophila. Genetics *142*, 195-204.

Hunter, T. (2000) Signaling-2000 and beyond. Cell *100*, 113-127.

Ikeda, S. R., and Kammermeier, P.J. (2002) M current mystery messenger revealed? Neuron *35*, 411-412.

Irie, M., Hata, Y., Deguchi, M., Ide, N., Hirao, K., Yao, I., Nishioka, H., and Takai, Y. (1999) Isolation and characterization of mammalian homologues of Caenorhabditis elegans lin-7: localization at cell-cell junctions. Oncogene *18*, 2811-2817.

Iverson, L. E., Tanouye, M. A., Lester, H. A., Davidson, N., and Rudy, B. (1988) A-type potassium channels expressed from Shaker locus cDNA. Proc Natl Acad Sci USA *85*, 5723-5727.

Jackson, M. B., Konnerth, A., and Augustine, G. J. (1991) Action potential broadening and frequency-dependent facilitation of calcium signals in pituitary nerve terminals. Proc Natl Acad Sci U S A *88*, 380-384.

Jacob, L. and Lum, L. (2007) Hedgehog signaling pathway in Drosophila. Science Stke *407*, cm6.

James, P., Vorherr, T., and Carafoli, E. (1995) Calmodulin-binding domains: just two faced or multi-faceted? Trends Biochem Sci *20*, 38-42.

Jan, L. Y. and Jan, Y. N. (1978) Genetic dissection of short-term and long-term facilitation at the Drosophila neuromuscular junction. Proc Natl Acad Sci U S A *75*, 515-519.

Jaramillo, A. M., Zheng, X., Zhou, Y., Amado, D. A., Sheldon, A., Sehgal, A., and Levitan, I. B. (2004) Pattern of distribution and cycling of SLOB, Slowpoke channel binding protein, in Drosophila. BMC Neurosci *5*, 3.

Jeng, C. J., Chang, C. C., and Tang, C. Y. (2005) Differential localization of rat Eag1 and Eag2 K+ channels in hippocampal neurons. Neuroreport *16*, 229-233.

Jiang, Y., Lee, A., Chen, J., Cadene, M., Chait, B. T., and Mackinnon, R. (2002) The open pore conformation of potassium channels. Nature 417, 523-526.

Kaczmarek, L. K. (2006) Non-conducting functions of voltage-gated ion channels. Nat Rev Neurosci *7*, 761-771.

Kaech, S. M., Whitfield, C. W., and Kim, S. K. (1998) The LIN-2/LIN-7/LIN-10 complex mediates basolateral membrane localization of the C. elegans EGF receptor LET-23 in vulval epithelial cells. Cell *94*, 761-771.

Kandel, E. R. and Schwartz, J. H. (1982) Molecular biology of learning: Modulation of transmitter release. Science *218*, 433-443.

Kandel E. eds. (2000) Principles of Neuroscience, 4th Ed. (New York, McGraw-Hill)

Kaplan, W. D., and Trout, W. E., 3rd (1969) The behavior of four neurological mutants of Drosophila. Genetics *61*, 399-409.

Karim, F. D., and Rubin, G. M. (1998) Ectopic expression of activated Ras1 induces hyperplastic growth and increased cell death in Drosophila imaginal tissues. Development *125*, 1-9.

Keen, J. E., Khawaled, R., Farrens, D. L., Neelands, T., Rivard, A., Bond, C. T., Janowsky, A., Fakler, B., Adelman, J. P., and Maylie, J. (1999) Domains responsible for constitutive and Ca(2+)-dependent interactions between calmodulin and small conductance Ca(2+)-activated potassium channels. J Neurosci *19*, 8830-8838.

Kidokoro, Y., Kuromi, H., Delgado, R., Maureira, C., Oliva, C., and Labarca, P. (2004) Synaptic vesicle pools and plasticity of synaptic transmission at the Drosophila synapse. Brain Res Rev *47*, 18-32.

Kim, E., Niethammer, M., Rothschild, A., Jan, Y. N., and Sheng, M. (1995) Clustering of Shaker-type K+ channels by interaction with a family of membrane-associated guanylate kinases. Nature *378*, 85-88.

Kim, E. and Sheng, M. (2004) PDZ domain proteins of synapses. Nature Rev Neurosci *5*, 771-781.

Klauck, T. M., Faux, M. C., Labudda, K., Langeberg, L. K. Jaken, S., Scott, J. D. (1996) Coordination of three signaling enzymes by AKAP79, a mammalian scaffold protein. Science *271*, 1589-1592.

Klyachko, V. A., Ahern, G. P., and Jackson, M. B. (2001) cGMP-mediated facilitation in nerve terminals by enhancement of the spike afterhyperpolarization. Neuron *31*, 1015-1025.

Knebel, A. (2003) Protein kinases as drug targets. Trends Drug Discov *4*, 60-62.

Krapivinsky, G., Medina, I., Krapivinsky, L., Gapon, S., and Clapham, D. E. (2004) SynGAP-MUPP1-CaMKII synaptic complexes regulate p38 MAP kinase activity and NMDA receptor-dependent synaptic AMPA receptor potentiation. Neuron *43*, 563-574.

Krasne, F. B. and Teshiba, T. M. (1995) Habituation of an invertebrate escape reflex due to modulation by higher centers rather than local events. Proc Natl Acad Sci USA *92*, 3362-3366.

Kubo, Y. et al., (2005) International Union of Pharmacology. LIV. Nomenclature and molecular relationships of inwardly rectifying potassium channels. Pharmacol Rev *57*, 509–526.

Kupershmidt, S., Yang, I. C-H., Hayashi, K., Wei, J., Chanthaphaychith, S., Petersen, C. I., Johns, D. C., George, A. L., Roden, D. M., Balser, J. R. (2003) The IKr drug response is modulated by KCR1 in transfected cardiac and noncardiac cell lines. FASEB J *17*, 2263-2265.

Lastraioli, E., Guasti, L., Crociani, O., Polvani, S., Hofmann, G., Witchel, H., Bencini, L., Calistri, M., Messerini, L., Scatizzi, M., *et al.* (2004) herg1 gene and HERG1 protein are overexpressed in colorectal cancers and regulate cell invasion of tumor cells. Cancer Res *64*, 606-611.

Laverty, H. G. and Wilson, J. B. (1998) Murine CASK is disrupted in a sex-linked cleft palate mouse mutant. Genomics *53*, 29-41.

LeBoeuf, B., Gruninger, T. R., and Garcia, L. R. (2007) Food deprivation attenuates seizures through CaMKII and EAG K+ channels. PLoS Genetics *3*, 1622-1632.

Lecain, E., Sauvaget, E., Crisanti, P., Van Den Abbeele, T., and Huy, P. T. (1999) Potassium channel ether a go-go mRNA expression in the spiral ligament of the rat. Hear Res *133*, 133-138.

Lechleiter, J. D., and Clapham, D.E. (1992) Molecular mechanisms of intracellular calcium excitability in X. laevis oocytes. Cell *69*, 283-294.

Lee, A., Wong, S. T., Gallagher, D., Li, B., Storm, D. R., Scheuer, T., and Catterall, W. A. (1999) Ca2+/calmodulin binds to and modulates P/Q-type calcium channels. Nature *399*, 157-159.

Levitan, I. B. (1999) It is calmodulin after all! Mediator of the calcium modulation of multiple ion channels. Neuron *22*, 645-648.

Levitan, I. B. (2006) Signaling protein complexes associated with neuronal ion channels. Nat Neurosci *9*, 305-310.

Lewis, R. S., and Cahalan, M. D. (1995) Potassium and calcium channels in lymphocytes. Annu Rev Immunol *13*, 623-653.

Li, M., Jan, Y-N., and Jan, L. Y. (1992) Specification of subunit assembly by the hydrophilic amino-terminal domain of the Shaker potassium channel. Science *257*, 1225-1230.

Lin, C. S., Boltz, R. C., Blake, J. T., Nguyen, M., Talento, A., Fischer, P. A., Springer, M. S., Sigal, N. H., Slaughter, R. S., Garcia, M. L., and et al. (1993) Voltage-gated

potassium channels regulate calcium-dependent pathways involved in human T lymphocyte activation. J Exp Med *177*, 637-645.

Lisman, J. and Raghavachari, S. (2006) A unified model of the presynaptic and postsynaptic changes during LTP at CA1 synapses. Science Stke *356*, 11.

Littleton, J. T. and Ganetzky B. (2000) Ion channels and synaptic viewpoint organization: analysis of the *Drosophila* genome. Neuron *26*, 35-43.

Lisman, J., Schulman, H., and Cline, H. (2002) The molecular basis of CaMKII function in synaptic and behavioural memory. Nat Rev Neurosci *3*:175-190.

Liu, J-H., Bijlenga, P., Fischer-Lougheed, J., Occhiodoro, T., Kaelin, A., Bader, C. R., and Bernheim, L. (1998) Role of an inward rectifier K+ current and of hyperpolarization in human myoblast fusion. J Physiol *510*, 467-476.

Liu, Q., Berry, D., Nash, P., Pawson, T., McGlade, C. J., and Li, S. S. (2003) Structural basis for specific binding of the Gads SH3 domain to an RxxK motif-containing SLP-76 peptide: a novel mode of peptide recognition. Molecular Cell *11*, 471-481.

Lnenicka, G. A., Grizzaffi, J., Lee, B., and Rumpal, N. (2006) Ca2+ dynamics along identified synaptic terminals in Drosophila larvae. J Neurosci *26*, 12283–12293.

Long, S. B., Campbell, E. B., and MacKinnon, R. (2005a) Crystal structure of a mammalian voltage-dependent Shaker family K+ channel. Science *309*, 897-903.

Long, S. B., Campbell, E. B., and MacKinnon, R. (2005b) Voltage sensor of Kv1.2: structural basis of electromechanical coupling. Science *309*, 903-908.

Lu, C. S., Hodge, J. J., Mehren, J., Sun, X. X., and Griffith, L. C. (2003) Regulation of the Ca2+/CaM-responsive pool of CaMKII by scaffold-dependent autophosphorylation. Neuron *40*, 1185-1197.

Ludwig, J., Terlau, H., Wunder, F., Bruggemann, A., Pardo, L. A., Marquardt, A., Stuhmer, W., and Pongs, O. (1994) Functional expression of a rat homologue of the voltage gated either a go-go potassium channel reveals differences in selectivity and activation kinetics between the Drosophila channel and its mammalian counterpart. Embo J *13*, 4451-4458.

Ludwig, J., Owen, D., and Pongs, O. (1997) Carboxy-terminal domain mediates assembly of the voltage-gated rat ether-a` -go-go potassium channel. EMBO J *16*, 6337–6345.

Ludwig, J., Weseloh, R., Karschin, C., Liu, Q., Netzer, R., Engeland, B., Stansfeld, C. and Pongs, O. (2000) Cloning and functional expression of rat eag2, a new member of the Ether-a` -go-go family of potassium channels and comparison of its distribution with that of eag1. Molec Cell Neurosci *16*, 59-70.

Lüscher, C., Nicoll, R. A., Malenka, R. C., and Muller, D. (2000) Synaptic plasticity and dynamic modulation of the postsynaptic membrane. Nat Neurosci *3*, 545-550.

Lynch, G. S., Dunwiddie, T., and Gribkoff, V. (1977) Heterosynaptic depression: a postsynaptic correlate of long-term potentiation. Nature *266*, 737-739.

MacKinnon, R. and Yellen, G. (1990) Mutations affecting TEA blockade and ion permeation in voltage-activated K+ channels. Science *250*, 276-279.

MacLean, J. N., Zhang, Y., Johnson, B. R., and Harris-Warrick, R. M. (2003) Activity-independent homeostasis in rhythmically active neurons. Neuron *37*, 109-120.

Macleod, G. T., Hegstrom-Wojtowicz, M., Charlton, M. P., and Atwood, H. L. (2002) Fast calcium signals in Drosophila motor neuron terminals. J Neurophysiol *88*, 2659-2663.

Maffai, A., Nelson, S. B., and Turrigiano, G. G. (2004) Selective reconfiguration of layer 4 visual cortical circuitry by visual deprivation. Nature Neurosci *7*, 1353-1359.

Malenka, R. C., Kauer, J. A., Perkel, D. J., Mauk, M. D., Kelly, P. T., Nicoll, R. A., and Waxham, M. N. (1989) An essential role for postsynaptic calmodulin and protein kinase activity in long-term potentiation. Nature *230*, 554-557.

Malenka, R. C. and Bear, M. F. (2004) LTP and LTD: An embarrassment of riches. Neuron *44*, 5-21.

Malhotra, J. D., Kazen-Gillespie, K., Hortsch, M., and Isom, L. L. (2000) Sodium channel beta subunits mediate homophilic cell adhesion and recruit ankyrin to points of cell-cell contact. J Biol Chem *275*, 11383-11388.

Mallart, A., Angaut-Petit, D., Bourret-Poulin, C., and Ferrus, A. (1991) Nerve terminal excitability and neuromuscular transmission in T(X:Y)V7 and Shaker mutants of Drosophila melanogaster. J Neurogenet 7, 75-84.

Marble, D. D., Hegle, A. P., Snyder, E. D., Dimitratos, S., Bryant, P. J., and Wilson, G. F. (2005) Camguk/CASK enhances Ether-a-go-go potassium current by a phosphorylation-dependent mechanism. J Neurosci *25*, 4898-4907.

Martin, J. R., and Ollo, R. (1996) A new Drosophila Ca2+/calmodulin-dependent protein kinase (Caki) is localized in the central nervous system and implicated in walking speed. EMBO J *15*, 1865-1876.

Martin, S. J. and Morris, R.G. M. (2002) New life in an old idea: The synaptic plasticity and memory hypothesis revisited. Hippocamp *12*, 609-636.

Martin, K. C. (2002) Synaptic tagging during synapse-specific long-term facilitation of Aplysia sensory-motor neurons. Neurobiol Learn Mem *78*, 489-497.

Marx, S. O., Kurokawa, J., Reiken, S., Motoike, H., D'Armiento, J., Marks, A. R., and Kass, R. S. (2002) Requirement of a macromolecular signaling complex for beta adrenergic receptor modulation of the KCNQ1-KCNE1 potassium channel. Science *295*, 496-499.

Massey, P. V. and Bashir, Z. I. (2007) Long-term depression: multiple forms and implications for brain function. Trends Neurosci *30*, 176-184.

Maximov, A., Sudhof, T. C., and Bezprozvanny, I. (1999) Association of neuronal calcium channels with modular adaptor proteins. Journal of Biological Chemistry *274*, 24453-24456.

McCormick, D. A. and Bal, T. (1997) Sleep and arousal: Thalamocortical mechanisms. Annu Rev Neurosci *20*,185–215.

McGee, A. W., Dakoji, S. R., Olsen, O., Bredt, D. S., Lim, W. A., and Prehoda, K. E. (2001) Structure of the SH3-guanylate kinase module from PSD-95 suggests a mechanism for regulated assembly of MAGUK scaffolding proteins. Molecular Cell *8*, 1291-1301.

McHugh, T. J., Blum, K. I., Tsien, J. Z., Tonegawa, S., and Wilson, M. A. (1996) Impaired hippocampal representation of space in CA1-specific NMDAR1 knockout mice. Cell *87*, 1339-1349.

Mee, C. J., Pym, E. C. G., Moffat, K. G., and Baines, R. A. (2004) Regulation of neuronal excitability through pumilio-dependent control of a sodium channel gene. J Neurosci *24*, 8695-8703.

Meyer, R., and Heinemann, S. H. (1998) Characterization of an eag-like potassium channel in human neuroblastoma cells. J Physiol *508 (Pt 1)*, 49-56.

Meyer, R., Schonherr, R., Gavrilova-Ruch, O., Wohlrab, W., and Heinemann, S. H. (1999) Identification of ether a go-go and calcium-activated potassium channels in human melanoma cells. J Membr Biol *171*, 107-115.

Meyer, T., Hanson, P. I., Stryer, L., and Schulman, H. (1992) Calmodulin trapping by calcium-calmodulin-dependent protein kinase. Science *256*, 1199-1202.

Miguel Corona, M., Gurrola, G. B., Merino, E., Restano Cassulini, R., Valdez-Cruz, N. A., Garcia, B., Ramirez-Dominguez, M . E., Coronas, F. I. V., Zamudio, F. Z., Wanke, E., and Possani, L. D. (2002) A large number of novel Ergtoxin-like genes and ERG Kþ-channels blocking peptides from scorpions of the genus Centruroides. FEBS Letters *532*, 121-126.

Miller, S. G. and Kennedy, M. B. (1986) Regulation of brain type II Ca2+/calmodulin-dependent protein kinase by autophosphorylation: A Ca2+-triggered molecular switch. Cell *44*, 861-870.

Miller, C. An overview of the potassium channel family. (2000) Genome Biology *1*, 1-5.

Misonou, H., Menegola, M., Mohapatra, D. P., Guy, L. K., Park, K-S., and Trimmer, J. S. (2006) Bidirectional activity-dependent regulation of neuronal ion channel phosphorylation. J. Neurosci *26*, 13505-13514.

Molleman, A., Thuneberg, L., and Huizinga, J. D. (1993) Characterization of the outward rectifying potassium channel in a novel mouse intestinal smooth muscle cell preparation. J Physiol *470*, 211-229.

Morais Cabral, J. H., Lee, A., Cohen, S. L., Chait, B. T., Li, M., and Mackinnon, R. (1998) Crystal structure and functional analysis of the HERG potassium channel N terminus: a eukaryotic PAS domain. Cell *95*, 649-655.

Morais-Cabral, J. H., Zhou, Y., and MacKinnon, R. (2001) Energetic optimization of ion conduction rate by the K^+ selectivity filter. Nature *414*, 37-42.

Mu, D., Chen, L., Zhang, X., See, L. H., Koch, C. M., Yen, C., Tong, J. J., Spiegel, L., Nguyen, K. C., Servoss, A., *et al.* (2003) Genomic amplification and oncogenic properties of the KCNK9 potassium channel gene. Cancer Cell *3*, 297-302.

Mulkey, R. M., Endo, S., Shenolikar, S., and Malenka, R. C. (1994) Involvement of a calcineurin/inhibitor-1 phosphatase cascade in hippocampal long-term depression. Nature *369*, 486-488.

Muller, B. M., Kistner, U., Kindler, S., Chung, W. J., Kuhlendahl, S., Fenster, S. D., Lau, L. F., Veh, R. W., Huganir, R. L., Gundelfinger, E. D., and Garner, C. C. (1996) SAP102, a novel postsynaptic protein that interacts with NMDA receptor complexes in vivo. Neuron *17*, 255-265.

Murakoshi, H. and Trimmer, J .S. (1999) Identification of the Kv2.1 K+ channel as a major component of the delayed rectifier K+ current in rat hippocampal neurons. J Neurosci *19*, 1728–1735.

Murata, Y., Iwasaki, H., Sasaki, M., Inaba, K., and Okamura, Y. (2005) Phosphoinositide phosphatase activity coupled to an intrinsic voltage sensor. Nature *435*, 1239-1243.

Nakajima, T., Hayashi, K., Viswanathan, P. C., Kim, M-Y. Anghelescu, M., Barksdale, K. A., Shuai, W., Balser, J. R. and Kupershmidt, S. (2007) HERG is protected from pharmacological block by α-1,2-glucosyltransferase function. J Biol Chem *282*, 5506-5513.

Narita, K., Akita, T., Hachisuka, J., Huang, S.-M., Ochi, K., and Kuba, K. (2000) Functional coupling of Ca2+ channels to ryanodine receptors at presynaptic terminals: Amplification of exocytosis and plasticity. J Gen Physiol *115*, 519-532.

Nelson, H. B., Heiman, R. G., Bolduc, C., Kovalick, G. E., Whitley, P., Stern, M., and Beckingham, K. (1997) Calmodulin point mutations affect Drosophila development and behavior. Genetics *147*, 1783-1798.

Nitabach, M. N., Blau, J., and Holmes, T. C. (2002) Electrical silencing of *Drosophila* pacemaker neurons stops the free-running circadian clock. Cell *109*, 485–495.

Occhiodoro, T., Bernheim, L., Liu, J. H., Bijlenga, P., Sinnreich, M., Bader, C. R., and Fischer-Lougheed, J. (1998) Cloning of a human ether-a-go-go potassium channel expressed in myoblasts at the onset of fusion. FEBS Lett *434*, 177-182.

Ogielska, E. M. and Aldrich, R. W. (1999) Functional consequences of a decreased potassium affinity in a potassium channel pore. Ion interactions and C-type inactivation. J Gen Physiol *113*, 347-358.

Oliveria, S. F., Dell'Acqua, M. L., and Sather, W. A. (2007) AKAP79/150 anchoring of calcineurin controls neuronal L-type Ca2+ channel activity and nuclear signaling. Neuron *55*, 261–275.

Ostrom, R. S., Naugle, J. E., Hase, M., Gregorian, C., Swaney, J. S., Insel, P. A., Brunton, L. L., and Meszaros, J. G. (2003) Angiotensin II enhances adenylyl cyclase signaling via Ca2+/calmodulin. J Biol Chem *278*, 24461-24468.

Papazian, D. M., Schwarz, T. L., Tempel, B. L., Jan, Y. N., and Jan, L. Y. (1987) Cloning of genomic and complementary DNA from Shaker, a putative potassium channel gene from Drosophila. Science *237*, 749-753.

Paradis, S., Sweeney, S. T., and Davis, G. W. (2001) Homeostatic control of presynaptic release is triggered by postsynaptic membrane depolarization. Neuron 30, 737-749.

Pardo, L. A. (2004) Voltage-gated potassium channels in cell proliferation. Physiology (Bethesda) *19*, 285-292.

Pardo, L. A., Bruggemann, A., Camacho, J., and Stuhmer, W. (1998) Cell cycle-related changes in the conducting properties of r-eag K+ channels. J Cell Biol *143*, 767-775.

Pardo, L. A., Contreras-Jurado, C., Zientkowska, M., Alves, F., and Stuhmer, W. (2005) Role of voltage-gated potassium channels in cancer. J Membr Biol *205*, 115-124.

Pardo, L. A., del Camino, D., Sanchez, A., Alves, F., Bruggemann, A., Beckh, S., and Stuhmer, W. (1999) Oncogenic potential of EAG K(+) channels. Embo J *18*, 5540-5547.

Patt, S., Preussat, K., Beetz, C., Kraft, R., Schrey, M., Kalff, R., Schonherr, K., and Heinemann, S. H. (2004) Expression of ether a go-go potassium channels in human gliomas. Neurosci Lett *368*, 249-253.

Pearson, G., Robinson, F., Beers Gibson, T., Xu, B. E., Karandikar, M., Berman, K., and Cobb, M. H. (2001) Mitogen-activated protein (MAP) kinase pathways: regulation and physiological functions. Endocrine Reviews *22*, 153-183.

Pemberton, K. E., Hill-Eubanks, L. J., and Jones, S. V. P. (2000) Modulation of low-threshold T-type calcium channels by the five muscarinic receptor subtypes in NIH 3T3 cells. Pflugers Archives -- European Journal of Physiology *440*, 452-461.

Petegem, F. V. and Minor, D.L. (2006) The structural biology of voltage-gated calcium channel function and regulation. Biochem Soc Trans *34*, 887-893.

Peterson, B. Z., DeMaria, C. D., Adelman, J. P., and Yue, D. T. (1999) Calmodulin is the Ca2+ sensor for Ca2+ -dependent inactivation of L-type calcium channels. Neuron *22*, 549-558.

Phelps, C. B., and Brand, A. H. (1998) Ectopic gene expression in Drosophila using GAL4 system. Methods *14*, 367-379.

Pillozzi, S., Brizzi, M. F., Balzi, M., Crociani, O., Cherubini, A., Guasti, L., Bartolozzi, B., Becchetti, A., Wanke, E., Bernabei, P. A., *et al.* (2002) HERG potassium channels are constitutively expressed in primary human acute myeloid leukemias and regulate cell proliferation of normal and leukemic hemopoietic progenitors. Leukemia *16*, 1791-1798.

Piros, E. T., Shen, L., and Huang, X-Y. (1999) Purification of an EH domain-binding protein from rat brain that modulates the gating of the rat ether-a-go-go channel. *274*, 33677–33683.

Pitt, G. S., Zuhlke, R. D., Hudmon, A., Schulman, H., Reuter, H., and Tsien, R. W. (2001) Molecular basis of calmodulin tethering and Ca2+-dependent inactivation of L-type Ca2+ channels. J Biol Chem *276*, 30794-30802.

Po, S., Roberds, S., Snyders, D.J., Tamkun, M.M., and Bennett, P.B. (1993) Heteromultimeric assembly of human potassium channels. Circ Res *72*, 1326-1336.

Pokorska, A., Vanhoutte, P., Arnold, F. J. L., Silvagno, F., Hardingham, G. E. and Bading, H. (2003) Synaptic activity induces signalling to CREB without increasing global levels of cAMP in hippocampal neurons. J Neurochem *84*, 447-452.

Pongs, O. (1992) Structural basis of voltage-gated K+ channel pharmacology. Trends Pharmacol Sci *13*, 359-365.

Pongs, O., Lindemeier, J., Zhu, X. R., Theil, T., Engelkamp, D., Krah-Jentgens, I., Lambrecht, H. G., Koch, K. W., Schwemer, J., Rivosecchi, R., et al. (1993) Frequenin--a

novel calcium-binding protein that modulates synaptic efficacy in the Drosophila nervous system. Neuron *11*, 15-28.

Potet, F., Scott, J.D., Mohammad-Panah, R., Escande, D., and Baró, I. (2001) AKAP proteins anchor cAMP-dependent protein kinase to KvLQT1/IsK channel complex. Am J Physiol Heart Circ Physiol *280*, 2038-2045.

Preisig-Muller, R., Schlichthorl, G., Goerge, T., Heinen, S., Bruggemann, A., Rajan, S., Derst, C., Veh, R. W., and Daut, J. (2002) Heteromerization of Kir2.x potassium channels contributes to the phenotype of Andersen's syndrome. Proc Natl Acad Sci U S A *99*, 7774-7779.

Price, M., Lee, S. C., and Deutsch, C. (1989) Charybdotoxin inhibits proliferation and interleukin 2 production in human peripheral blood lymphocytes. Proc Natl Acad Sci U S A *86*, 10171-10175.

Prinz, A. A., Bucher, D., and Marder, E. (2004) Similar network activity from disparate circuit parameters. Nat Neurosci *7*, 1345-1352.

Putkey, J. A., and Waxham, M. N. (1996) A peptide model for calmodulin trapping by calcium/calmodulin-dependent protein kinase II. Journal of Biological Chemistry *271*, 29619-29623.

Qian, J. and Saggau, P. (1999) Activity-dependent modulation of K+ currents at presynaptic terminals of mammalian central synapses. J Physiol *519*, 427-437.

Ramsey, I. S., Moran, M. M., Chong, J. A., and Clapham, D. E. (2006) A voltage-gated proton-selective channel lacking the pore domain. Nature *440*, 1213-1216.

Rashid, A., Khurshid, R., Begum, M., Gul-e-Raana, Latif, M. and Salimd, A. (2004) Modeling the mutational effects on calmodulin structure: prediction of alteration in the amino acid interactions. Biochem Biophys Res Comm *317*, 363-369.

Rehm, H., Pelzer, S., Cochet, C., Chambaz, E., Tempel, B. L., Trautwein, W., Pelzer, D., and Lazdunski, M. (1989) Dendrotoxin-binding brain membrane protein displays a potassium channel activity that is stimulated by both cAMP-dependent and endogenous phosphorylations. Biochem *28*, 6455-6460.

Reiner, D. J., Newton, E. M., Tian, H., and Thomas, J. H. (1999) Diverse behavioural defects caused by mutations in Caenorhabditis elegans unc-43 CaM kinase II. Nature 402, 199-203.

Rettig, J., Heinemann, S. H., Wunder, F., Lorra, C., Parcej, D. N., Dolly, J. O., and Pongs, O. (1994) Inactivation properties of voltage-gated K+ channels altered by presence of beta-subunit. Nature *369*, 289-294.

Reuther, G. W., Fu, H., Cripe, L. D., Collier, R. J., and Pendergast, A. M. (1994) Association of the protein kinases c-Bcr and Bcr-Abl with proteins of the 14-3-3 family. Science *266*, 129-133.

Rho, J. M., Szot, P., Tempel, B. L., and Schwartzkroin, P. A. (1999) Developmental seizure susceptibility of Kv1.1 potassium channel knockout mice. Dev Neurosci *21*, 320-327.

Robertson, G. A., Warmke, J. M., and Ganetzky, B. (1996) Potassium currents expressed from Drosophila and mouse eag cDNAs in Xenopus oocytes. Neuropharmacology *35*, 841-850.

Rodrigues, S. M., Farb, C. R., Bauer, E. P., LeDoux, J. E., and Schafe, G. E. (2004) Pavlovian fear conditioning regulates Thr286 autophosphorylation of Ca2+/calmodulin-dependent protein kinase II at lateral amygdala synapses. J Neurosci *24*, 3281-3288.

Rohrbough, J., Pinto, S., Mihalek, R.M., Tully, T., and Broadie, K. (1999) latheo, a Drosophila gene involved in learning, regulates functional synaptic plasticity. Neuron *23*, 55-70.

Rohrbough, J., Grotewiel, M.S., Davis, R.L., and Broadie, K. (2000) Integrin-mediated regulation of synaptic morphology, transmission, and plasticity. J Neurosci *20*, 6868-6878.

Rosen, L. B., Ginty, D. D., Weber, M. J., and Greenberg, M. E. (1994) Membrane depolarization and calcium influx stimulate MEK and MAP kinase via activation of Ras. Neuron *12*, 1207-1221.

Roth, A. and Häusser, M. (2001) Compartmental models of rat cerebellar Purkinje cells based on simultaneous somatic and dendritic patch-clamp recordings. J Physiol *535*, 445-472.

Runnels, L. W., Yue, L., and Clapham, D. E. (2001) TRP-PLIK, a bifunctional protein with kinase and ion channel activities. Science *291*, 1043-1047.

Rutter, J., Michnoff, C. H., Harper, S. M., Gardner, K. H., and McKnight, S. L. (2001) PAS kinase: An evolutionarily conserved PAS domain-regulated serineythreonine kinase. Proc Natl Acad Sci USA *98*, 8991–8996.

Saganich, M. J., Vega-Saenz de Miera, E., Nadal, M. S., Baker, H., Coetzee, W. A., and Rudy, B. (1999) Cloning of components of a novel subthreshold-activating K+ channel with a unique pattern of expression in the cerebral cortex. J Neurosci *19*,10789-10802.

Saganich, M. J., Machado, E., and Rudy, B. (2001) Differential expression of genes encoding subthreshold-operating voltage-gated K+ channels in brain. J Neurosci *21*, 4609-4624.

Sanguinetti, M. C., Curran, M. E., Zou, A., Shen, J., Spector, P. S., Atkinson, D. L., and Keating, M. T. (1996) Coassembly of KvLQT1 and minK (IsK) proteins to form cardiac IKs potassium channel. Nature *384*, 80-83.

Sanguinetti, M. C. and Xu, Q. P. (1999) Mutations of the S4-S5 linker alter activation properties of HERG potassium channels expressed in Xenopus oocytes. J Physiol *514*, 667-675.

Saimi, Y., and Kung, C. (2002) Calmodulin as an ion channel subunit. Annu Rev Physiol *64*, 289-311.

Salinas, M., Duprat, F., Heurteaux, C., Hugnot, J-P., and Lazdunski, M. (1997) New modulatory α subunits for mammalian *Shab* K+ channels. J Biol Chem *272*, 24371–24379.

Sano, Y., Mochizuki, S., Miyake, A., Kitada, C., Inamura, K., Yokoi, H., Nozawa, K., Matsushime, H., and Furuichi, K. (2002) Molecular cloning and characterization of Kv6.3, a novel modulatory subunit for voltage-gated K+ channel Kv2.1. FEBS Letters *512*, 230-234.

Sasaki, M., Takagi, M., and Okamura, Y. (2006) A voltage sensor-domain protein is a voltage-gated proton channel. Science *312*, 589-592.

Schonherr, R., and Heinemann, S. H. (1996) Molecular determinants for activation and inactivation of HERG, a human inward rectifier potassium channel. J Physiol *493 (Pt 3)*, 635-642.

Schonherr, R., Lober, K., and Heinemann, S. H. (2000) Inhibition of human ether a go-go potassium channels by Ca(2+)/calmodulin. Embo J *19*, 3263-3271.

Schonherr, R., Mannuzzu, L. M., Isacoff, E. Y., and Heinemann, S. H. (2002) Conformational switch between slow and fast gating modes: allosteric regulation of voltage sensor mobility in the EAG K+ channel. Neuron *35*, 935-949.

Schopperle, W. M., Holmqvist, M. H., Zhou, Y., Wang, J., Wang, Z., Griffith, L. C., Keselman, I., Kusinitz, F., Dagan, D., and Levitan, I. B. (1998) Slob, a novel protein that interacts with the Slowpoke calcium-dependent potassium channel. Neuron *20*, 565-573.

Schreiber, M., Wei, A., Yuan, A., Gaut, J., Saito, M., and Salkoff, L. (1998) Slo3, a novel pH-sensitive K+ channel from mammalian spermatocytes J Biol Chem *273*, 3509–3516.

Schulman, H. (2004) Activity-dependent regulation of calcium/calmodulin-dependent protein kinase II localization. J Neurosci *24*, 8399–8403.

Schumacher, M. A., Rivard, A. F., Bachinger, H. P., and Adelman, J. P. (2001) Structure of the gating domain of a Ca2+-activated K+ channel complexed with Ca2+/calmodulin. Nature *410*, 1120-1124.

Schuster, C. M., Davis, G. W., Fetter, R. D., and Goodman, C. S. (1996) Genetic dissection of structural and functional components of synaptic plasticity. II. Fasciclin II controls presynaptic structural plasticity. Neuron *17*, 655–667.

Schwarz, J. R. and Bauer, C. K. (2004) Functions of erg K+ channels in excitable cells. J Cell Mol Med *8*, 22-30.

Scully, A. L., and Kay, S. A. (2000) Time flies for Drosophila. Cell *100*, 297-300.

Selyanko, A. A., Delmas, P., Hadley, J. K., Tatulian, L., Wood, I. C., Mistry, M., London, B., and Brown, D. A. (2002) Dominant-negative subunits reveal potassium channel families that contribute to M-like potassium currents. J Neurosci *22*, RC212 1-5.

Shen, N. V., Chen, X., Boyer, M. M., and Pfaffinger, P.J. (1993) Deletion analysis of K+ channel assembly. Neuron *11*, 67-76.

Shen, N. V. and Pfaffinger, P. J. (1995) Molecular recognition and assembly sequences involved in the subfamily-specific assembly of voltage-gated K + channel subunit proteins. Neuron *14*, 625-633.

Sheng, M., McFadden, G., and Greenberg, M. E. (1990) Membrane depolarization and calcium induce c-fos transcription via phosphorylation of transcription factor CREB. Neuron *4*, 571-582.

Sheng, M., Liao, Y. J., Jan, Y. N., Jan, L. Y. (1993) Presynaptic A-current based on hterommultimeric K+ channels detected in vivo. Nature *365*, 72-75.

Shi, W., Wang, H-S., Pan, Z., Wymore, R. S., Cohen, I. S., McKinnon, D., and Dixon, J. E. (1998) Cloning of a mammalian *elk* potassium channel gene and EAG mRNA distribution in rat sympathetic ganglia. J Physiol *511*, 675-682.

Shifman, J. M., Choi, M. H., Mihalas, S., Mayo, S. L., and Kennedy, M. B. (2006) Ca2+/calmodulin-dependent protein kinase II (CaMKII) is activated by calmodulin with two bound calciums. Proc Natl Acad Sci USA *103*, 13968-13973.

Siegel, R. W., and Hall, J. C. (1979) Conditioned responses in courtship behavior of normal and mutant Drosophila. Proc Natl Acad Sci USA *76*, 3430-3434.

Silva, A. J., Paylor, R., Wehner, J. M., and Tonegawa, S. (1992a) Impaired spatial learning in alpha-calcium-calmodulin kinase II mutant mice. Science *257*, 206-211.

Silva, A. J., Stevens, C. F., Tonegawa, S., and Wang, Y. (1992b) Deficient hippocampal long-term potentiation in alpha-calcium-calmodulin kinase II mutant mice. Science *257*, 201-206.

Silverman, W. R., Tang, C-Y., Mock, A. F., Huh, K-B., and Papazian, D. M (2000) Mg2+ modulates voltage-dependent activation in Ether-à-go-go potassium channels by binding between transmembrane segments S2 and S3. J Gen Physiol *116*, 663–677.

Silverman, W. R., Roux, B., and Papazian, D. M. (2003) Structural basis of two-stage voltage-dependent activation in K+ channels. Proc Natl Acad Sci U S A *100*, 2935-2940.

Silverman, W. R., Bannister, J. P. A., and Papazian, D. M. (2004) Binding site in Eag voltage sensor accommodates a variety of ions and is accessible in closed channel. Biophys J *87*, 3110–3121.

Singer-Lahat, D. et al., (2007) K+ channel facilitation of exocytosis by dynamic interaction with syntaxin. J Neurosci *27*, 1651-1658.

Smith, P. L., Baukrowitz, T., and Yellen, G. (1996) The inward rectification mechanism of the HERG cardiac potassium channel. Nature *379*, 833-836.

Smith, P. L., and Yellen, G. (2002) Fast and slow voltage sensor movements in HERG potassium channels. J Gen Physiol *119*, 275-293.

Soderling, T. R. (1993) Calcium/calmodulin-dependent protein kinase II: role in learning and memory. Mol Cell Biochem *127-128*, 93-101.

Sparks, A. B., Rider, J. E., Kay, B. K., Curriculum in, G., and Molecular Biology, U.o.N.C. a.C.H.U.S.A. (1998) Mapping the specificity of SH3 domains with phage-displayed random-peptide libraries. Methods in molecular biology (Clifton, NJ) *84*.

Stansfeld, C. E., Roper, J., Ludwig, J., Weseloh, R. M., Marsh, S. J., Brown, D. A., and Pongs, O. (1996) Elevation of intracellular calcium by muscarinic receptor activation induces a block of voltage-activated rat ether-a-go-go channels in a stably transfected cell line. Proc Natl Acad Sci U S A *93*, 9910-9914.

Stern, M. Ganetzky, B. (1989) Altered synaptic transmission in Drosophila hyperkinetic mutants. J Neurogen *5*, 215-228.

Stevens, C. F. and Wesseling, J. F. (1998) Activity-dependent modulation of the rate at which synaptic vesicles become available to undergo exocytosis. Neuron *21*, 415-424.

Stewart, B. A., Atwood, H. L., Renger, J. J., Wang, J., and Wu, C. F. (1994) Improved stability of Drosophila larval neuromuscular preparations in haemolymph-like physiological solutions. J Comp Physiol *175*, 179-191.

Stukenberg, P. T., Lustig, K. D., McGarry, T. J., King, R. W., Kuang, J. and Kirschner, M. W. (1997) Systematic identification of mitotic phosphoproteins. Curr Biol *7*, 338-348.

Suh, B. C. and Hille, B. (2002) Recovery from muscarinic modulation of M current channels requires phosphatidylinositol 4,5-bisphosphate synthesis. Neuron *35*, 507–520.

Sun, X. X., Hodge, J. J., Zhou, Y., Nguyen, M., and Griffith, L. C. (2004) The eag potassium channel binds and locally activates calcium/calmodulin-dependent protein kinase II. J Biol Chem *279*, 10206-10214.

Sutton, K. G., McRory, J. E., Guthrie, H., Murphy, T. H., and Snutch, T. P. (1999) P/Q-type calcium channels mediate the activity-dependent feedback of syntaxin-1A. Nature *401*, 800-804.

Sweatt, J. D. (2004) Mitogen-activated protein kinases in synaptic plasticity and memory. Curr Opin Neurobiol *14*, 311-317.

Tabuchi, K., Biederer, T., Butz, S. and Sudhof, T. C. (2002) CASK participates in alternative tripartite complexes in which Mint 1 competes for binding with Caskin1, a novel CASK-binding protein. J Neurosci 22, 4264–4273.

Takeda, K., Matsuzawa, A., Nishitoh, H., Tobiume, K., Kishida, S., Ninomiya-Tsuji, J., Matsumoto, K., and Ichijo, H. (2004) Involvement of ASK1 in Ca2+-induced p38 MAP kinase activation. EMBO Rep *5*, 161-166.

Tang, Y-P., Shimizu, E., Dube, G. R., Rampon, C., Kerchner, G. A., Zhuo, M., Liu, G., and Tsien, J. Z. (1999) Genetic enhancement of learning and memory in mice. Nature *401*, 63-69.

Tang, C. Y., Bezanilla, F., and Papazian, D. M. (2000) Extracellular Mg(2+) modulates slow gating transitions and the opening of Drosophila ether-a-Go-Go potassium channels. J Gen Physiol *115*, 319-338.

Tang, W., Halling, D. B., Black, D. J., Pate, P., Zhang, J. Z., Pedersen, S., Altschuld, R. A., and Hamilton, S. L. (2003) Apocalmodulin and Ca2+ calmodulin-binding sites on the Ca(V)1.2 channel. Biophysical Journal *85*, 1538-1547.

Taylor, B. L., and Zhulin, I. B. (1999) PAS domains: internal sensors of oxygen, redox potential, and light. Microbiol Mol Biol Rev *63*, 479-506.

Tempel, B. L., Papazian, D. M., Schwarz, T. L., Jan, Y. N., and Jan, L. Y. (1987) Sequence of a probable potassium channel component encoded at Shaker locus of Drosophila. Science *237*, 770-775.

Tempel, B. L., Jan, Y. N., and Jan, L. Y. (1988) Cloning of a probable potassium channel gene from mouse brain. Nature *332*, 837-839.

Terlau, H., Ludwig, J., Steffan, R., Pongs, O., Stuhmer, W., and Heinemann, S. H. (1996) Extracellular Mg2+ regulates activation of rat eag potassium channel. Pflugers Arch *432*, 301-312.

Thomas, G. M., and Huganir, R. L. (2004) MAPK cascade signalling and synaptic plasticity. Nat Rev Neurosci *5*, 173-183.

Tibbs, V. C., Gray, P. C., Catterall, W. A., and Murphy, B. J. (1998) AKAP15 anchors cAMP-dependent protein kinase to brain sodium channels. J Biol Chem *273*, 25783–25788.

Timpe, L. C., Schwarz, T. L., Tempel, B. L., Papazian, D, M., Jan, Y. N., and Jan, L. Y. (1988) Expression of functional potassium channels from Shaker cDNA in Xenopus oocytes. Nature *331*,143-145.

Titus, S. A., Warmke, J. W., and Ganetzky, B. (1997) The Drosophila erg K+ channel polypeptide is encoded by the seizure locus. J Neurosci *17*, 875–881.

Trudeau, M. C., Titus, S. A., Branchaw, J. L., Ganetzky, B., and Robertson, G. A. (1999). Functional analysis of a mouse brain Elk-type K+ channel. J Neurosci *19*, 2906-2918.

Trudeau, M. C., Warmke, J. W., Ganetzky, B., and Robertson, G. A. (1995) HERG, a human inward rectifier in the voltage-gated potassium channel family. Science *269*, 92-95.

Tseng, G-N. (2001) Basic cardiac electrophysiology. IKr: The hERG channel. J Mol Cell Cardiol *33*, 835–849.

Tsien, J. Z., Huerta, P. T., and Tonegawa, S. (1996) The essential role of hippocampal CA1 NMDA receptor–dependent synaptic plasticity in spatial memory. Cell *87*, 1327-1338.

Turrigiano, G. (2007) Homeostatic signaling: the positive side of negative feedback. Curr Opin Neurobiol *17*:318–324.

Turrigiano, G. G. and Nelson, S. B. (2004) Homeostatic plasticity in the developing nervous system. Nature Rev Neurosci *5*, 97-107.

Turrigiano, G. G., Leslie, K. R., Desai, N. S., Rutherford, L. C., Nelson, S. B. (1998) Activity-dependent scaling of quantal amplitude in neocortical neurons. Nature *391*, 892-896.

Ullrich, N. (1999) The role of ion channels in cell proliferation. The Neuroscientist *5*, 70-73.

Valiyaveetil, F. I., Leonetti, M., Muir, T. W., and MacKinnon, R. (2006) Ion selectivity in a semisynthetic K+ channel locked in the conductive conformation. Science *314*, 1004-1007.

Vautier, F., Belachew, S., Chittajallu, R., and Gallo, V. (2004) Shaker-type potassium channel subunits differentially control oligodendrocyte progenitor proliferation. Glia *48*, 337-345.

Wang, H., Kunkel, D. D., Martin, T. M., Schwartzkroin, P. A., and Tempel, B. L. (1993) Herteromultimeric K+ channels in terminal juxtaparanodal regions of neurons. Nature 365, 75-78.

Wang, L., Xu, B., White, R. E., and Lu, L. (1997) Growth factor-mediated K+ channel activity associated with human myeloblastic ML-1 cell proliferation. Am J Physiol Cell Physiol *273*, 1657-1665.

Wang, H-S., Pan, Z., Shi, W., Brown, B. S., Wymore, R. S., Cohen, I. S., Dixon., J. E., McKinnon, D. (1998) KCN2 and KCNQ3 Potassium Channel Subunits: Molecular Correlates of the M Current. Science *282*, 1890-1893.

Wang, J., Zhou, Y., Wen, H., and Levitan, I. B. (1999) Simultaneous binding of two protein kinases to a calcium-dependent potassium channel. J Neurosci *19*, RC4.

Wang, H., Zhang, Y., Cao, L., Han, H., Wang, J., Yang, B., Nattel, S., and Wang, Z. (2002a) HERG K+ channel, a regulator of tumor cell apoptosis and proliferation. Cancer Res *62*, 4843-4848.

Wang, Z., Wilson, G. F., and Griffith, L. C. (2002b) Calcium/calmodulin-dependent protein kinase II phosphorylates and regulates the Drosophila eag potassium channel. J Biol Chem *277*, 24022-24029.

Wang, H., Ferguson, G. D., Pineda, V. V., Cundiff, P. E., and Storm, D. R. (2004) Overexpression of type-1 adenylyl cyclase in mouse forebrain enhances recognition memory and LTP. Nat Neurosci *7*, 635-642.

Warmke, J., Drysdale, R., and Ganetzky, B. (1991) A distinct potassium channel polypeptide encoded by the Drosophila eag locus. Science *252*, 1560-1562.

Warmke, J. W., and Ganetzky, B. (1994) A family of potassium channel genes related to eag in Drosophila and mammals. Proc Natl Acad Sci U S A *91*, 3438-3442.

Waxham, M. N., Tsai, A. L,, and Putkey, J. A. (1998) A mechanism for calmodulin (CaM) trapping by CaM-kinase II defined by a family of CaM-binding peptides. J Biol Chem *273*, 17579-17584.

Wei, X., Neely, A., Lacerda, A. E., Olcese, R., Stefani, E., Perez-Reyes, E., and Birnbaumer, L. (1994) Modification of Ca2+ channel activity by deletions at the carboxyl terminus of the cardiac alpha 1 subunit. J Biol Chem *269*, 1635-1640.

Weinshenker, D., Wei, A., Salkoff, L., and Thomas, J. H. (1999) Block of an ether-a-go-go-like K+ channel by imipramine rescues egl-2 excitation defects in Caenorhabditis elegans. J Neurosci *19*, 9831–9840.

Wen, H., and Levitan, I. B. (2002) Calmodulin is an auxiliary subunit of KCNQ2/3 potassium channels. J Neurosci *22*, 7991-8001.

Weng, J., Cao, Y., Moss, N., and Zhou, M. (2006) Modulation of voltage-dependent Shaker family potassium channels by an aldo-keto reductase. J Biol Chem *281*, 15194-15200.

Wilson, G. F., and Chiu, S. Y. (1993) Mitogenic factors regulate ion channels in Schwann cells cultured from newborn rat sciatic nerve. J Physiol *470*, 501-520.

Wilson, G. F., Wang, Z., Chouinard, S. W., Griffith, L. C., and Ganetzky, B. (1998) Interaction of the K channel beta subunit, Hyperkinetic, with eag family members. J Biol Chem *273*, 6389-6394.

Wimmers, S., Bauer, C. K., and Schwarz, J. R. (2002) Biophysical properties of heteromultimeric erg K+ channels. Eur J Physiol *445*, 423–430.

Wonderlin, W. F., and Strobl, J. S. (1996) Potassium channels, proliferation and G1 progression. J Membr Biol *154*, 91-107.

Wong, K., Karunanithi, S., and Atwood, H. L. (1999) Quantal unit populations at the Drosophila larval neuromuscular junction. J Neurophysiol *82*, 1497-1511.

Wong, H. K., Sakurai, T., Oyama, F., Kaneko, K., Wada, K., Miyazaki, H., Kurosawa, M., De Strooper, B., Saftig, P., and Nukina, N. (2005) beta Subunits of voltage-gated sodium channels are novel substrates of beta-site amyloid precursor protein-cleaving enzyme (BACE1) and gamma-secretase. J Biol Chem *280*, 23009-23017.

Wu, C. F., Suzuki, N., and Poo, M. M. (1983a) Dissociated neurons from normal and mutant Drosophila larval central nervous system in cell culture. J Neurosci *3*, 1888-1899.

Wu, C. F., Ganetzky, B., Haugland, F. N., and Liu, A. X. (1983b) Potassium currents in Drosophila: different components affected by mutations of two genes. Science *220*, 1076-1078.

Wu, C. F., Tsai, M. C., Chen, M. L., Zhong, Y., Singh, S., and Lee, C. Y. (1989) Actions of dendrotoxin on K+ channels and neuromuscular transmission in Drosophila melanogaster, and its effects in synergy with K+ channel-specific drugs and mutations. J Exper Biol *147*, 21-41.

Wu, Y., Kawasaki, F., and Ordway, W. R. (2005) Properties of short-term synaptic depression at larval neuromuscular synapses in wild-type and temperature-sensitive paralytic mutants of Drosophila. J Neurophysiol *93*, 2396-2405.

Xia, X. M., Fakler, B., Rivard, A., Wayman, G., Johnson-Pais, T., Keen, J. E., Ishii, T., Hirschberg, B., Bond, C. T., Lutsenko, S., *et al.* (1998) Mechanism of calcium gating in small-conductance calcium-activated potassium channels. Nature *395*, 503-507.

Xu, J., Yu, W. Jan, Y-N., Jan, L. Y., and Li, M. (1995) Assembly of voltage-gated potassium channels. J Biol Chem *270*, 24761–24768.

Xu, B., Wilson, B. A., and Lu, L. (1996) Induction of human myeloblastic ML-I cell G1 arrest by suppression of K+ channel activity. Am J Physiol 271, C2037-C2044.

Xu, J., He, L., and Wu, L-G. (2007) Role of Ca2+ channels in short-term synaptic plasticity. Curr Opin Neurobiol *17*, 352–359.

Xu-Friedman, M. A. and Regehr, W. G. (2004) Structural contributions to short-term synaptic plasticity. Physiol Rev *84*, 69-85.

Yoshimura, Y., Aoi, C., and Yamauchi, T. (2000) Investigation of protein substrates of Ca(2+)/calmodulin-dependent protein kinase II translocated to the postsynaptic density. Brain Res Mol Brain Res *81*, 118-128.

Young, K. A. and Caldwell, J. H. (2005) Modulation of skeletal and cardiac voltage-gated sodium channels by calmodulin. J Physiol *565*, 349-370.

Yu, F. H., and Catterall, W. A. (2004) The VGL-chanome: a protein superfamily specialized for electrical signaling and ionic homeostasis. Sci STKE *2004*, re15.

Zagotta, W. N., Hoshi, T., and Aldrich, R. W. (1990) Restoration of inactivation in mutants of Shaker potassium channels by a peptide derived from ShB. Science *250*, 568-571.

Zeng, H., Fei, H., and Levitan, I. B. (2004) The slowpoke channel binding protein Slob from Drosophila melanogaster exhibits regulatable protein kinase activity. Neurosci Lett *365*, 33-38.

Zhang, W., Hirschler-Laszkiewicz, I., Tong, Q., Conrad, K., Sun, S. C., Penn, L., Barber, D. L., Stahl, R., Carey, D. J., Cheung, J. Y., and Miller, B. A. (2006). TRPM2 is an ion channel that modulates hematopoietic cell death through activation of caspases and PARP cleavage. Am J Physiol Cell Physiol *290*, C1146-1159.

Zhong, Y. and Wu, C-F. (1991) Alteration of four identified K+ currents in Drosophila muscle by mutations in eag. Science *252*, 1562-1564.

Zhong, Y. and Wu, C-F. (1993) Modulation of different K+ currents in Drosophila: A hypothetical role for the Eag subunit in multimeric K+ channels. J Neurosci *73*, 4669-4679.

Zhou, Y., Schopperle, W. M., Murrey, H., Jaramillo, A., Dagan, D., Griffith, L. C., and Levitan, I. B. (1999) A dynamically regulated 14-3-3, Slob, and Slowpoke potassium channel complex in Drosophila presynaptic nerve terminals. Neuron *22*, 809-818.

Zhou, Y., Wang, Z., Griffith, L. C., and Levitan, I. B. (2001) Temperature-sensitive functional expression of Drosophila EAG potassium channels. Society for Neuroscience Abstracts *27*, 812-830.

Zhou, L., Olivier, N. B., Yao, H., Young, H. C., and Siegelbaum, S. A. (2004) A conserved tripeptide in CNG and HCN channels regulates ligand gating by controlling C-terminal oligomerization. Neuron *44*, 823–834.

Zhu, J. J., Qin, Y., Zhao, M., Van Aelst, L., and Malinow, R. (2002) Ras and Rap control AMPA receptor trafficking during synaptic plasticity. Cell *110*, 443-455.

Ziechner, U., Schonherr, R., Born, A-K., Gavrilova-Ruch, O., Glaser, R. W., Malesevic, M., Kullertz, G., and Heinemann, S. H. (2006) Inhibition of human ether a` go-go potassium channels by Ca2+⁄calmodulin binding to the cytosolic N- and C-termini. FEBS J *273*, 1074-1086.

Zordan, M. A., Massironi, M., Ducato, M. G., te Kronnie, G., Costa, R., Reggiani, C., Chagneau, C., Martin, J-R., and Megighian, A. (2005) Drosophila CAKI/CMG protein, a homolog of human CASK, is essential for regulation of neurotransmitter vesicle release. J Neurophysiol *94*, 1074-1083.

Zou, A., Lin, Z., Humble, M., Creech, C. D., Wagoner, P. K., Krafte, D., Jegla, T.J., and Wickenden, A. D. (2003) Distribution and functional properties of human KCNH8 (Elk1) potassium channels. Am J Physiol Cell Physiol *285*, C1356–C1366.

Zucker, R. S. and Regehr, W. G. (2002) Short-term synaptic plasticity. Annu Rev Physiol *64*, 355–405.

Zuhlke, R. D., Pitt, G. S., Deisseroth, K., Tsien, R. W., and Reuter, H. (1999) Calmodulin supports both inactivation and facilitation of L-type calcium channels. Nature *399*, 159-162.